THE ROLE OF CANONICAL AND NON-CANONICAL WNT SIGNALLING PATHWAYS IN LOAD INDUCED CARTILAGE DEGRADATION.

Ayesha Al-Sabah

A thesis submitted to Cardiff University in accordance with the requirements for the degree of Doctor of Philosophy in the school of Biosciences

September 2014

Dedicated to my

Family

For their

unconditional love and support

Acknowledgements

I would like to firstly thank my supervisors Prof. Vic Duance and Dr. Emma Blain for their help and guidance throughout not only my PhD, but also when I was an undergraduate project student. If it were not for their support and encouragement, I would not be where I am today. Thank you for taking me as your student and spending the time and effort to guide me.

A big thank you for my parents, my baby brother and sister who have encouraged me and made the effort to come all the way here to see me and shower me with their unconditional love and support. I am very lucky to have them always by my side whenever things felt a bit bleak. My nanny who has raised me and been by my side ever since I can remember, I owe her everything and the person I am today is because of her.

I would like to thank my international family, starting with Dr. Yadan Zhang A.K.A lab mom, for helping and guiding me through lab and setting me straight when it was required. Dr. Marisol Vazquez for her support and amazing cakes which always gets me through any stressful day. Dr. Cleo Bonnet for her unconditional support and care as well as being the sunshine in our office and making it ever so lively. Dr. Sophie Gilbert for her help and guidance throughout my undergraduate project year and PhD. Dr. Tom Davies for his friendship, support, and encouragement in his own geeky way.

I would like to mostly thank the future Dr. Paulina Stadnik for her unconditional care, love, and support and keeping me sane throughout my PhD. Without her support, I do not think I could have completed this. Thank you for being there for me in the ups and downs of this roller coaster of a PhD.

I would like to say a big thank you to my previous lab, Prof. Bruce Caterson's lab, where I did my MRes degree. Thank you Dr. Clare Hughes and Prof. Bruce Caterson for supporting me through my PhD and your words of encouragement meant a lot to me. Dr. Shane Wainwright, for being the lab guru that he is and his infinite wisdom in able to troubleshoot.

Although I have been away from home for nearly 9 years (undergrad studies, masters, and now PhD), I have not felt I was ever away from home thanks to everyone I met during my PhD.

Abbreviations

3D	Three-dimensional
ADAMTS	A disintegrin and metalloproteinase with thrombospondin motifs
ANOVA	Analysis of variance
AP-1	Activator protein-1
APC	Adenomatous polyposis coli
APS	Ammonium persulphate
At	Annealing temperature
ATP	Adenosine triphosphate
BCA	Bicinchoninic acid
Bp	Base pair
BSA	Bovine serum albumin
Ca2+	Calcium
$CaCl_2$	Calcium chloride
CaMKII	Calcium calmodulin-dependent protein kinase II
cAMP	Cyclic adenosine monophosphate
cDNA	Complementary DNA
CILP	Cartilage intermediate layer protein
CO_2	Carbon dioxide
COMP	Cartilage oligomeric protein
CREB	Cyclic adenosine monophosphate response element binding protein
Ct	Threshold cycle
DAAM-1	Dishevelled associated activator of morphogenesis 1
DAG	Diacyl glycerol
DKK	Dickkopf
DMA	Dynamic mechanical analysis
DMEM	Dulbecco's Modified Eagle's Medium
DNA	Deoxyribonucleic acid
DVL	Dishevelled

ECL	Enhanced chemiluminescence
ECM	Extracellular matrix
FAK	Focal adhesion kinase
FITC	Fluorescein isothiocyanate
FZD	Frizzled
GAG	Glycosaminoglycans
GSK 3β	Glycogen synthase kinase 3β
HBSS	Hanks' Buffered Salt Solution
HRP	Horseradish peroxidase
IGD	Interglobular domain
IL-1β	Interleukin-1β
IP_3	Inositol 1, 4, 5-triphosphate
ITS	Insulin-transferrin-sodium selenium
JNK	C-Jun N-terminal kinase
LEF	Lymphoid enhancer-binding factor-1
LRP5/6	Low-density lipoprotein receptor-related protein 5/6
M	Molar
MAPK	Mitogen activated protein kinase
mM	Millimolar
mm	Millimeters
MMP	Matrix metalloproteinase
MPa	Megapascal
mRNA	Messenger ribonucleic acid
MT-MMP	Membrane-type matrix metalloproteinase
NaCl	Sodium chloride
NFκβ	Nuclear transcription factors nuclear factor kappa beta
NTPPHase	nucleotide triphosphate pyrophosphohydrolase
PBS	Phosphate buffered saline
PCP	Planar cell polarity

PCR	Polymerase chain reaction
PEA3	Polyomavirus enhancer A binding protein 3
PKC	Protein kinase C
PVDF	Polyvinylidene fluoride
qPCR	Quantitative polymerase chain reaction
RNA	Ribonucleic acid
ROCK	Rho-associated kinase
ROR	RAR-related orphan receptors
RPM	Revolutions per minute
rRNA	Ribosomal ribonucleic acid
SDS	Sodium dodecyl sulfate
SDS-PAGE	Sodium dodecyl sulphate-polyacrylamide gel electrophoresis
SEM	Standard error of the mean
SFRP	Secreted frizzled related-protein
siRNA	Small interfering RNA
SLRPs	Small leucine-rich proteoglycans
SNP	single nucleotide polymorphism
SZP	Superficial zone protein
TBS	Tris Buffered Saline
TBS-T	Tris Buffered Saline-Tween
TCF	T-cell factor
TEMED	Tetramethylethylenediamine
TIMP	Tissue inhibitors of metalloproteinase
TNFα	Tumour necrosis factor α
U	Unit
v/v	Volume per volume
w/v	Weight per volume
WIF	WNT-inhibitory factor
WISP-1	Wnt-1 induced secreted protein-1

Abstract:

Introduction:

WNT signalling is a major driving force in cartilage development, chondrocyte differentiation, and homeostasis. Due to its major role in cartilage homeostasis, deregulation of this pathway was suggested to be involved in the pathophysiology of osteoarthritis, which causes cartilage degeneration. Studies have identified mutations in inhibitors of WNT signalling in OA tissue in addition to up-regulation of related WNT components. However, these studies have focused on the end stage of the disease and have not factored in mechanical loading which is one of the main regulators of cartilage homeostasis.

Results:

Canonical WNT signalling was activated in response to both tensile and compressive loading. Furthermore, WNT signalling was observed to be differentially regulated in bovine cartilage explants in response to physiological (2.5MPa, 1Hz, 15 minutes) and degradative (7MPa, 1Hz, 15 minutes) compressive loading in a zone dependent manner as indicated by β-catenin nuclear translocation. Based on periods post-cessation of load, physiological and degradative loads have induced differential matrix gene expression. In addition, both loading regimes have shown differential regulation of WNT signalling components displaying more WNT signalling activation in degradative loading regime. DKK-1 and NFATC, WNT signalling components which have shown to have a role in cartilage homeostasis, have been chosen for functional analysis studies. Treatment of recombinant DKK-1 in combination with degradative load have shown that DKK-1 primarily inhibited canonical WNT signalling pathway, whereas treatment with NFAT inhibitor induced inhibition of both WNT signalling pathways. In addition, both treatments were observed to inhibit some of the load-induced matrix gene changes.

Conclusions:

WNT signalling is mechano-regulated in articular cartilage. The differential expression of WNT signalling components in response to different mechanical load regimes indicates a role for these components in maintaining cartilage homeostasis.

List of Figures:

Chapter 1

Chapter 2

Chapter 3

Chapter 4

Chapter 5

Chapter 6:

List of tables

Chapter 1

Chapter 2

Chapter 5

Chapter 6

Chapter 1:

Introduction

1.1 Articular cartilage

1.1.1 Function

Articular cartilage is an avascular, aneural and hypo-cellular tissue located at the ends of long bones to ensure reduced friction and smooth transition of force during movement. As a result of everyday motion, articular cartilage is subjected to compressive, hydrostatic, shear and tensile forces. Consequently, the composition and structure of articular cartilage is designed to withstand the forces transmitted, dispersing these forces across the entire joint. Articular cartilage tissue is primarily composed of a highly hydrated extracellular matrix (ECM) containing collagens, proteoglycans, and a single cell type, the chondrocyte, which regulates cartilage matrix turnover.

1.1.2 Structure

1.1.2.1 Cartilage zones

Cartilage zones are divided according to the variation in chondrocyte morphology and alignment, collagen fibril orientation and biochemical composition of the ECM (Figure 1-1) (Athanasiou et al., 2013). The four distinct zones are the superficial, middle, deep and calcified zones. The concentration and organisation of the ECM macromolecules within each layer provides different functional significance to maintain cartilage integrity in response to mechanical forces.

1.1.2.2 Superficial zone

In human cartilage, the uppermost 10-20% of the total volume of articular cartilage is categorised as the superficial zone (Pearle et al., 2005). The top layer of the superficial zone contains a single cell layer referred to as the lamina splendens which contains lubricin for smooth articulation (Kumar et al., 2001, Jones et al., 2007). The superficial zone consists primarily of densely packed type II collagen fibrils and elongated chondrocytes orientated in a parallel manner to the articulating surface (Figure 1-1). In addition, the superficial zone contains less proteoglycan content with respect to the deeper zones (Buckwalter et al., 2005). The orientation of the collagen fibrils provides resistance to tensile forces which the tissue is subjected to as a result of joint movement. Furthermore, the sheet of collagen acts as a barrier restricting transport of molecules in and out of cartilage (Buckwalter et al., 2005).

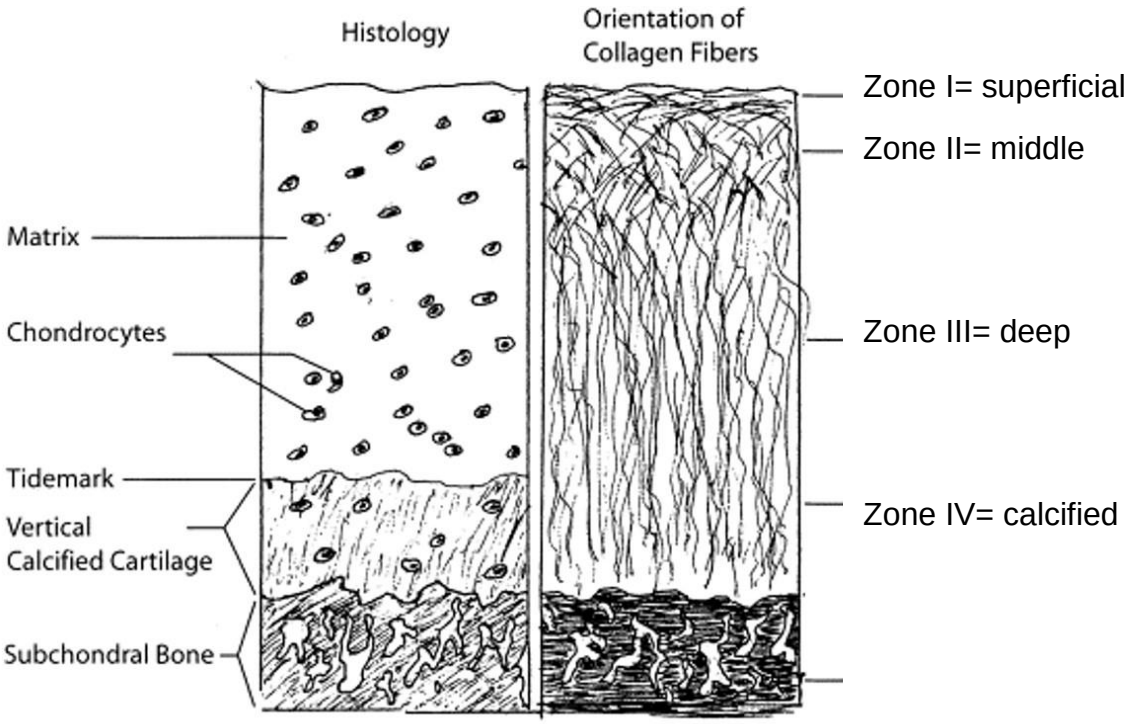

Figure 1-1: Illustration of full-depth articular cartilage histology showing the orientation of collagen fibrils throughout the different zones (Seal et al., 2001).

1.1.2.3 Middle zone

The middle zone comprises the bulk of the human articular cartilage volume (40-60%) (Pearle et al., 2005). Chondrocytes present are spherical in shape and have an abundance of organelles, endoplasmic reticulum and Golgi membranes, which support anabolic processes (Buckwalter et al., 2005). As a result, chondrocytes are able to synthesise a matrix containing an abundant proteoglycan content and thicker collagen fibrils (Buckwalter et al., 2005). Collagen fibrils in this zone are organised as an arcade-like structure and are referred to as the "Benninghoff Arcades" (Eyre, 2002, Benninghoff, 1925). The composition of this matrix enables resistance against compressive loading.

1.1.2.4 Deep zone

The deep zone encompasses 30-40% of the total human cartilage volume. Chondrocytes are arranged in columns and are parallel to the collagen fibrils and perpendicular to the articulating surface (Figure 1-1) (Pearle et al., 2005) The matrix in this layer contains large diameter collagen fibrils, the highest concentration of proteoglycans and lowest concentration of water (Pearle et al., 2005). The collagen fibrils present are organised in large bundles orientated in a perpendicular manner to the articulating surface (Athanasiou et al., 2013). The high proteoglycan concentration in the deep zone allows maximal resistance to compressive forces (Roughley, 2006).

1.1.2.5 Calcified zone

A basophilic line referred to as the tidemark differentiates the calcified zone from the deep zone. In the calcified zone, chondrocytes are smaller in size and have a relatively low metabolism as indicated by the limited number of synthetic organelles (Buckwalter et al., 2005). The calcified zone has a significant role in anchoring cartilage to bone thus allowing the transition of mechanical load across the joint (Oegema et al., 1997). The attachment of cartilage to the subchondral bone is facilitated by the calcified zone fastening of collagen fibrils from the deep zone to the subchondral bone (Eyre and Wu, 2005).

1.1.3 Cartilage composition

1.1.3.1 Chondrocytes

Chondrocytes are the only specialised resident cell type in cartilage tissue and comprises approximately 1% of the volume of adult human articular cartilage (Buckwalter et al., 2005). The phenotype of a chondrocyte is variable based on which zone the chondrocyte is residing (Lee et al., 1998). However, despite the variation in the phenotype of chondrocytes, all chondrocytes possess the necessary machinery (synthetic organelles) to synthesise a specialised matrix to maintain cartilage homeostasis (Buckwalter et al., 2005). The constituents of this specialised matrix and the organisation of these constituents determines the mechanical properties of articular cartilage. Some of the main constituents of the matrix include collagens, non-collagenous proteins and proteoglycans. The correct form and quantity of the previously mentioned macromolecules must be produced and structured into the appropriate framework for normal joint mobility and function (Buckwalter et al., 2005). In order for the chondrocyte to be able to synthesise the appropriate matrix composition to replace the degraded matrix components, it needs to be able to detect modifications in the biochemical composition of the ECM (Buckwalter et al., 2005, Goldring and Marcu, 2009). The ECM provides biochemical and biomechanical cues which chondrocytes are able to perceive and respond appropriately to synthesise the required macromolecules to sustain tissue integrity (Allen et al., 2012, Melrose and Whitelock, 2006).

1.1.3.1.1 Primary cilia

The primary cilium is a microtubule-based cellular organelle that projects from cells into the ECM (Irianto et al., 2014). The primary cilium is mechanosensitive, and the location of these primary cilia on chondrocytes allows their interaction with collagen fibres allowing them to sense deformation resulting from mechanical load (Wann et al., 2012). Furthermore, the primary cilia were demonstrated to regulate ECM synthesis in response to a mechanical stimulus via calcium signalling mediated by ATP release (Wann et al., 2012). The presence of primary cilia was shown to be integral for cartilage homeostasis as chondrocytes with depleted numbers of primary cilia exhibited enhanced expression of markers associated with ECM catabolism (Irianto et al., 2014).

1.1.3.2 Collagen

Collagen comprises 60% of the dry weight of articular cartilage and is the most abundant matrix macromolecule (Eyre, 2002). The structure of a collagen molecule is composed of three polypeptide chains which intertwine to form a triple helix, however the role, size and distribution is variable, dependent on collagen type and the localisation of the collagen molecules in the tissue (Gelse et al., 2003). Several collagen types are present in cartilage tissue mainly types II, VI, IX, X and XI (Buckwalter et al., 2005); small quantities of collagen types I and III have also been detected in the superficial zone of cartilage (Eyre, 2002, Wardale and Duance, 1993). However, collagen type II accounts for 90% of the collagens in articular cartilage (Eyre, 2002, Pearle et al., 2005).

Type II collagen is classified as a fibril-forming collagen, where it self-assembles in a quarter staggered arrangement to form fibrils (Gelse et al., 2003). The distribution of type II collagen throughout the depth of the tissue provides cartilage with a structural scaffold with the biomechanical properties to withstand both compressive and tensile strains (Gelse et al., 2003).

Type VI collagen, a microfibrillar collagen, is mainly localised around the perimeter of chondrocytes and is interspersed within the spaces of the collagen framework (Eyre, 2002, Duance et al., 1998). It is suggested to have a role in attaching chondrocytes to the matrix, associating matrix macromolecules to each other and stabilising fibril bundles (Hagiwara et al., 1993).

The other minor collagens, type IX and XI, have a role in associating with and regulating the diameter of type II collagen fibrils (Eyre, 2002). In addition, the interaction of these collagens with the type II collagen is stabilised by the cross-linking mechanism mediated by lysyl oxidase (Eyre and Wu, 2005). The cross-linking of these collagens is essential to reinforce the collagen network against the effects of repetitive mechanical loading and injury (Eyre and Wu, 2005).

The other type of collagen found in cartilage is type X, and expression is restricted to the calcified zone. This localisation has suggested a potential role

for type X collagen in matrix mineralisation and endochondral ossification (Gelse et al., 2003).

1.1.3.3 Non-collagenous proteins

1.1.3.3.1 Proteoglycans

Proteoglycans are comprised of a protein core with covalently bonded polysaccharide chains known as glycosaminoglycans (GAG). GAGS contain repeating disaccharide blocks of *N*-acetylglucosamine or *N*-acetylgalactosamine and an uronic acid (Esko et al., 2009). The GAGs present in cartilage include chondroitin sulphate, dermatan sulphate and keratan sulphate (Buckwalter et al., 2005). Proteoglycans resist compressive forces through hydration of the tissue by creating an osmotic pressure derived from the negative charge of the GAGs (Chahine et al., 2005). In cartilage there are two classes of proteoglycans, the large aggregating proteoglycans and small non-aggregating proteoglycans.

1.1.3.3.1.1 Large aggregating proteoglycan of articular cartilage

Aggrecan, a large aggregating proteoglycan, is the predominant structural proteoglycan in articular cartilage. One of the main functions of aggrecan is to provide resistance to compressive loading to maintain cartilage integrity. The mobility of aggrecan is limited due to its large size, contributed by its GAG chains and aggregation with hyaluronan - a non-sulphated GAG, which results in it being entrapped within the collagen meshwork (Kiani et al., 2002, Roughley, 2006). The negatively charged chondroitin and keratan sulphate chains attract cationic ions e.g. sodium, calcium, thus creating an imbalance in ionic concentration relative to the surrounding tissues (Kiani et al., 2002). The difference in ionic concentration and the entrapment of aggrecan within the collagen results in hydration of the tissue (Buschmann et al., 1996). As water causes the expansion of the matrix, the tissue becomes resistant to deformation (Kiani et al., 2002). The stabilisation of aggrecan aggregates is facilitated by link protein, a small glycoprotein (Figure 1-2) (Kiani et al., 2002). Structurally aggrecan is a multi-modular molecule containing three globular domains termed G1, G2 and G3 (Figure 1-3). Aggrecan exists in cartilage as aggregates through non-covalent bonding with hyaluronan and the aggrecan G1 domain (Aspberg, 2012). Anchorage of the aggrecan aggregates to the matrix is mediated through the G3 domain (Aspberg, 2012).

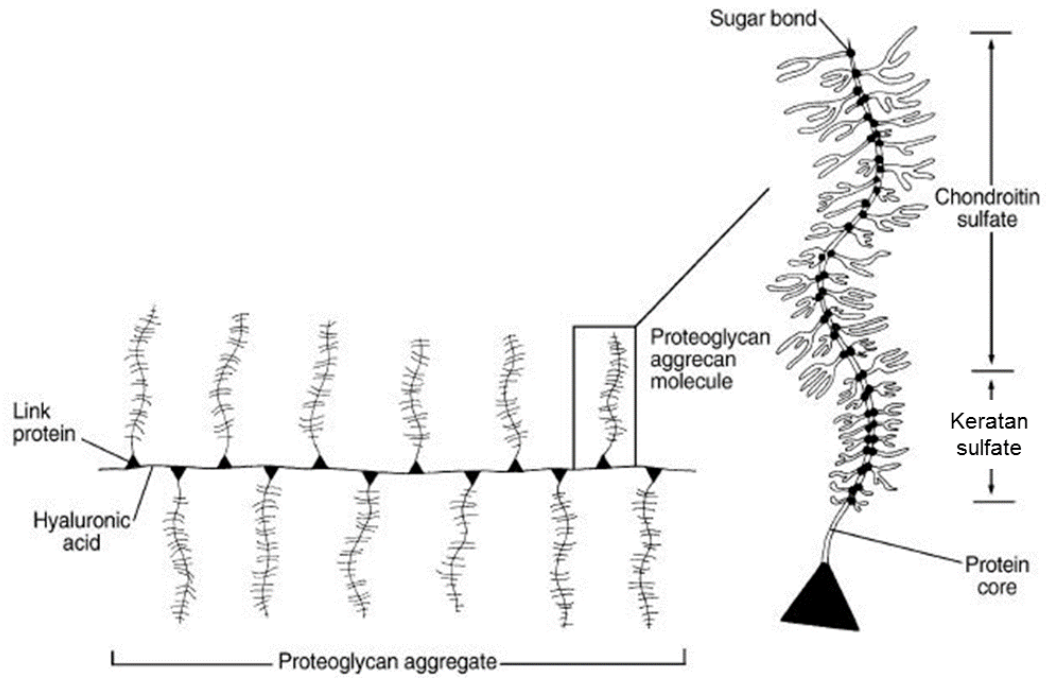

Figure 1-2: Schematic diagram of proteoglycan aggregates.

Diagram illustrates the structure and composition of proteoglycan aggregates and an individual aggrecan monomer (Pearle et al., 2005).

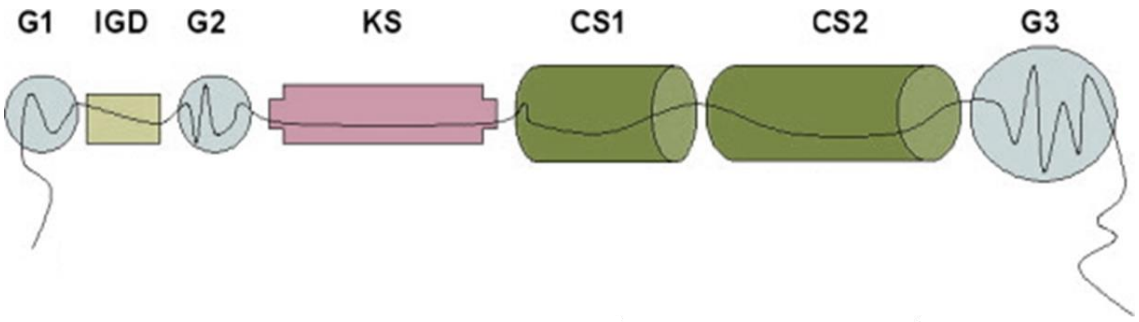

Figure 1-3: Illustration of the globular domains of aggrecan. Aggrecan has three globular domains (G1-G3) which are separated by an interglobular domain (IGD) and regions of keratan sulphate (KS) or chondroitin sulphate (CS) rich regions (Garvican et al., 2010).

1.1.3.3.1.2 Small non-aggregating proteoglycans

1.1.3.3.1.2.1 Small leucine rich proteoglycans

Small leucine-rich proteoglycans (SLRPs) form an integral component of the cartilage ECM. The main structural components of SLRPs are the protein core and the glycosaminoglycan chains, whose number and type varies between members (Dellett et al., 2012). Members of SLRPs are characterised structurally by several repeats of leucine residues at conserved regions (Heinegard, 2009). The SLRPs are classified according to the number of leucine-rich repeats and the type of GAG attached (Roughley, 2006). In cartilage, the first sub-family of SLRPs which include biglycan and decorin are categorised as class I. Biglycan and decorin contain 12 leucine-rich repeats and have either dermatan sulphate or chondroitin sulphate chains (Dellett et al., 2012). The second class of SLRPs found in cartilage comprise fibromodulin, lumican and keratocan. All three SLRPs contain 12 leucine-rich repeats and have keratan sulphate chains (Dellett et al., 2012).

SLRPS have multiple regulatory functions which contribute to maintaining cartilage homeostasis. In cartilage, SLRP members were found to associate with matrix macromolecules, such as collagens, through their protein core to regulate the spatial organisation, proteolytic degradation and diameter of collagen fibrils (Dellett et al., 2012). Class I SLRPs were found to associate with collagen type VI via their core protein and orchestrate the assembly of collagen and act as a platform for further interactions with other components in the matrix (Heinegard, 2009). Similarly, class II SLRPs bind to fibrillar collagen through their leucine-rich repeats (Heinegard, 2009). Furthermore, studies have shown that SLRPs directly regulate multiple signalling pathways by interacting with the ligands or receptors associated with the activation of these pathways (Dellett et al., 2012). SLRPs have a wide affinity for various growth factors, cytokines and signalling molecules. For instance, decorin is able to associate with insulin-like growth factor receptor, transforming growth factor-β and Wnt-1 induced secreted protein-1 (WISP-1) (Dellett et al., 2012). As a result of such modulations, SLRPs are able to regulate several cellular processes such as cell differentiation, growth survival and adhesion (Dellett et al., 2012).

1.1.3.3.1.3 Glycoproteins

Glycoproteins in articular cartilage are present to support and maintain the organisation of the matrix. Examples of glycoproteins present in cartilage include link protein, cartilage oligomeric matrix protein (COMP), cartilage intermediate layer protein (CILP), annexin V and matrilins. One of the integral roles of link protein in cartilage is to facilitate the formation and stabilisation of aggrecan aggregates (Roughley, 2006). Link protein promotes the formation of aggregates by inducing a conformational change in the G1 domain of aggrecan which enhances the ability of aggrecan monomers to associate with hyaluronan (Roughley, 2006). COMP is primarily expressed in cartilage tissue, however it is expressed in other tissues which are subjected to mechanical load (Heinegard, 2009). One of the main functions of COMP in developing cartilage is catalysing fibril formation. Due to the minimal turnover of type II collagen in adult cartilage, COMP is suggested to maintain the structural integrity of the collagen network (Heinegard, 2009). However, an elevated expression of COMP was demonstrated to dysregulate collagen fibrillogenesis thus supporting its role in modulating fibril formation (Heinegard, 2009). Annexin V, also known as anchorin CII, is found to be localised at the chondrocyte surface. Due to its localisation, its role was suggested to be securing chondrocytes to the matrix through association with type II collagen (Mollenhauer et al., 1999). Furthermore, annexin V is involved in regulating calcium influx into matrix vesicles resulting in matrix mineralisation, and influx into the cytoplasm resulting in cell death (Ea et al., 2008).

Other non-collagenous structural proteins which have been identified in cartilage include tenascin-C, fibronectin, cartilage intermediate layer protein (CILP) and superficial zone protein (SZP). The expression of the protein tenascin-C is altered in response to tissue injury and repair (Chiquet et al., 1996). Studies have revealed tenascin-C fragments as possible endogenous inducers of cartilage degradation in disease state (Sofat et al., 2012). Fibronectin has a role in mediating cell-matrix interactions through anchoring chondrocytes to the matrix (van der Kraan et al., 2002). Fibronectin has the ability to bind to multiple matrix macromolecules such as SLRPs and collagens (Martin and Buckwalter, 1998). Similar to tenascin-C, fragments of fibronectin were observed to promote

cartilage degradation and were observed to be elevated in diseases of cartilage degeneration such as osteoarthritis (Roughley, 2001).

CILP was found to be highly expressed in the middle to deep zones of cartilage (Yao et al., 2004). The carboxy terminus of CILP contains a region that is homologous to nucleotide triphosphate pyrophosphohydrolase (NTPPHase) (Yao et al., 2004). The hypothesised role of NTPPHase enzyme in cartilage is to facilitate the formation of calcium pyrophosphate dihydrate due to its parallel expression (Hirose et al., 2000). Calcium pyrophosphate dihydrate was found to accumulate in osteoarthritic tissue promoting articular cartilage degradation (Derfus et al., 1998). Furthermore, CILP was up-regulated with ageing and in cartilage degenerative diseases like osteoarthritis (Yao et al., 2004). SZP, otherwise known as lubricin, is a proteoglycan which is produced by chondrocytes at the superficial layer of articular cartilage and is secreted into synovial fluid (Iwakura et al., 2013). The hypothesised role of SZP is to reduce friction and therefore mediate smooth articulation of the joint (Neu et al., 2007). Furthermore, SZP promotes adhesion of molecules to the matrix and cell proliferation (Iwakura et al., 2013).

Matrilins are one of the non-collagenous proteins in cartilage which contribute to the organisation and maintenance of the integrity and function of the tissue (Heinegard, 2009). Some of the roles of matrilins include mediating interactions between matrix macromolecules, promoting matrix assembly and matrix degradation (Klatt et al., 2011). All 4 members of the matrilin family are expressed in cartilage. Matrilin-1 and matrilin-3 are the predominant matrilin members in cartilage, whereas matrilin-2 and matrilin-4 are more ubiquitously expressed (Klatt et al., 2011). In cartilage, these proteins are suggested to act as adaptors in facilitating matrix assembly. Matrilin-1, -3 and -4 were found to associate and form complexes with SLRPs which provide anchorage to other matrix macromolecules such as type II collagen or aggrecan (Klatt et al., 2011). Furthermore, it has been reported that matrilins have a role in mechanotransduction; it was suggested that the alteration in matrilin content, specifically matrilin-1 and -3, in the matrix surrounding the chondrocytes can modify the mechano-response of chondrocytes (Kanbe et al., 2007).

1.2 Cartilage turnover

In order to maintain cartilage homeostasis, chondrocytes maintain the balance between catabolic and anabolic processes. Catabolic events in cartilage are primarily mediated by the disintegrin and metalloproteinase with thrombospondin motifs family and the matrix metalloproteinase family of proteolytic enzymes.

1.2.1 A disintegrin and metalloproteinase with thrombospondin motifs family

Aggrecan turnover is mediated by members of the A disintegrin and metalloproteinase with thrombospondin motifs (ADAMTS) family, primarily ADAMTS-4 and ADAMTS-5 in articular cartilage (also referred to as aggrecanase-1 and aggrecanse-2 respectively) (Bondeson et al., 2008). ADAMTS structure includes a signal peptide, a prodomain, a disintegrin domain, a metalloproteinase domain, a thrombospondin type I motif and a spacer domain; a second thrombospondin domain is only present in ADAMTS-5 (Figure 1-4). The ancillary domains of these enzymes modulate substrate specificity and proteolytic activity (Kashiwagi et al., 2004).

ADAMTS-4 and ADAMTS-5 have multiple cleavage sites along the chondroitin sulphate-2 domain of aggrecan (Nagase and Kashiwagi, 2003). The most integral cleavage site which has pathological relevance and is characterized as a mark of aggrecanase activity is at glutamate 373 - alanine 374 in the IGD (Troeberg and Nagase, 2012). Cleavage at this site results in the release of the fragment where the majority of the GAG chains are attached, thus nullifying the contribution of the aggrecan molecule to maintaining cartilage homeostasis (Troeberg and Nagase, 2012). Consequently, ADAMTS-4 and ADAMTS-5 are tightly modulated through post-translational processing as a result of their effects on cartilage homeostasis (Nagase and Kashiwagi, 2003).

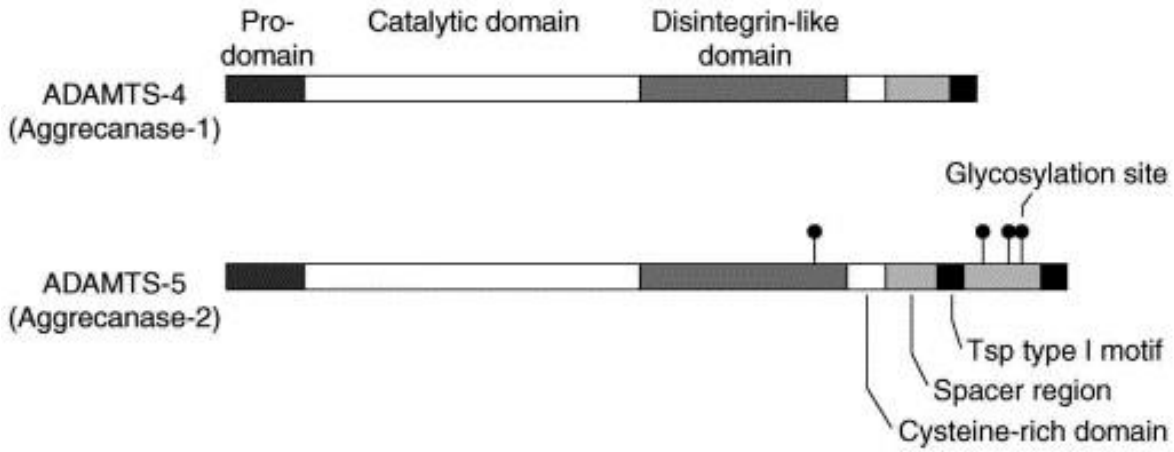

Figure 1-4: Catalytic and ancillary domain organisation of ADAMTS-4 and ADAMTS-5. Key: Tsp= thrombospondin (Arner, 2002).

1.2.2 Matrix metalloproteinases

Matrix metalloproteinases (MMPs) are a major family of multi-domain zinc-dependent enzymes which facilitate ECM turnover (Chakraborti et al., 2003). Although historically MMPs are recognised simply as degradative enzymes of matrix constituents, recent studies have shown that through the degradation of such constituents, alterations occur between cell-matrix and cell-cell interactions (Nagase et al., 2006). As a consequence of matrix degradation, growth factors and other bioactive molecules are released, thus resulting in altered cell metabolism (Nagase et al., 2006). There are 23 different MMPs in the human genome, however they share some common structural features including a signal peptide, a pro-peptide, a catalytic metalloproteinase domain, a hinge region and a hemopexin domain (Figure 1-5) (Nagase et al., 2006). The pro-peptide is responsible for the dormancy of MMPs. This domain contains a conserved sequence motif known as the “cysteine switch” and this cysteine residue interacts with a zinc ion present in the catalytic domain to maintain enzyme latency (Chakraborti et al., 2003). This interaction prevents the binding of a water molecule to the catalytic zinc ion, present in the catalytic domain, required for MMP activation to occur (Murphy et al., 2002). Binding of a substrate is dictated by the structure of the active site of the MMP and a hydrophobic pocket termed “S1 pocket” (Murphy and Nagase, 2008). The hinge domain is believed to confer MMP specificity by manipulating the positioning of the catalytic and hemopexin domain (Ganea et al., 2007); it does this partly due to the presence of proline residues which confers some structural rigidity in this region (Murphy and Nagase, 2008). The hemopexin domain is suggested to control substrate specificity (Ganea et al., 2007) and is integral in MMPs which cleave collagens (Murphy and Nagase, 2008). Members of the MMP family are assembled into sub-families based on their domain arrangement and substrate specificity. MMPs are categorised as collagenases, gelatinases, stromelysins, matrilysins, membrane-type MMPs and a category for other MMPs which do not conform with these categories (Nagase et al., 2006); many of these MMPs have been detected in articular cartilage (Table 1-1).

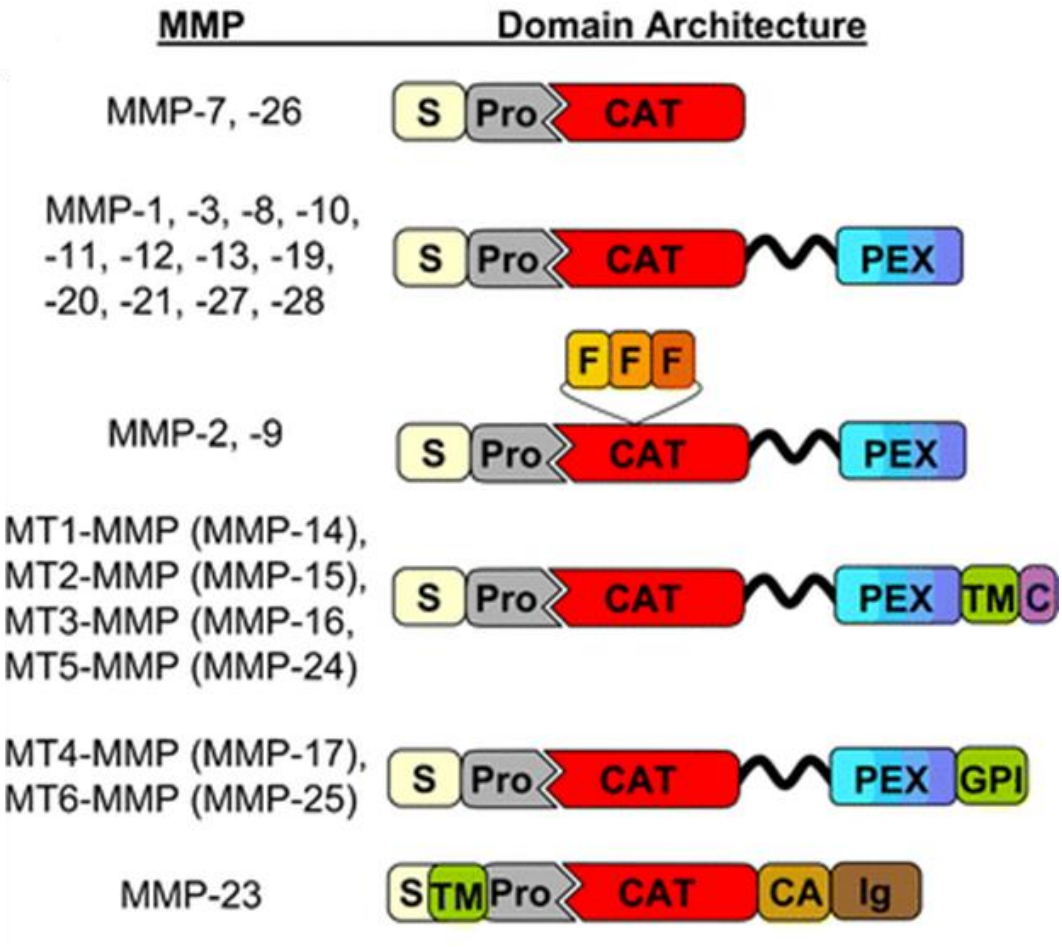

Figure 1-5: MMP domain organisation.
Key: S=signal peptide; Pro= pro-peptide; CAT= catalytic domain; F= fibronectin repeats; PEX= hemopexin domain; TM= transmembrane domain; GPI= glycophosphatidylinositol membrane anchor; C= cytoplasmic domain; CA= cysteine array; Ig= immunoglobulin-like domain.

Table 1-1: Properties and known substrates of those MMPs which have been detected in articular cartilage, adapted from (Murphy et al., 2002).

MMP	Enzyme	M_r latent	M_r active	Known substrates
MMP-1	Interstitial collagenase	55,000	45,000	Collagens I, II, III, VII, VIII, and X, gelatin, aggrecan, versican, protein link protein, casein, α_2-M, pregnancy zone protein, ovostatin, nidogen, MBP, proTNF, L-selectin, proMMP-2, proMMP-9
MMP-2	Gelatinase A	72,000	66,000	Collagens I, IV, V, VII, X, XI and XIV, gelatin, elastin, fibronectin, aggrecan, versican, proteoglycan link protein, MBP, proTNF, α1-proteinase inhibitor, proMMP-9, proMMP-13
MMP-3	Stromelysin-1	57,000	45,000	Collagens III, IV, IX and X, gelatin, aggrecan, versican, perlecan, nidogen, proteoglycan link protein, fibronectin, laminin, elastin, casein, fibrinogen, antithrombin-III, α2M, ovostatin, α1-proteinase inhibitor, MBP, proTNF, proMMP-1, proMMP-7, proMMP-8, proMMP-9, proMMP-13
MMP-8	Neutrophil collagenase	75,000	58,000	Collagens I, II, III, V, VII, VIII and X, gelatin, aggrecan, α1-proteinase (collagenase-2) inhibitor, α2-antiplasmin, fibronectin
MMP-9	Gelatinase B	92,000	86,000	Collagens IV, V, VII, X and XIV, gelatin, elastin, aggrecan, versican, proteoglycan link protein, fibronectin, nidogen, α1-proteinase inhibitor, MBP, proTNF
MMP-13	Collagenase-3	60,000	48,000	Collagens I, II, III and IV, gelatin, plasminogen activator inhibitor 2, aggrecan, perlecan, tenascin
MMP-14	MT1-MMP	66,000	56,000	Collagens I, II and III, gelatin, casein, elastin, fibronectin, laminin B chain, vitronectin, aggrecan, dermatan sulfate proteoglycan, MMP-2, MMP-13, proTNF
MMP-15	MT2-MMP	72,000	60,000	proMMP-2, gelatin, fibronectin, tenascin, nidogen, laminin
MMP-16	MT3-MMP	64,000	52,000	proMMP-2
MMP-17	MT4-MMP	57,000	53,000	?

1.2.3 Tissue inhibitors of metalloproteinases

Regulation of MMP and ADAMTS activities in cartilage is primarily controlled by the tissue inhibitors of metalloproteinases (TIMPs). TIMPs (TIMP-1, TIMP-2, TIMP-3 and TIMP-4) are endogenous MMP inhibitors which regulate their activity during tissue remodelling and matrix turnover (Brew and Nagase, 2010). The levels of TIMPs are regarded to be vital in maintaining homeostasis due to their direct effect on MMP activity (Visse and Nagase, 2003). Although TIMPs can inhibit almost all MMPs and ADAMTSs, the efficiency at which it inhibits an MMP or ADAMTS is variable (Bourboulia and Stetler-Stevenson, 2010, Brew and Nagase, 2010). The structure of TIMPs consist of N and C-terminal subdomains, in which each subdomain comprises three disulphide bonds (Nagase et al., 2006). Inhibition by TIMPs is facilitated through its amino-terminal where it binds to the active site of MMPs (Murphy, 2011). The efficiency of TIMP inhibition of MMPs is determined by the wedge shaped ridge at the amino-terminal which binds to the active site of the MMP (Murphy, 2011).

1.3 Biomechanical properties and function of cartilage

The biomechanical properties of articular cartilage tissue are governed by the major constituents of its ECM, namely proteoglycans and collagens. These components provide resistance to loads which cartilage are exposed to as a result of everyday movement. The loads or stresses which cartilage is exposed to include tension, compression, shear, and hydrostatic stress, as summarised in Figure 1-6. Tensile load is the application of a pulling force resulting in the stretching of cartilage and it becoming longer and thinner (Watkins, 2014). Compressive stress is defined as the ratio of the force applied to the cross-sectional area (where the units of stress are N/m^2). When a stress is applied, the tissue is subjected to deformation and experiences a change in length/height i.e. becomes shorter and wider (Watkins, 2014). This change in length/height relative to the original length/height is defined as compressive strain (strain has no units). Stress is proportional to strain and is defined by a constant called Young's modulus (E). Once the force is removed from cartilage, the tissue returns to its original dimensions, and therefore cartilage is considered to have viscoelastic properties. The degree of deformation will depend on whether the shape change is constrained by attachment to subchondral bone. One of the functions of

cartilage is to reduce contact stress to the underlying bone by increasing the contact area. This is achieved due to the ability of cartilage to deform more than bone (Sokoloff, 2014).

When an articulating joint is subjected to load, cartilage deformation results in interstitial fluid flow through the ECM; this generation of fluid movement is defined by fluid-induced shear stresses (Watkins, 2014, Kerr, 2010). Furthermore, shear stresses can be exerted due to friction induced by the extent of joint lubrication and amount of contact stress at the tissue surface under compressive load. In addition, mechanical loading induces the generation of hydrostatic pressure. Hydrostatic pressure occurs due to the restriction of fluid flow within the tissue (Kerr, 2010, Lee et al., 2005a).

Properties of the cartilage ECM are governed by the chemical structure and physical interactions of the proteoglycan aggregates (Ratcliffe and Mow, 1996). These macromolecules have an abundance of negatively charged sulphate and carboxylate groups, creating a high concentration of fixed negative charges which contribute to the strong intra- and intermolecular charge-charge repulsive forces within the tissue, referred to as the Donnan osmotic pressure (Donnan, 1924, Buschmann et al., 1995). These repulsive forces extend and stiffen the proteoglycan macromolecules within the surrounding collagen network. However, this repulsion generated by the sulphate and carboxylate groups on the proteoglycans is counter-balanced by the attraction of positively charged ions (mainly Na^+, Ca^{2+} and Cl^-) into the cartilage to maintain electro-neutrality. The net effect of this attraction of cations into the matrix is a swelling pressure (determined by the Donnan osmotic pressure law), which is resisted by tension conferred by the collagen network (Maroudas, 1976, Mow and Ratcliffe, 1997). As a consequence of this swelling pressure, the collagen network is subjected to a “pre-stress” even in the absence of external mechanical loads (Setton et al., 1995 referred to in Mow and Hung, 2001). Due to the inhomogeneous distribution of proteoglycans through the depth of the cartilage ECM, the cartilage is exposed to inhomogeneous swelling also. When subjected to mechanical compression, this external stress causes an internal pressure in the cartilage ECM to exceed that of the swelling pressure, hence fluid is expelled. As the fluid is expelled, the concentration of proteoglycans increases sufficiently

to increase the Donnan osmotic swelling pressure and bulk compressive stress until equilibrium is met with the external stress (Mow and Hung, 2001) (Mow and Hung, 2001). Collectively, the physicochemical properties of the proteoglycans entrapped within the collagen network protects the cartilage against high levels of stress and strain developing in the ECM, facilitating its ability to resist compression. Hence, the interactions of the cartilage proteoglycan and collagen networks are of huge significance for maintaining mechanical functionality.

However, when cartilage is subjected to a load, zone-dependent responses are observed (Wong et al., 1997). This is due to the variation in the organisation, composition and quantity of ECM macromolecules within the cartilage tissue zones. This is suggested to be an adaptive mechanism to the loads applied. It is widely accepted that mechanical loading within the physiological range induces matrix synthesis to maintain tissue integrity (Kiviranta et al., 1988). Although it is known that the superficial zone undergoes the highest magnitude of stress, analysis of zonal chondrocyte subpopulations demonstrate distinct levels of metabolic activities in response to mechanical stimuli (Lee et al., 1998). The variation in response in intact cartilage is known to be attributed to the differences in the degree chondrocytes are deformed as a result of the variation in chondrocyte stiffness between zonal chondrocyte subpopulations (Lee et al., 1998). However, it was demonstrated that the application of mechanical load on chondrocytes isolated from each zone cultured separately in agarose constructs have maintained distinct metabolic responses (Lee et al., 1998). For example, the application of mechanical compression at a frequency of 1 Hz inhibited glycosaminoglycan synthesis in the superficial zone whereas it was induced in the deep zone (Lee et al., 1998).

Mechanical loading is one of the principal regulators of cartilage turnover and homeostasis. In the absence of such mechanical forces cartilage tissue will atrophy (Palmoski and Brandt, 1981). In response to moderate levels of mechanical loading, articular cartilage is able to adapt to the load it is subjected to by inducing an anabolic response and suppressing the catabolic reaction (Yokota et al., 2011). This is reflected in areas which are subjected to high levels of mechanical stress such as femoral condyles where the matrix in that area contains a highly organised collagen network to maintain tissue integrity

(Arokoski et al., 2000). Therefore, disuse or excessively high mechanical loads result in articular cartilage degradation (Millward-Sadler and Salter, 2004). Over the past decades, many studies have been conducted on articular cartilage, both *in vivo* and *in vitro*, to elucidate the mechanism(s) of action arising from the tissue's response to mechanical load, and how this can initiate cartilage degeneration.

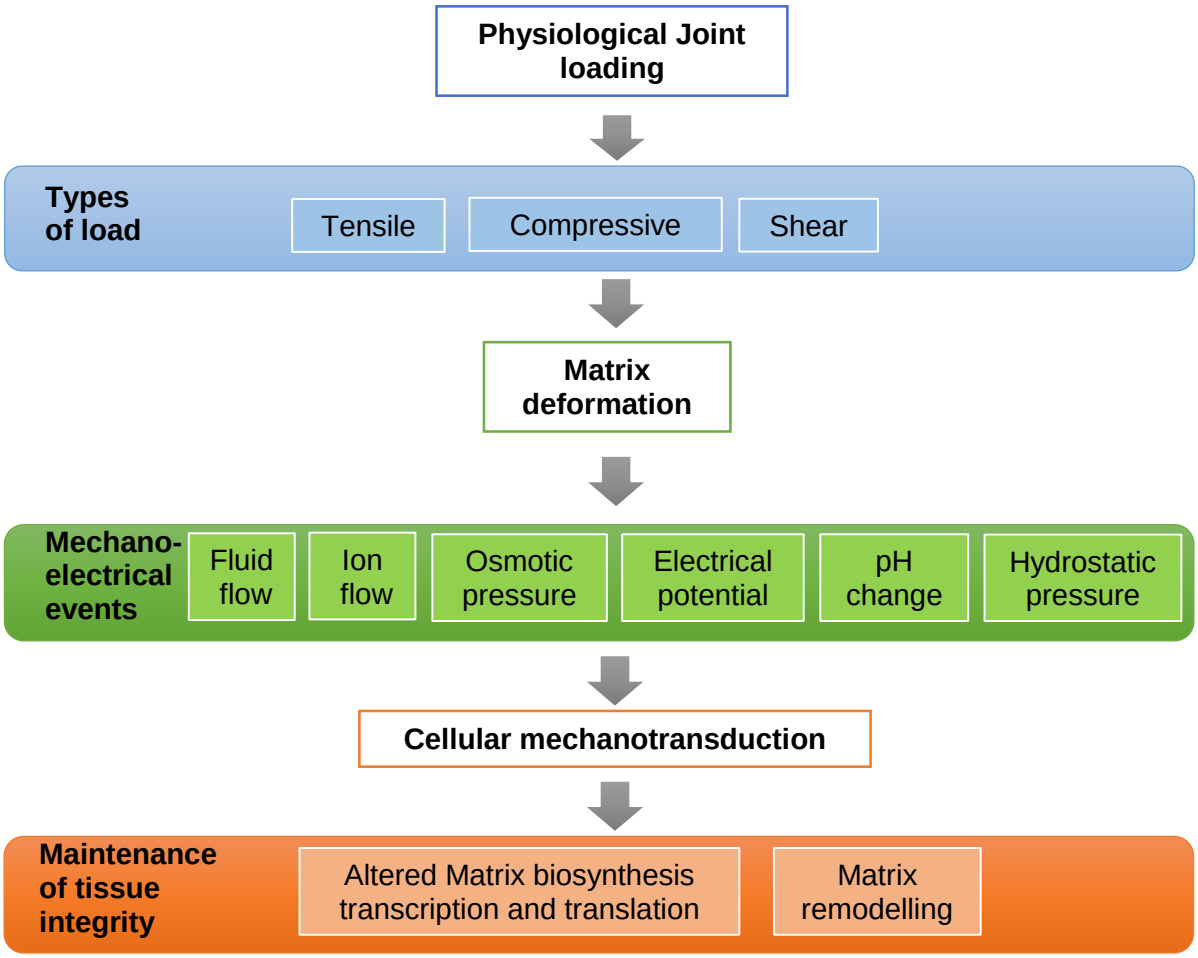

Figure 1-6: Illustration of the types of loads which are exerted upon the joint and the mechano-electrical events involved which lead to the maintenance of cartilage tissue integrity.

1.3.1 *In vivo* studies on the effect of mechanical loading on cartilage

Several early *in vivo* studies have shown that joint motion in the absence of mechanical loading is not sufficient to maintain homeostasis (Palmoski et al., 1980, Kiviranta et al., 1987). This is reflected in a study examining the effect of load bearing exercises in hamsters. The study demonstrated that the group of inactive hamsters had reduced proteoglycan levels in the cartilage as well as a lower synovial fluid volume (Otterness et al., 1998). The observed alteration in the matrix is contributed to by cartilage fibrillation and fissuring. In contrast, the group of active hamsters which had undergone daily wheel running exercises (6-12km/day) were protected against such damage and had normal articular cartilage (Otterness et al., 1998). Furthermore, a study using canines to examine the effects of physical exercise by running for 1 hour, five days a week for 15 weeks showed increased cartilage thickness and in regions bearing the highest amplitude of load stimulated a local alteration in cartilage composition (Kiviranta et al., 1988). In addition, there was differential zonal expression of GAGs. Most of the up-regulation in GAG expression was observed in the intermediate and deep zones only (Kiviranta et al., 1988). Physiological loads using young rabbits was shown to have contributed to the maturation process of matrix proteins and improved collagen network integrity (Julkunen et al., 2010); the collagen fibril network was observed to have undergone maturation-related changes as assessed by collagen fibril orientation in response to load. During the maturation process, the collagen network slowly develops as it adapts to the load it is exposed to. It has been suggested that the collagen network may play a role in chondrocyte deformation and thus modulate cellular metabolic responses and maintain cartilage homeostasis (Julkunen et al., 2010). Similar observations were made in foals, where exposure to mechanical loading at a young age led to the maturation of matrix components (van Weeren et al., 2008). In addition to compressive load, studies have proposed that cartilage tissue induces mechanotransduction responses via stimulation from interstitial fluid flow. The resulting biosynthetic response is suggested to be associated with the shear-induced deformation of chondrocytes (Jin et al., 2001).

1.3.2 *In vitro* studies on the effect of mechanical loading on cartilage

In vitro studies investigating the effect of mechanical load on chondrocytes have been conducted using either a monolayer or three-dimensional (3D) cell culture system, or cartilage explants. The benefit of these *in vitro* systems is that the cellular response to a mechanical stimulus and the signalling pathways involved as a result are easier to elucidate as it removes the interference and responses of the surrounding tissues that occur *in vivo*.

Studies using a monolayer system involved seeding chondrocytes onto flexible tissue culture plates and fluid-induced shear, tensile stretch or pressure-induced strain was applied. GAG synthesis was increased in bovine chondrocytes exposed to fluid-induced shear stress (200 revolutions per minute, 24 hours), and this increase was suggested to be as a result of nitric oxide and G protein dependent pathways (Das et al., 1997). Furthermore, it was demonstrated that cells have a differential response to the magnitude and frequency of stress applied. For example, in response to the application of a low frequency tensile strain (10 cycles/ hour, 5% elongation), bovine chondrocytes displayed an up-regulation in proteoglycan synthesis, whereas high magnitude and frequency (10 cycles/minute, 17% elongation) had the opposite effect (Fukuda et al., 1997). Similar results were also observed in studies using cyclic pressure-induced strain, whereby human chondrocytes exposed to pressure pulses of 1 atmosphere (0.33Hz, 20 minutes) had enhanced proteoglycan synthesis and down-regulation of MMP-3 via integrin and interleukin-4 signalling (Millward-Sadler et al., 2000). Collectively, these studies reflect the necessity for moderate loading to maintain cartilage homeostasis, however beyond a specific loading threshold the cellular response becomes catabolic.

An alternative method of assessing cellular responses to mechanical stimuli is through the use of 3D cell cultures whereby chondrocytes are seeded in agarose. The benefit of this method is that chondrocytes are suspended in a 3D environment where over time the matrix synthesised by these cells shows a similar composition to native cartilage. The cells can also be maintained in culture for long periods without loss of phenotypic stability which can occur in monolayer systems (Buschmann et al., 1992, Hauselmann et al., 1994). As observed previously in the monolayer systems, application of 15% dynamic compressive

load (1Hz, 48 hours) on agarose-chondrocyte (chondrocytes isolated from bovine cartilage) constructs induced proteoglycan synthesis, however very low (0.3Hz) or high (3Hz) frequencies inhibited proteoglycan synthesis (Lee and Bader, 1997). Similarly, Mauck et al demonstrated significant up-regulation of total GAG and collagen content as an outcome of 10% compressive strain (1Hz, 3 times of 1 hour on, 1 hour off stimulation per day) over a period of 4 weeks using bovine chondrocytes (Mauck et al., 2000). In contrast, the application of static compressive loading (up to 50%) was shown to decrease overall matrix synthesis, whilst dynamic compression stimulated matrix synthesis (Buschmann et al., 1995). These observations again imply the importance of physiological loading for the maintenance of cartilage matrix homeostasis.

The use of cartilage explants *in situ*, where chondrocytes and the matrix retain their zonal variation, provides a more physiologically relevant environment to investigate the effects of mechanical load *in vitro*. Studies have shown that mechanical load induces differential responses through the tissue depth i.e. zonal effects, in cartilage explants. Application of dynamic cyclical compression (5kg, 0.3Hz) for 7 days on an anatomically intact bovine cartilage specimen induced proteoglycan synthesis primarily in the superficial to mid zones (Korver et al., 1992). Furthermore, exposure of full-depth bovine cartilage explants to 4.1 MPa (0.5 Hz, 20 hours) induced alterations in the zonal properties of cartilage, with a marked increase in thickness within the superficial and intermediate zones (41.4% and 434% respectively) (Király et al., 1998); however a reduction in thickness was observed in the deep zone (18.5-27.8%) (Kiraly et al., 1998). Moreover, collagen fibril orientation was altered in the superficial zone, and in the deep zone enhanced proteoglycan synthesis was observed suggesting a mechanism in which to maintain tissue integrity (Kiraly et al., 1998). As observed previously in other *in vitro* systems, chondrocyte metabolism is sensitive to the frequency and magnitude of load it is exposed to. In a study by Wong and co-workers, cyclical compression of full thickness bovine cartilage explants (10%, 0.1 Hz) led to a dramatic increase in protein synthesis, particularly COMP and fibronectin, but in response to static compression (10%) a dose-dependent reduction in overall biosynthetic response was observed (Wong et al., 1999).

These results indicate that cartilage tissue is able to modulate biosynthetic activities based on functional requirements (Wong et al., 1999).

Collectively, these *in vitro* studies demonstrate that chondrocytes are mechano-responsive to tensile, shear and compressive loading. As a countermeasure to exposure to mechanical loads, chondrocytes demonstrate the ability to adapt and modulate biosynthetic processes to maintain cartilage homeostasis.

1.3.3 Mechanotransduction

Mechanical cues are transduced into a biological response by chondrocytes through a process referred to as “mechanotransduction”. The process of mechanotransduction is initiated by interactions between the ECM and the chondrocyte cell membrane (Leong et al., 2011a). Mechanical loading of cartilage results in the deformation of both the matrix and chondrocytes (Ramage et al., 2009, Guilak, 1995, Lee et al., 2000), and as a result of tissue deformation and biochemical changes in the ECM, chondrocytes respond via activation of mechano-receptors expressed on the cell membrane (Millward-Sadler and Salter, 2004). Some of these mechano-signalling intermediaries expressed in chondrocytes include ion channels, the actin cytoskeleton and integrin receptors (Leong et al., 2011a). The purpose of such mechano-sensors is to induce extensive transcriptional changes which result in the maintenance of the ECM and tissue integrity.

A change in the intracellular ion concentration is one of the major rapid alterations that occur in response to load. One of the first responses to mechanical stimulation in chondrocytes is an increase in intracellular Ca^{2+} (Nuki and Salter, 2007). As a result, signalling molecules such as calmodulin become activated. The Ca^{2+}-calmodulin complex leads to the activation of calmodulin kinase which in turn phosphorylates and activates the transcription factor AP-1, resulting in an alteration of gene expression (Ramage et al., 2009). Furthermore, an increase in intracellular Ca^{2+} also activates phospholipase C which cleaves the phospholipid phosphatidylinositol 4,5-bisphosphate into diacyl glycerol (DAG) and inositol 1, 4, 5-triphosphate (IP_3) (Nuki and Salter, 2007). IP_3 up-regulation leads to further increases in intracellular Ca^{2+} and activation of protein kinase C; this culminates in the downstream activation of cyclic adenosine monophosphate (cAMP) response element binding protein (CREB) and AP-1 transcription factor to modulate gene expression to maintain tissue homeostasis (Drissi et al., 2005).

The integrin heterodimer, α5β1, was identified as one of the major mechanoreceptors in chondrocytes (Wright et al., 1997). Integrins are heterodimeric extracellular glycoprotein receptors composed of α and β monomers in which the different combinations of these monomers governs ligand specificity (Ramage et al., 2009). Chondrocytes express several integrins on the

cell surface including α1β1, α10β1, αvβ5 and α5β1 (Salter et al., 1992). Chondrocyte integrins comprise an extracellular domain and a cytoplasmic domain which interacts with cytoplasmic proteins and the actin cytoskeleton, thus enabling the transduction of mechanical signals to biochemical responses (Ramage, 2011). In addition, they mediate binding to ECM proteins to mediate adhesion to the matrix (Loeser, 2014). In response to mechanical stimulation, integrin ligand binding is able to affect actin organisation with phosphorylation of actin regulatory proteins such as focal adhesion kinase (FAK) and paxillin (Guilak, 1995). This results in activation of signalling cascades that influence gene expression, thereby maintaining tissue homeostasis (Lee et al., 2002, Loeser, 2014, Salter et al., 1992).

As alluded to above, another major component of the chondrocyte mechanotransduction pathway is the actin cytoskeleton. A critical function of the actin cytoskeleton is to provide the chondrocyte with resistance against compressive forces and maintain the structural integrity of the cell (Blain, 2011, Trickey et al., 2004, Guilak et al., 1995). As a result of deformation, the actin cytoskeleton undergoes remodelling by reversibly disassembling and reforming to adapt to the mechanical loads being exerted on the chondrocytes, and to propagate the mechano-signalling response. Load-induced actin remodelling is suggested to be facilitated via integrins which provide a link between the ECM and the chondrocyte (Blain, 2011). Alterations in the actin cytoskeleton are variable and are dependent on the type of load applied. For example, the actin network re-organised as a reaction to osmotic stress (Erickson et al., 2003). This re-organisation was suggested to be required for the regulatory volume decrease responses (Chao et al., 2006). In addition, it was demonstrated that in response to increasing hydrostatic pressure (15-30MPa, 0.125-0.05Hz, 2 hours), a loss of actin organisation was observed, which was reversed after a two hour recovery period (Parkkinen et al., 1995). In contrast, chondrocytes exposed to static (5MPa) or cyclical compressive force (5MPa, 1Hz) for 2 hours demonstrated a shift in actin assembly from cortical to a more punctate appearance (Knight et al., 2006). The different responses observed between the two different loads was suggested to be a consequence of the activation of different signalling pathways (Knight et al., 2006). However, the signalling intermediaries described here is by

no means an exhaustive list, as many more signalling molecules and/or pathways have been implicated in articular chondrocyte mechanotransduction.

1.4 WNT signalling pathway

The WNTs are a family of secreted glycoproteins comprising 19 members. The term “WNT” is derived from the amalgamation of Drosophila *wingless* and mouse *Int1* which were shown to belong to an evolutionary conserved family of secreted signalling molecules (van Amerongen and Nusse, 2009). WNT signalling is critical to many cellular processes and mediates the generation of cell polarity, cell fate determination and embryonic development to name but a few (Cadigan and Nusse, 1997). WNT signalling can elicit a response via two mechanisms (Figure 1-7), either β-catenin dependent (canonical pathway) or independent pathways (non-canonical pathway) (Kim et al., 2013).

1.4.1 Canonical WNT signalling

The canonical WNT pathway regulates the expression of β-catenin, a transcriptional activator, which influences transcriptional activity (MacDonald et al., 2009). In the absence of WNT ligand, cytoplasmic β-catenin is normally phosphorylated and degraded by a destruction complex comprising glycogen synthase kinase 3β (GSK 3β), casein kinase, axin and adenomatous polyposis coli (APC) (Gordon and Nusse, 2006). However, once the pathway is activated, a WNT ligand binds to a receptor complex comprising members of the frizzled (FZD) transmembrane receptors and low density lipoprotein receptor-related protein 5 or 6 (LRP5 or 6). Association of the WNT ligand results in phosphorylation of the cytoplasmic tail of LRP5/6 followed by activation of dishevelled, a phosphoprotein (Metcalfe et al., 2010). Dishevelled inhibits β-catenin phosphorylation which leads to its accumulation and nuclear translocation (Nusse, 2005). In the nucleus, β-catenin associates with the transcription factors T-cell factor (TCF) and lymphoid enhancer-binding factor-1 (LEF-1) resulting in an alteration of the transcriptional output (Habas and Dawid, 2005). Some of the downstream targets of β-catenin include c-Myc, cyclin D1, cyclooxygenase-2, CD44, WISP-1 and MMP-7 (Luo et al., 2007, Blom et al., 2010).

1.4.2 Non-canonical WNT signalling

All WNT signalling pathways which are not mediated through β-catenin are classified as non-canonical. Non-canonical WNT pathways include the WNT planar cell polarity and WNT/Ca^{2+} pathways. The planar cell polarity pathway was found to promote polarisation within the plane of cells and control convergent extension movements in zebrafish and Xenopus (Schlessinger et al., 2009, Wallingford et al., 2002). In the planar cell polarity pathway, the WNT signal is transduced via frizzled receptors leading to the activation of dishevelled (Komiya and Habas, 2008). Dishevelled contains three conserved domains which are DIX, PDZ and DEP (Boutros et al., 1998, Yanagawa et al., 1995). The DIX domain is required for mediating canonical WNT signalling (Boutros et al., 1998), whereas PDZ and DEP domains mediate the activation of two pathways which activate Rho and Rac, members of the small GTPase family (Komiya and Habas, 2008). Dishevelled associated activator of morphogenesis 1 (DAAM-1) mediates the formation of the dishevelled-Rho complex which leads to the activation of Rho (Habas et al., 2001). Consequently, the activation of Rho GTPase results in the activation of Rho-associated kinase (ROCK) and myosin which cause the reorganisation of the actin cytoskeleton (Komiya and Habas, 2008). In contrast, activation of the Rac pathway is mediated via the DEP domain of dishevelled which then stimulates JNK activity thus promoting cytoskeletal changes (Komiya and Habas, 2008).

Signal transduction via the WNT/Ca^{2+} pathway is mediated by the interaction of a WNT ligand with a G-protein coupled frizzled receptor resulting in a temporary elevation in intracellular Ca^{2+} levels. This results in the activation of phospholipase C which hydrolyses membrane phospholipid, phosphatidylinositol 4,5-bisphosphate, into DAG and IP_3 (De, 2011). IP_3 interacts with Ca^{2+} channels localised on the endoplasmic reticulum inducing an influx of Ca^{2+} ions (Kuhl et al., 2000). In cooperation with the Ca^{2+} ions, calmodulin stimulates Ca^{2+} calmodulin-dependent protein kinase II (CaMKII) (Kuhl et al., 2000). In contrast, DAG and the released Ca^{2+} ions from the endoplasmic reticulum induce the activation of protein kinase C (PKC). PKC and CaMKII collectively stimulate the expression of the nuclear transcription factors: nuclear factor kappa beta (NFκβ) and CREB to induce downstream effects (De, 2011).

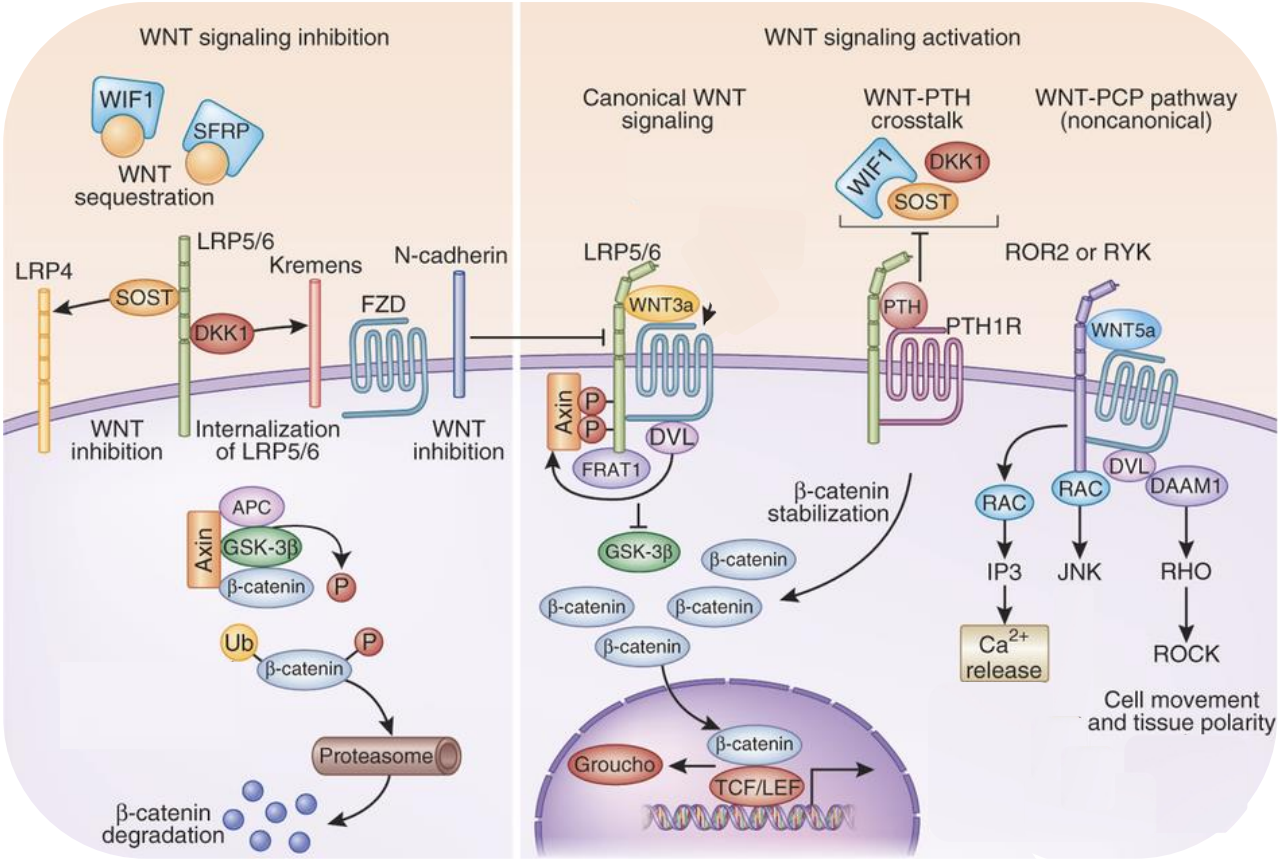

Figure 1-7: Schematic diagram of canonical and non-canonical WNT signalling. Activation of canonical WNT signalling induces β-catenin nuclear translocation which mediates transcriptional regulation of downstream genes. The non-canonical WNT pathway encompasses the planar cell polarity and Ca^{2+} pathways. The activation of the non-canonical WNT pathway involves the regulation of several cellular processes such as alterations in cytoskeletal arrangement to mediate migration (Baron and Kneissel, 2013).

1.4.3 Inhibitors and stimulators of canonical WNT signalling

Due to its regulatory role in several developmental processes, the WNT signalling pathway is tightly regulated to maintain homeostasis through the activity of endogenous inhibitors. Inhibitors include the secreted frizzled related-proteins (SFRPs), WNT-inhibitory factor (WIF), sclerostin (SOST) and Dickkopf (DKK) (Mii and Taira, 2011, Li et al., 2011a). SFRPs and WIF regulate WNT signalling by binding to canonical and non-canonical WNT ligands to prevent their association with WNT ligand target receptors (Li et al., 2008, Surmann-Schmitt et al., 2009). In contrast, DKK and SOST promote inhibition of WNT signalling through association with receptors of WNT ligands. The mechanism of action of DKK involves binding with LRP6 and another class of receptors, Kremen1 and Kremen2, to promote LRP6 receptor internalisation (Figure 1-6) (Mao et al., 2002).

WNT ligands are the main inducers of WNT signalling activation. Based on the receptors the ligands bind to, either the canonical or non-canonical WNT signalling pathway may be activated. This is achieved through the coupling of a frizzled receptor with LRP5/6 to activate canonical WNT signalling and retinoic acid-receptor-related orphan receptors (ROR) for activation of the non-canonical WNT pathway (Grumolato et al., 2010).

1.4.4 Role of WNT signalling in cartilage development

WNT signalling has a pivotal role in regulating embryonic skeletal development, chondrocyte differentiation, chondrocyte function, joint and digit formation (Yates et al., 2005). During embryonic development, chondrocytes form the template for skeletal formation. This process is initiated by the formation of mesenchymal condensation in which cells differentiate into chondrocytes to form a cartilage anlage (template) for bone formation. This process of bone formation is called endochondral ossification (Figure 1-8). β-catenin plays an integral role in orchestrating this process as it acts as a molecular switch regulating osteoblast and chondrocyte differentiation (Kang et al., 2013). WNT ligands are also involved in the regulation of endochondral ossification. WNT3A promotes the expansion of the mesenchymal stem cell pool by decreasing apoptosis, and chondrogenesis only occurs once its expression is down-regulated (Hwang et al., 2005).

Osteoblasts, cells involved in synthesising and mineralising bone, form the periostal bone collar on either side of the cartilage anlage (Mackie et al., 2008). Chondrocytes located at the end of the anlage, termed resting chondrocytes, will form the articular cartilage which caps the end of the epiphysis, whereas the population of chondrocytes underneath will undergo proliferation. WNT4 expression at the end of the epiphysis induces chondrocyte maturation, whereas WNT5A and WNT5B expression is implicated in the recruitment of mesenchymal cells to undergo chondrogenic differentiation (Church et al., 2002, Hartmann, 2002). Proliferating chondrocytes in the growth plate become enlarged (pre-hypertrophic) and ultimately undergo hypertrophy. The ECM surrounding these cells becomes calcified and resorbed and is subsequently substituted by bone i.e. primary centre of ossification (Figure 1-8) (Mackie et al., 2008). The regulation of these WNT components are mediated by the presence of endogenous inhibitors which include FRZB, a member of the SFRP family, and DKK-1. FRZB expression was demonstrated to be localised to cells which have differentiated down the chondrogenic lineage, as it is known that high levels of WNT signalling promotes an osteogenic lineage (Day et al., 2005, Hoang et al., 1996). DKK-1 displayed a similar role but was not as effective as FRZB (Im and Quan, 2010).

Studies have mis-expressed WNT signalling components i.e. expressing a gene at a time and location in which it is not endogenously expressed, to elucidate the contributions of the individual WNT components in limb development. In chick limb development, the mis-expression of WNT14 in mesenchymal condensation prevented mesenchymal cells undergoing chondrogenesis (Hartmann and Tabin, 2001). The mis-expression of WNT5a, WNT5b, Frizzled1, Frizzled 7 or FRZB inhibited chondrocyte maturation (Kawakami et al., 1999, Church et al., 2002, Hartmann and Tabin, 2000, Kitagaki et al., 2003). Furthermore, studies mis-expressing β-catenin signalling led to the interruption of chondrocyte differentiation (Hartmann and Tabin, 2000). In contrast, loss-of-function studies demonstrated that the chondrocyte life cycle cannot be completed without appropriate WNT signalling (Yates et al., 2005). Studies in WNT5A$^{-/-}$ mice demonstrated that the cartilage anlagen did not extend along the proximal-distal axis as a consequence of insufficient proliferation of

chondrocytes (Yamaguchi et al., 1999). Furthermore, other studies have highlighted the role WNT5a plays in condensation of mesenchymal cells and chondrocyte maturation (Topol et al., 2003, Yang et al., 2003). Similarly, loss of β-catenin in differentiated chondrocytes in mouse embryos resulted in a dwarfism phenotype (Akiyama et al., 2004). Collectively, these studies show that WNT signalling is tightly regulated to facilitate this multistep process that is chondrogenesis and skeletal formation.

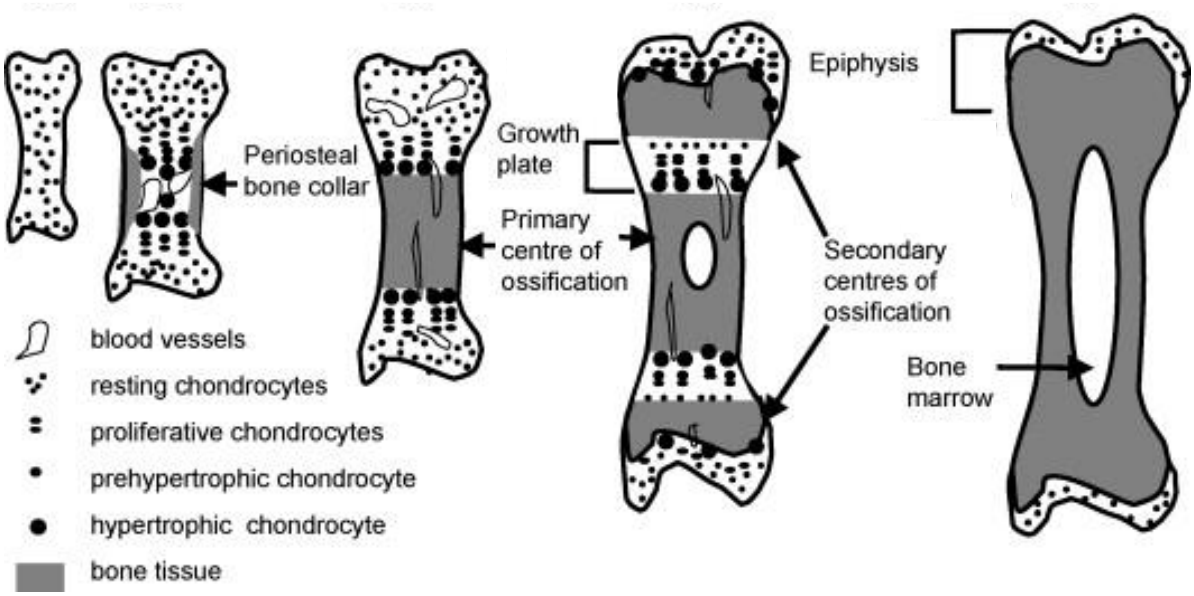

Figure: 1-8: Schematic representation illustrating the process of endochondral ossification. (Mackie et al., 2008).

1.4.5 Role of WNT signalling in cartilage homeostasis

WNT signalling also has an integral role in maintaining postnatal cartilage homeostasis as demonstrated by *in vivo* studies. Studies using transgenic mice where a constitutively active form of β-catenin was conditionally expressed have shown deleterious effects on cartilage homeostasis (Yuasa et al., 2009). Transient activation of β-catenin signalling in young adult mice resulted in severe defects in the formation of the knee joint. Furthermore, a vast number of apoptotic cells were observed in the femoral and tibial growth plates before irreversible deterioration (Yuasa et al., 2009). In addition, there was a significant loss in proteoglycan content and an increase in cell proliferation, density and cartilage thickness (Yuasa et al., 2009). In contrast, mice conditionally deficient in β-catenin had significantly reduced cell numbers, malformation of the growth plate and a significant reduction in bone volume, as well as a surge in cell apoptosis leading to eventual cartilage destruction (Yuasa et al., 2009, Zhu et al., 2008). Moreover, conditional inhibition of β-catenin signalling in mice induced significant down-regulation in the expression of genes associated with chondrocyte maturation like type X collagen, MMP-13 and alkaline phosphatase, in addition to a reduction in chondrocyte proliferation and differentiation (Chen et al., 2008). Regulation of the chondrogenic phenotype was more recently demonstrated to be governed by cross-talk between the canonical and non-canonical WNT signalling pathways. WNT3A, a prototypical activator of the canonical WNT signalling pathway, was demonstrated to regulate chondrogenesis by activation of both canonical and non-canonical mechanisms (Nalesso et al., 2011). Furthermore, it was demonstrated that the canonical WNT pathway inhibits the WNT/Ca^{2+} pathway and promotes loss of chondrogenic marker expression. However, inhibition of the canonical WNT pathway results in a rescue of the WNT/Ca^{2+} pathway and restores the expression of chondrogenic markers (Nalesso et al., 2011), highlighting the interactions that occur between these two pathways which were previously thought of as working in isolation.

Studies in normal human cartilage have shown that there is a high concentration of endogenous WNT inhibitors expressed, particularly FRZB and DKK-1 (Leijten et al., 2012). Enhanced expression of these inhibitors was proposed to be the reason why healthy cartilage was highly resistant to

hypertrophic differentiation, which occurs in pathological conditions. This was demonstrated in chondrogenically differentiated mesenchymal stem cells treated with recombinant FRZB and DKK-1, where the presence of these exogenous inhibitors prevented matrix mineralisation and hypertrophy (Leijten et al., 2012). Taken together, these studies highlight the importance of the regulation of WNT signalling and the necessity of appropriate levels of WNT signalling in maintaining homeostasis in postnatal cartilage. Clearly, dysregulation of WNT signalling can impact on tissue homeostasis promoting the onset of cartilage degeneration and/or tissue ossification.

1.5 Osteoarthritis

Osteoarthritis (OA) is a multifactorial disease and is characterised by cartilage degeneration, subchondral bone remodelling, osteophyte development, inflammation and loss of joint function. Although multi-factorial in origin, risk factors which increase OA predisposition include abnormal mechanical loading, trauma and genetics. Trauma or injurious loading are risk factors for developing OA due to alterations in the properties of cartilage and/or subchondral bone remodelling that occurs in response to such conditions (Heinegard and Saxne, 2011). Furthermore, the amount of load exerted on cartilage may initiate and promote the progression of cartilage degeneration. This was demonstrated in a study by Hodge et al. (1986), where physiological loading in the hip was determined and the disuse of joint was found to be detrimental and leads to pathology (Hodge et al., 1986). Disuse of the knee joint has been demonstrated to alter the biomechanical composition of cartilage, thus increasing the risk of pathology. Immobilisation studies facilitated by casting the joint have shown atrophic alterations in cartilage tissue (Helminen, 1987). Although joint immobilisation did not affect proteoglycan synthesis, there was a significant reduction in GAGs in the superficial zone of cartilage (Jortikka et al., 1997). Furthermore, although the collagen network was not affected by joint immobilisation, there was a marked decrease in collagen cross-links resulting in a reduction in cartilage stiffness (Haapala et al., 1999, Jurvelin et al., 1986). In addition, the overuse of the joint can also lead to the development of OA. The result of repetitive motion could lead to the accumulation of microtrauma and thus not allowing the tissue sufficient time to recover. As a result the catabolic

processes would be greater than anabolic and result in cartilage degeneration (O'Keeffe et al., 2009).

Genetic factors which contribute to OA aetiology include bone mineral density, obesity and muscle weakness (Chapman and Valdes, 2012). In addition, single nucleotide polymorphisms (SNPs) in certain genes have been shown to be associated with an increased risk of developing OA. SNPs identified in growth differentiation factor 5, SMAD3 and asporin, which are part of the bone morphogenetic protein signalling pathway, are implicated in knee OA (Chapman and Valdes, 2012). Furthermore, other studies have found SNPs in FRZB and LRP5 which are associated with an increased incidence of knee and spine OA (Blom et al., 2010). As a result of these SNPs, dysregulation of WNT signalling was hypothesised to be associated with an increased risk of developing OA, however the association was not found to be statistically significant (Evangelou et al., 2009). Although not statistically significant, clearly there is a significant role for WNT signalling in cartilage homeostasis as asserted in studies investigating WNT signalling in human end-stage OA cartilage and experimentally induced-OA in animal models (Blom et al., 2009)

1.5.1 *In vivo* studies investigating the role of WNT signalling in cartilage degeneration

In vivo studies using transgenic mice were conducted to further elucidate the role of WNT signalling in cartilage degeneration. Conditional inhibition of β-catenin, achieved via overexpression of a peptide which selectively associates with the armadillo repeats in β-catenin thus preventing its interaction with TCF, in mice was demonstrated to induce apoptosis and cartilage degeneration (Zhu et al., 2008). Interestingly, mice with conditional activation of β-catenin, achieved by deletion of exon 3 of the β-catenin gene, also displayed an OA-like phenotype including surface fibrillation, osteopyte formation, cartilage degeneration and synthesis of new subchondral bone (Zhu et al., 2009). As these *in vivo* studies demonstrated, both inhibition of or sustained canonical WNT signalling results in deleterious effects in cartilage, thus recent studies have moved on to examine more specifically the role of enhanced WNT signalling in mouse models of OA.

The effect of enhanced WNT signalling was investigated in FRZB$^{-/-}$ mice in which OA was induced using papain, collagenase or methylated bovine serum albumin (BSA). Deletion of FRZB, which enhanced WNT signalling, resulted in significant cartilage degeneration in all three mouse models of OA (Lories et al., 2007). Based on transcriptomic results, cartilage degeneration was induced through WNT-dependent MMP expression, particularly MMP-3 (Lories et al., 2007). FRZB$^{-/-}$ mice subjected to mechanical loading (2,400 cycles/day at 4 Hz for 10 days) resulted in an anabolic response, as evidenced by enhanced cortical bone thickness and density in long bones (Lories et al., 2007). This increase in bone stiffness may produce larger strains on articular cartilage during every day loading thus contributing to its degeneration.

Corroborating evidence for the role of excessive WNT signalling in cartilage degeneration was demonstrated in mice over-expressing the WNT target gene WISP-1. An OA-like phenotype was observed as indicated by the presence of enzymes responsible for cartilage degradation, specifically MMP-3 and MMP-13 in the cartilage and synovium, and ADAMTS-4 and ADAMTS-5 primarily in the synovium (Blom et al., 2009). These findings illustrate that dysregulation of the canonical WNT pathway may play a major role in cartilage degeneration, and therefore OA initiation and progression *in vivo*.

1.5.2 *In vitro* studies investigating the role of WNT signalling in cartilage degeneration

Recent *in vivo* studies have implicated WNT signalling in promoting cartilage degeneration due to its potential dysregulation in OA (Section 1.5.1). This hypothesis is supported by *in vitro* studies using recombinant WISP-1 which was found to induce cartilage degradation through activation of MMPs and ADAMTSs (Blom et al., 2009). Similarly, enhancing canonical WNT signalling through inhibition of GSK3β in chondrocytes induced a loss of expression of cartilage markers, induction of MMP expression and inhibition of cell proliferation, features often observed in OA (Miclea et al., 2011). Furthermore, analysis of human OA tissue demonstrated an up-regulation in WNT7B in chondrocytes, whereas FRZB was down-regulated (Nakamura et al., 2005). All of these findings indicate that dysregulation of the WNT signalling pathway may play a prominent role in promoting cartilage degeneration.

1.6 Mechano-regulation of WNT signalling

WNT signalling is known to be mechanically regulated in other tissues i.e. tendon, bone and muscle. In tendon-derived stem cells, it was demonstrated that application of tensile strain (2% elongation, 0.5Hz, 3 days) activates non-canonical WNT signalling and induces osteogenic differentiation via WNT5A (Shi et al., 2012). WNT signalling was shown to be necessary in maintaining bone homeostasis, whereby *in vivo* loading of mouse tibiae (6-7N, 36 cycles, 2 Hz) activated the canonical WNT signalling pathway as indicated by the up-regulation of WNT target genes such as cyclin D1 and WISP-2 (Robinson et al., 2006). Mechano-regulation of WNT signalling was additionally observed in mouse myoblasts, where application of mechanical strain (20% elongation, 6 cycles/minute) induced WNT10B resulting in the maintenance of the myogenic phenotype (Akimoto et al., 2005). Collectively these studies emphasise the importance of mechano-regulation of WNT signalling in maintaining homeostasis within the respective tissues.

1.7 PhD hypothesis and objectives

At the start of this PhD, studies investigating the role of WNT signalling in cartilage degeneration or OA had not considered the role mechanical loading may have on WNT-mediated initiating events of this disease process. The one exception was a study performed in our laboratory which demonstrated the partial translocation of β-catenin to the nucleus in high-density monolayer chondrocytes subjected to tensile strain (7.5%, 1Hz, 30 minutes); however, comparable studies in articular cartilage had not been reported (Thomas et al., 2011). Due to the significant involvement of mechanical load and WNT signalling in cartilage development and homeostasis, I hypothesise that WNT signalling is activated in response to mechanical load in articular cartilage; further to this, I hypothesise that, as yet unidentified, WNT signalling components are differentially regulated in response to abnormal mechanical load which contributes to a degenerative cartilage phenotype. Specifically, the objectives of this PhD are:

i. Confirm mechano-regulation of β-catenin in isolated chondrocytes subjected to tensile strain

ii. To identify and characterise loading regimes which either induce cartilage homeostasis (physiological load) or catabolism (degradative load)
iii. To determine which WNT signalling components are regulated by physiological load
iv. To determine whether there is a differential WNT response in cartilage subjected to a degradative loading regime
v. To investigate the downstream effects of specific WNT signalling components identified in objectives ii and iii

Chapter 2

Methodology

All reagents were purchased from Sigma Aldrich (Poole, UK) unless otherwise stated and were of analytical grade or above. All molecular biology plasticware, filter tips and reagents were DNase and RNase free. All experiments conducted were n of 6 and repeated as three independent experiments unless otherwise indicated.

2.1 Chondrocytes

2.1.1 Isolation of primary articular chondrocytes

Feet from 7-10 day old bovine animals (F. Drury and sons, Swindon, UK), obtained within 6 hours of slaughter, were washed thoroughly and skinned. A sterile scalpel was used to shave off slivers of full-depth articular cartilage tissue from the *metacarpophalangeal* joint. Tissue was washed three times for 20 minutes each with Hanks' Buffered Salt Solution (HBSS) (Invitrogen, Paisley, UK) supplemented with 400µg/ml penicillin and 400U/ml streptomycin (Invitrogen, Paisley, UK), followed by a fourth wash of HBSS containing 100µg/ml penicillin and 100U/ml streptomycin only. Chondrocytes were released from the cartilage matrix by incubation in 0.1% (w/v) pronase (Roche, West Sussex, UK) [in Dulbecco's Modified Eagle's Medium (DMEM)/ Hams F12 with Glutamax™ (Invitrogen, Paisley, UK) containing 5% (v/v) foetal calf serum (Invitrogen, Paisley, UK) and 100µg/ml penicillin and 100U/ml streptomycin] for 50 minutes with gentle agitation (37°C, 5% CO_2). Subsequently, cartilage was digested in 0.04% (w/v) collagenase type II isolated from *Clostridium histolyticum* (Invitrogen, Paisley, UK), in the media described above, overnight with gentle agitation at 37°C (5% CO_2). The solution was filtered using a 40µm cell strainer (Fisher Scientific, Loughborough, UK), and the enzymatically-released chondrocytes were pelleted by centrifugation at 1,118g for 5 minutes. The cell pellet was resuspended in fresh media, as described above, supplemented with 100µg/ml penicillin and 100U/ml streptomycin. However, foetal calf serum was replaced by 1× insulin-transferrin-selenium (ITS) (Invitrogen, Paisley, UK) to prevent chondrocyte dedifferentiation (Kisiday et al., 2005) and 50µg/ml ascorbate-2-phosphate to sustain collagen synthesis (Murad et al., 1981). Unless indicated otherwise, this media supplementation was used for all subsequent tissue culture of cells and explants. The cell suspension was diluted 1:100 to enable cell

counting using a haemocytometer. Chondrocytes (4×10^6) seeded into the wells of a pronectin coated BioFlex® 6-well culture plate (Dunn Labortechnik, Asbach, Germany) were maintained for 24 hours.

2.1.2 Application of cyclic tensile strain to chondrocytes

A regimen of either 7.5%, 10% or 14% tensile strain at a frequency of 1Hz was applied to the chondrocytes using the FX3000 system (FlexCell Int, Hillsborough, NC, USA) for 1, 2 or 4 hours and either processed immediately post cessation of load or after 4 hours post load (Figure 2-1). The pronectin coated plates seeded with chondrocytes were placed on a baseplate containing 6 Teflon indenters which align with each well. Tensile strain was then applied by vacuum to deform the membrane of the wells over the Teflon indenters. The tensile strain applied to the chondrocytes lies within the range described as representative of physiological (Guterl et al., 2009). Cells seeded onto pronectin coated plates but not subjected to tensile strain were used as a control.

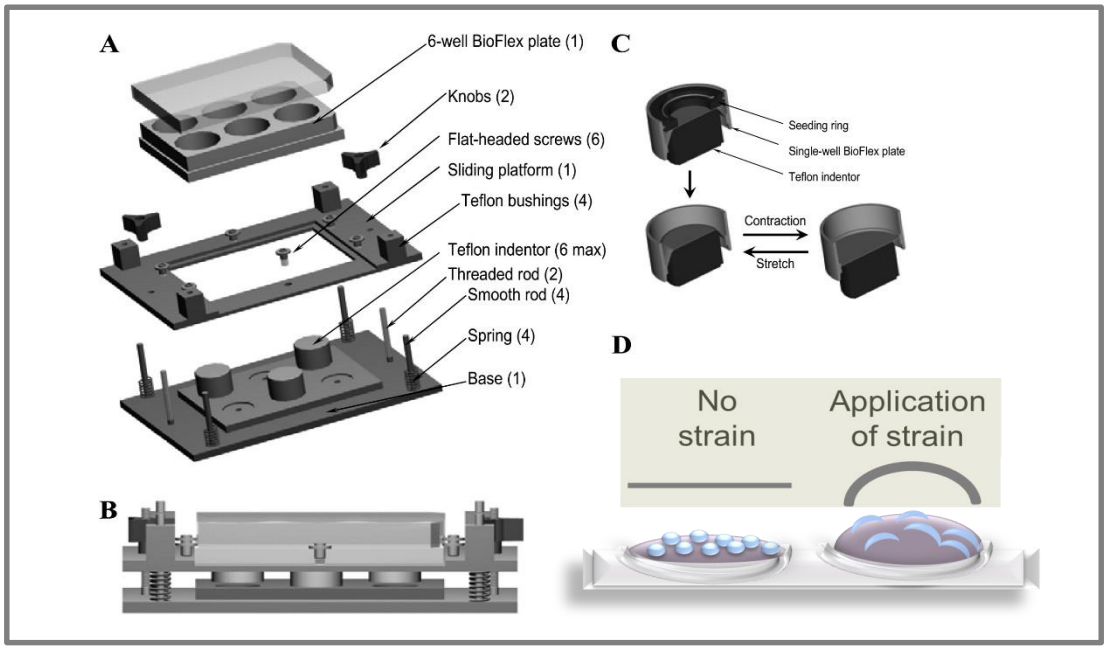

Figure 2-1: Schematic diagram of the FX3000 system (adapted from (Boudreault and Tschumperlin, 2010). Figures A-C illustrate the constituents of the FX3000 system. Figure D demonstrates the effect of tensile strain on seeded chondrocytes.

2.1.3 Bioflex® specimen preparation for confocal analysis

Primary articular chondrocytes cultured on pronectin coated Bioflex® plates were fixed with 2% (w/v) paraformaldehyde for 30 minutes at room temperature. The wells were washed once with 1× phosphate buffered saline (PBS) and the membranes excised using a sterile scalpel. The plate membranes were then cut into nine pieces. One piece was placed into a well of a 24 well tissue culture plate for immunohistochemical analysis, whereas the rest of the membranes were placed in a 6 well tissue culture plate and stored at -80°C for later processing.

2.2 Cartilage explants

2.2.1 Isolation of cartilage explants

Full thickness cartilage explants were obtained from the *metacarpophalangeal* joints of 7-10 day old bovine calves (as described in section 2.1.1) using sterile 5mm biopsy punches (Selles Medical, Hull, UK). Explants were washed and cultured in the media as previously described (section 2.1.1).

2.2.2 Application of load to cartilage explants

Cartilage explants were cultured for 72 hours for the tissue to stabilise after excision from the joint. The application of cyclical compressive load was conducted using an ElectroForce® 3200, controlled via WinTest dynamic mechanical analysis (DMA) software (Bose Corporation, ElectroForce® Systems Group, Minnesota, USA) (Figure 2-2A). An explant was placed in media in a glass petri dish which was placed on the ElectroForce 3200 stage; the platen was brought down until it made contact with the tissue. The machine was auto-tuned in both displacement (air) and load control (tissue) prior to loading. Contact between the tissue and loading platen was confirmed as an increase in force registered by the software (-0.1N).

Three loading regimes including 2.5MPa, 5MPa and 7MPa were tested to assess which was a suitable representation of either physiological or degradative compressive load as it had previously been reported that loads $\leq$ 3MPa were deemed physiological and loads exceeding 6MPa were deemed non-

physiological ; non loaded explants served as controls (Hodge et al., 1986, Bader et al., 2011). Subsequent to loading, media was replenished and explants were cultured in a CO_2 incubator (37°C, 5% CO_2, 95% humidity) for up to 24 hours post-load. Explants were then snap-frozen using liquid nitrogen and stored in liquid nitrogen prior to RNA extraction.

2.2.2.1 Recombinant DKK-1 and NFATC inhibitor treatments in conjunction with loading

In order to determine the role of DKK-1 and NFATC in cartilage homeostasis, recombinant human DKK-1 (Peprotech, London, UK) and NFAT inhibitor (Tocris, Bristol, UK) were used. NFATC inhibitor is a selective inhibitor of calcineurin-mediated dephosphorylation of all NFATC members except NFAT5. Recombinant human DKK-1 (100ng/ml, 250ng/ml, 500ng/ml) and NFATC inhibitor (10µM, 25µM, 50µM) were added to the media of bovine cartilage explants for 24 hours before loading. Fresh media with the respective treatments were added to the explants during application of degradative load (7MPa, 1Hz, for 15 minutes). After application of load, explants were left in culture with the respective treatments for either 4 or 24 hours post-cessation of load.

2.2.2.2 Measurement of cell viability

Explant chondrocyte viability following treatment with either recombinant DKK-1 or NFATC1 inhibitor was determined using the Cytotox 96® non-radioactive cytotoxicity assay (Promega, Southampton, UK) following the manufacturer's protocol. The assay measures the release of lactate dehydrogenase into the culture medium which occurs as a result of cell death (Koh and Choi, 1987). Briefly, 50µl of conditioned media was added to the 96-well plate followed by the addition of 50µl of reconstituted substrate mix. After an incubation period of 30 minutes, the absorbance values were determined at 492nm (FLUOstar OPTIMA. BMG Labtech, UK), and LDH levels compared to the control explants which had not been subjected to load.

2.3 Immunofluoresence analysis using confocal microscopy

2.3.1 Cryosectioning of cartilage explants

Snap-frozen cartilage explants, cut in half through the tissue depth and embedded in Tissue-Tek® OCT™ Compound (Sakura Finetek, Alphen aan den Rijn, Netherlands), were placed onto cryostat chucks and the tissue aligned perpendicularly to the chuck to section full-depth cartilage. Explants were sectioned using an OTF5000 cryostat (Bright instruments, Cambridgeshire, UK) and cut at a thickness of 25µm. Sections were placed on X-tra® slides (Leica, Wetzlar, Germany) which contain a permanent positive charge enabling the binding of cartilage tissue to the slide. Prior to immunohistochemical analysis, a Super Pap pen, a liquid blocker, (Daido Sangyo, Tokyo, Japan) was used around the sections to facilitate immuno-labelling and prevent cross-contamination of labels. Cryosections were fixed using 2% (w/v) paraformaldehyde (in 1x PBS) for 30 minutes at room temperature followed by one wash with PBS prior to immuno-labelling.

2.3.2 Immunofluorescence labelling

Samples (pieces of Bioflex® membrane or tissue cryosections) were permeabilised in 5% (v/v) Triton X-100 for 1 hour at room temperature. Samples were then blocked using 4% (v/v) goat serum at room temperature for 1 hour. Samples were incubated in primary antibody (diluted in 1× PBS, 0.1% (v/v) Tween-20 (PBS-T)) overnight at 4°C (refer to table 2-1 for specific antibodies and dilutions used). Samples were subsequently washed three times with PBS-T followed by incubation with secondary antibody diluted in PBS-T (table 2-1). Residual secondary antibody was removed using three washes in PBS-T, sections mounted in Vectashield® mounting medium containing 1.5µg/ml DAPI (Vector Laboratories, Peterborough, UK) and stored in the dark. Negative controls were treated exactly the same but no primary antibody was added.

Table 2-1: Dilutions of antibodies used in immunofluorescence analysis

Primary antibody	Dilution	Secondary antibody	Dilution
Monoclonal Anti-β-Catenin produced in mouse	1:500	Anti-Mouse IgG (whole molecule)–FITC antibody produced in goat	1:64
Anti-WIF1 (353-365) produced in rabbit	1:150	Anti-rabbit IgG (whole molecule)–FITC antibody produced in goat	1:64

2.3.3 Confocal scanning laser microscopy

Immunofluorescence labelling was examined using a Leica DM6000N upright digital microscope (Leica, Wetzlar, Germany). The microscope was controlled via the Leica Control software which was set up for sequential channel fluorescence recordings using the 63× oil immersion objective lens, (×8.85 zoom) to image representative chondrocytes with the suitable excitation and emission settings for FITC and DAPI. Three isolated single chondrocytes were selected at random as representative for each treatment per section. For each experiment, three explants were imaged, and data is representative of three independent experiments. Low power images were taken of the explants to capture an overview, and then high power images were taken of individual chondrocytes from each zone or each membrane. Chondrocytes were scanned continuously to generate a series of 2-dimensional images (30-35 serial sections) which were reconstructed to generate a 3-dimensional image of the chondrocyte using the Leica software. Total nuclear fluorescence was determined using ImageJ software. Using ImageJ, the nuclear region was selected and the area was calculated as well as the integrated density. To minimise background, a similar area was selected adjacent to the cell of interest. Thus, the following equation was utilised to determine the corrected total cell fluorescence, integrated density - (nuclear area X background readings).

2.4 RNA extraction from cartilage explants

Total RNA was extracted from cartilage tissue using Trizol® (Invitrogen, Paisley, UK). Cartilage tissue was powdered in Trizol® (50mg of wet weight tissue per ml of Trizol®) using liquid nitrogen cooled chambers in a Mikro-Dismembrator at 2,000rpm for 90 seconds (Braun Biotech, Melsungen, Germany). After a brief incubation at room temperature, 150µl of chloroform was added and mixed by vortex followed by a 10 minute incubation period at room temperature. Homogenised explants were then centrifuged at 12,500g for 15 minutes at 4°C to achieve phase separation. The aqueous phase was transferred to a 1.5ml tube followed by precipitation of RNA in a 1:1 volume of 100% ethanol and mixed by inversion 3-4 times at room temperature. RNA was then purified using the Qiagen RNeasy™ mini kit following the manufacturer's protocols

(Qiagen, West Sussex, UK). All centrifugation steps were carried out at room temperature. Briefly, samples were applied to the RNeasy spin columns and centrifuged at 8,000g for 15 seconds. The flow-through was discarded and the spin columns were then washed twice with 300µl of RW1 wash buffer followed by centrifugation at 8,000g for 45 seconds. Spin columns were then washed twice with 500µl of RPE buffer and centrifuged at 8,000g for 2 minutes. Finally, 30µl of RNase-free water was added to the spin columns followed by centrifugation at 8,000g for 1 minute to elute the RNA, which was then stored at -80°C for subsequent analysis.

2.4.1 Assessment of RNA quality and yield

RNA integrity was evaluated using the Agilent 2100 Bioanalyser (performed by Central Biological Services, School of Medicine, Cardiff University) using 1.5µl of purified total RNA. The ratio of 18S and 28S ribosomal bands, and the presence of degradation products were assessed for each sample by gel electrophoresis, and an RNA integrity number (RIN) assigned from 1 (completely degraded RNA) to 10 (perfect RNA quality) (Figure 2-2). RNA concentration was then determined using the Nanodrop Lite Spectrophotometer (Fisher Scientific, Loughborough, UK), and RNA purity was assessed by the ratio of the absorbance at 260nm and 280nm where a ratio of ~2 is desired.

2.4.2 Synthesis of cDNA from RNA template

cDNA was reverse transcribed from the purified RNA (300ng) using SuperScript™ III Reverse Transcriptase (Invitrogen, Paisley, UK). Following the manufacturer's protocol, cDNA was synthesised in a 20µl reaction containing 250ng random hexamers (Promega, Southampton, UK), and 500µM dNTP mix (Invitrogen, Paisley, UK). Samples were placed in a Prime Techne thermocycler (Bibby Scientific Limited, Staffordshire, UK) and incubated at 65°C for 5 minutes followed by an incubation at 4°C for 2 minutes. At the end of the incubation period, 100U SuperScript III Reverse Transcriptase, 4µl of 5× first-strand buffer (250mM Tris pH 8.3, 375mM KCl, 15mM $MgCl_2$), 2µl of 100mM dithiothreitol and 125U of recombinant RNase inhibitor (Promega, Southampton, UK) were added to the initial reaction followed by an incubation period of 10 minutes at 25°C. The

reaction mixture was then incubated for 50 minutes at 42°C. The reaction was terminated by inactivation of the reverse transcriptase at 70°C for 15 minutes.

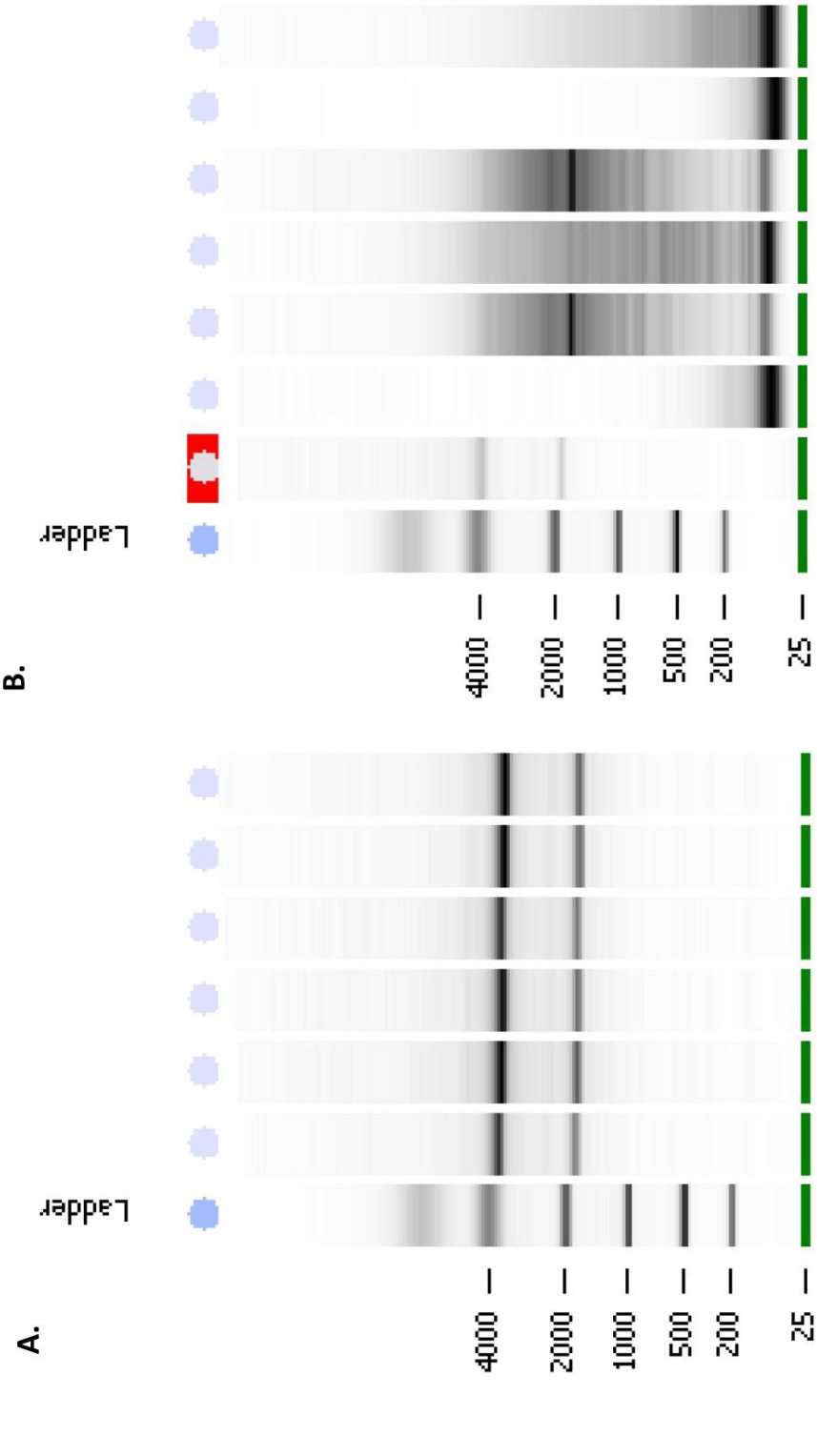

Figure 2-2: Representative bioanalyzer gel image. A) An example of how intact RNA is visualised on a gel, with low background and sharp bands depicting ribosomal 28S (top band) and 18S (bottom band), B) whereas poor RNA quality is identified by a high background in addition to the absence of distinct 28S and 18S bands which also is an indicator of RNA degradation.

2.5 Quantitative polymerase chain reaction (qPCR)

2.5.1 *Primer design*

Primers were designed using Primer-Blast software to span exon-exon boundaries, produce a PCR product within the range of 70-200bp and were specific for bovine. Selected primers were run through the NCBI BLAST database to ensure no homology to other genes. Primers (Eurofins Genomics, Ebersberg, Germany) were optimised according to the manufacturer's protocol using polymerase chain reaction (PCR) and GoTaq® Flexi DNA Polymerase kit (Promega, Southampton, UK).

2.5.2 Quantification of transcripts

Quantification of mRNA levels of genes of interest were measured using qPCR with Brilliant III Ultra-Fast SYBR® Green QPCR Master Mix (Agilent Genomics, Berkshire, UK). The master mix contains a variant of *Taq* DNA polymerase which is mutated to allow faster replication. SYBR® Green I fluorescent dye specifically binds to double stranded DNA resulting in an increase in fluorescence signal which is proportional to the amount of DNA present. The point at which the fluorescence signal is significantly higher than the baseline set (threshold) is referred to as threshold cycle (Ct) value. Ct values were used to determine relative quantification. Reactions were performed using RNase/DNase-free 96-well plates in conjunction with the Mx3000P® QPCR System and MxPro QPCR software (Stratagene, Cambridge, UK). cDNA was analysed in a reaction of 20µl containing the components listed (table 2-2); the exclusion of cDNA which was replaced by water acted as the negative control for the PCR. The plates were centrifuged at 1,000g for 1 minute to collect the contents. cDNA was amplified for 40 cycles under the conditions listed (table 2-3). The annealing step was carried out at 60°C unless indicated otherwise (table 2-4). One cycle of dissociation was performed at the end of the amplification process to confirm that only the gene of interest was amplified as indicated by the presence of a single peak (Figure 2-3). Relative quantification was calculated using the $2^{-\Delta\Delta CT}$ method (Livak and Schmittgen, 2001). Briefly, unloaded and/or untreated samples were used as a control group to measure relative changes in the target gene in the experimental samples. The relative change in gene

expression is presented as a fold change which is normalised to a combination of two housekeeping genes whose expression we have ascertained is not affected by treatment or loading.

Table 2-2: Components of a single quantitative PCR reaction

Component	Volume
Brilliant III Ultra-Fast SYBR® Green QPCR Master Mix	10µl
Forward and reverse primers (0.2µM) from a 10µM stock (Eurofins MWG, Ebersberg, Germany)	0.4µl
Water	8.6µl
cDNA (or water for non-template control)	1µl
Total	20µl

Table 2-3: Quantitative PCR cycling conditions used to amplify genes of interest

Reaction steps	Cycles	Duration of cycle	Temperature
Activation of DNA polymerase	1	3 mins	95°C
Annealing and extension	40	15 sec 30 sec	95°C 60°C
Generation of dissociation curve	1	1 min 30 sec 30 sec	95°C 60°C 95°C

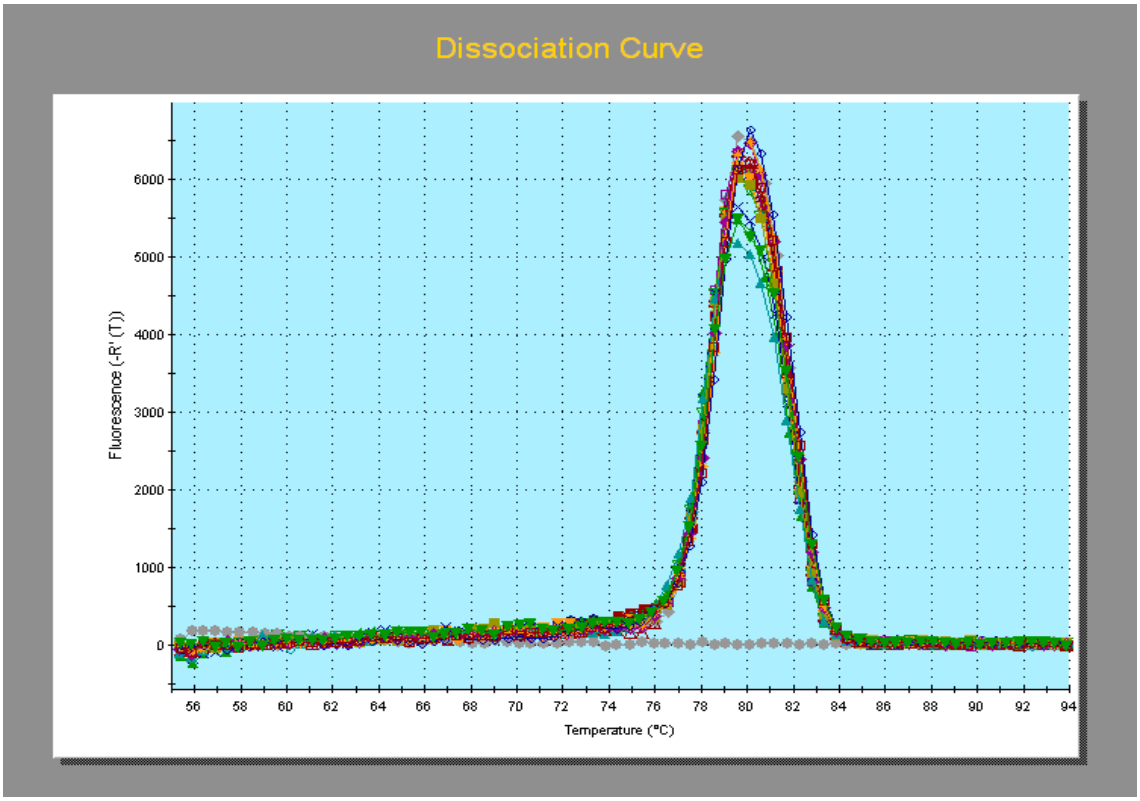

Figure 2-3: Representative dissociation curve (aggrecan) for quantitative PCR showing a single peak that is indicative of a single PCR product. The grey line denotes the negative control which contains water instead of cDNA indicating that there was no contamination in the qPCR reactions.

Table 2-4: Primer sequences of matrix genes.

Name	*Annealing temperature*	*Product size (BP) Reference*	*Sequences 5'-3'*
COL2-F	60	69 (Deng et al., 2007)	AAC GGT GGC TTC CAC TTC
COL2-R			GCA GGA AGG TCA TCT GGA
AGG-F	60	76 (Thomas et al., 2011)	GCT ACC CTG ACC CTT CAT C
AGG-R			AAG CTT TCT GGG ATG TCC AC
MMP3-F	60	221 (Li et al., 2011b)	TGG AGA TGC TCA CTT TGA TGA TG
MMP3-R			GAG ACC CGT ACA GGA ACT GAA TG
MMP9-F	60	121 (Blain et al., 2010)	TAG CAC GCA CGA CAT CTT TC
MMP9-R			GAA GGT CAC GTA GCC CAC AT
MMP13-F	60	202 (Blain et al., 2010)	CCC TTG ATG CCA TAA CCA GT
MMP13-R			GCC CAA AAT TTT CTG CCT CT
TS4-F	60	169 (Blain et al., 2010)	CTC CAT GAC AAC TCG AAG CA
TS4-R			CTA GGA GAC AGT GCC CGA AG
TS5-F	60	155 (Blain et al., 2010)	CTC CCA TGA CGA TTC CAA GT
TS5-R			TAC CGT GAC CAT CAT CCA GA
TIMP1-F	60	75 (Li et al., 2011b)	CTG CGG ATA CTT CCA CAG GT
TIMP1-R			ATG GAT GAG CAG GGA AAC AC
TIMP3-F	60	119	GAC ATC GTG ATC CGA GCC AA
TIMP3-R			TGG GGC ATC TTG GTG AAT CC
CJUN-F	60	100 (Thomas et al., 2011)	TAA ACT AAG CCC ACG CGA AG
CJUN-R			CTC AGA CTG GAG GAA CGA GG
BCAT-F	60	175	GCC GGC TAT TGT AGA AGC TGG
BCAT-R			ATC TGA GCC CAG AAG CTG GA

2.5.3 Selection and valid of appropriate housekeeping genes

A panel of reference genes selected from a paper by Anstaett et al. (2010) were used to identify the most stable reference genes in the experimental model (table 2-4). Experimental cDNA which was derived from explants loaded under different regimes were pooled to make up a 10-fold serial dilution to create a standard curve. The standard curve generated assesses the efficiency of the PCR reaction which needs to fall within 95-110% to produce reliable data for cross-comparison with other genes of interest. The most stable combination of reference genes was selected using the RefFinder software. RefFinder integrates the three most common computational programmes (BestKeeper, geNorm, and NormFinder) which selects the most stable reference genes tested based on Ct values of the experimental samples. Each software has its own unique method in selecting the best reference genes. BestKeeper gene selection is established by pair-wise correlation analysis of all reference genes used and calculates the geometric mean of the optimal single or combination of two genes. geNorm determines stability of reference genes by calculating average pair-wise variation between a single reference gene and the other group of reference genes. In contrast, NormFinder software is different as it takes into consideration experimental design and variation between and within groups to assess gene stability (Anstaett et al., 2010). RefFinder then uses the results of all three programmes to assign a value to the individual genes and calculates the geometric mean to rank the genes from most to least stable. Primer sequences of the reference genes and their reported functions are listed (table 2-5;2-6).

Table 2-5: List of reference genes used and their functions

Nomenclature	Gene names	Function	Reference
18S	18s ribosomal RNA	Ribosomal subunit	(Doudna and Rath, 2002)
β-actin	β-actin	Cytoskeletal protein	(Glare et al., 2002)
GAPDH	Glyceraldehyde 3-phosphate dehydrogenase	An enzyme involved in glycolysis	(Glare et al., 2002)
HPRT	Hypoxanthine guanine phosphoribosyltransferase	Biosynthetic enzyme that synthesizes purine nucleotides from intermediates generated from RNA and DNA degradation.	(Kang et al., 2013)
PPIA	Peptidylprolyl isomerase A	A protein involved in assisting the folding of proteins	(Thali et al., 1994)
RPL4	Ribosomal protein 4	A component of 60S ribosome large subunit	(Yang et al., 2005)
SDHA	Succinate Dehydrogenase subunit A	Encodes one of the flavoprotein subunit of the SDH complex II which is involved in oxidative phosphorylation in the inner membrane of the mitochondria	(Italiano et al., 2012)
YWHAZ	tyrosine 3 monooxygenase/tryptopha n 5monooxygenase activation protein—zeta polypeptide	A metastasis enhancer gene and has a potential novel role in regulating β-catenin	(Chen et al., 2012)

Table 2-6: Primer sequences of housekeeping genes.

Name	*Annealing temperature*	*Product size (BP)*	*Sequences*
GAPDH-F	60	133	TTG TCT CCT GCG ACT TCA ACA GCG
GAPDH-R			CAC CAC CCT GTT GCT GTA GCC AAA T
YWHAZ-F	60	180	CTG AGG TTG CAG CTG GTG ATG ACA
YWHAZ-R			AGC AGG CTT TCT CAG GGG AGT TCA
HPRT-F	60	127	TAA TTA TGG ACA GGA CCG AAC GGCT
HPRT-R			TTGATGTAATCCAACAGGTCGGCA
PPIA-F	60	186	GGT GGT GAC TTC ACA CGC CAT AATG
PPIA-R			CTT GCC ATC CAA CCA CTC AGT CTT G
RPL4-F	60	199	TTT GAA ACT TGC TCC TGG TGG TCA C
RPL4-R			TCG GAG TGC TCT TTG GAT TTC TGG
SDHA-F	60	104	GAT GTG GGA TCT AGG AAA AGG CCT G
SDHA-R			ACA TGG CTG CCA GCC CTA CAG A
BACT-F	60	157	CAT CGC GGA CAG GAT GCA GAA A
BACT-R			CCT GCT TGC TGA TCC ACA TCT GCT
18S-F	60	123	GCA ATT ATT CCC CAT GAA CG
18S-R			GGC CTC ACT AAA CCA TCC AA

All taken from (Anstaett et al., 2010), except 18S primer sequences (Balacescu et al., 2011).

2.6 RT^2 Profiler PCR Array System

2.6.1 cDNA synthesis

RT^2 First Strand Kit (Qiagen, West Sussex, UK) was used to synthesise cDNA for use with the PCR array as it includes an external RNA control which is necessary for assessment of the reverse-transcription control on the RT^2 Profiler PCR Array. Total RNA extracted from bovine explants (section 2.2.3) was pooled to create a representative sample for either unloaded, 2.5MPa or 7MPa loaded explants. From each set (n=6) equal amounts of RNA (200ng) was taken to create the pooled sample. Following the manufacturer's protocol, 500ng of pooled RNA was mixed with 2µl of genomic DNA elimination buffer (GE buffer). RNase-free water was then added to bring the total volume to 10µl. The reaction was placed in the Prime Techne thermocycler (Bibby Scientific Limited, Staffordshire, UK) and incubated for 5 minutes at 42°C followed by placement on ice for 1 minute. The reverse transcription mix composed of 4µl of 5× BC3 buffer, 1µl of Control P2 buffer, 2µl RE3 Reverse Transcriptase Mix and 3µl of RNase-free water was added to each sample and mixed by pipetting. The reaction was then placed in the thermocycler and incubated at 42°C for 15 minutes. The reaction was terminated by incubation at 95°C for 5 minutes followed by the addition of 91µl of RNase-free water. Samples were then stored at -20°C.

2.6.2 WNT RT^2 Profiler PCR Array

A custom-designed bovine-specific WNT RT^2 Profiler PCR Array (Qiagen, West Sussex, UK) was used to assess the expression of WNT related genes. The PCR array is comprised of a 96-well qPCR plate which has 84 WNT related genes and 12 wells which contain housekeeping genes, positive controls and reverse transcription controls. In a loading reservoir, 1350µl 2× RT^2 SYBR® Green Mastermix (Qiagen, West Sussex, UK), 102µl of cDNA and 1248µl RNase-free water were mixed and 25µl pipetted into each well using a multi-channel pipette. Reactions were performed using the Mx3000P® QPCR System and MxPro QPCR software (Stratagene, Cambridge, UK). The PCR array was performed under the following conditions: 1 cycle of 10 minutes at 95°C to activate HotStart DNA *Taq* Polymerase and denature cDNA, and 40 cycles of 15 seconds at 95°C for melt curve analysis, and 1 minute at 60°C for

annealing/extension step. Transcript levels of WNT related genes were analysed using the RT² Profiler PCR Array Data Analysis software (Qiagen, West Sussex, UK). Gene targets were normalised to a panel of housekeeping genes selected automatically by the software. A single array plate was used per experimental condition and three independent experiments were conducted per condition to confirm the consistency of results obtained.

2.6.2.1 Validation of WNT PCR array

Results from WNT PCR arrays were validated by RT^2 qPCR Primer Assays (Qiagen, West Sussex, UK) to confirm reliability and accuracy of the PCR array results. A selection of fifteen WNT related genes were chosen based on two criteria: [1] at least a 2-fold difference in gene expression between the loading regimens at defined time points, and [2] a relevance to cartilage homeostasis or have potential association with OA pathology as reported in the literature. Primers (sequences not made available by Qiagen) for the selected genes were used to run all individual samples. cDNA was synthesised using 500ng of RNA following the same protocol as previously described (section 2.4.1). The qPCR reaction consisted of 12.5µl RT^2 SYBR® Green Mastermix, 1µl of cDNA, 1µl of the respective RT^2 Primer assay (0.4µM) and 10.5µl of RNase-free water. The qPCR reaction was run under the same conditions as previously described (section 2.4.2). Transcripts were quantified using the $2^{-\Delta\Delta CT}$ method and normalised to the housekeeping genes SDHA and YWHAZ.

2.7 Statistical analysis

All data is representative of three independent experiments unless stated otherwise. QPCR data are presented as mean ± SD after normalisation to the geomean of YWHAZ and SDHA relative to the unloaded control explants (n=6-8). The distribution of the data was analysed using the Anderson-Darling test to confirm the normality of the data and differences in variances tested using Bartlett's test (Minitab 16). Data that was not normal or of equal distribution was subject to log transformation. Two-way analysis of variance (ANOVA) (Minitab 16) was performed to determine the significance of mechanical load on gene expression. Results were considered statistically significant at $P \leq 0.05$. Data

points which were two standard deviations from the mean were considered outliers and removed from the data set.

Chapter 3

Mechanoregulation of WNT signalling in primary articular chondrocytes

3.1 Backgound

Mechanical load induces progressive structural and compositional alterations in the matrix of articular cartilage over time. These alterations may involve maintaining the homeostatic balance of the tissue, however if they are deleterious, then accumulation of these changes may lead to the development of degenerative diseases such as OA. As a result of OA, the cartilage matrix becomes compromised and unable to resist the mechanical forces exerted on the tissue as a result of everyday movement. One of the hallmarks of OA is the tendency of tissue to lose its morphological integrity (Kamineni et al., 2012). The effect of mechanical load on OA progression is largely unknown. The studies that do exist have mostly focused on investigating the effect of compression because it is the predominant force experienced by the articular joint at the gross level (Kamineni et al., 2012, Buschmann et al., 1995, Buschmann et al., 1996, Knight et al., 2006). However, at the cellular level chondrocytes are likely to be exposed to different types of loading including compressive, hydrostatic, shear and tensile strain.

Tensile strain is predominantly experienced at the articulating surface of cartilage. However, due to the differential zonal composition of the matrix it is likely that chondrocytes are loaded by compression and tension in different directions (Kamineni et al., 2012). Alterations in matrix composition, such as in OA, results in changes in the tensile modulus and hence the ensuing tensile strain that chondrocytes are exposed to (Mawatari et al., 2010). Chondrocytes embedded near regions containing fissures or cracks on the articulating surface are exposed to high tensile strain compared to intact areas (Vanderploeg et al., 2004). The increase in tensile strain may contribute to the propagation of cartilage degeneration. Due to chondrocytes being the primary cell type involved in regulating matrix turnover, it is important to understand the effect of tensile strain on chondrocyte metabolism with respect to cartilage homeostasis (Mawatari et al., 2010).

In vitro studies have demonstrated that chondrocyte metabolism is altered in response to various magnitudes of tensile strain and frequencies. In a fibrin gel culture system, application of 10% and 20% tensile strain displacement (1Hz)

for 48 hours repressed proteoglycan production in chondrocytes, whereas lesser strains had no effect (Connelly et al., 2004). Similarly, the application of high tensile stress (17 kPa, 30 cycles/min) reduced proteoglycan synthesis in chondrocytes, concomitant with a significant up-regulation in the expression of MMP-1, MMP-3 and MMP-9 (Honda et al., 2000). Furthermore, a study by Huang et al. reported that in response to 10% cyclic tensile strain (0.5 Hz, 3 hours), there was an initial up-regulation of anabolic genes e.g. collagen type II and aggrecan (Huang et al., 2007). However, after 12 hours of loading, expression of anabolic genes were significantly down-regulated, whereas MMP-1 transcription was elevated (Huang et al., 2007). These results suggest that chondrocytes transiently express anabolic genes in an attempt to adapt to mechanical stress and initiate repair, however prolonged exposure results in an alteration in chondrocyte metabolism (Huang et al., 2007).

In addition to the magnitude of strain applied, the frequency of strain was also observed to contribute to an alteration in chondrocyte behaviour. The application of a high frequency, irrespective of the magnitude of tensile strain, induced a catabolic response through the expression of inflammatory mediators and MMPs, and a reduction in proteoglycan synthesis (Honda et al., 2000, Fujisawa et al., 1999, Fukuda et al., 1997). In contrast, the application of low magnitude and frequency of strain promoted an anabolic response by increasing proteoglycan production (Fukuda et al., 1997).

Overall, the outcomes of these studies show that chondrocytes are responsive to tensile strain, and as a result alter their metabolic activity to create a matrix which is sufficient to withstand the stress exerted on it by mechanical load. All of these studies mentioned previously, have monitored the changes in matrix-related genes. However, tensile strain can additionally stimulate various pathways such as WNT signalling as observed in endothelial cells, osteoblasts and osteocytes (Balachandran et al., 2011, Case et al., 2008, Lau et al., 2013).

In articular cartilage, WNT signalling has been demonstrated to be a possible mediator in cartilage degeneration i.e. OA (section 1.5.1 and 1.5.2). Therefore, it is important to determine the mechano-responsiveness of WNT signalling due to abnormal mechanical load being a major risk factor in OA.

Analysing the effect of mechanical load on WNT signalling activation may assist in elucidating the initial events that lead to OA pathophysiology. Therefore, a preliminary study previously performed in our laboratory demonstrated activation of the canonical WNT pathway in high density primary chondrocytes exposed to physiological tensile strain (7.5%, 1Hz, 30 minutes), as observed by the partial translocation of β-catenin to the nucleus (Thomas et al., 2011). A physiological strain is determined by assessment of anabolic and catabolic genes mRNA levels. If the levels of catabolic to anabolic genes are relatively in balance then that regime is deemed to be physiological. The purpose of this chapter was to validate the previous *in vitro* findings, and furthermore determine whether the magnitude of strain, and/or the period of loading influenced canonical WNT signalling in primary chondrocytes.

3.2 Results

3.2.1 Canonical WNT signalling is activated in response to physiological tensile strain in chondrocytes

Tensile strain (7.5% 1Hz) was applied to high-density primary chondrocytes for 1, 2 or 4 hours to determine if canonical WNT signalling was activated by physiological tensile strain. Activation of WNT signalling in chondrocytes was assessed at the protein level by the presence of nuclear translocation of β-catenin using confocal microscopy. After 1 hour, unstrained (control) chondrocytes exhibited weak cytoplasmic β-catenin staining (Figure 3-1A), whereas in contrast, tensile strain induced a transient β-catenin nuclear translocation with very minimal cytoplasmic β-catenin (Figure 3-1D). The maximum response, as illustrated by nuclear β-catenin translocation, was observed in chondrocytes exposed to 2 hours of tensile strain (Figure 3-1E), as confirmed by quantification of nuclear staining intensity by ImageJ (Figure 3-1B). After 4 hours of tensile strain (Figure 3-1F), β-catenin became predominantly cytoplasmic returning to near basal levels as reflected in the unstrained control cells (Figure 3-1C).

3.2.2 Physiological strain induces maximal β-catenin nuclear translocation in chondrocytes

Different magnitudes of strain (7.5%, 10% and 14% strain, 1Hz) were applied to primary chondrocytes for 2 hours to determine whether there was a strain-dependent effect on β-catenin nuclear translocation. As observed previously, β-catenin was localised to the cytoplasm in chondrocytes not exposed to tensile strain (Figure 3-2A and E). Interestingly, maximal β-catenin nuclear translocation was observed within the reported physiological range of 7.5% (Figure 3-2B and F) and 10% (Figure 3-2C and G), whereas at the higher strain

(14%) β-catenin translocation was reduced and was predominantly localised in the cytoplasm (Figure 3-2D and H).

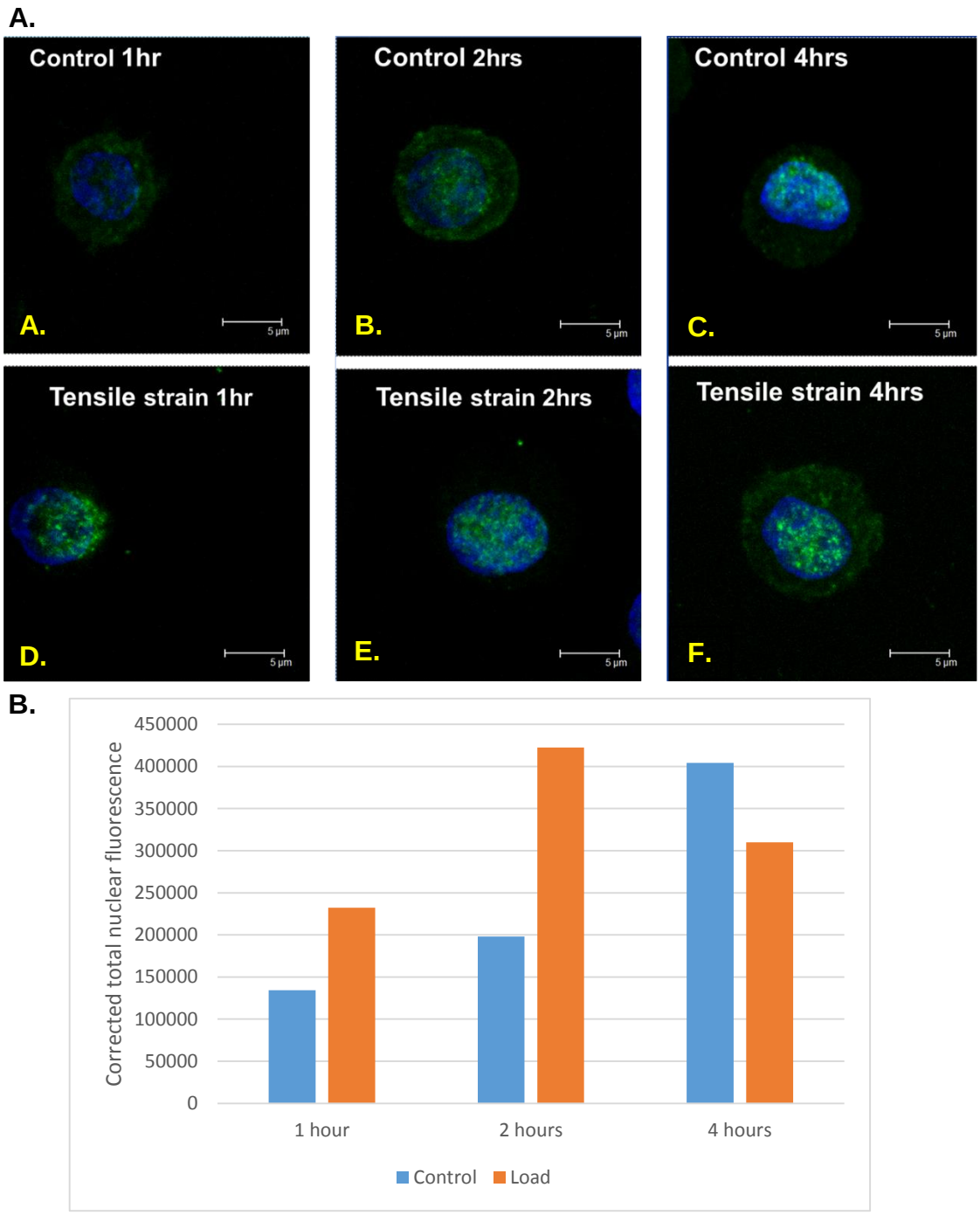

Figure 3-1: Effect of tensile strain (7.5%, 1Hz) on β-catenin localisation in primary articular chondrocytes loaded for 1, 2 or 4 hours. A) Cells were labelled with monoclonal anti-β-catenin antibody in conjunction with goat anti-mouse FITC-conjugated secondary antibody (green): nuclei were counterstained with DAPI (blue) and visualised using confocal microscopy. Representative 3D reconstructions are presented [scale bar = 5µm]. B) Quantification of nuclear staining intensity using ImageJ.

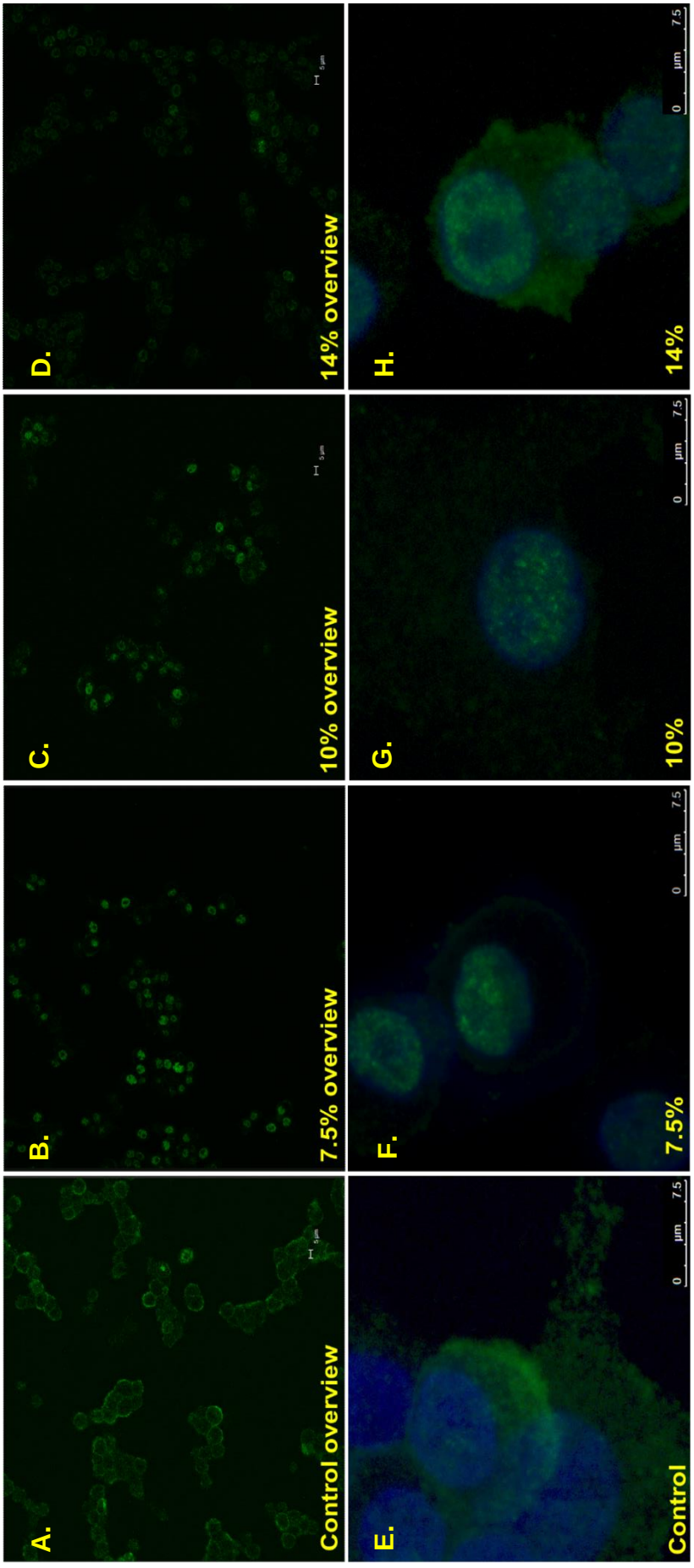

Figure 3-2: Effect of tensile strain (7.5%, 10% and 14%, 1Hz) on β-catenin localisation in primary articular chondrocytes loaded for 2 hours. Cells were labelled with monoclonal anti-β-catenin antibody in conjunction with goat anti-mouse FITC-conjugated secondary antibody (green): nuclei were counterstained with DAPI (blue) and visualised using confocal microscopy. Representative 3D reconstructions are presented [scale bar = 7.5μm].

3.2.3 WIF-1 expression is enhanced in response to levels of strain

WIF-1 expression was investigated as recent studies have implicated its involvement in fine-tuning WNT signalling and regulating cartilage turnover (Stock et al., 2013). WIF-1 protein localisation was investigated in primary chondrocytes subjected to 7.5%, 10% and 14% strain (1Hz) for 2 hours. In unstrained (control) chondrocytes, WIF-1 staining was localised to the cytoplasm (Figure 3-3A and E). In contrast, in chondrocytes subjected to 7.5% (Figure 3-3B and F) or 14% strain (Figure 3-3D and H), WIF-1 was also localised to the cytoplasm but expression appeared to be higher. It is appreciated that immunofluorescence microscopy is not quantitative, but having been processed together, the low power images suggest more WIF1 localised in the cytoplasm of cells exposed to 7.5% (Figure 3-3B) or 14% strain (Figure 3-3D) compared to the unstrained cells (Figure 3-3A). Surprisingly, WIF1 localisation and staining intensity in the 10% strained cells (Figure 3-3C and G) appeared comparable to the unstrained cells.

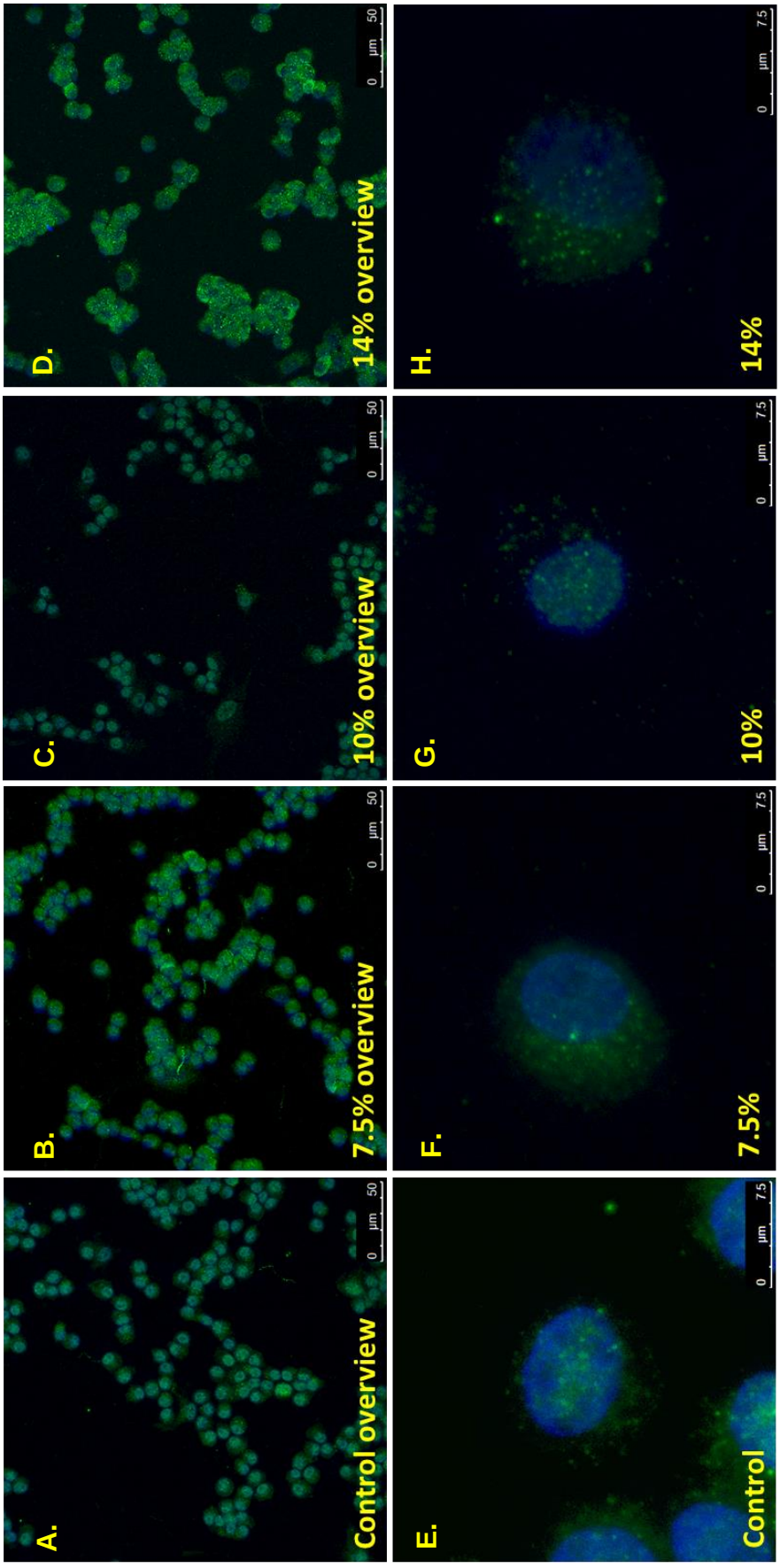

Figure 3-3: Effect of tensile strain (7.5%, 10% and 14%, 1Hz) on WIF-1 localisation in primary articular chondrocytes loaded 2 hours. Cells were labelled with polyclonal anti-WIF-1 antibody in conjunction with goat anti-rabbit FITC-conjugated secondary antibody (green): nuclei were counterstained with DAPI (blue) and visualised using confocal microscopy. Representative 3D reconstructions are presented [scale bar = 7.5µm].

3.3 Discussion

A primary high-density chondrocyte monolayer system was adopted as a preliminary screen to confirm nuclear translocation of β-catenin, which is indicative of canonical WNT signalling activation. Chondrocytes were mechanically stimulated by application of a 7.5% tensile strain (1 Hz) for 1, 2, or 4 hours. This regime was selected as it had previously been reported to be representative of physiological load (Guterl et al., 2009, Perera et al., 2010); furthermore, our laboratory had previously reported the partial nuclear translocation of β-catenin in primary chondrocytes in response to this loading regime (analysed 4 hours post-cessation of a 30 minute stimulation) (Thomas et al., 2011). β-catenin was found to be maximally translocated after 2 hours of strain application, in comparison to the localisation profiles of chondrocytes subjected to either 1 or 4 hours of tensile load.

Having identified a loading timeframe in which β-catenin appeared to be maximally translocated to the nucleus i.e. confirmation of mechano-regulation of the WNT pathway, the effect of higher strains on WNT signalling were further investigated to determine if there was a load-induced threshold of activation. For this, tensile strains representing 7.5%, 10% and 14% elongation (1 Hz) were applied to the chondrocytes for 2 hours. Nuclear translocation of β-catenin primarily occurred in chondrocytes exposed to the 7.5%-10% elongation, reported to be representative of a normal to high physiological load; limited cytoplasmic β-catenin was detected in these cells. However, in response to 14% elongation, considered a damaging strain, there was an increase in both cytoplasmic and nuclear β-catenin, possibly implying enhanced WNT signalling. The difference in β-catenin localisation observed between the physiological (7.5-10%) and damaging non-physiological strains (14%) may arise due to the requirement of the chondrocyte to maintain homeostasis, as it is well established that WNT signalling is necessary to maintain this critical function in cartilage (Zhu et al., 2008, Zhu et al., 2009). As a result, transient activation of β-catenin signalling is necessary to mediate the balance in anabolic and catabolic processes, as it is an effector protein which influences several downstream targets including the early response genes and MMPs (Vidya Priyadarsini et al., 2012). Consequently, the higher levels of β-catenin signalling observed in

response to the non-physiological strain, which may reflect sustained activation of this pathway, could result in the increased expression of degradative enzymes such as the MMPs, thus tipping the balance towards catabolic processes. Furthermore, localisation of WIF-1, an inhibitor of WNT signalling, was assessed using confocal immunofluorescence analysis, to examine how inhibitors of the WNT molecules respond to different levels of strain. As demonstrated, the localisation of WIF-1 mirrored that of β-catenin, whereas in response to the 10% regime, WIF-1 staining appeared nuclear; this pattern of expression was slightly surprising as WIF-1 is a secreted protein (Wissmann et al., 2003). The increase in WIF-1 expression may have occurred to neutralise load-induced canonical WNT signalling as a potential negative feedback mechanism, but this requires further investigation. WIF-1 prevents cartilage degradation through regulation of canonical WNT signalling (Stock et al., 2013). The induction of experimental OA through crossbreeding WIF-1 deficient mice with TNFα-transgenic mice demonstrated that WIF-1 deficiency increased cartilage degradation in comparison to TNFα-transgenic mice as a result of increased canonical WNT signalling by TNFα (Stock et al., 2013).

Based on these results, it was clear that tensile strain activated WNT signalling in high-density primary chondrocytes, confirming previous observations (Thomas et al., 2011). Furthermore, the data demonstrated that activation of canonical WNT signalling was dependent on the magnitude and duration of strain applied. However, one of the major limitations of the monolayer chondrocyte model is that the cells have no surrounding ECM. As many mechano-sensing events occur via matrix to cell interactions, it was imperative to confirm these novel observations in a more biologically relevant model.

3.4 Summary

- Canonical WNT signalling is activated in response to physiological tensile strain, and maximum nuclear translocation was demonstrated to be at 2 hours of strain.
- Canonical WNT signalling is differentially regulated by magnitude of strain as shown by β-catenin and WIF-1 expression.

Chapter 4

Characterisation of physiological and degradative loading regimes on articular cartilage metabolism

4.1 Background

In articular cartilage, mechanical loading regulates homeostatic tissue remodelling processes. In response to mechanical loading, chondrocytes are able to initiate biosynthetic or catabolic processes depending on the extent of force applied (Chen et al., 2013). Physiological loading on cartilage is known to promote a balance between anabolic and catabolic processes. As a result, cartilage tissue integrity and function are maintained whilst promoting turnover of new tissue (Nicodemus and Bryant, 2010). However, when the mechanical load exceeds what is considered to be physiological, catabolic processes dominate the tissue remodelling process leading to cartilage degeneration (Bader et al., 2011). By taking into consideration these observations, many loading studies have been conducted *in vitro* with different durations and magnitudes of load to determine what constitutes physiological load and to understand the downstream biological effects. In many of these reported studies, cartilage explants were loaded for at least 3 hours to several days using static (Fitzgerald et al., 2004) or dynamic loading regimes (Kurz et al., 2001). Static loading of bovine cartilage explants (to a final compressive strain of 50%) for 8 hours elevated expression of aggrecan, collagen type II and link protein mRNA (Fitzgerald et al., 2004); however, the expression of these genes returned to below basal levels after 24 hours of static load (Fitzgerald et al., 2004). Furthermore, a study where bovine cartilage explants were cyclically loaded at 4.1 MPa (0.5Hz) for 1-20 hours showed enhanced proteoglycan synthesis (Kiraly et al., 1998). These studies demonstrated that mechanical forces elicit biosynthetic responses in cartilage.

Previously, our laboratory demonstrated that bovine cartilage explants subjected to a peak load of 2.5MPa (1Hz) for 15 minutes was capable of inducing the expression of both anabolic and catabolic genes, thereby promoting tissue homeostasis (unpublished data). Furthermore, when higher loads >5MPa were applied to the cartilage, a predominantly catabolic phenotype was observed as exemplified by increased MMP and ADAMTS transcription. These observations were in line with other studies that reported up-regulation of catabolic genes in bovine cartilage explants following a repetitive impact load of at 5MPa 0.3 Hz for 2 hours (Chen et al., 2001), whereas application of loads below 5MPa induced expression of anabolic genes. Application of a cyclic load (1MPa, 0.5 Hz, 3 days)

on bovine cartilage explants demonstrated an increase in proteoglycan synthesis (Steinmeyer et al., 1999, Fehrenbacher et al., 2003).

In addition to the magnitude of load, the period of time post load was also investigated to determine the optimal time frame in which mechano-sensitive target genes were regulated. To accurately assess mRNA levels of these target genes, appropriate reference genes were required. Reference genes, otherwise referred to as housekeeping genes, are genes in which their expression does not alter in response to experimental treatments. Commonly used housekeeping genes include 18S ribosomal RNA, β2-microglobulin, β-actin and glyceraldehyde-3-phosphate dehydrogenase (GAPDH) (Thellin et al., 1999, Dheda et al., 2005). However, over the past decades, these commonly used housekeeping genes were utilised in many loading studies without considering their relative stability in response to a mechanical stimulus. As a result, normalising data to inappropriate reference genes could lead to false positive or negative results as has been discovered in other tissue types and stimuli (Dheda et al., 2004, Dheda et al., 2005). Methodologies have rapidly developed and software such as Bestkeeper or NormFinder, which assess reference gene stability relative to the experimental parameter(s) is now routinely used to determine the most appropriate reference genes for normalisation of qPCR data (Anstaett et al., 2010).

As a result, the aims of this experimental chapter were: i) to identify appropriate reference genes that were stable in cartilage explants exposed to load, ii) characterise physiological and degradative loading regimes based on gene expression profiles, iii) determine the optimal period post-load to monitor early mechanically-regulated transcriptional changes.

4.2 Results

4.2.1 Characterisation of physiological and degradative loading regimes

A preliminary study was conducted to establish loading regimes, in articular cartilage, that either promoted an anabolic or homeostatic response (termed “physiological”) or induced a predominantly catabolic response (termed “degradative”) where increased transcriptional expression of proteolytic enzymes was observed. Explants were subjected to loading regimes of 2.5MPa, 5MPa and 7MPa (1Hz, 15 minutes) and analysed 24 hours post-cessation of load, by characterising changes in gene expression.

4.2.1.1 Confirmation of RNA quality

RNA integrity was evaluated using the Agilent 2100 Bioanalyzer to confirm quality and concentration prior to quantitative analyses. As shown on a representative gel (Figure 4-1A and B), all experimental samples comprised distinctive 28S and 18S ribosomal bands with low background; a RIN number of $\geq$8 indicative of intact RNA was obtained for all of the experimental RNA samples confirming suitability for downstream processing.

A.

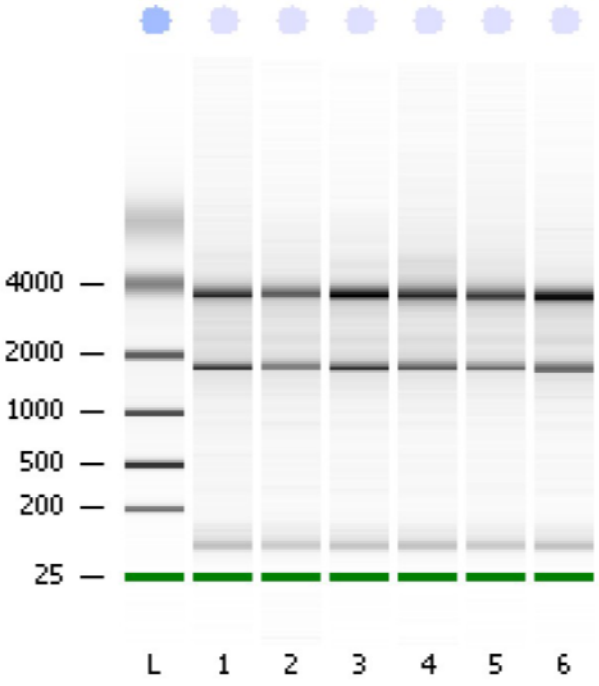

B.

Lane	RIN
1	8.4
2	8.1
3	8.7
4	8.4
5	8.4
6	8.9

Figure 4-1: Confirmation of RNA quality using the Bioanalyzer.

A) Representative gel depicting distinct 28S (top) and 18S (bottom) ribosomal RNA bands from experimental cartilage samples. B) Table showing RIN values relating to the corresponding lanes of the gel.

4.2.1.2 Selection of candidate reference genes for gene expression analysis

Identification of stable reference genes i.e. housekeeping genes for normalisation of target gene expression in response to different loading regimes is essential for interpreting data generated by quantitative PCR. Eight endogenous bovine reference genes were selected from a study by Anstaett et al. (2010) to identify the best combination of reference genes to use for qPCR analysis (Anstaett et al., 2010). To identify the most stable reference genes for the cartilage explant model system, samples from three independent experiments, utilising material from explants which had been subjected to no load or loads of 2.5MPa, 5MPa and 7MPa were tested using qPCR. The stability of these reference genes was evaluated using RefFinder software which integrates the main programmes available (geNorm, Normfinder, Bestkeeper and the comparative ΔCt method) to assess the most suitable to use for normalisation of qPCR data (Liang et al., 2014). Each programme ranks the genes by assigning an appropriate value and calculates the geometric mean of their values to give a final ranking of which gene is the most stable within an experimental data set (Liang et al., 2014). Genes assigned with high values are least stable, whereas genes with values close to one are considered most stable. Based on the outcome of RefFinder, the best combination of housekeeping genes which were most consistent across all of the experimental loading variables were Succinate Dehydrogenase subunit A (SDHA: stability value of 1.19) and tyrosine 3 monooxygenase/tryptophan 5 monooxygenase activation protein—zeta polypeptide (YWHAZ: stability value of 3.22) (Figure 4-2). The least stable reference genes across the experimental loading variables were glyceraldehyde-3-phosphate dehydrogenase (GAPDH: stability value of 7.24) and hypoxanthine guanine phosphoribosyltransferase (HRPT: stability value of 7.74) (Figure 4-2). After confirming the best combination of housekeeping genes, standard curves were generated using 10-fold dilutions of pooled cDNA samples from each experimental set to confirm PCR efficiency. Both SDHA and YWHAZ had PCR efficiencies of 94.4% and 99.4% respectively (Figure 4-3A and B), which is within the accepted range of 90 – 110%. Therefore, experiments were subsequently

normalised to the geometric mean of SDHA and YWHAZ Ct values for each independent data set.

Method	Ranking Order (Better--Good--Average) 1	2	3	4	5	6	7	8
Delta CT	sdha	ppia	rpl4	bactin	18s	ywhaz	GAPDH	hprt
BestKeeper	sdha	18s	ywhaz	bactin	ppia	rpl4	hprt	GAPDH
Normfinder	rpl4	sdha	ppia	bactin	18s	ywhaz	GAPDH	hprt
Genorm	ywhaz | sdha		18s	bactin	ppia	rpl4	GAPDH	hprt
Recommended comprehensive ranking	**sdha**	**ywhaz**	**rpl4**	**18s**	**ppia**	**bactin**	**GAPDH**	**hprt**

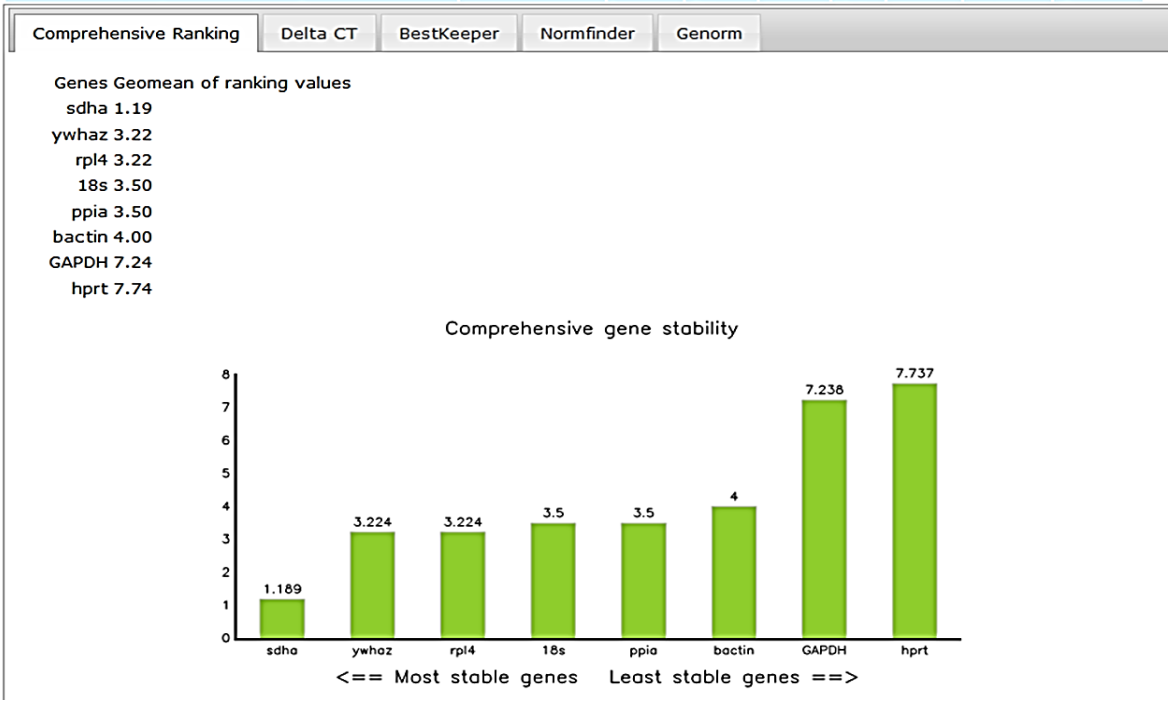

Figure 4-2: Results output from RefFinder software ranking the most stable reference genes (lowest number) to the most unstable (highest number). The output also includes results from other well-known softwares (described in section 2.5.3) that are used to identify the most appropriate reference genes. The comprehensive ranking order takes into consideration the results of all of the software outputs. Genes selected for all experimental data normalisation were based on the comprehensive ranking results.

A.

SDHA

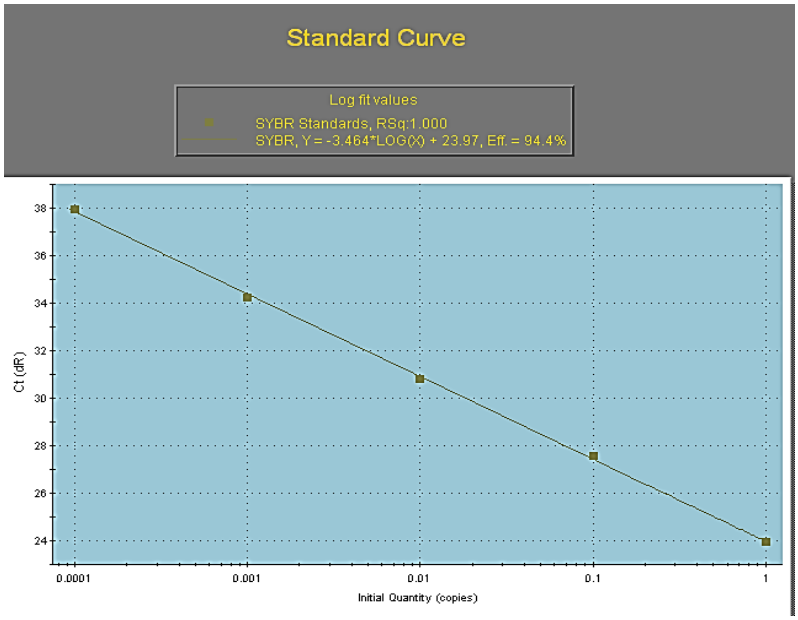

B.

YWHAZ

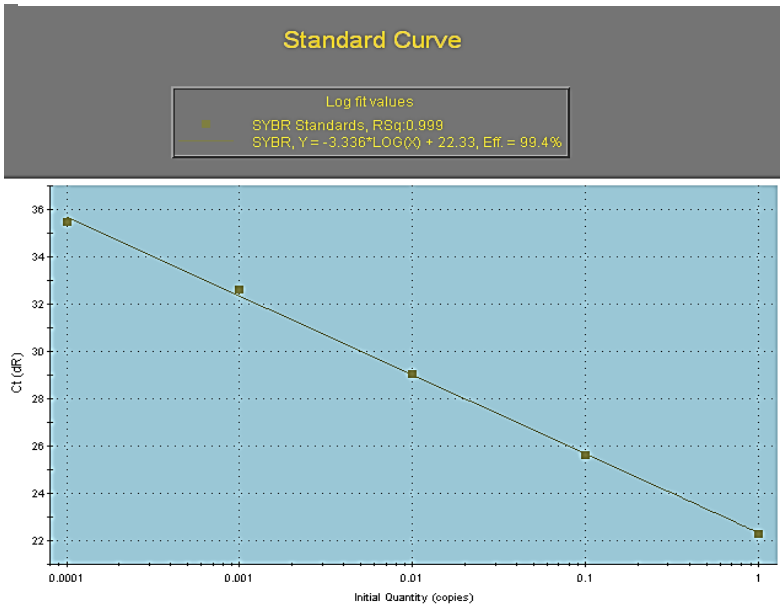

Figure 4-3: Representative quantitative PCR standard curves of A) SDHA and B) YWHAZ performed on pooled cDNAs from unloaded cartilage explants and explants subjected to 2.5, 5 and 7MPa loads. The standard curves demonstrate that the efficiencies of the quantitative PCR reaction are within the accepted 95-110% range which is necessary for accurate data interpretation.

4.2.1.3 Matrix gene analysis to establish physiological and degradative loading regimes

Characterisation of physiological and degradative loading regimes was conducted on explants subjected to a cyclic load of either 2.5MPa, 5MPa or 7MPa (1Hz, 15 minutes). Cartilage was harvested 24 hours post-load to assess mechanical responses at the transcriptional level. qPCR data presented was initially normalised to the reference genes SDHA and YWHAZ, and further normalised to the unloaded control explants.

- ***2.5MPa regime*:** Analysis of key matrix genes involved in anabolic and catabolic processes demonstrated that after 15 minutes at a peak load of 2.5MPa, there was no significant alteration in either aggrecan (Figure 4-4A) or collagen type II mRNA expression (Figure 4-4C). However, there was significant down-regulation in the transcription of catabolic genes including MMP-9 (6.25-fold, $p<0.01$; Figure 4-5C) and MMP-13 (5.5-fold, $p<0.001$; Figure 4-5E). Of the two ADAMTS genes, only ADAMTS-4 appeared to be sensitive to 2.5MPa, with a significant increase in mRNA expression (2.2-fold, $p<0.01$; Figure 4-6A); ADAMTS-5 transcription remained unchanged (Figure 4-6C). Interestingly, there were subtle elevations in TIMP-1 (1.6-fold, $p<0.01$) and TIMP-3 (1.8-fold, $p<0.05$) mRNA levels (Figure 4-7A and C).

- ***5MPa regime:*** As observed at 2.5MPa, at 5MPa, mRNA levels of the ECM genes aggrecan (Figure 4-4A) and collagen type II (Figure 4-4C) remained comparable to levels detected in the unloaded control explants. Furthermore, at 5MPa, transcripts of the catabolic matrix genes were significantly elevated including MMP3 (2.5-fold, $p<0.05$; relative to control, 4.4-fold, $p<0.001$ relative to 2.5MPa Figure 4-5A), and ADAMTS4 (5.1-fold, $p<0.001$ relative to control; 2.4-fold, $p<0.01$ Figure 4-6A); again, ADAMTS5 did not alter appreciably in response to this higher load (Figure 4-6C). Surprisingly, both MMP9 (7-fold, $p<0.001$; Figure 4-5C) and MMP13 (5.5-fold, $p<0.001$; Figure 4-5E) mRNA levels were significantly down-regulated after cartilage explants were exposed to a 5MPa load (1Hz, 15mins). In a load-dependent manner, transcription of TIMP-1 (2.6-fold, $p<0.001$ relative to control; 1.6-fold, $p<0.01$ relative to 2.5MPa Figure 4-7A)

and TIMP-3 (6-fold, $p<0.001$ relative to control; 4.25-fold, $p<0.001$ relative to 2.5MPa Figure 4-7C) were significantly elevated in response to a 5MPa load.

- ***7MPa regime:*** The highest loading regime utilised in this optimisation study, namely 7MPa, demonstrated similar trends to that observed at 5MPa. Although it appears that the fold change is considerably higher in the cartilage explants in response to 7MPa, an absolute cross-comparison between them could not be performed as they were prepared and analysed independently of the other two regimes conducted; however, potential trends have been alluded to. As observed previously for the other loading regimes, aggrecan (Figure 4-4B) and collagen type II mRNA levels (Figure 4-4D) remained unchanged. As previously observed, MMP3 transcription (6.8-fold, $p<0.001$; Figure 4-5B) was significantly elevated in explants subjected to a 7MPa regime, and appeared to increase in a load-dependent manner. MMP9 and MMP13 levels were not significantly altered (Figure 4-5D and F). Interestingly, 7MPa was the only loading regime that elicited a significant elevation in both the expression of ADAMTS-4 (6-fold, $p<0.001$; Figure 4-6B) and ADAMTS-5 (5.5-fold, $p<0.001$; Figure 4-6D). Furthermore, mRNA expression levels of TIMP-1 (3.6-fold, $p<0.001$; Figure 4-7B) and TIMP-3 (10.2-fold, $p<0.001$; Figure 4-7D) were significantly enhanced compared to the unloaded controls and the explants subjected to the other loading regimes.

Due to the absence of any significant changes in matrix gene expression and a general reduction in MMP transcription, 2.5MPa was selected as a representation of physiological loading. The loading regime of 7MPa was selected to represent degradative load as a result of the significant elevation in mRNA levels of catabolic genes i.e. MMP3, ADAMTS-4 and -5.

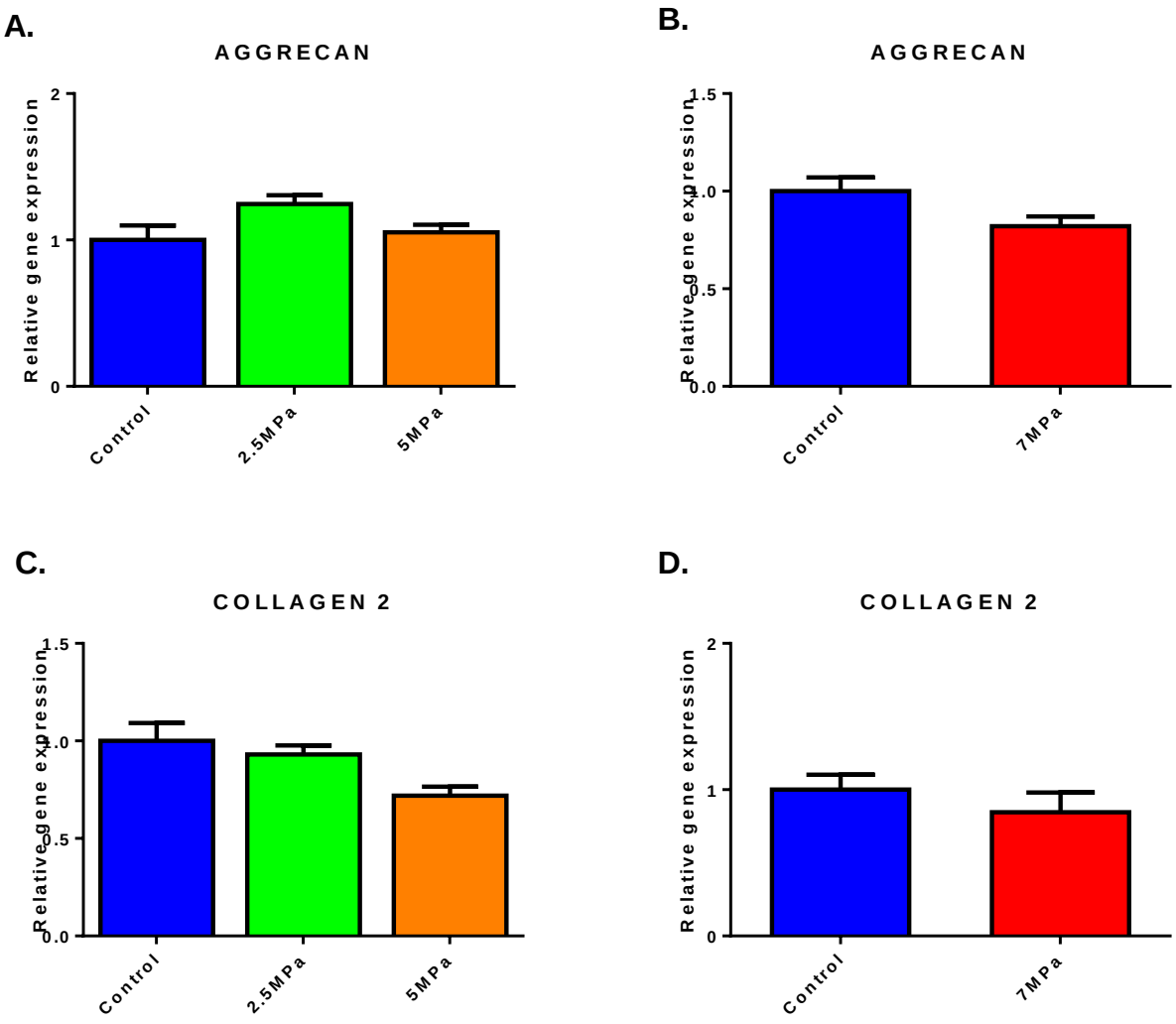

Figure 4-4: mRNA quantification of A, B) aggrecan, and C, D) collagen type II levels in cartilage explants subjected to 2.5 and 5MPa, or 7MPa respectively, where unloaded explants served as controls. mRNA levels were assessed 24 hours post-load using qPCR. All data were normalised to the geometric mean of reference genes SDHA and YWHAZ and relative to the unloaded control. Results presented are mean ± SD. Two graphs for each gene show data of independent experiments. Controls from independent experiments demonstrated no significant differences thus allowing cross comparison between all loading regimes. Statistical analysis was performed using a two way ANOVA with Tukey's post hoc test (n=6).

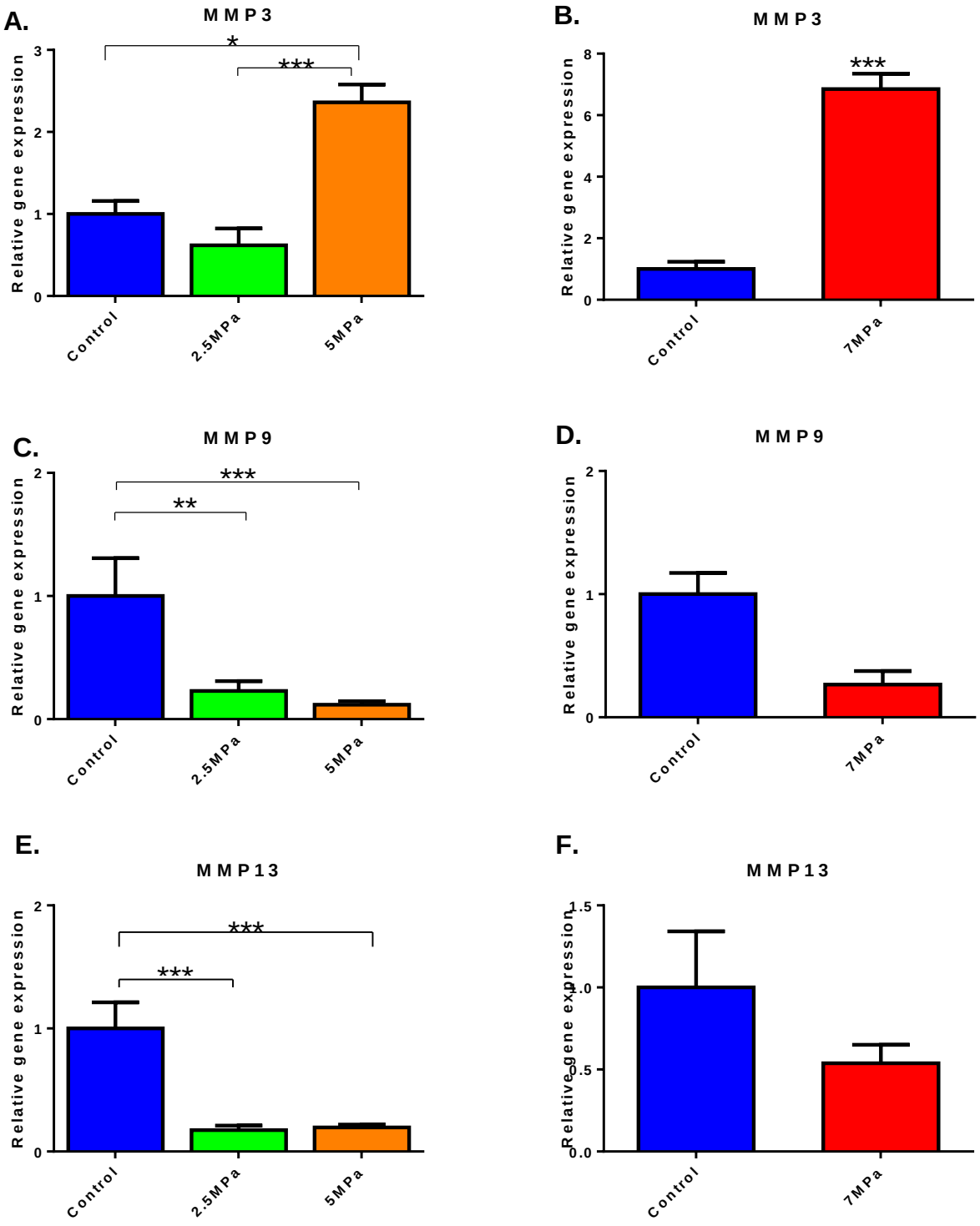
A.
MMP3
Relative gene expression
*
***
Control
2.5MPa
5MPa
B.
MMP3
Relative gene expression
***
Control
7MPa
C.
MMP9
Relative gene expression
***
**
Control
2.5MPa
5MPa
D.
MMP9
Relative gene expression
Control
7MPa
E.
MMP13
Relative gene expression
***
***
Control
2.5MPa
5MPa
F.
MMP13
Relative gene expression
Control
7MPa

Figure 4-5: mRNA quantification of A, B) MMP3, C, D) MMP9, and E, F) MMP13 levels in cartilage explants subjected to 2.5 and 5MPa, or 7MPa respectively, where unloaded explants served as controls. mRNA levels were assessed 24 hours post-load using qPCR. All data were normalised to the geometric mean of reference genes SDHA and YWHAZ and relative to the unloaded control. Results presented are mean ± SD. Two graphs for each gene show data of independent experiments. Controls from independent experiments demonstrated no significant differences thus allowing cross comparison between all loading regimes. Statistical analysis was performed using a two way ANOVA with Tukey's post hoc test (n=6). [*: $p<0.05$, **: $p<0.01$, ***: $p<0.001$]

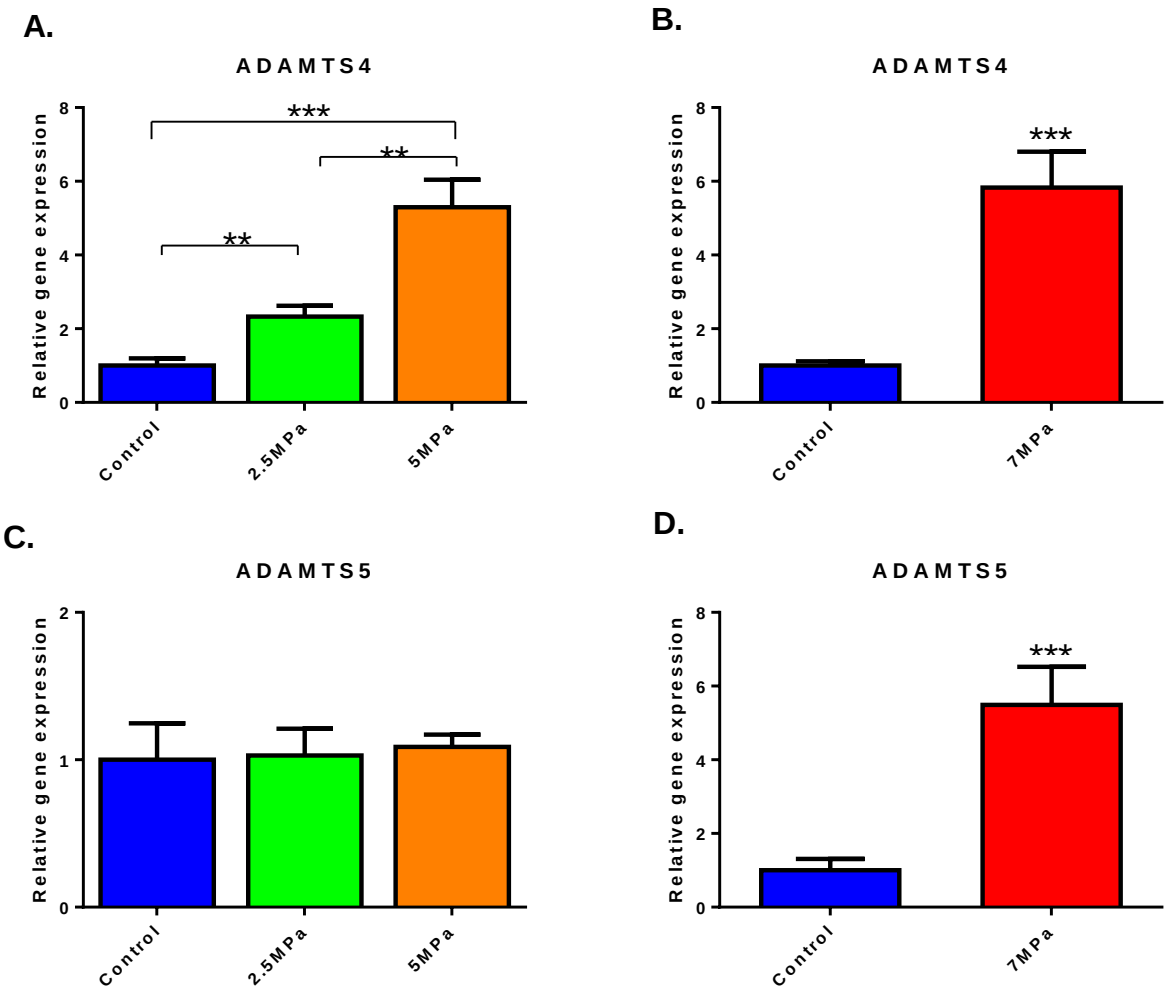

Figure 4-6: mRNA quantification of A, B) ADAMTS4 and C, D) ADAMTS5 levels in cartilage explants subjected to 2.5 and 5MPa, or 7MPa respectively, where unloaded explants served as controls. mRNA levels were assessed 24 hours post-load using qPCR. All data were normalised to the geometric mean of reference genes SDHA and YWHAZ and relative to the unloaded control. Results presented are mean ± SD. Two graphs for each gene show data of independent experiments. Controls from independent experiments demonstrated no significant differences thus allowing cross comparison between all loading regimes. Statistical analysis was performed using a two way ANOVA with Tukey's post hoc test (n=6). [*: $p<0.05$, **: $p<0.01$, ***: $p<0.001$]

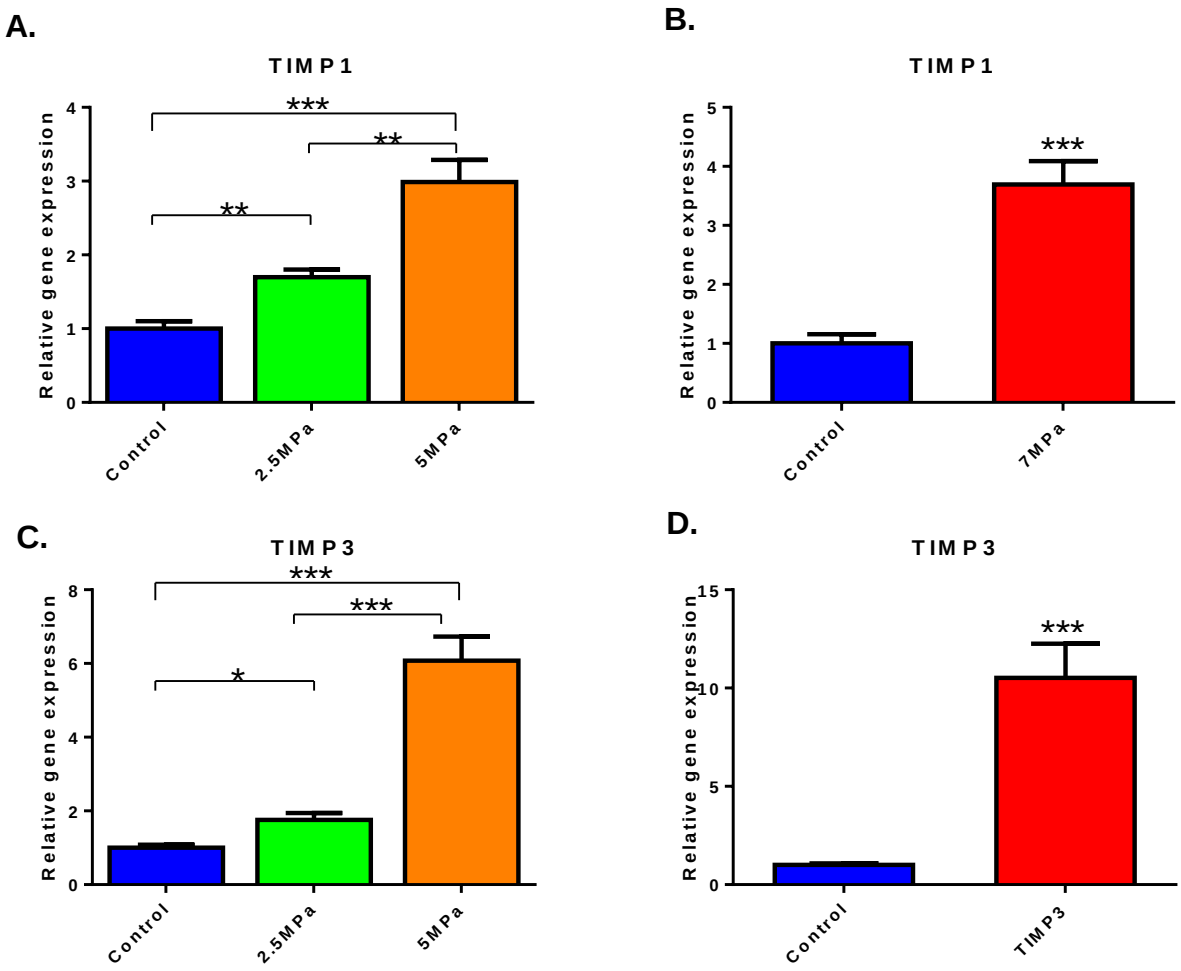

Figure 4-7: mRNA quantification of A, B) TIMP1 and C, D) TIMP3 levels in cartilage explants subjected to 2.5 and 5MPa, or 7MPa respectively, where unloaded explants served as controls. mRNA levels were assessed 24 hours post-load using qPCR. All data were normalised to the geometric mean of reference genes SDHA and YWHAZ and relative to the unloaded control. Results presented are mean ± SD. Two graphs for each gene show data of independent experiments. Controls from independent experiments demonstrated no significant differences thus allowing cross comparison between all loading regimes. Statistical analysis was performed using a two way ANOVA with Tukey's post hoc test (n=6). [*: $p<0.05$, **: $p<0.01$, ***: $p<0.001$]

4.2.1.4 Optimisation of period post-load required to detect differential expression of mechano-responsive genes

Loading regimes that either induced a homeostatic response i.e. physiological (2.5MPa) or a predominantly catabolic response i.e. degradative (7MPa) were optimised with analysis of the transcriptional response initially performed 24 hours post-cessation of load. However, it was then necessary to identify the optimal transcriptional window to monitor gene expression changes downstream of the initial 15 minutes of mechanical stimulus. To identify the most appropriate time to monitor early load-induced changes in gene expression, explants were loaded for 15 minutes as performed previously, but explants were either processed for RNA immediately post-loading or maintained in culture post-load for different periods e.g. 4hrs, 8hrs or 24hrs post-cessation of load prior to mRNA analysis. Gene transcripts were then evaluated to determine the most appropriate time post-cessation of load to monitor mechanically induced gene expression changes. In addition to matrix genes, C-JUN, an early response gene and downstream target of WNT signalling, was also assessed to determine the most appropriate time point post-load to quantify transcriptional changes in WNT signalling genes in subsequent experiments.

- ***2.5MPa*:** Analysis of key matrix genes involved in anabolic and catabolic processes demonstrated that directly post-load and at 4 hours post-cessation of load (2.5MPa, 1 Hz, 15 minutes), many of the genes remained unaffected. However, C-JUN was significantly up-regulated at 4 hours (2.73-fold, $p<0.001$; Figure 4-8A), but returned to basal levels thereafter. Interestingly, aggrecan was initially down-regulated, which was significant at 4hrs (2-fold, $p<0.05$; Figure 4-8C), but then returned to basal expression levels. MMP3 and MMP13 expression were elevated at 8 hours post-load only (2.5-fold, $p<0.01$ and 2.55-fold, $p<0.01$; Figure 4-9A and C), whereas ADAMTSs were not significantly affected (Figure 4-10). In contrast, TIMP3 was significantly up-regulated at 4 (2-fold, $p<0.05$) and 24 hours post-load (2.8-fold, $p<0.00$; Figure 4-11A).

- ***7MPa*:** Overall, under the higher loading regime (7MPa, 1 Hz, 15 minutes), most transcriptional changes were observed primarily at 4 hours post-load. Significantly increased mRNA levels of C-JUN (5.7-fold, $p<0.001$; Figure 4-8B),

MMP3 (6-fold, $p<0.001$; Figure 4-9B), ADAMTS4 (4-fold, $p<0.01$; Figure 4-10B) and TIMP-3 (3.7-fold, $p<0.01$; Figure 4-11B) were observed after 4 hours. In contrast, aggrecan levels were down-regulated (3.7-fold, $p<0.001$; Figure 4-8D). Of the changes observed at 8 hours, most notable were the up-regulation of MMP3 (14.5-fold, $p<0.001$; Figure 4-9B) and TIMP-3 (4.2-fold, $p<0.001$; Figure 4-11B). Mechanically-induced effects observed at the earlier time points were also observed at 24 hours post-load, but the transcriptional changes were not as dramatic. Enhanced expression of MMP3 (3-fold, $p<0.001$; Figure 4-9B), ADAMTS4 (3.3-fold, $p<0.01$; Figure 4-10B) and TIMP3 (4.8-fold, $p<0.001$; Figure 4-11B) were still evident at 24 hours post-load, whereas the other genes returned to constitutive levels comparable with the unloaded controls. MMP13 (Figure 4-9D) and ADAMTS-5 levels (Figure 4-10D) remained unaffected throughout the time course.

Based on these preliminary results, 4 hours post-cessation of load was considered the most appropriate time frame to monitor the mechano-responsiveness of WNT signalling transcription in articular cartilage.

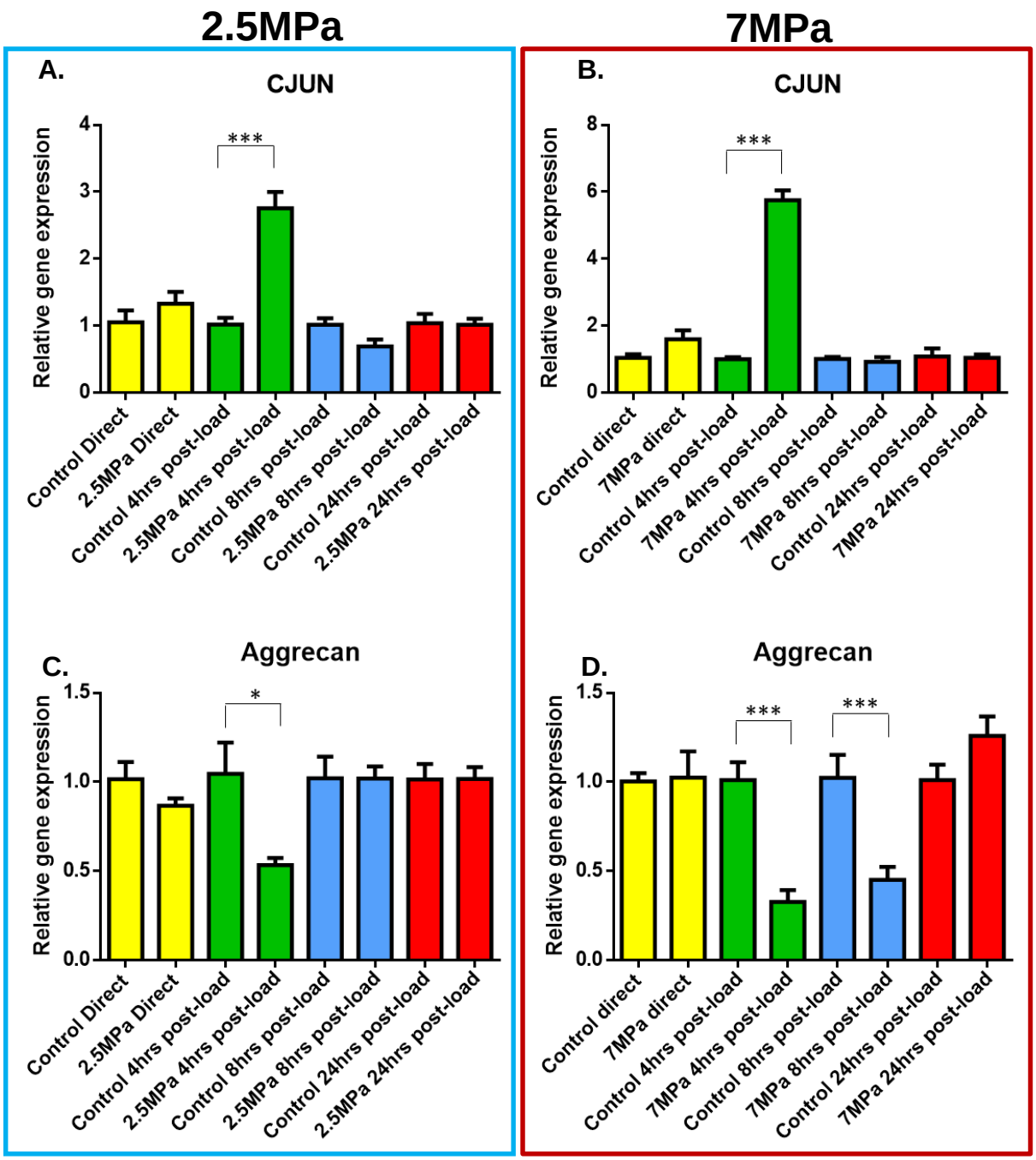

Figure 4-8: mRNA quantification of A, B) C-JUN and C, D) aggrecan levels in cartilage explants subjected to a load of either 2.5MPa or 7MPa (1Hz, 15 minutes), where unloaded explants served as controls. mRNA levels were assessed directly, 4, 8 and 24 hours post-load using qPCR. All data were normalised to the geometric mean of reference genes SDHA and YWHAZ and relative to the unloaded control. Results presented are mean ± SE. Statistical analysis was performed using a two way ANOVA with Tukey's post hoc test (n=4). [*: $p<0.05$, **: $p<0.01$, ***: $p<0.001$]

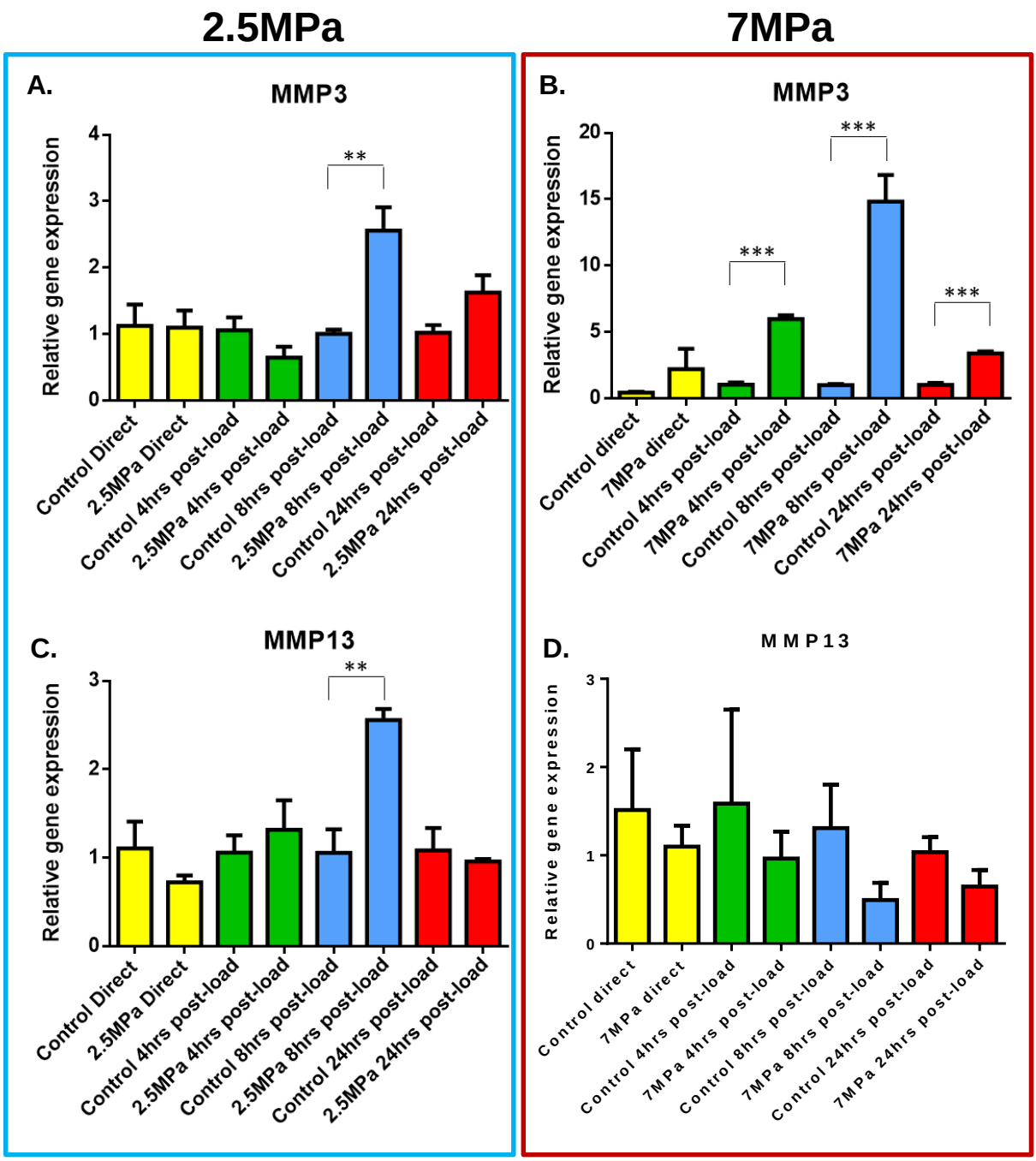

Figure 4-9: mRNA quantification of A, B) MMP3 and C, D) MMP13 levels in cartilage explants subjected to a load of either 2.5MPa or 7MPa (1Hz, 15 minutes), where unloaded explants served as controls. mRNA levels were assessed directly, 4, 8 and 24 hours post-load using qPCR. All data were normalised to the geometric mean of reference genes SDHA and YWHAZ and relative to the unloaded control. Results presented are mean ± SE. Statistical analysis was performed using a two way ANOVA with Tukey's post hoc test (n=4). [*: $p<0.05$, **: $p<0.01$, ***: $p<0.001$]

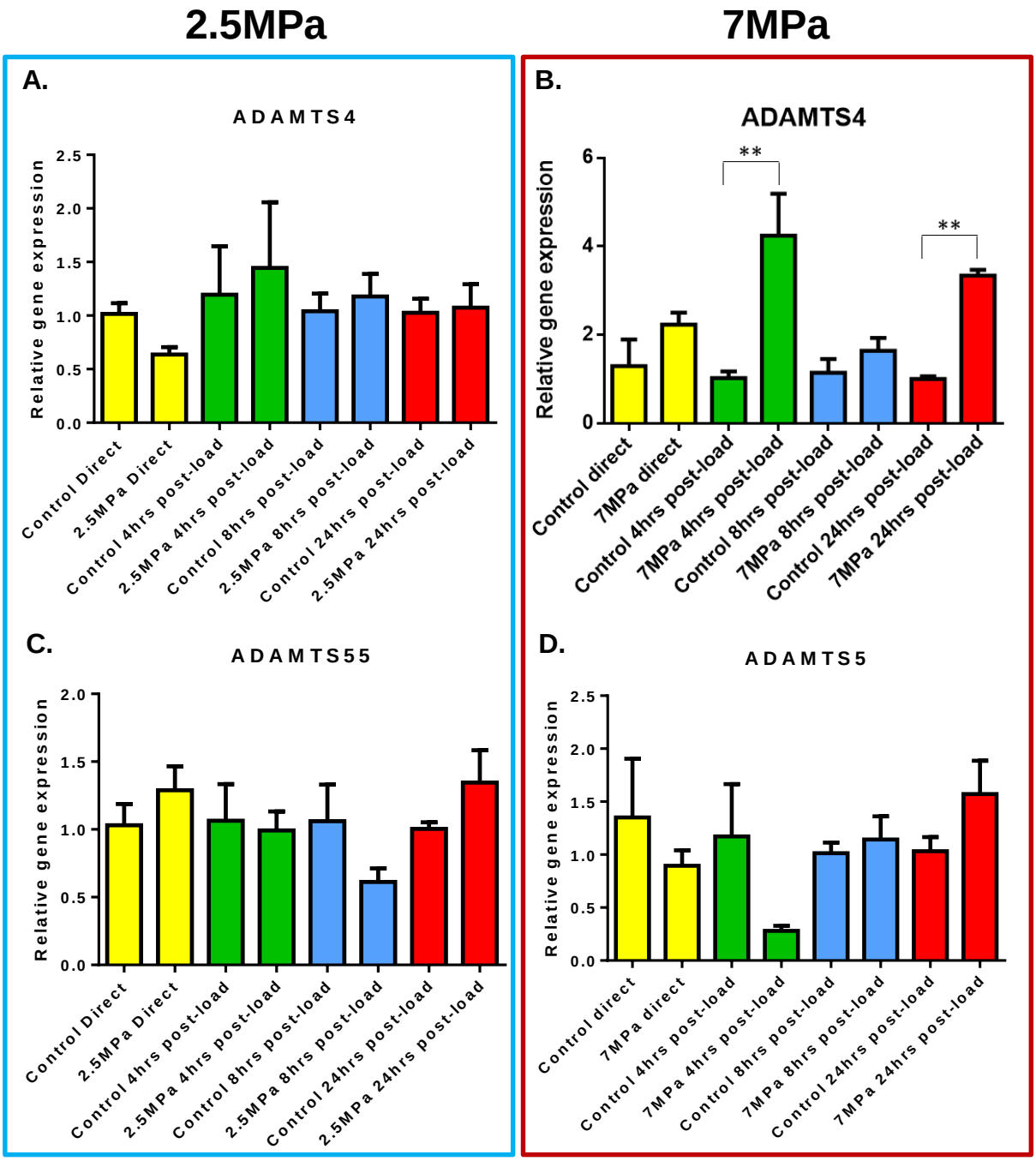

Figure 4-10: mRNA quantification of A, B) ADAMTS-4 and C, D) ADAMTS-5 levels in cartilage explants subjected to a load of either 2.5MPa or 7MPa (1Hz, 15 minutes), where unloaded explants served as controls. mRNA levels were assessed directly, 4, 8 and 24 hours post-load using qPCR. All data were normalised to the geometric mean of reference genes SDHA and YWHAZ and relative to the unloaded control. Results presented are mean ± SE. Statistical analysis was performed using a two way ANOVA with Tukey's post hoc test (n=4). [*: $p<0.05$, **: $p<0.01$, ***: $p<0.001$]

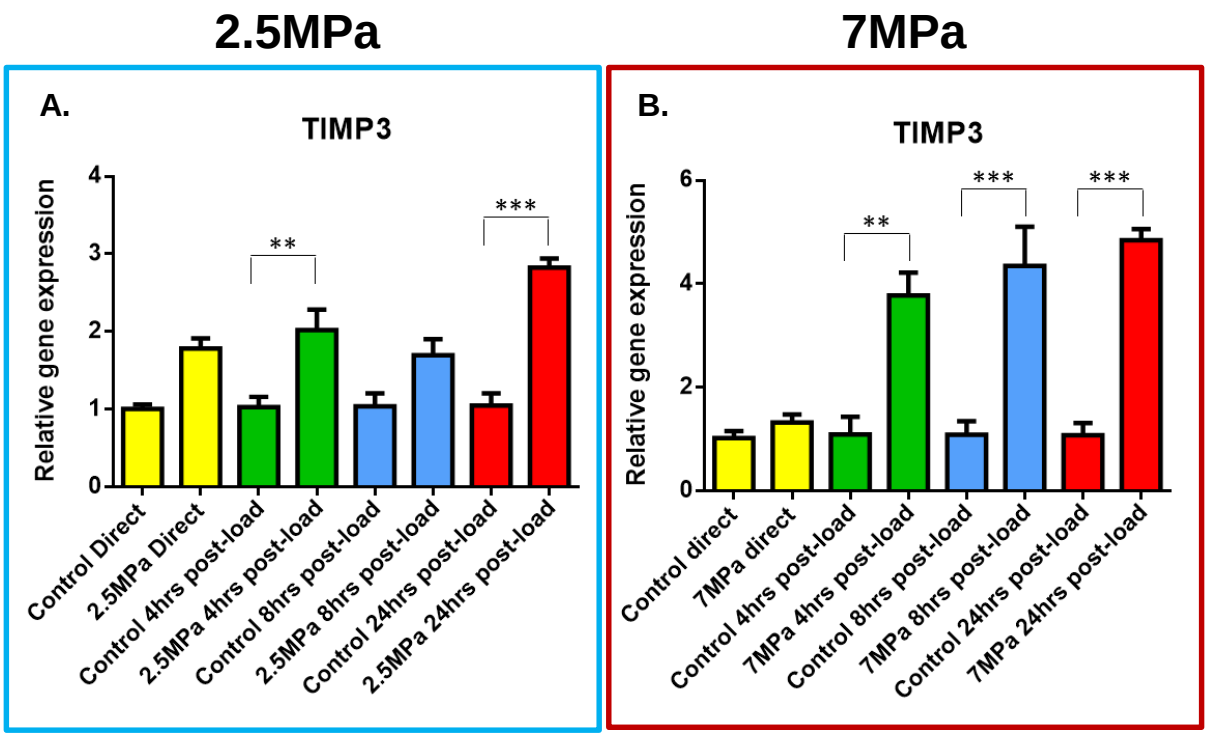

Figure 4-11: mRNA quantification of A, B) TIMP3 levels in cartilage explants subjected to a load of either 2.5MPa or 7MPa (1Hz, 15 minutes), where unloaded explants served as controls. mRNA levels were assessed directly, 4, 8 and 24 hours post-load using qPCR. All data were normalised to the geometric mean of reference genes SDHA and YWHAZ and relative to the unloaded control. Results presented are mean ± SE. Statistical analysis was performed using a two way ANOVA with Tukey's post hoc test (n=4). [*: $p<0.05$, **: $p<0.01$, ***: $p<0.001$]

4.3 Discussion

Numerous studies have shown that cartilage tissue subjected to dynamic mechanical loading initiates either a biosynthetic or catabolic response based on the magnitude and duration of the loading regime (Lee et al., 2005b, Lee and Bader, 1997, Bader et al., 2011). The aim of this chapter was to identify two loading regimes to replicate either a physiological or a degradative response in articular cartilage. Both the magnitude and duration post-cessation of load were modulated to monitor early mechano-responsive changes in gene expression using qPCR. Hence, the nomenclature referring to these loading regimes herein relates to either primarily a homeostatic (physiological) or degradative (non-physiological) response at the gene level. Quantifying mechano-responsive changes in transcript levels by qPCR required the selection of appropriate reference genes for normalisation of the ensuing data to characterise the loading regimes.

4.3.1 Selection of appropriate reference genes unaffected by a mechanical stimulus

Historically, many studies have utilised common reference genes including β-actin, GAPDH, β-tubulin, β2-microglobulin and 18s to assess mechanically-regulated transcriptional responses. However, it is becoming more apparent how vital it is to use appropriate reference genes as the use of unstable reference genes can lead to inaccurate interpretation of qPCR data. Studies have shown that normalising data using inappropriate i.e. unstable reference genes can lead to false negative or positive results due to the influence of the experimental conditions on the expression of these genes themselves (Dheda et al., 2004, Kozera and Rapacz, 2013). Therefore, a panel of reference genes taken from a study by Anstaett et al. were assessed for their stability using pooled cDNA generated from the three loading regimes and the unloaded cartilage (Anstaett et al., 2010). This was conducted by running experimental samples for each reference gene and using the software RefFinder. This software identifies the most stable genes, by assessing the Ct values, and provides an output of the recommended single or combination of reference genes for data normalisation. Interestingly, the most stable reference genes in cartilage cDNAs pooled from

unloaded and different loading regimes were SDHA and YWHAZ, which were used to normalise the resulting data. 18s, used in many mechanical studies and previously used in our laboratory, was relatively stable as was β-actin. The β-actin result was quite surprising as the actin cytoskeleton is known to reorganise in response to load (Guilak et al., 2002, Knight et al., 2006, Haudenschild et al., 2008a, Blain, 2009). The least stable reference genes, determined from the panel analysed, were GAPDH and HRPT. For example, GAPDH is an enzyme involved in glycolysis, and therefore likely to alter in situations where the metabolic demands on the tissue is increased e.g. in cartilage subjected to load.

4.3.2 Characterisation of physiological and degradative loading regimes

Cartilage explants were loaded using three different loading regimes (2.5MPa, 5MPa and 7MPa; 1 Hz, 15 minutes) and tissue harvested 24 hours post-load to assess mRNA levels of markers of cartilage matrix homeostasis to allow characterisation of the loading regimes at the transcriptional level. The magnitude of load used here i.e. $\leq$5MPa, was reported in the literature as being physiological and values above this were considered degradative, however the frequency used here is considered the equivalent to walking (Bader et al., 2011, Chen et al., 2001, Steinmeyer et al., 1999, Jahn et al., 2000). Matrix genes which included markers of both catabolism (MMP3, MMP9, MMP13, ADAMTS4 and ADAMTS5) and anabolism (aggrecan, collagen type II, TIMP-1 and TIMP-3) were selected to monitor and establish which loading regimes most appropriately represented physiological or non-physiological responses in the cartilage. Genes selected as markers of ECM catabolism were chosen due to their role in cartilage homeostasis and pathology; furthermore, these genes were observed to be up-regulated in response to mechanical injury (Kurz et al., 2005). The panel of genes selected to assess for an anabolic response to loading were chosen due to their known involvement in maintaining cartilage integrity and also their reported mechano-responsiveness (Kiraly et al., 1998, Kurz et al., 2001).

Assessment of gene expression by qPCR indicated that after 15 minutes of loading at a peak stress of 2.5MPa (1Hz), MMP mRNA levels decreased whereas there were subtle increases in ADAMTS-4, and TIMPs-1 and -3 transcription compared to the unloaded control explants; aggrecan and collagen

type II transcription were unresponsive to this loading regime. These results are in line with previous studies which demonstrated, using a similar loading regime on rat cartilage explants for a longer duration (1 hour), the significant down-regulation of MMP expression (Leong et al., 2011b). Due to this loading regime producing a fairly static balance between the expression of anabolic and catabolic genes, and in keeping with its report of being physiological in other studies (Madej et al., 2014, Leong et al., 2011b), this loading regime was therefore selected to represent physiological load i.e. a homeostatic response, for all subsequent experiments.

By doubling the magnitude of load to 5MPa, a differential effect on matrix gene expression was observed, mainly in the expression of the MMPs and TIMPS. MMP3 was the only MMP up-regulated in response to 5MPa; mechano-regulation of MMP3 has been observed in previous studies using bovine cartilage explants where a single impact load of 50% final strain (at a velocity of 1 mm/second) increased MMP3 mRNA levels as early as 2 hours, and peaked as high as 250-fold 24 hours post-load (Lee et al., 2005b, Patwari et al., 2003). However, MMP9 and MMP13 were found to be significantly down-regulated in response to a 5MPa load; these results were surprising and inconsistent with the results of several other studies which demonstrated that high levels of mechanical load results in MMP9 up-regulation, whereas MMP13 was shown be either transient or unaffected by load (Lee et al., 2005b, Patwari et al., 2003). The discrepancies between our results and other studies could be explained by the differences in loading protocols and specimen preparations across studies (Kurz et al., 2005). As a result, it may be difficult to cross compare results directly with these published studies. In the experiments reported in this chapter, the specimens used did not contain any underlying subchondral bone and the age of the bovine calves was approximately 7 – 10 days old i.e. immature cartilage tissue. As a result, due to the maturity of cartilage tissue used, chondrocytes present in immature cartilage may not absolutely respond in a manner as has been reported previously for mature tissue, although apart from MMP9 and MMP13 all other effects are consistent with the literature. Furthermore, at 5MPa, only ADAMTS-4 mRNA levels was elevated; ADAMTS-5, aggrecan and collagen type II expression were unaltered by this loading regime. However, increases in

both TIMP-1 and TIMP-3 expression were observed at 5MPa which is in line with previous studies (Fitzgerald et al., 2006). Based on these results, the 5MPa loading regime may be classified as high physiological due to the transient up-regulation of only MMP-3 and ADAMTS-4 from the group of catabolic genes, the maintenance of anabolic genes i.e. unaltered expression of aggrecan and collagen type II, and the increased expression of TIMP-1 and TIMP-3 to likely counterbalance the consequences of proteolytic enzyme transcription. The balance between catabolic and anabolic gene expression is suggestive that this 5MPa loading regime is not sufficiently high enough to be classified as a degradative load, as characterised by the gene expression profile, at the time points analysed.

At the highest load evaluated (7MPa), mRNA levels of catabolic genes were dramatically increased. As observed previously with the 5MPa findings, MMP3 was significantly elevated indicating a load-dependent response over the peak stresses tested. Furthermore, 7MPa was the only loading regime which induced the expression of both ADAMTS-4 and ADAMTS-5; at the lower loads, ADAMTS-5 transcription was not significantly modulated. Therefore, it is likely that ADAMTS-4 may be constitutively expressed for load-induced matrix turnover and maintenance of homeostasis, whereas the mechano-regulation of both may be indicative of a degradative load; this remains to be confirmed. However, similar results were observed by Lee et al., where ADAMTS-5 was significantly up-regulated in response to, 50% strain degradative mechanical load (Lee et al., 2005b). Due to their efficiency in aggrecan catabolism, ADAMTSs' are tightly regulated via TIMPS. As these results indicate, at 7MPa both TIMP-1 - but mainly TIMP-3 were up-regulated in a load-dependent manner. TIMP-3 is known to inhibit a wide range of MMPs as well as ADAMTSs (Murphy, 2011). TIMP-3 knockout mice studies have shown that TIMP-3 is essential in regulating ADAMTS-4 and 5 activity which is evident from the enhanced degradation of aggrecan shown by histological analysis of the knee joint (Sahebjam et al., 2007). Therefore, this may be a response to maintain cartilage integrity by regulating the process of aggrecan catabolism through ADAMTS-4 and ADAMTS-5 inhibition.

4.3.3 Optimisation of period post-load required to detect differential expression of mechano-responsive genes

Following the selection of 2.5MPa and 7MPa as the best representations of physiological and degradative loading respectively, as assessed at the gene level, culture times post-cessation of load were then optimised to determine the period in which early transcriptional events induced by these loading regimes was initiated. For these post-load optimisation experiments, the matrix gene panel selected was chosen on the basis of their reported mechano-responsiveness from previous experiments conducted in our lab (data not shown). As this preliminary experiment was used to assess the most appropriate transcriptional window for subsequent experiments, not all matrix genes were analysed. However, expression levels of C-JUN, an early response gene and a down-stream target of WNT signalling, was included, allowing the optimal transcriptional time frame for detection of mechanically-induced WNT signalling to be established. Gene expression changes in cartilage explants loaded using the optimised physiological or degradative regimes was either assessed directly post-cessation of load or maintained in culture and analysed at 4, 8 and 24 hours post-load.

In response to a load of 2.5MPa, most of the genes analysed were unaffected, however a more dynamic temporal expression profile was observed in response to the 7MPa regime. C-JUN transcription was significantly up-regulated at 4 hours post-load in response to both 2.5MPa and 7MPa. C-JUN, a component of the activator protein-1 (AP-1) complex and an early response gene, has previously been demonstrated to be mechano-responsive in cartilage (Fitzgerald et al., 2004). Furthermore, C-JUN has been shown to initiate MMP transcription (Han et al., 2002). Aggrecan expression was shown to be temporarily down-regulated at 4 (2.5MPa) and 8 hours (7MPa) post-load, however expression returned to basal levels by 24 hours in response to both loading regimes. This transient response was not unexpected due to the short loading duration used, as other studies have shown alterations in aggrecan expression occurred after a minimum of 1.5 hours of continuous dynamic load (Parkkinen et al., 1992).

Expression of most of the catabolic genes demonstrated a maximal response at 4 and 8 hours post-load. With regard to MMP expression, MMP3 and MMP13 mRNA levels were both transiently up-regulated at 8 hours (both 2.5-fold) in response to 2.5MPa. MMP3 up-regulation appeared to be sustained and was elevated at 4, 8 and 24 hours post-cessation of the 7MPa load, with expression peaking at 8 hours post-load (15-fold). Similar trends were reported by Lee et al., where MMP3 was significantly up-regulated in immature bovine cartilage tissue in response to degradative load (Lee et al., 2005). MMP3 is known to be a mechano-sensitive gene and is implicated in the activation of other MMPs (Lee et al., 2005b, Blain, 2007). Expression of ADAMTSs were unaffected by the 2.5MPa load, however in response to the 7MPa load, ADAMTS-4 expression was significantly induced at 4 hours and, to a lesser extent, 24 hours post-load. Expression of TIMP-3, a regulator of both MMPs and ADAMTSs (Sahebjam et al., 2007), was shown to increase over time.

Based on the results in this chapter, representative physiological and degradative loading regimes were identified that either induced homeostatic or predominantly catabolic effects respectively, at the transcriptional level, in articular cartilage. Furthermore, a period of 4 hours post-cessation of load was identified as being the optimal timeframe to monitor the early mechano-responsive transcriptional effects.

4.4 Summary of findings

- SDHA and YWHAZ were the most appropriate reference genes, in articular cartilage subjected to various loading regimes, for normalisation of qPCR data.
- Assessment of a panel of matrix genes indicated that loads of 2.5MPa and 7MPa induced effects in articular cartilage ECM that characterised homeostasis or predominantly catabolism respectively, at the transcriptional level, reflecting physiological and degradative loading regimes.

- A period of 4 hours post-cessation of load was identified as being the optimal timeframe to monitor the early mechano-responsive transcriptional effects.

Chapter 5

Analysis of mechanically regulated WNT signalling components in articular cartilage

5.1 Background

WNT signalling has numerous roles in facilitating biological processes such as embryonic development, tumorigenesis and limb development (Chun et al., 2008). These processes are mediated through either β-catenin dependent (canonical pathway) or independent pathways (non-canonical pathways). The canonical WNT pathway becomes active by the binding of a WNT ligand to frizzled and lipoprotein-related receptors resulting in the phosphorylation of the phosphoprotein dishevelled (DVL). Ordinarily, in the absence of WNT ligand, the glycogen synthase complex (APC, GSK3β, casein kinase, axin) forms facilitating phosphorylation of β-catenin and its destruction by ubiquitination. Conversely, the inhibition of the glycogen synthase complex leads to the accumulation of non-phosphorylated cytoplasmic β-catenin and its nuclear translocation, where it associates with TCF/LEF transcription factors to regulate expression of WNT target genes (Daniels and Weis, 2005). In contrast, the non-canonical pathways are more complex and are not as linear as the canonical pathway. The non-canonical pathways either act via elevating levels of intracellular calcium (Ca^{2+}) through phospholipase C and phosphodiesterase activation, or via activation of Rho GTPases to control planar cell polarity (Chun et al., 2008). There is still limited understanding of how the non-canonical pathways are regulated. However, what is clear is the involvement of both canonical and non-canonical WNT signalling pathways in chondrogenesis, chondrocyte maturation, endochondral ossification and maintenance of the chondrogenic phenotype.

As WNT signalling has numerous integral roles in maintaining cartilage homeostasis it has been suggested that dysregulation of this pathway may result in disease. Numerous studies have reported the differential expression of WNT components associated with cartilage pathology. A study by Loughlin et al. identified a single nucleotide polymorphism (SNP) in FRZB, a WNT inhibitor, which results in an Arg324Gly substitution associated with hip OA in women (Loughlin et al., 2004). This SNP i.e. amino acid substitution induces a conformational change in the structure of the protein thereby reducing the ability of FRZB to inhibit WNT signalling; as a result, enhanced WNT signalling occurs. Furthermore, studies of end-stage human OA cartilage have shown enhanced expression of WNT signalling components including β-catenin, WISP-1, FOSL1,

C-JUN and WNT5A (Thorfve et al., 2012). *In vitro* studies have also demonstrated that enhanced WNT signalling induces MMP and aggrecanase expression promoting cartilage degeneration (Blom et al., 2009). These *in vitro* observations were validated in *in vivo* studies; conditional activation of β-catenin in articular chondrocytes of skeletally mature mice demonstrated that enhanced canonical WNT signalling leads to the development of OA-like symptoms which include osteophyte formation, chondrocyte differentiation and degradation of cartilage tissue (Zhu et al., 2009). Furthermore, a study by the same group demonstrated that inhibition of β-catenin in cartilage tissue of skeletally mature mice promotes apoptosis and loss of cartilage tissue (Zhu et al., 2008).

Based on these studies, it is clear that WNT signalling is essential for cartilage homeostasis. However, these studies have not elucidated the involvement of mechanical load in regulating WNT signalling components, particularly considering that mechanical load is one of the main regulators of cartilage homeostasis. Mechano-regulation of WNT signalling has been demonstrated in several tissue types including blood vessels, ligaments and bone (Li et al., 2014, Premaraj et al., 2011, Yokota et al., 2011). Mechano-regulation of WNT signalling in bone tissue is well documented. Studies on mechanically loaded bone have shown enhanced canonical WNT signalling to maintain tissue integrity (Robinson et al., 2006). Furthermore, our laboratory previously demonstrated the partial translocation of β-catenin into the nucleus of high-density primary chondrocytes subjected to tensile strain (7.5%, 1Hz, 30 minutes) (Thomas et al., 2011) .

Due to the implication of WNT signalling in disease progression combined with the few studies performed on the mechano-responsiveness of β-catenin in primary chondrocytes, the experiments in this chapter sought to determine how WNT signalling components respond to the two loading regimes established in Chapter 4, namely turnover and degradative loads, in cartilage explants. WNT signalling activation was determined using confocal microscopy by assessing the presence of nuclear β-catenin. mRNA levels of WNT components were assessed using customised bovine WNT signalling arrays and findings validated by qPCR. An understanding of how these components respond in a defined loading

environment will help elucidate the role of WNT signalling in the pathophysiology of load-induced cartilage degeneration.

5.2 Results

5.2.1 Canonical WNT signalling is activated in response to physiological and degradative load in cartilage explants

Having confirmed that the canonical Wnt pathway, as characterised by nuclear translocation of β-catenin, is activated in response to tensile strain in isolated chondrocytes (Chapter 3), the next objective was to assess if this effect was also evident in articular cartilage. To address this, explants were either subjected to physiological load (2.5MPa, 1Hz, 15 minutes) or a load resulting in a degradatory genotype (7MPa, 1Hz, 15 minutes). Explants were harvested directly post-cessation of load, or alternatively at 4, 8 or 24 hours post-load to assess β-catenin localisation. Directly post-cessation of load, β-catenin was predominantly localised in the cytoplasm of the chondrocytes throughout the tissue depth of unloaded explants (Figure 5-1A). In contrast, nuclear translocation of β-catenin was only evident in the deep zone chondrocytes directly post-cessation of the 2.5MPa load (Figure 5-1H; Figure 5-3H). These observations were confirmed by quantification of nuclear staining intensity (Figure 5-2). Interestingly, after application of the 7MPa load, minimal β-catenin expression was observed in the superficial (Figure 5-1C; Figure 5-3C) and mid zone chondrocytes (Figure 5-1F; Figure 5-3F); however nuclear β-catenin was observed in deep zone chondrocytes (Figure 5-1I; Figure 5-3I), an effect that mirrored the response to the physiological loading regime.

At 4 hours post-cessation of load, β-catenin was localised to the nucleus primarily in deep zone chondrocytes in unloaded explants (Figure 5-4G; Figure 5-6G). However, the quantification of nuclear staining intensity have not reflected these results (Figure 5-5). In contrast, nuclear β-catenin was observed throughout the depth of explants subjected to a 2.5MPa load (Figure 5-4B; Figure 5-4E; Figure 5-4H), however labelling was still predominantly in the deep zone (Figure 5-4H; Figure 5-6H), which is in line with quantification of staining intensity results (Figure 5-5). In contrast, explants subjected to the 7MPa load (analysed 4 hours post-cessation) demonstrated enhanced β-catenin nuclear translocation

in the mid (Figure 5-4F; Figure 5-6F) and deep zone chondrocytes (Figure 5-4I; Figure 5-6I), when compared to the localisation profile of directly post-loaded explants (Figure 5-1I; Figure 5-3I). These results do not agree with the staining intensity quantification results due to the absence of β-catenin staining in the earlier timepoint, thus the measurement of staining intensity reflects only the nuclear staining (Figure 5-5). However, there was also a significant increase in cytoplasmic β-catenin levels in deep zone chondrocytes 4 hours post-cessation of the 7MPa load (Figure 5-4I; Figure 5-6I).

β-catenin localisation profiles were comparable in explant chondrocytes following either 8 (Figure 5-7) or 24 hours post-cessation of load (Figure 5-10), and in the equivalent unloaded explants. At both time points post-load, β-catenin was localised to the edges of the nucleus in unloaded and 2.5MPa loaded explants; in the low power images (Figure 5-7; Figure 5-10) this labelling appeared to be nuclear, however under higher magnification it was apparent that the protein had not translocated to the nucleus (Figure 5-9 and Figure 5-12). The quantification of nuclear intensity reflects what was observed at low-powered images (Figure 5-8; Figure 5-11) as these results reflect the intensity of staining but does not confirm if the protein is translocated, unless higher magnification indicate the merge of the two stains showing a cyan-like colour thus confirming nuclear translocation. Although there was no evidence of β-catenin translocation in explant chondrocytes subjected to 7MPa, and analysed 8 hours post-cessation of load (Figure 5-9), nuclear translocation was apparent again following 24 hours post-cessation of this higher loading regime; interestingly, punctate β-catenin labelling was also present in the cytoplasm of deep zone chondrocytes (Figure 5-12I).

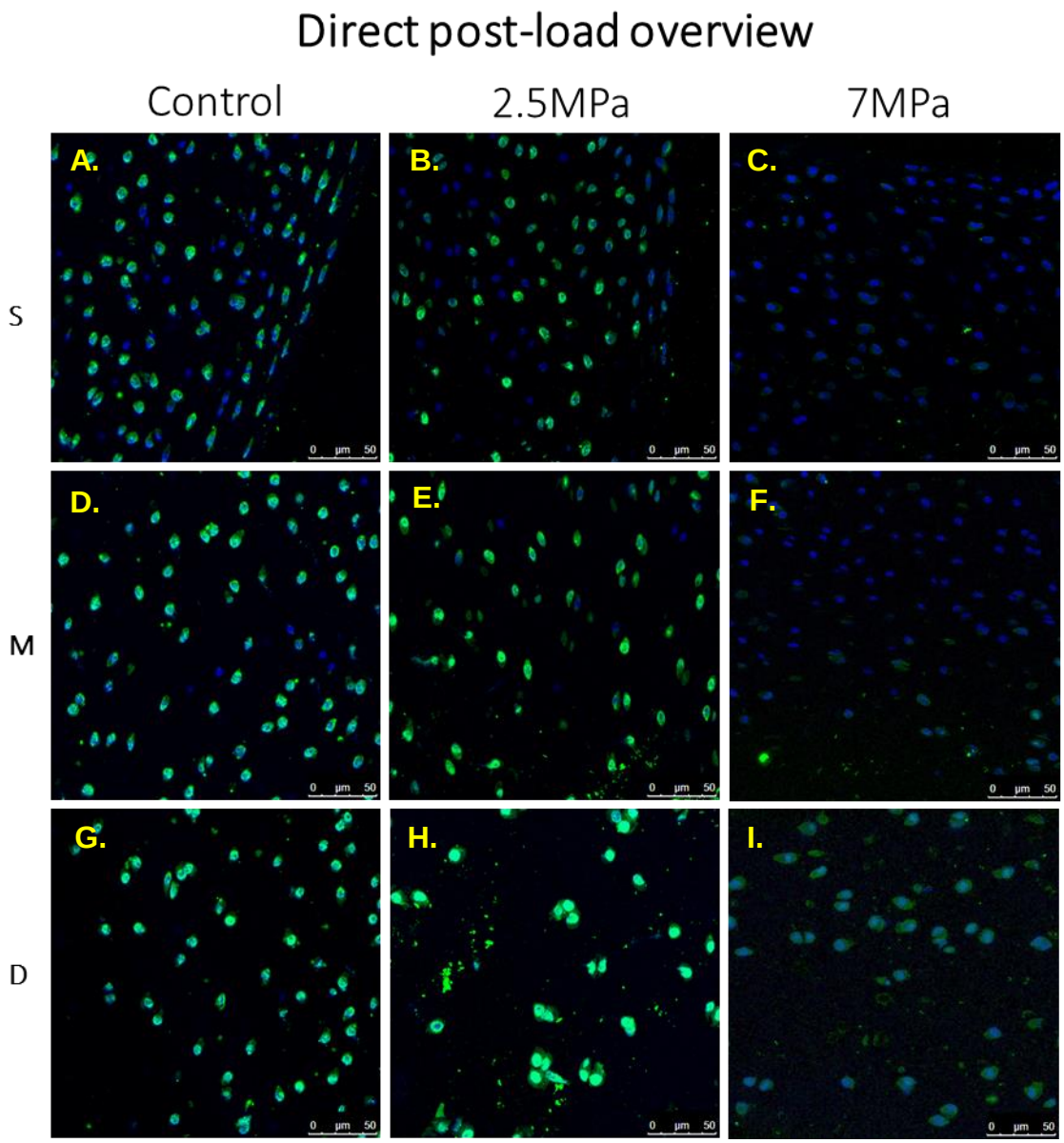

Figure 5-1: Effect of mechanical load (2.5MPa or 7MPa, 1Hz, 15 minutes) on β-catenin localisation in articular chondrocytes directly post-cessation of load. Low power confocal images of explant chondrocytes labelled with monoclonal anti-β-catenin and visualised using goat anti-mouse FITC-conjugated antibody to confirm activation of WNT signalling pathway, i.e. β-catenin nuclear translocation (scale bar= 50µm). [Key: S: superficial zone, M: middle zone, D: deep zone].

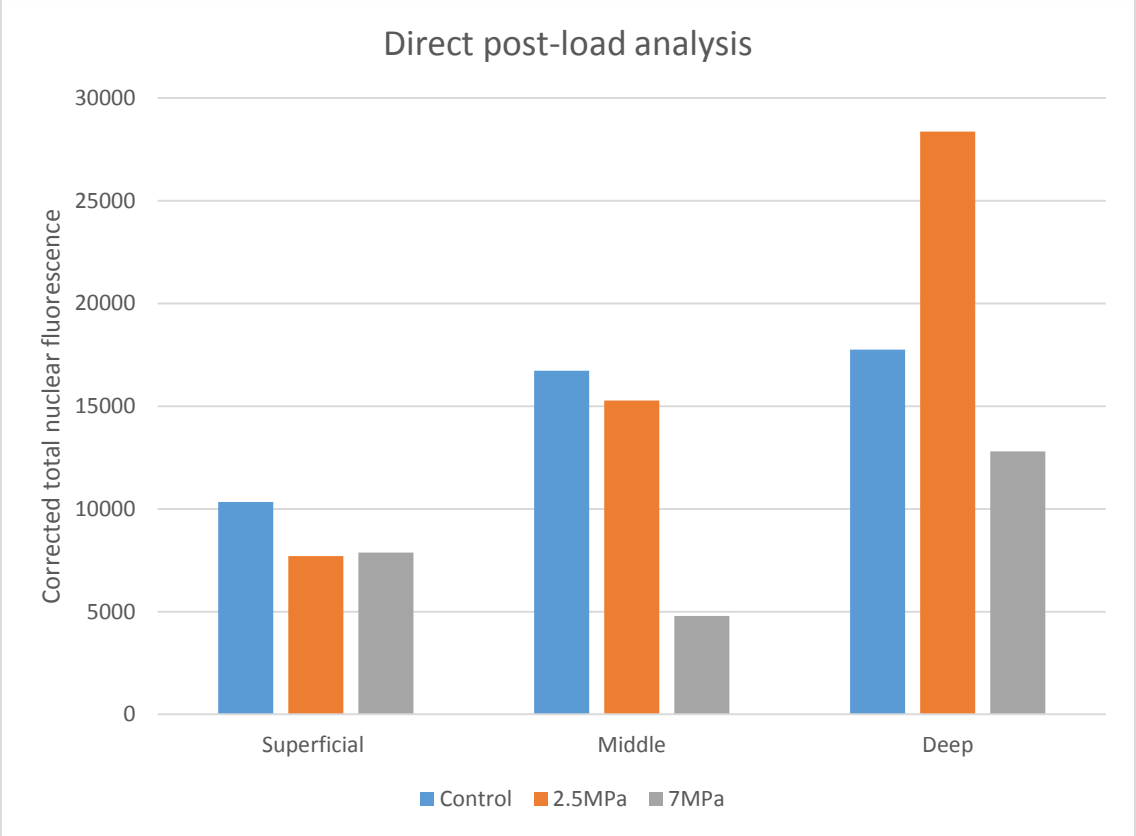

Figure 5-2: Quantification of nuclear staining intensity in mechanically loaded explant chondrocytes (2.5MPa or 7MPa, 1Hz 15 minutes) directly post-load in superficial, middle, and deep zones. Unloaded explants were used as control. Quantification of fluorescence was performed by calculating the intensity of staining within the nuclear region using ImageJ software. Each bar represents the average of nuclear staining of six chondrocytes from respective zones of articular cartilage.

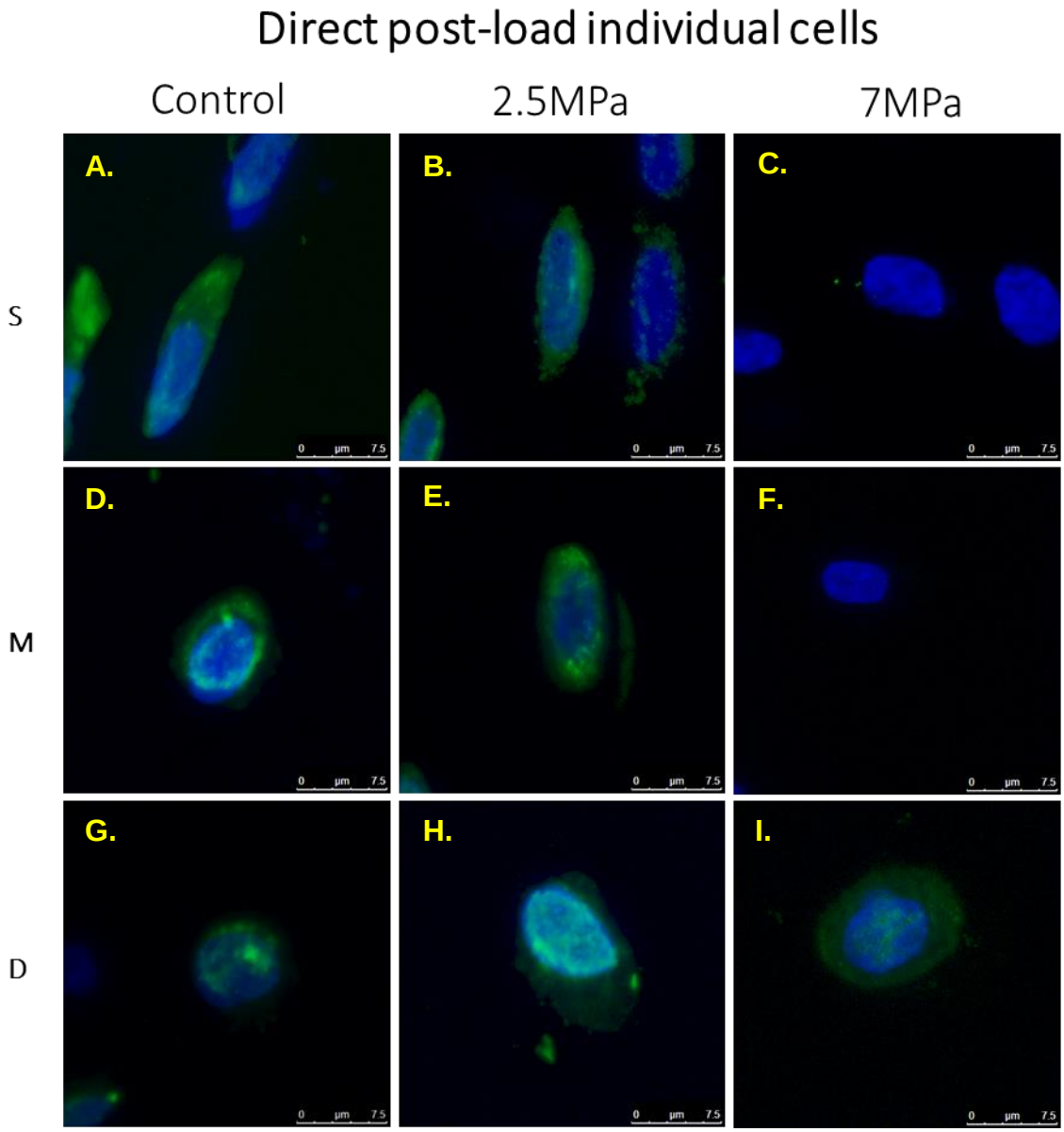

Figure 5-3: Effect of mechanical load (2.5MPa or 7MPa, 1Hz, 15 minutes) on β-catenin localisation in articular chondrocytes directly post-cessation of load. Confocal 3D reconstructions of chondrocytes labelled with monoclonal anti-β-catenin and visualised using goat anti-mouse FITC-conjugated antibody to confirm activation of WNT signalling pathway, i.e. β-catenin nuclear translocation (scale bar= 7.5μm). [Key: S: superficial zone, M: middle zone, D: deep zone].

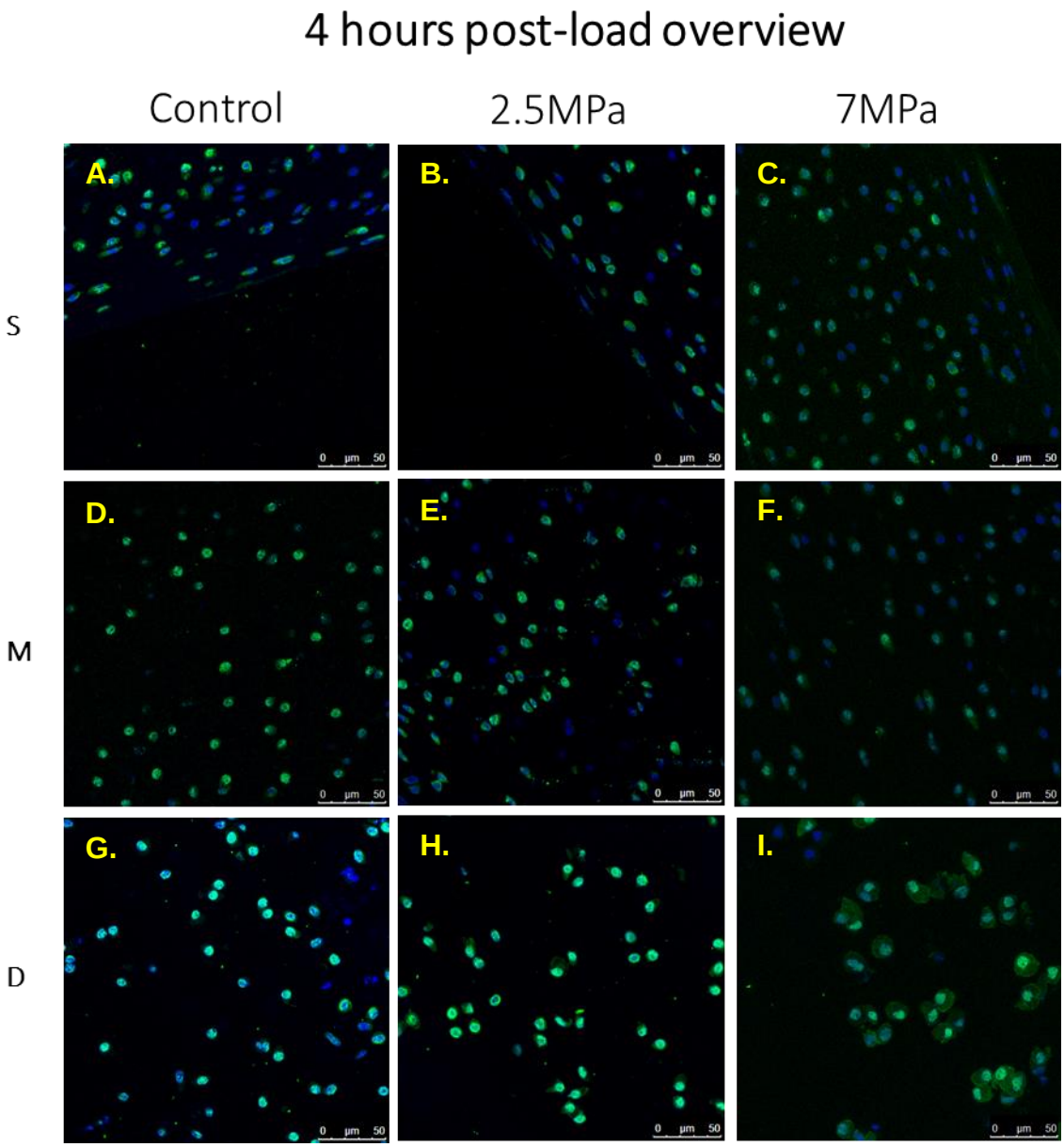

Figure 5-4: Effect of mechanical load (2.5MPa or 7MPa, 1Hz, 15 minutes) on β-catenin localisation in articular chondrocytes 4 hours post-cessation of load. Low power confocal images of explant chondrocytes labelled with monoclonal anti-β-catenin and visualised using goat anti-mouse FITC-conjugated antibody to confirm activation of WNT signalling pathway, i.e. β-catenin nuclear translocation (scale bar= 50µm). [Key: S: superficial zone, M: middle zone, D: deep zone].

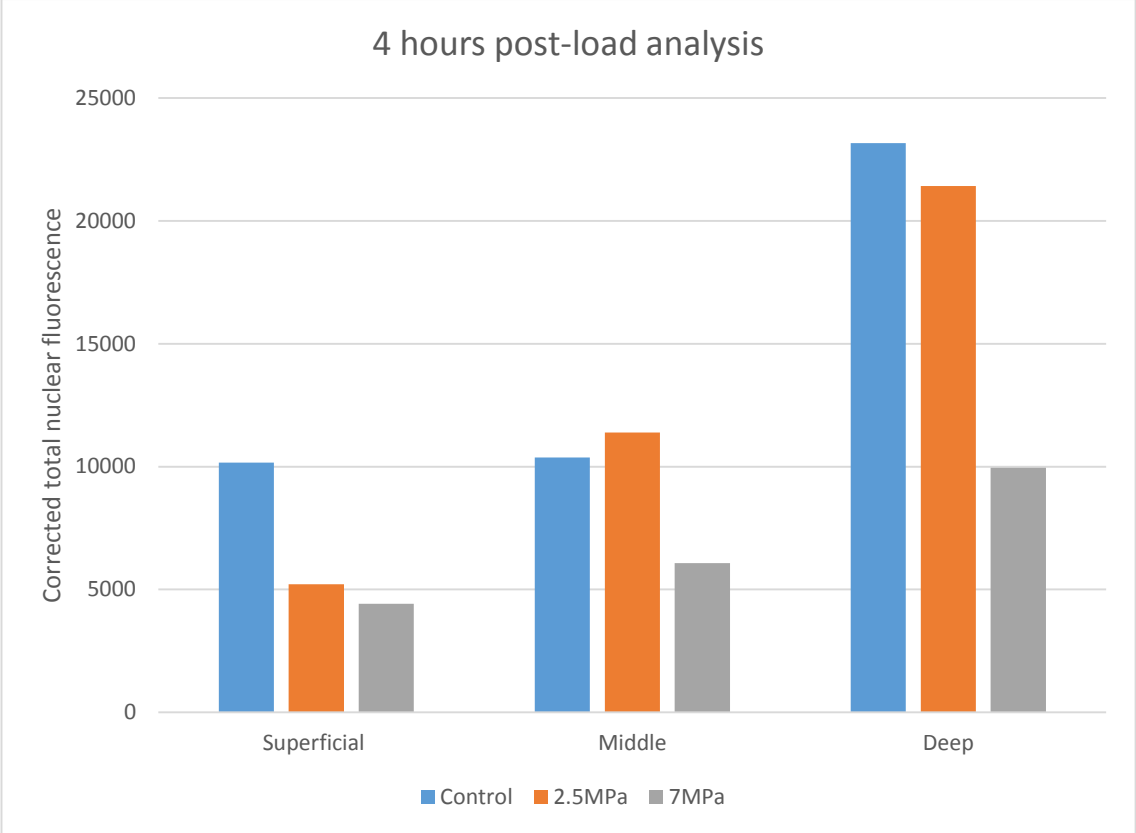

Figure 5-5: Quantification of nuclear staining intensity in mechanically loaded explant chondrocytes (2.5MPa or 7MPa, 1Hz 15 minutes 4 hours post-load in superficial, middle, and deep zones. Unloaded explants were used as control. Quantification of fluorescence was performed by calculating the intensity of staining within the nuclear region using ImageJ software. Each bar represents the average of nuclear staining of six chondrocytes from respective zones of articular cartilage.

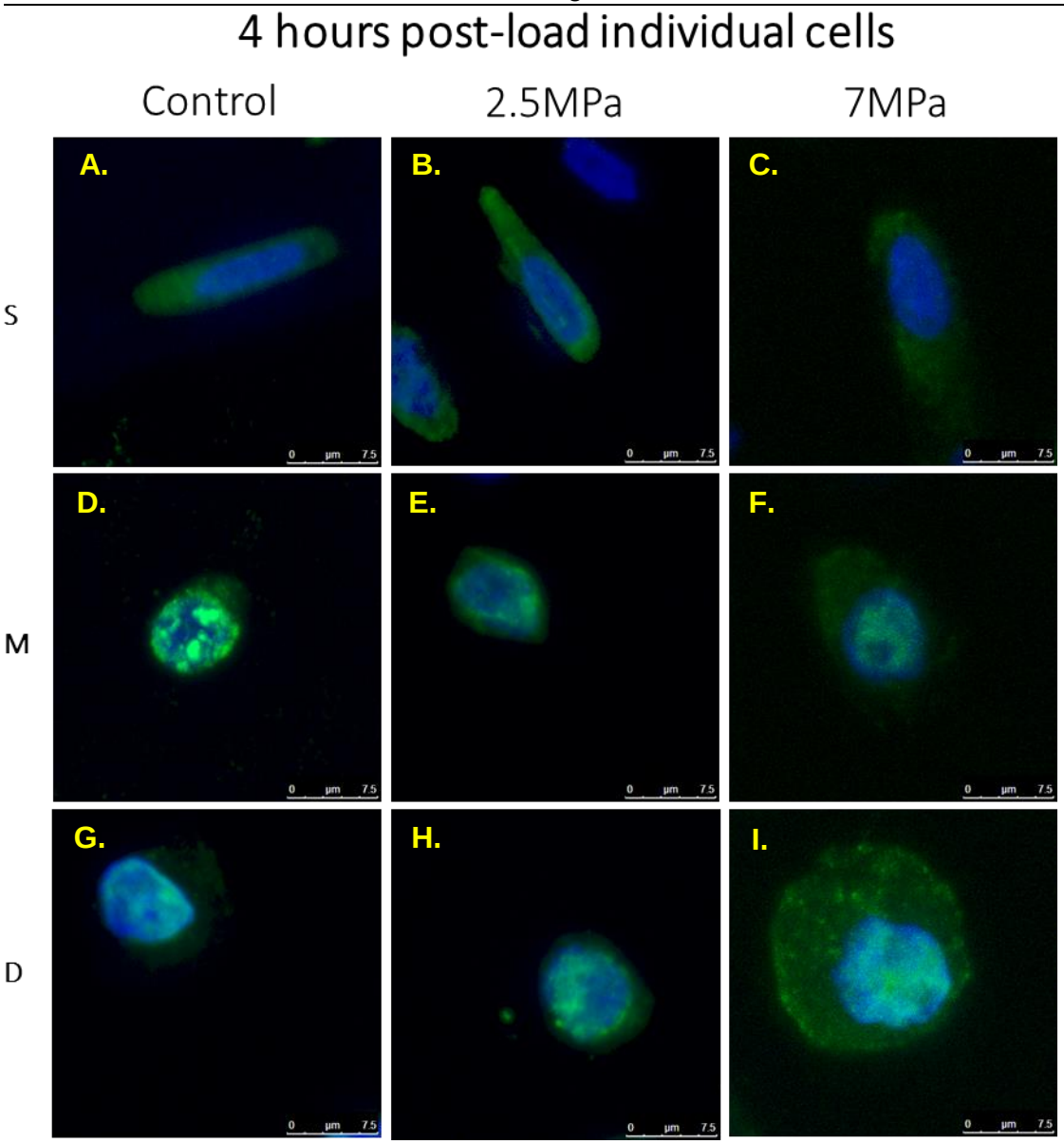

Figure 5-6: Effect of mechanical load (2.5MPa or 7MPa, 1Hz, 15 minutes) on β-catenin localisation in articular chondrocytes 4 hours post-cessation of load. Confocal 3D reconstructions of chondrocytes labelled with monoclonal anti-β-catenin and visualised using goat anti-mouse FITC-conjugated antibody to confirm activation of WNT signalling pathway, i.e. β-catenin nuclear translocation (scale bar= 7.5μm). [Key: S: superficial zone, M: middle zone, D: deep zone].

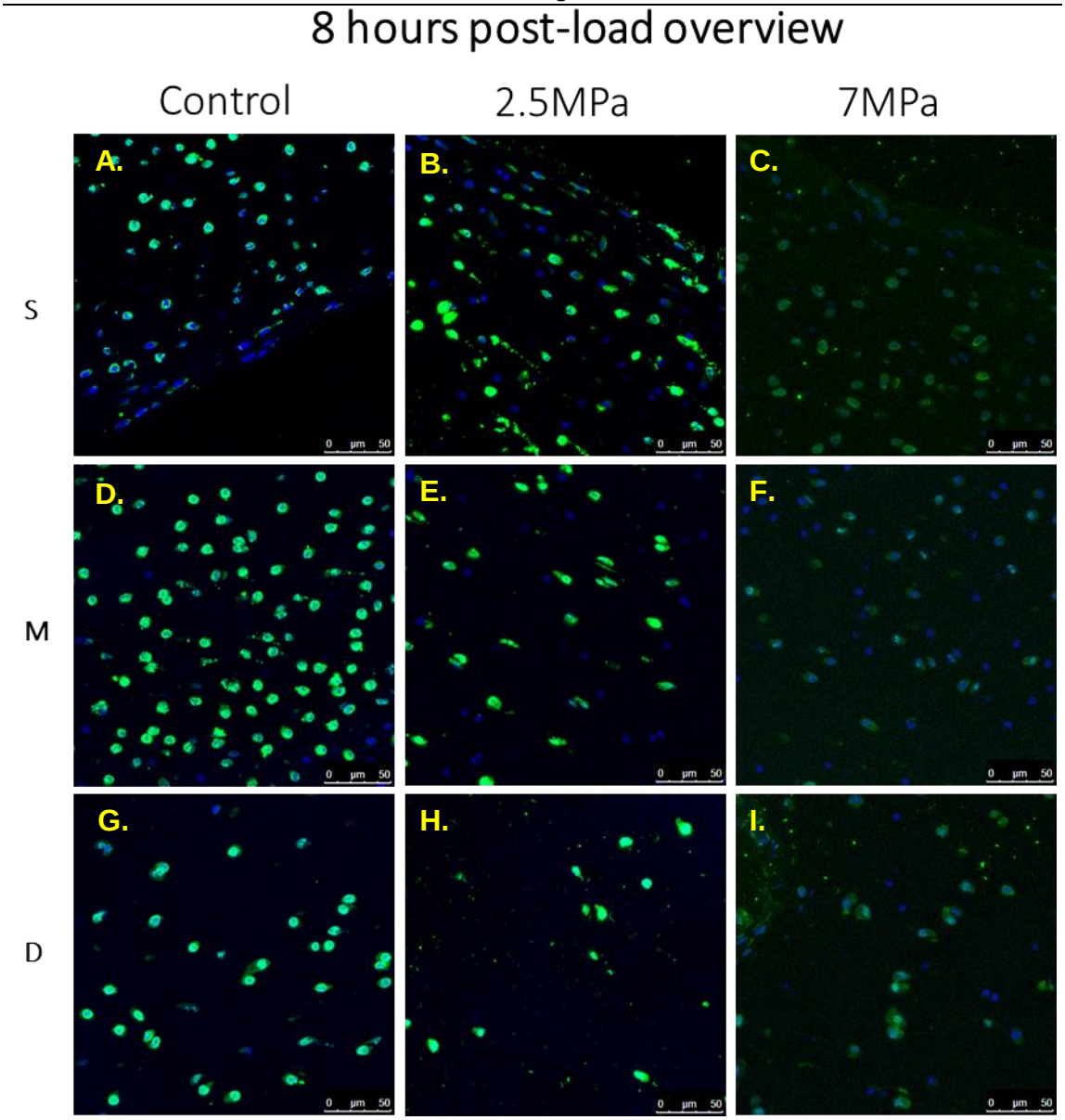

Figure 5-7: Effect of mechanical load (2.5MPa or 7MPa, 1Hz, 15 minutes) on β-catenin localisation in articular chondrocytes 8 hours post-cessation of load. Low power confocal images of explant chondrocytes labelled with monoclonal anti-β-catenin and visualised using goat anti-mouse FITC-conjugated antibody to confirm activation of WNT signalling pathway, i.e. β-catenin nuclear translocation (scale bar= 50µm). [Key: S: superficial zone, M: middle zone, D: deep zone].

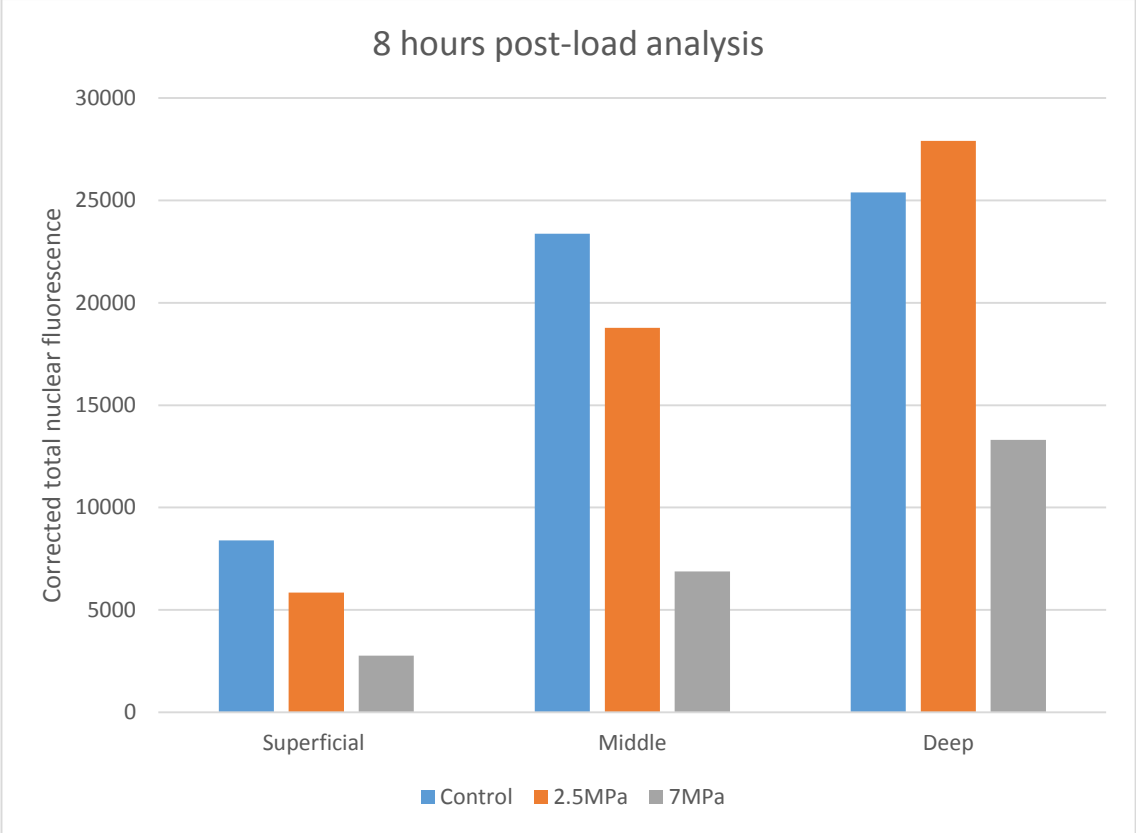

Figure 5-8: Quantification of nuclear staining intensity in mechanically loaded explant chondrocytes (2.5MPa or 7MPa, 1Hz 15 minutes) 8 hours post-load in superficial, middle, and deep zones. Unloaded explants were used as control. Quantification of fluorescence was performed by calculating the intensity of staining within the nuclear region using ImageJ software. Each bar represents the average of nuclear staining of six chondrocytes from respective zones of articular cartilage.

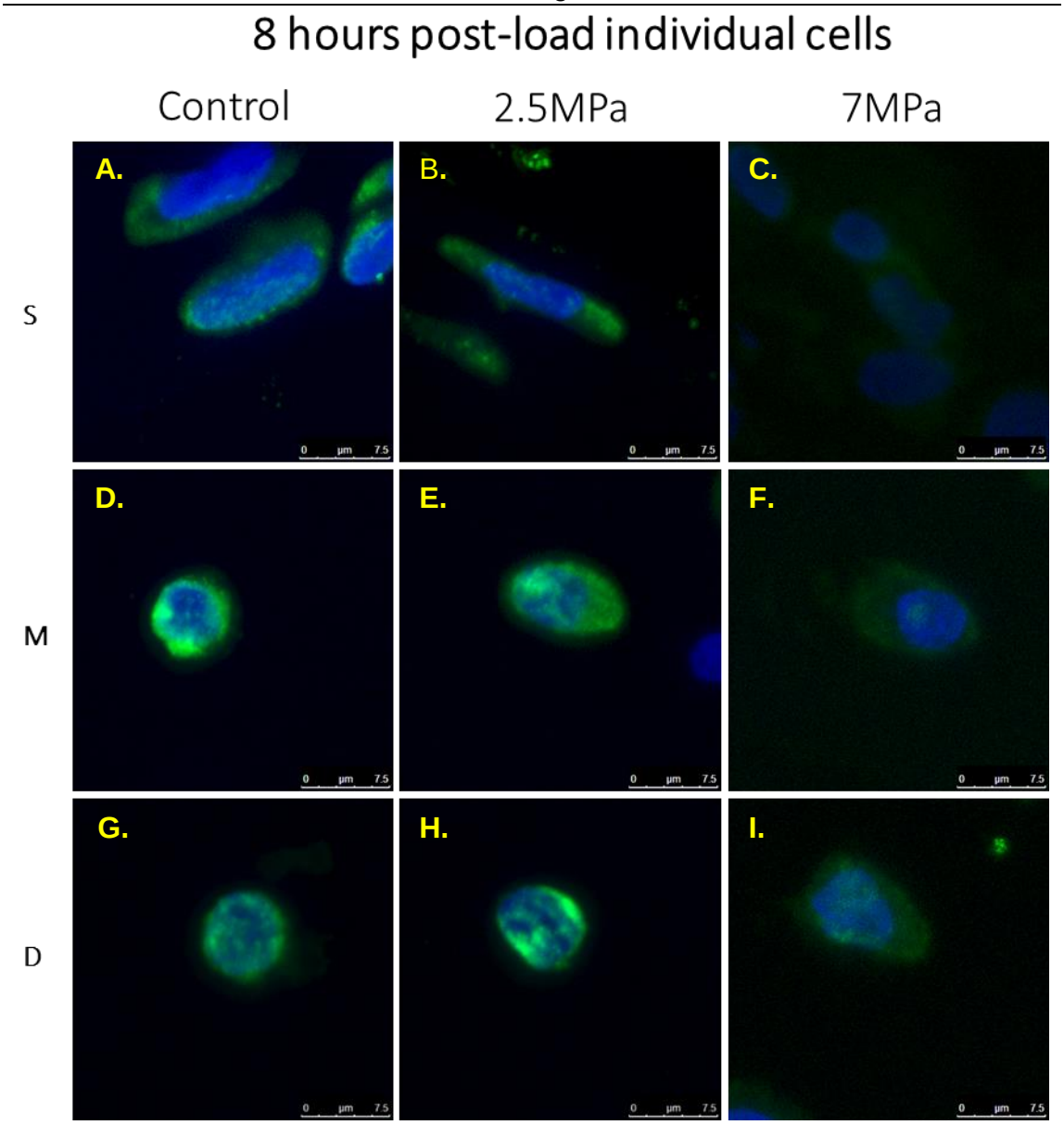

Figure 5-9: Effect of mechanical load (2.5MPa or 7MPa, 1Hz, 15 minutes) on β-catenin localisation in articular chondrocytes 8 hours post-cessation of load. Confocal 3D reconstructions of chondrocytes labelled with monoclonal anti-β-catenin and visualised using goat anti-mouse FITC-conjugated antibody to confirm activation of WNT signalling pathway, i.e. β-catenin nuclear translocation (scale bar= 7.5µm). [Key: S: superficial zone, M: middle zone, D: deep zone].

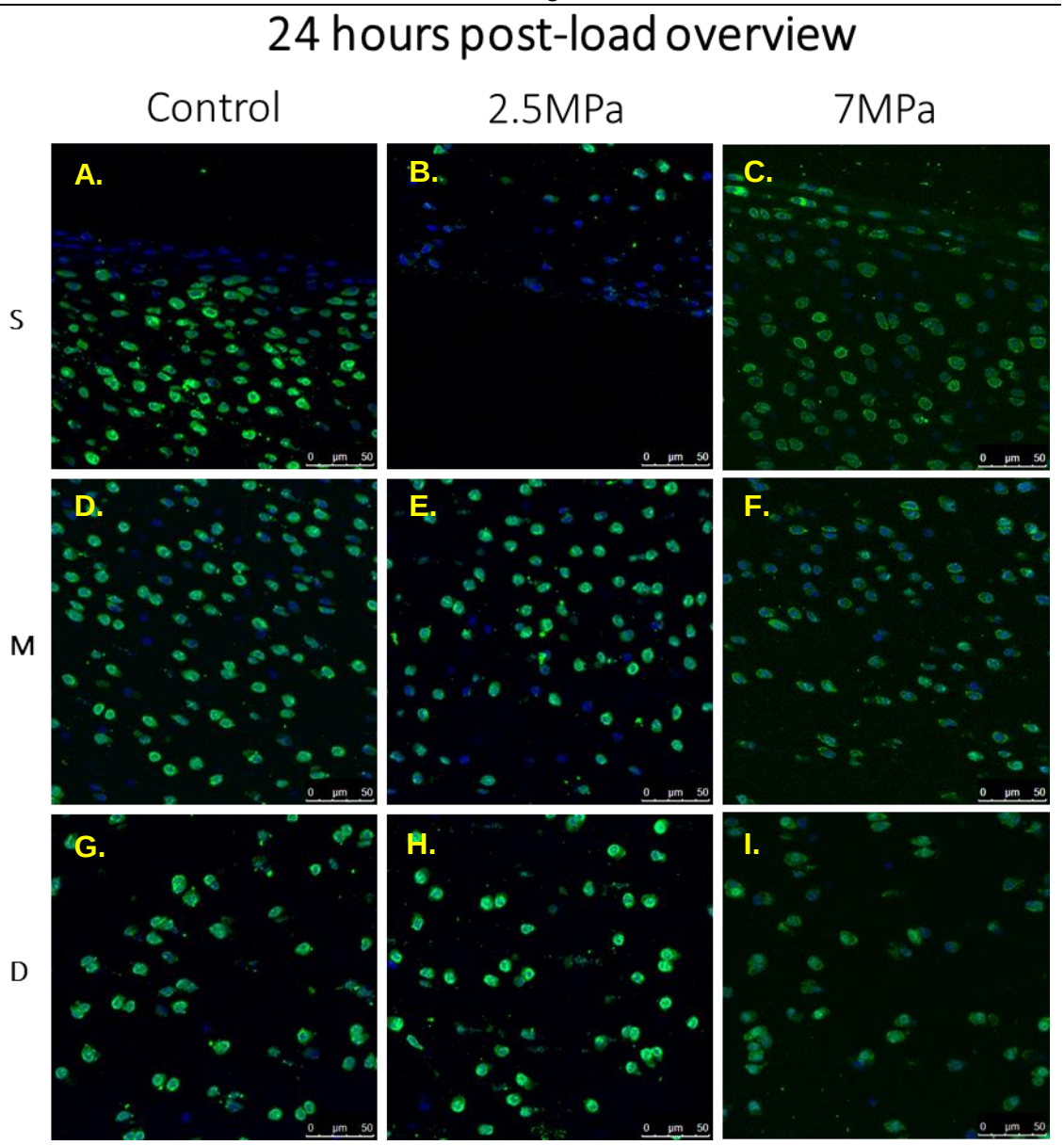

Figure 5-10: Effect of mechanical load (2.5MPa or 7MPa, 1Hz, 15 minutes) on β-catenin localisation in articular chondrocytes 24 hours post-cessation of load. Low power confocal images of explant chondrocytes labelled with monoclonal anti-β-catenin and visualised using goat anti-mouse FITC-conjugated antibody to confirm activation of WNT signalling pathway, i.e. β-catenin nuclear translocation (scale bar= 50µm). [Key: S: superficial zone, M: middle zone, D: deep zone].

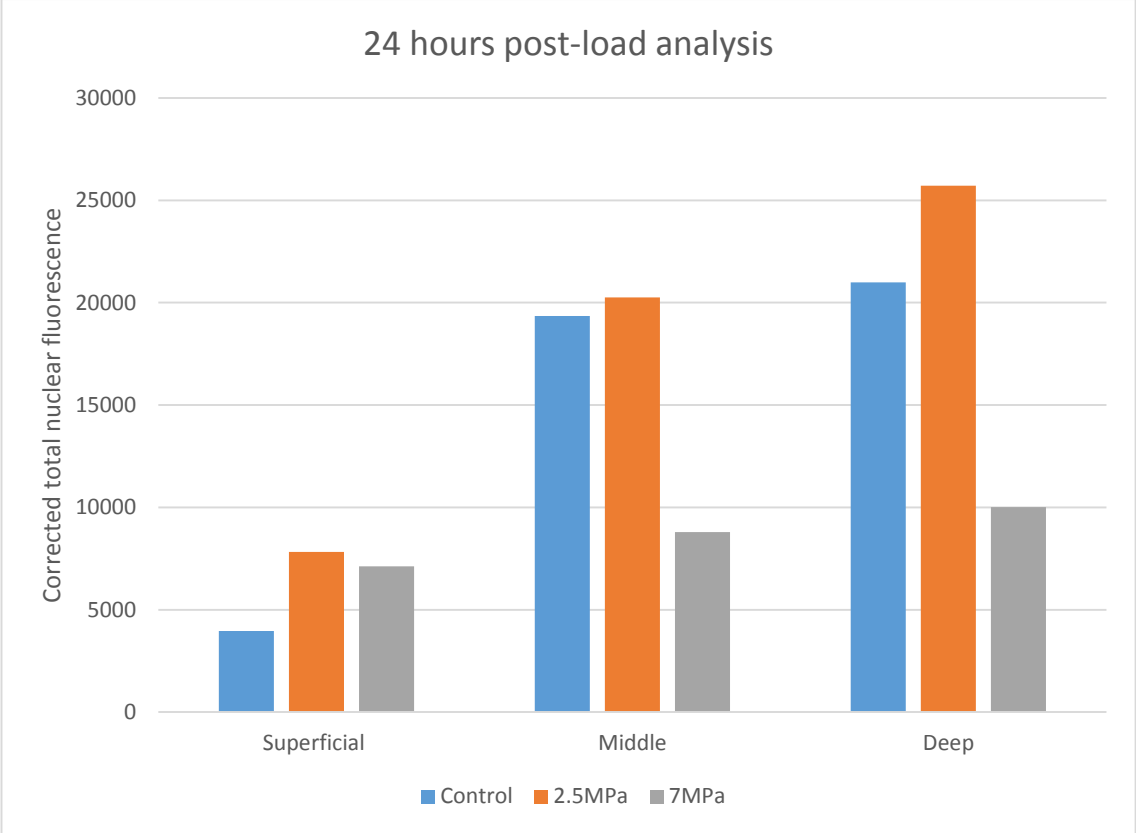

Figure 5-11: Quantification of nuclear staining intensity in mechanically loaded explant chondrocytes (2.5MPa or 7MPa, 1Hz 15 minutes) 24 hours post-load in superficial, middle, and deep zones. Unloaded explants were used as control. Quantification of fluorescence was performed by calculating the intensity of staining within the nuclear region using ImageJ software. Each bar represents the average of nuclear staining of six chondrocytes from respective zones of articular cartilage.

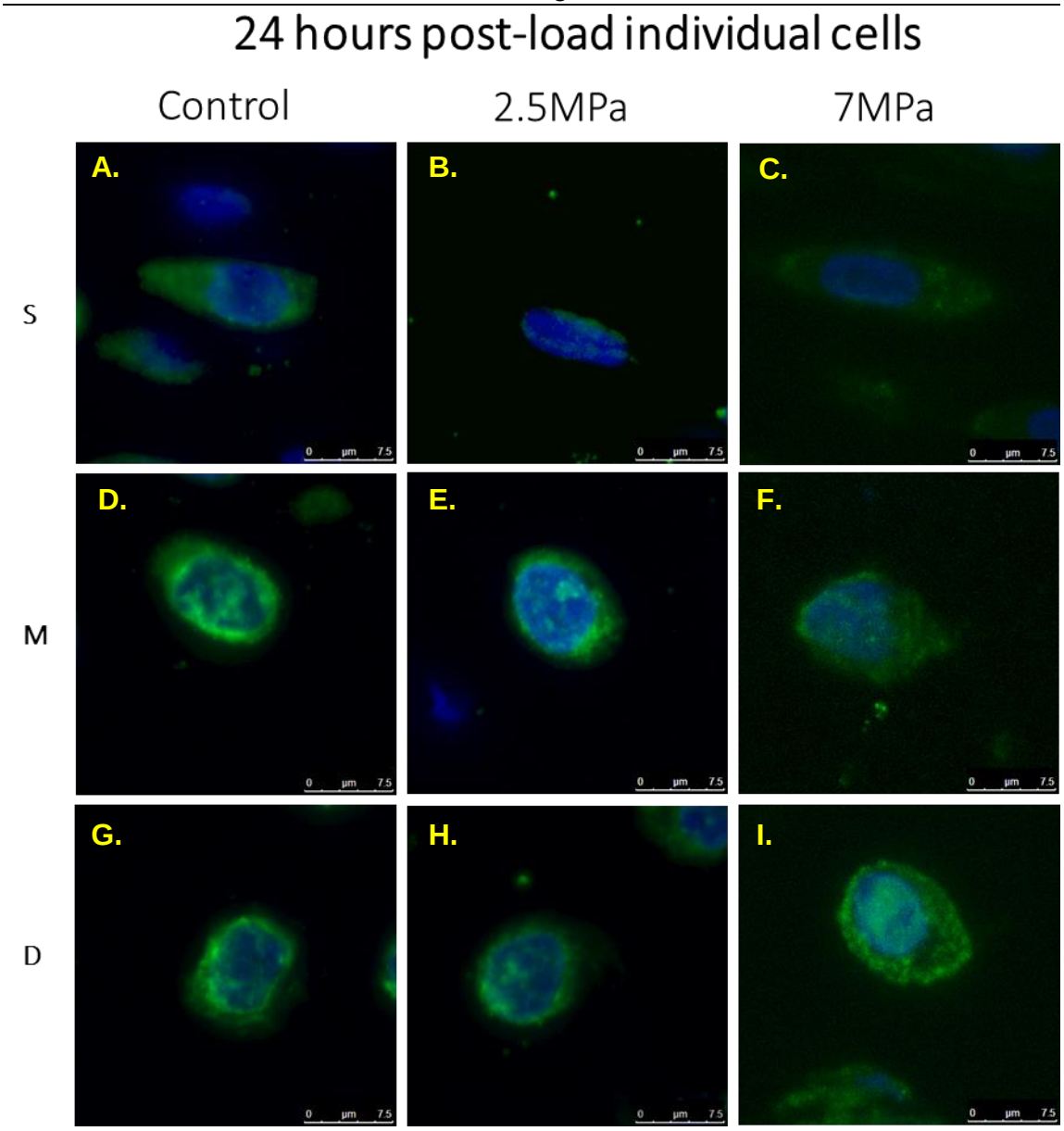

Figure 5-12: Effect of mechanical load (2.5MPa or 7MPa, 1Hz, 15 minutes) on β-catenin localisation in articular chondrocytes 24 hours post-cessation of load. Confocal 3D reconstructions of chondrocytes labelled with monoclonal anti-β-catenin and visualised using goat anti-mouse FITC-conjugated antibody to confirm activation of WNT signalling pathway, i.e. β-catenin nuclear translocation (scale bar= 7.5µm). [Key: S: superficial zone, M: middle zone, D: deep zone]

5.2.2 Differential regulation of WNT signalling components in response to physiological and degradative loads.

Clearly, mechanical load is sufficient to activate Wnt signalling in explant cartilage chondrocytes. To determine which WNT related molecules are mechano-sensitive at the transcriptional level, mRNA levels of the WNT signalling components were assessed in explants exposed to either physiological load (2.5MPa 1Hz 15 minutes) or a load inducing a degradative genotype (7MPa 1Hz 15 minutes) using custom-built bovine-specific WNT signalling PCR arrays. The PCR arrays contained 84 WNT related genes and were categorised according to gene function. The genes assessed fell into the following categories: targets of WNT signalling, components of canonical WNT signalling, WNT/Ca^{2+} pathway, planar cell polarity (PCP) pathway and inhibitors of WNT signalling. The effect of the loading regimes on WNT related gene transcription were assessed in explants 2, 4 and 24 hours post-cessation of load. As demonstrated previously (section 4.2.1.4), the optimal timeframe for observing mechanically regulated WNT target gene transcription, as indicated by increased C-JUN expression, was at 4 hours. Based on these observations, time points were selected prior to (2 hours) and beyond (24 hours) this 4 hour time point to gain a better understanding of the expression profile of WNT signalling components in response to load. PCR array data were normalised to housekeeping genes present on the array, which were selected automatically using the online Qiagen Data Analysis centre software, and changes in gene expression normalised to the unloaded control explants; however, further comparisons were also performed to establish how increasing the magnitude of load affected the transcriptional responses. For data analysis, genes were assessed according to their functional grouping and data is presented for those genes which were differentially regulated by at least 2-fold.

5.2.2.1 Differential mechano-regulation of WNT signalling components 2 hours post-cessation of load

At 2 hours post-cessation of load, regulation of the WNT signalling components were nearly identical in response to physiological and degradative loading regimes (Figure 5-13A and B). In response to physiological load (Figure 5-13A), there was an up-regulation of the early response genes (WNT signalling

targets): C-JUN (11.5-fold), MYC (3.2-fold) and FOSL1 (21-fold), FRAT1 (4-fold) (canonical WNT signalling), NFATC1 (4.6-fold) (WNT/Ca^{2+}) and the Wnt inhibitor AXIN2 (2.3-fold); in contrast, transcription of the WNT inhibitor DKK-1 was down-regulated (5.2-fold). Furthermore, the higher loading regime (7MPa; Figure 5-13B) also modulated transcript levels of the same genes, but to a greater extent (C-JUN 25.6-fold; MYC 4.9-fold; FOSL-1 35.2-fold; FRAT-1 7.3-fold; NFATC1 4.3-fold; AXIN2 2.1-fold; DKK-1 4-fold). Interestingly, following application of the higher load, additional genes were up-regulated including the WNT/Ca^{2+} related genes WNT5B (2.4-fold) and WNT9A (2.3-fold).

5.2.2.2 Differential mechano-regulation of WNT signalling components 4 hours post-cessation of load

At 4 hours post-cessation of load, the greatest number of genes were found to be differentially regulated with respect to the loading regime applied (Figure 5-14A and B). Expression of approximately 15% of the WNT signalling genes altered in cartilage explants subjected to physiological load. In addition, there was a significant increase in expression of the same WNT signalling targets (C-JUN 3.5-fold; MYC 3.7-fold; FOSL-1 12.9-fold) as those observed at 2 hours post-load, however PPARD was additionally found to be up-regulated (2.2-fold; Figure 5-14A). Of the canonical WNT signalling genes, TCF transcript levels were elevated (2.1-fold), whereas other canonical WNT signalling components such as FZD1 and FZD5 were down-regulated (both 3-fold). NFATC1 expression was still elevated (3-fold), however WNT11, another component of the WNT/Ca^{2+} pathway was reduced (2.2-fold). Interestingly, one of the first detected changes in genes involved in the PCP pathway was the down-regulation of PRICKLE-1 expression (3.7-fold); at 2 hours post-load changes in this pathway were not observed for either of the loading regimes. Additionally, the WNT inhibitors DKK-1, DKK-3 and WIF-1 were all down-regulated (2.4-fold, 3.5-fold and 3.8-fold respectively).

In contrast, expression of approximately 32% of the WNT signalling genes altered in cartilage explants subjected to the higher 7MPa loading regime, 4 hours post-cessation of load (Figure 5-14B). The early response WNT signalling target genes were up-regulated in response to this higher load (C-JUN 10.5-fold; MYC

14-fold; FOSL-1 109-fold; PPARD 5.6-fold); furthermore, expression levels were significantly greater than those observed in cartilage subjected to the physiological regime (Figure 5-14A). In addition, the WNT target gene WISP-1 was also elevated during this timeframe (2.6-fold). Most of the changes in gene expression, in response to the 7MPa load, involved up-regulation of members of the canonical WNT signalling group including: BCL9 (2.2-fold), CSNK1A1 (3.2-fold), CTNNB1 (β-catenin) (2.8-fold), FZD8 (3-fold), FZD4 (2.2-fold), NKD1 (2.1-fold), TCF7 (10.4-fold), RUVBL1 (2.8-fold), WNT1 (8-fold) and WNT3 (2.4-fold). As observed at the earlier time point (Figure 5-13B), the same genes involved in the WNT/ Ca^{2+} pathway were up-regulated at 4 hours post-load including NFATC1 (8.4-fold), WNT5B (2.5-fold) and WNT9A (3.3-fold). Furthermore, the PCP pathway genes DAAM1 and RHOA were also elevated (2.1-fold and 2.7-fold respectively). The decreased expression in PRICKLE-1 mRNA levels observed in cartilage exposed to physiological load was also apparent in response to this higher loading regime (2.7-fold). As for the WNT inhibitors, expression of FBXW11 (2.4-fold) and AXIN2 (3.2-fold) were elevated. However, DKK-1 transcription was decreased (3.8-fold), consistent with the observations of its reduction at 2 hours (Figure 5-13B), and in response to physiological load also (Figure 5-13A and Figure 5-14A).

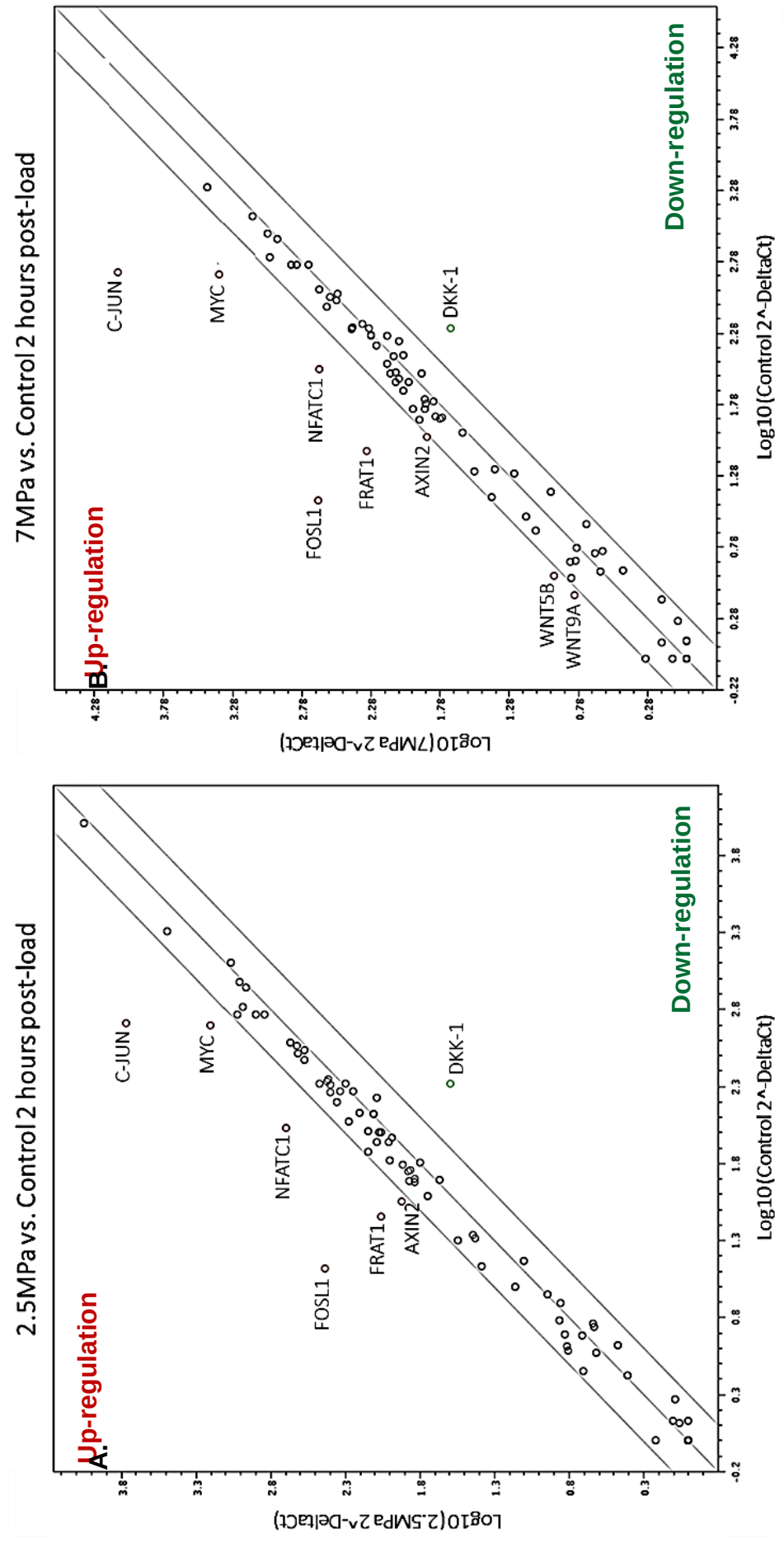

Figure 5-13: Scatterplots of WNT signalling array data comparing A) Control and 2.5MPa, B) Control and 7MPa 2 hours post-load. Explants were loaded at 2.5MPa or 7MPa for 15mins at 1Hz. Data are presented as a mean of 3 independent experiments, in which for each loading regime 6 explants were used. The lines represent the 2-fold threshold. For each experiment, RNA from 6 explants was pooled to create cDNA for use on a single array. Unloaded explants served as controls.

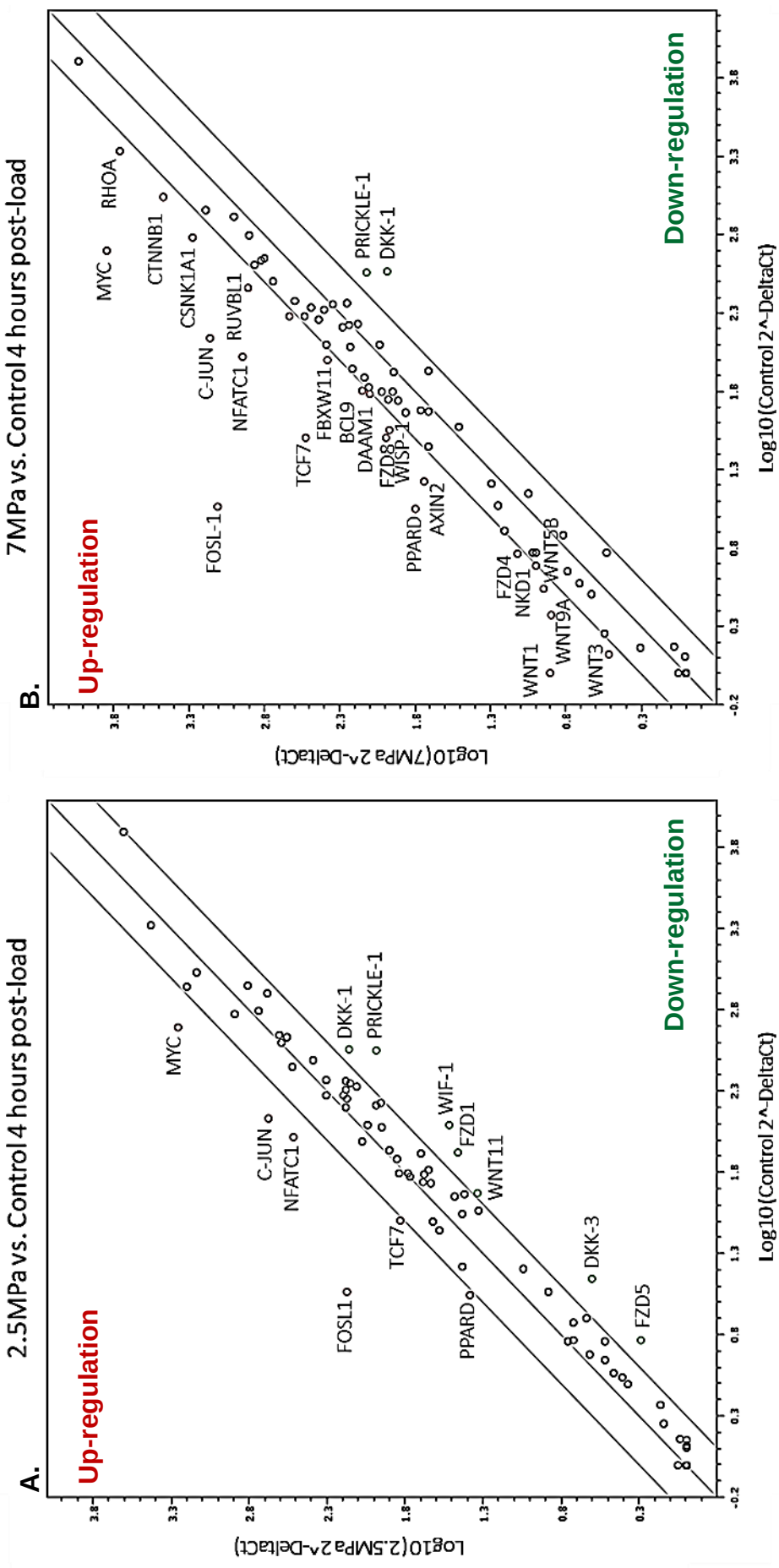

Figure 5-14: Scatterplots of WNT signalling array data comparing A) Control and 2.5MPa, B) Control and 7MPa 4 hours post-load. Explants were loaded at 2.5MPa or 7MPa for 15mins at 1Hz. Data are presented as a mean of 3 independent experiments, in which for each loading regime 6 explants were used. The lines represent the 2-fold threshold. For each experiment, RNA from 6 explants was pooled to create cDNA for use on a single array. Unloaded explants served as controls.

5.2.2.3 Differential mechano-regulation of WNT signalling components 24 hours post-cessation of load

Evaluation of the transcriptional expression of the WNT signalling components 24 hours post-cessation of load demonstrated that many of the genes which had previously been up-regulated by the physiological load at the earlier time points had either returned to basal levels or were significantly down-regulated, approximately 33% of all WNT genes (Figure 5-15A). When compared to data for the earlier time points, a period of 24 hours post-load displayed the least number of physiological load induced changes in WNT target gene expression; across the data set only one gene, namely CCND1 was observed to increase (2-fold). In contrast, many of the canonical WNT signalling related genes were down-regulated at this time point including AES (2.4-fold), FZD9 (3-fold), CTBP1 (2.4-fold), LRP5 (3-fold), FZD1 (6.3-fold), FZD8 (2-fold), FZD3 (2.3-fold), NKD1 (2.5-fold), DVL1 (2.8-fold), FZD4 (3.9-fold), LEF-1 (2.8-fold) and DVL2 (2.8-fold). Of the genes involved in the WNT/ Ca^{2+} pathway, the WNT ligands WNT11 (2-fold), WNT5A (2.5-fold), WNT5B (2.3-fold) and WNT9A (4-fold) were all decreased 24 hours post-cessation of physiological load. Moreover, the PCP pathway genes PRICKLE-1 and RHOU were also decreased (2.1-fold and 2.2-fold respectively). Interestingly, at 24 hours post-load, changes in WNT inhibitor gene expression was most noticeable in explants subjected to physiological load with reductions in FRZB (2.2-fold), WIF-1 (2.5-fold), NLK (2-fold), KREMEN1 (2-fold), AXIN1 (3.5-fold), AXIN2 (2.4-fold) and DKK-3 transcription (2-fold).

In contrast, there were limited changes in gene expression in response to the higher loading regime (7MPa) (Figure 5-15B). However, the WNT signalling target genes were still elevated including FOSL1 (27-fold), WISP1 (4.7-fold), CCDN1 (2.1-fold) and PPARD (3-fold) (Figure 5-15B); the differential expression of these genes was observed across all of the time points in response to the 7MPa load. In contrast, transcript levels of the other WNT related genes were significantly reduced at 24 hours including FZD1 (5-fold), WNT5A (3-fold), PRICKLE-1 (2-fold), and the WNT inhibitors FRZB (2.7-fold) and WIF-1 (2.8-fold).

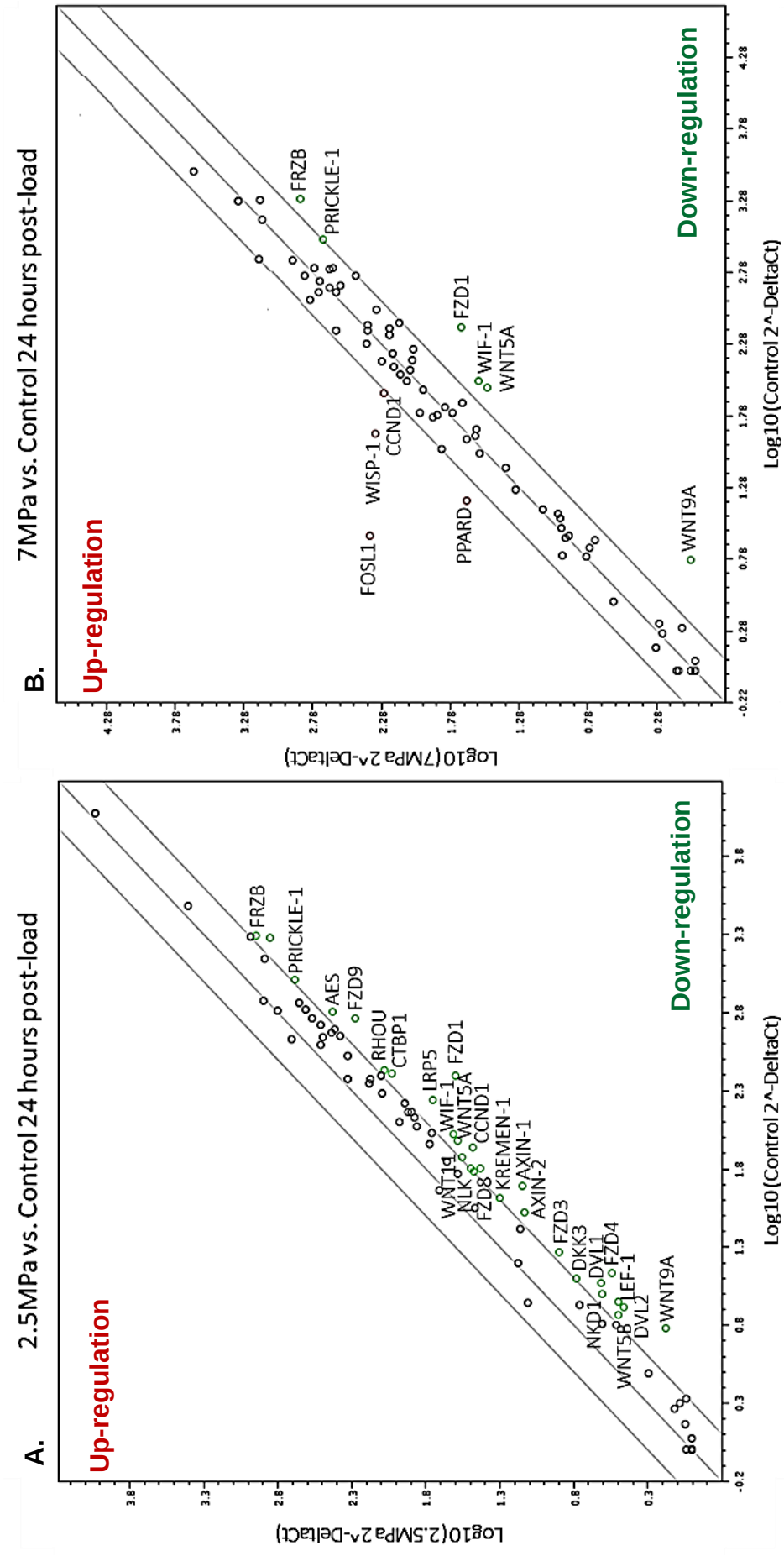

Figure 5-15: Scatterplots of WNT signalling array data comparing A) Control and 2.5MPa, B) Control and 7MPa 24 hours post-load. Explants were loaded at 2.5MPa or 7MPa for 15mins at 1Hz. Data are presented as a mean of 3 independent experiments, in which for each loading regime 6 explants were used. The lines represent the 2-fold threshold. For each experiment, RNA from 6 explants was pooled to create cDNA for use on a single array. Unloaded explants served as controls.

5.2.3 Quantitative PCR validation of mechanically regulated genes identified from the PCR arrays

Having identified putative mechanically-regulated components of the WNT signalling pathway using PCR arrays (Figures 5-13 – 5-15), results obtained were validated using quantitative PCR (with Sybr green technology). Putative genes were selected for validation based on two criteria: [1] at least a 2-fold difference in gene expression between the loading regimens at defined time points, and [2] a relevance to cartilage homeostasis or have potential association with OA pathology. The literature was searched to determine if any of the putative genes had previously been identified as mechano-responsive in other cell types. Fifteen genes were selected based on these criteria including DKK-1, NFATC1, WISP1, WNT1, FRIZZLED1, WIF-1, FOSL1, C-JUN, MYC, WNT16, KREMEN2, LEF1, WNT3A, WNT9A, and PRICKLE-1. However, not all of the genes were mechano-sensitive at each time point post-cessation of load, hence the respective genes which were regulated are presented below.

After 2 hours post-cessation of load, six genes were identified as fitting the criteria above; these included C-JUN, DKK-1, FOSL-1, MYC, NFATC1 and WNT9A (Figure 5-16). Quantification of these genes indicated that five out of the six followed the trends observed on the array (table 5-1). Although relative expression levels differed slightly between the two methodologies, significant increases in C-JUN and FOSL-1 were observed in response to both loading regimes ($p<0.001$); furthermore, DKK1 transcription was significantly reduced in response to load ($p<0.001$). Surprisingly, expression levels of MYC and WNT9A did not reach significance possibly due to the smaller difference in mRNA levels detected using qPCR. NFATC1 mRNA levels were elevated in response to load, as detected using the PCR arrays however the trend was not validated at this time point. In addition, although the genes described were mechano-responsive at this time point post-cessation of load, a differential response to the two loading regimes was not apparent (table 5-1).

Ten genes were identified 4 hours post-cessation of load according to the criteria specified above including C-JUN, DKK-1, FZD1, FOSL1, MYC, NFATC1, PRICKLE-1, WIF-1, WISP-1 and WNT-1 (Figure 5-17). Significant increases in

C-JUN, FOSL1, NFATC1 and WNT-1 ($p<0.001$) were confirmed in response to both loading regimes (table 5-2). Furthermore, a significant differential load-induced increase in FOSL1 and WNT-1 transcription was observed when comparing the response of explants to 2.5MPa versus 7MPa regimes ($p<0.05$). In contrast, DKK-1, FZD1 and PRICKLE-1 mRNA levels were significantly reduced in response to load ($p<0.01$). Interestingly, there was a further differential reduction in DKK1 mRNA levels between explants exposed to the two loading regimes ($p<0.05$). Of the remaining genes that were validated, expression levels of the WNT inhibitor WIF-1 were significantly reduced (9.7-fold, $p<0.01$) in response to physiological load, but appeared unaffected by the higher loading regime (Figure 5-17). This response was consistent between the PCR arrays and qPCR data, identifying another putative differentially regulated gene ($p<0.05$, table 5-2). In contrast, WISP-1 regulation was only apparent at the higher loading regime, as detected both by PCR array (2.6-fold increase) and qPCR (2.3-fold; $p<0.01$), again indicative of a further putative differentially regulated gene ($p<0.01$, table 5-2).

Of the fifteen genes selected for validation, seven were investigated 24 hours post-cessation of load including FOSL-1, FZD1, KREMEN-1, LEF-1, PRICKLE-1, WIF-1 and WISP-1 (Figure 5-18). A significant increase in FOSL-1 was confirmed in response to both loading regimes ($p<0.001$); this effect was more pronounced in explants subjected to the 7MPa load when compared to the physiological 2.5MPa regime ($p<0.001$, table 5-3). Increased WISP-1 transcription in response to load was confirmed ($p<0.01$, Figure 5-18), however no differential effect of the loading regimes was observed (table 5-3). This trend was also apparent for FZD1 ($p<0.05$), LEF-1 ($p<0.01$) and PRICKLE-1 expression ($p<0.01$); mechanical load decreased their mRNA levels but this did not significantly alter between the regimes (table 5-3). Although the PCR arrays had indicated that WIF-1 transcription was regulated by both loading regimes, qPCR validation demonstrated that mRNA levels were only reduced in response to the 7MPa load (2.3-fold). Surprisingly this effect was not statistically significant ($p= 0.05$) although the data suggested that there was a significant load-induced regulation when compared to the physiological load ($p<0.05$, table 5-3). Reduction in mRNA levels of Kremen, which according to the PCR arrays was

regulated by physiological load, was not validated using qPCR (Figure 5-18; table 5-3).

Importantly, nearly all of the genes, detected using the custom-built PCR arrays, which were identified as mechanically regulated in the cartilage explants were verified using qPCR. Furthermore, several sub-groups of genes were identified that were either: [1] regulated in response to load, irrespective of the regime, [2] only regulated by either the 2.5MPa or 7MPa loads respectively, or alternatively [3] a load-induced differential effect whereby the effect was more pronounced as the load increased.

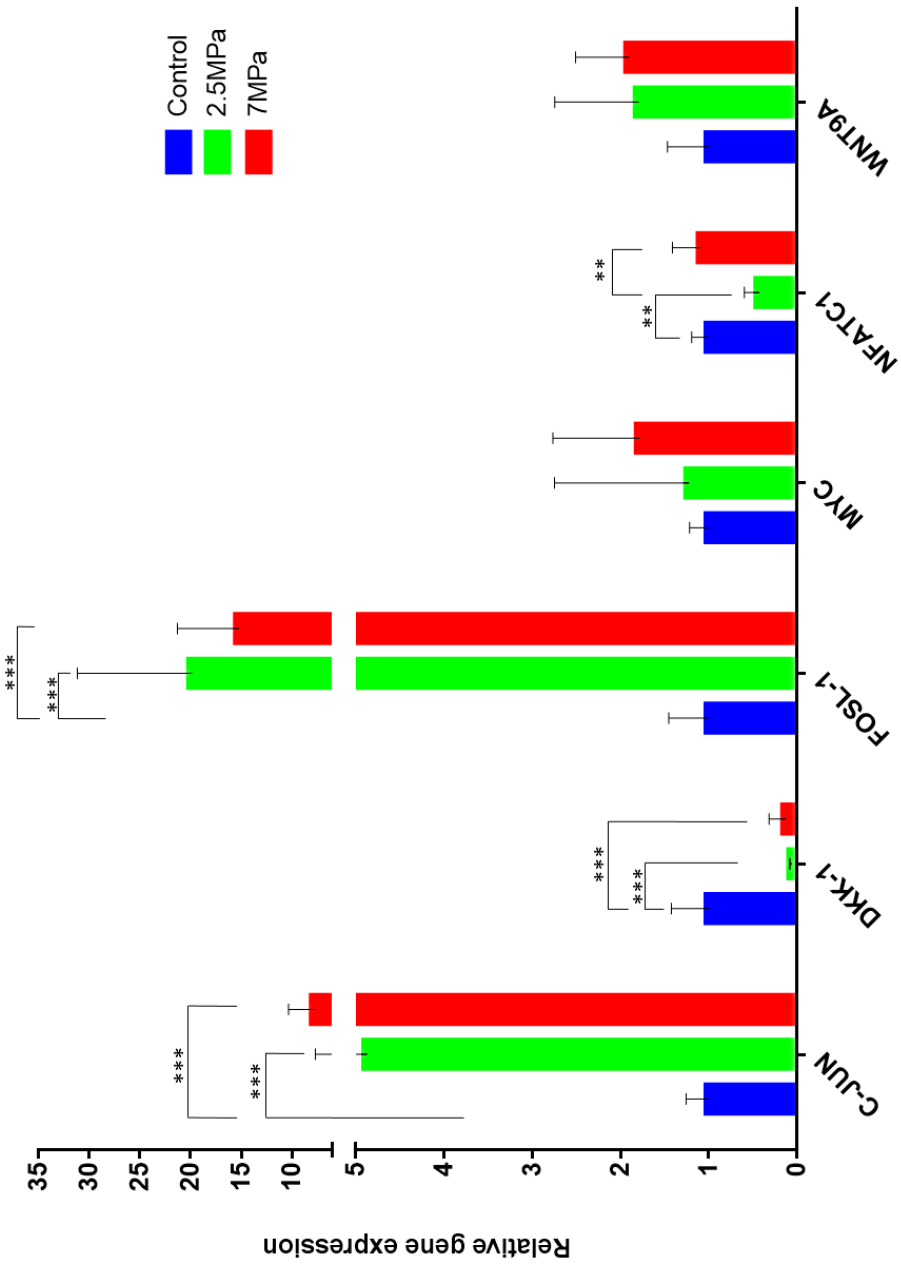

Figure 5-16: Validation of putative mechanically regulated genes using quantitative PCR 2 hours post-load. Putative genes were selected for validation from the WNT signalling arrays (as described in the text); cartilage explants were subjected to loads of either 2.5MPa or 7MPa (1Hz, 15 minutes) and transcriptional effects analysed 2 hours post-cessation of load. Results were normalised to the geometric mean of housekeeping genes SDHA and YWHAZ, and further normalised to the unloaded explants which served as controls. Data is presented as Mean ± SD (n=6) and analysed using 1-way ANOVA [***: $p<0.001$, **: $p<0.01$].

Table 5-1: Comparison of transcript levels of mechano-responsive WNT components 2 hours post-cessation of load identified using PCR arrays and validated using qPCR. Results were normalised to the geometric mean of the housekeeping genes SDHA and YWHAZ, and further normalised to the unloaded control explants. Statistical analysis was performed using a two way ANOVA with Tukey's post hoc test (n=6). [Key: Green filled cells represent agreement with PCR array results, whereas pink cells represent differences between PCR array and qPCR validation results, NS= no significance].

Gene	Unloaded vs.2.5MPa			Unloaded vs.7MPa			2.5MPa vs. 7MPa
	Array result	Validation Fold change	Validation p-value	Array result	Validation Fold change	Validation p-value	Validation p-value
C-JUN	11.5	4.9	p<0.001	25.6	10.3	p<0.001	NS
DKK-1	-5.24	-2.4	p<0.001	-4.04	-1.9	p<0.001	NS
FOSL-1	21	20	p<0.001	35.3	15.3	p<0.001	NS
MYC	3.2	1.2	NS	4.9	1.8	NS	NS
NFATC1	4.6	-2.5	p<0.01	4.3	1.1	NS	P<0.01
WNT9A	1.8	1.8	NS	2.3	2	NS	NS

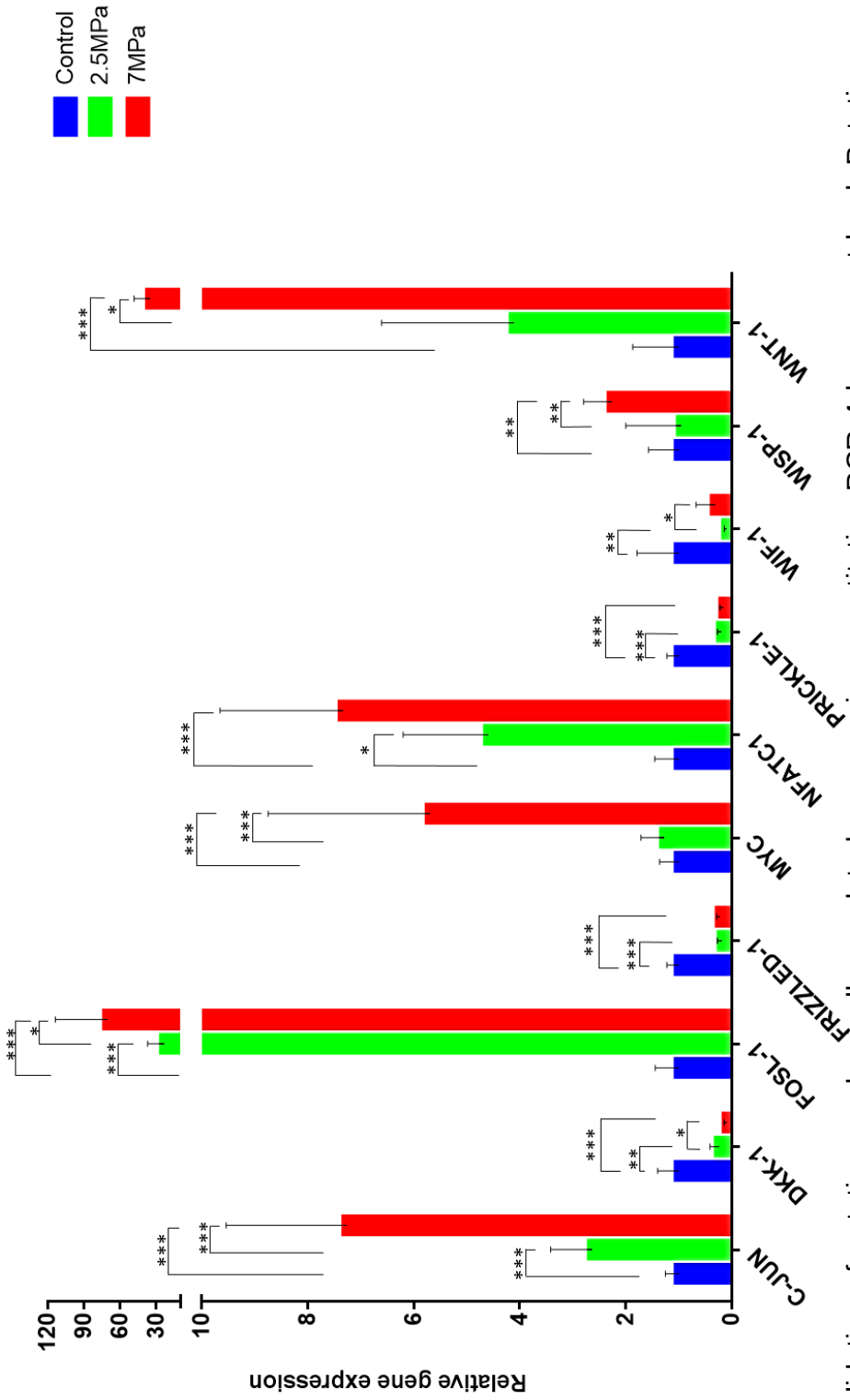

Figure 5-17: Validation of putative mechanically regulated genes using quantitative PCR 4 hours post-load. Putative genes were selected for validation from the WNT signalling arrays (as described in the text); cartilage explants were subjected to loads of either 2.5MPa or 7MPa (1Hz, 15 minutes) and transcriptional effects analysed 4 hours post-cessation of load. Results were normalised to the geometric mean of housekeeping genes SDHA and YWHAZ, and further normalised to the unloaded explants which served as controls. Data is presented as Mean ± SD (n=6) and analysed using 1-way ANOVA [***: p<0.001, **: p<0.01].

Table 5-2: Comparison of transcript levels of mechano-responsive WNT components 4 hours post-cessation of load identified using PCR arrays and validated using qPCR. Results were normalised to the geometric mean of the housekeeping genes SDHA and YWHAZ, and further normalised to the unloaded control explants. Statistical analysis was performed using a two way ANOVA with Tukey's post hoc test (n=6). [Key: Green filled cells represent agreement with PCR array results, whereas pink cells represent differences between PCR array and qPCR validation results, NS= no significance].

Gene	Unloaded vs.2.5MPa			Unloaded vs.7MPa			2.5MPa vs. 7MPa
	Array result	Validation Fold change	Validation p-value	Array result	Validation Fold change	Validation p-value	Validation p-value
C-JUN	3.5	2.6	p<0.001	10.5	7.3	p<0.001	NS
DKK-1	-2.5	-4.1	p<0.01	-3.8	-10.4	p<0.001	p<0.05
FOSL-1	12.9	23.7	p<0.001	109	70.9	p<0.001	p<0.05
FRIZZLED-1	-2.9	-5.2	p<0.001	-1.6	-4.4	p<0.001	NS
MYC	3.6	1.3	NS	14	5.7	p<0.001	p<0.001
NFATC1	3.1	4.6	p<0.05	8.4	7.3	p<0.001	NS
PRICKLE-1	-3.6	-4.9	p<0.001	-2.7	-6.3	p<0.001	NS
WIF-1	-3.8	-9.7	p<0.01	-1.2	1.5	NS	p<0.05
WISP-1	-1.3	-1	NS	2.6	2.3	p<0.01	p<0.01
WNT-1	1.1	3.568	NS	8	16.8	p<0.001	p<0.05

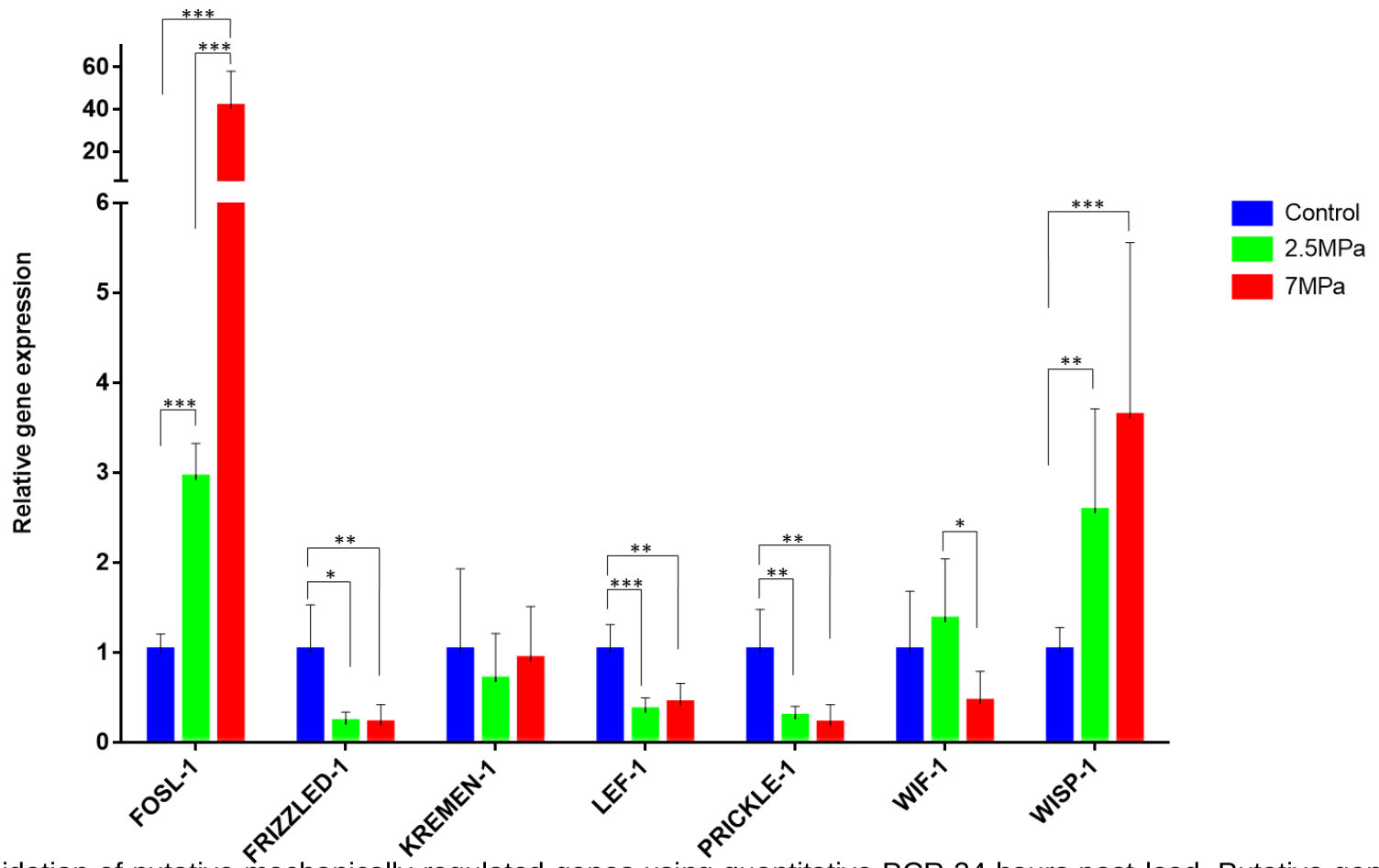

Figure 5-18: Validation of putative mechanically regulated genes using quantitative PCR 24 hours post-load. Putative genes were selected for validation from the WNT signalling arrays (as described in the text); cartilage explants were subjected to loads of either 2.5MPa or 7MPa (1Hz, 15 minutes) and transcriptional effects analysed 24 hours post-cessation of load. Results were normalised to the geometric mean of housekeeping genes SDHA and YWHAZ, and further normalised to the unloaded explants which served as controls. Data is presented as Mean ± SD (n=6) and analysed using 1-way ANOVA [***: $p<0.001$, **: $p<0.01$].

Table 5-3: Comparison of transcript levels of mechano-responsive WNT components 24 hours post-cessation of load identified using PCR arrays and validated using qPCR. Results were normalised to the geometric mean of the housekeeping genes SDHA and YWHAZ, and further normalised to the unloaded control explants. Statistical analysis was performed using a two way ANOVA with Tukey's post hoc test (n=6). [Key: Green filled cells represent agreement with PCR array results, whereas pink cells represent differences between array and qPCR validation results, NS= no significance].

Gene	Unloaded vs.2.5MPa			Unloaded vs.7MPa			2.5MPa vs. 7MPa
	Array result	Validation Fold change	Validation p-value	Array result	Validation Fold change	Validation p-value	Validation p-value
FOSL-1	1.5	3.5	p<0.001	26.5	40	p<0.001	p<0.001
FRIZZLED-1	-6.3	-5	p<0.05	-5	-5.3	p<0.01	NS
KREMEN-1	-2.1	-1	NS	1.1	1.3	NS	NS
LEF-1	-2.8	-3	p<0.001	-1	-2.4	p<0.01	NS
PRICKLE-1	-2.1	-3.8	p<0.01	-2	-5.4	p<0.01	NS
WIF-1	-2.5	1.3	NS	-2.7	-2.3	NS	p<0.05
WISP-1	1.1	2.5	p<0.01	4.7	3.6	p<0.001	NS

5.3 Discussion

It has been recognised for a few years that mechanical loading is associated with activation of the WNT signalling pathway in several tissues such as bone and tendon (Burgers and Williams, 2013, Shi et al., 2012). However, at the start of my PhD, very few studies had been conducted to determine whether there was an association between mechanical loading and activation of the WNT signalling pathway in cartilage chondrocytes. In this chapter, the data clearly demonstrates that WNT signalling, via both the canonical and non-canonical pathways, is differentially regulated according to the level of load applied, at both the gene and protein levels.

5.3.1 Effect of physiological and degradative loading on the regulation of WNT signalling components in cartilage explants

5.3.1.1 Differential localisation of β-catenin in explant cartilage chondrocytes post-cessation of load

As performed previously with the high-density chondrocyte monolayer system, the simplest way to detect WNT signalling activation is by immunofluorescence confocal analysis of β-catenin nuclear translocation. Explants were subjected to compressive load at either 2.5MPa (physiological) or 7MPa (degradative) for 15 minutes (1 Hz) and were analysed either directly or 4, 8 and 24 hours post-cessation of load (see appendix 1-3 for serial sections).

As observed in the chondrocyte monolayer system, mechanical stimulation resulted in the nuclear translocation of β-catenin, mainly in the deep zone chondrocytes at all time points post-cessation of load. In the unloaded explants and in explants directly after the application of 2.5MPa, β-catenin was predominantly cytoplasmic in the superficial and mid zone cells, but in the deep zone cells, both cytoplasmic and nuclear β-catenin was present. In contrast, a marked decrease in β-catenin expression was observed in the superficial and mid zones of cartilage analysed directly after the application of a 7MPa load. In the explant model, nuclear translocation of β-catenin was most abundant 4 hours post-cessation of load; this differs to the 2 hours that was found to be maximal in the chondrocyte monolayer system possibly reflecting the period of time necessary to transduce the biomechanical signals through the matrix to the cell

to effect a response. After 4 hours post-load, β-catenin nuclear translocation was again observed throughout the different zones of cartilage but again predominantly in the deep zone in response to 2.5MPa, an effect observed directly after load application. In a similar fashion, nuclear translocation of β-catenin was observed throughout the mid and deep zone chondrocytes in cartilage exposed to the 7MPa load however, increased cytoplasmic accumulation was also evident. Interestingly, this increase in cytoplasmic β-catenin in explants subjected to the 7MPa loading regime was also observed in the high-density monolayer chondrocytes exposed to 14% elongation (deemed a non-physiological regime). At 8 and 24 hours post-cessation of the 2.5MPa load, β-catenin localisation had returned to basal levels comparable with the unloaded control explants. Interestingly, the β-catenin localisation profile observed at the earlier time points in response to the 7MPa load was also apparent at 8 and 24 hours, with increased nuclear β-catenin in the deep zone chondrocytes and punctate cytoplasmic β-catenin localised throughout all zones, but particularly in the deep zone.

The zone specific nature of the nuclear translocation of β-catenin may arise as a consequence of the cartilage tissue attempting to maintain integrity. Although the superficial zone is the closest to the site of mechanical stimulation and thus it might be anticipated that WNT signalling might therefore be invoked in this region first, interestingly more activation was observed in the deep zone. The nuclear localisation of β-catenin in deep zone chondrocytes may have occurred due to the deep zone containing higher levels of sulphated GAGs, therefore the chondrocytes are in an environment designed to withstand such forces and can adapt adequately by activation of key signalling pathways to promote either catabolic or anabolic processes to maintain tissue homeostasis. Other studies applying compressive load to cartilage chondrocytes have observed a similar phenomenon whereby cells in the deep zone seem to respond more overtly to compressive load compared with cells residing in the superficial and mid zones (Lee et al., 2000, Durrant et al., 1999).

5.3.1.2 Differential mechano-regulation of WNT signalling components

Having confirmed the mechano-regulation of the WNT signalling pathway in cartilage chondrocytes, as exemplified by increased nuclear translocation of β-catenin, the next step was to determine how this effect might be propagated. To address this, the gene expression profile of WNT signalling components were evaluated using custom-built bovine specific PCR arrays containing 84 WNT signalling related genes grouped according to function. The assigned groups included targets of WNT signalling, components of canonical WNT signalling, WNT/Ca^{2+} pathway, planar cell polarity (PCP) pathway and inhibitors of WNT signalling (see appendix 4-6 for all WNT genes). Cartilage explants were subjected to either a load of 2.5MPa or 7MPa and were analysed 2, 4 or 24 hours post-cessation of load; unloaded explants processed at identical time points served as controls. The periods post-load selected for this set of experiments were based on the optimal timeframe identified in the characterisation experiments, where establishment of the "transcriptional window" to capture changes in early-response genes and downstream targets was conducted (section 4.2.1.4).

The gene expression profile of explants subjected to a load of 2.5MPa or 7MPa and analysed 2 hours post-cessation of load demonstrated a similar response. Both loading regimes increased the expression of the early response genes C-JUN, MYC and FOSL1 (WNT signalling targets), FRAT1 (canonical WNT signalling), NFATC1 (WNT/Ca^{2+}) and AXIN2 (inhibitor), while DKK-1 expression was decreased. Interestingly, the higher load (7MPa) also induced the up-regulation of the WNT/Ca^{2+} related genes WNT5B and WNT9A. Although, at this time point of analysis, several genes were differentially regulated as the load increased, the majority of the genes exhibited altered expression in response to both loading regimes. The similarity in gene expression profiles within this time point likely suggests that these WNT genes are the first to be transcriptionally altered in response to load, regardless of whether the loading regime was physiological or degradative. These results are in line with other studies, which demonstrated increases in load induced early-response gene expression

indicating a mechano-responsive effect (Thomas et al., 2011, Fitzgerald et al., 2004, Sironen et al., 2002).

By 4 hours post-cessation of load, many more genes were affected by the loading regimes, and their differences in expression levels were also amplified compared to the earlier point. In addition to the WNT signalling target genes regulated at 2 hours post-load (2.5MPa), PPARD was also up-regulated. However, after 4 hours the canonical WNT signalling components were differentially regulated with increased expression of TC7, and a significant reduction in FZD1 and FZD5 transcription. TC7 is a transcription factor known to associate with nuclear β-catenin to facilitate canonical WNT signalling (Wu et al., 2012), thus its up-regulation confirms mechano-activation of canonical WNT signalling at the transcriptional level. The other canonical component, FZD, encodes a family of receptor proteins in which WNT ligands bind to mediate the inhibition of β-catenin phosphorylation via the glycogen synthase kinase-3β complex. Down-regulation of FZD expression has been associated with inhibition of canonical WNT signalling (Chigita et al., 2012), therefore, its reduction in response to the 2.5MPa load may reflect a means of controlling the extent of WNT activation. Regulation of the WNT/Ca^{2+} pathway genes was still evident at 4 hours post-cessation of load with the consistent up-regulation of NFATC1 and down-regulation of WNT11. The consequences of NFATC1 regulation in cartilage are conflicting. Some studies have associated NFATC expression with markers of cartilage catabolism (Ranger et al., 2000), but a recent study hypothesised this molecule to be a suppressor of OA development (Greenblatt et al., 2013), whereas WNT11 is known to regulate collagen type II expression via activation of protein kinase C (Ryu and Chun, 2006). Alterations in the PCP gene pathway, namely PRICKLE-1 down-regulation was only evident at 4 hours post-cessation of the 2.5MPa load. Furthermore, all the inhibitors analysed (DKK-1, -3 and WIF-1) were down-regulated at 2.5MPa.

A similar differential regulation of the genes observed in cartilage loaded at 2.5MPa was also evident in response to the higher regime (7MPa) 4 hours post-load, but WISP-1 transcription was also up-regulated. induction of WISP-1, a WNT signalling target, in response to the 7MPa load only may be a specific response to higher magnitudes of load, as its expression is implicated in inducing

MMP and ADAMTS synthesis in murine and human chondrocytes (Blom et al., 2009). This would agree with the previous observations of increased MMP and ADAMTS transcription in response to the 7MPa load (Chapter 4). Enhanced expression of genes related to canonical WNT signalling were most abundant in response to the 7MPa load including BCL9, CSNK1A1, CTNNB1, FZD8, FZD4, NKD1, TCF7, RUVBL1, WNT1 and WNT3. Increased transcription of CTNNB1 demonstrates that the confocal immunofluorescence analysis depicting activation of canonical WNT signalling is not only mediated through nuclear translocation at the protein level, but is also effected at the gene level. It is interesting to note that some components of the PCP gene group are differentially regulated i.e. DAAM1 and RHOA were up-regulated and PRICKLE-1 down-regulated in response to load. DAAM1 was reported to activate RHOA via WNT signalling (Matusek et al., 2006), which may explain their co-up-regulation only within this time point (these genes were not expressed at other time points or loading regimes). These results corroborate a study demonstrating the mechano-responsiveness of RHOA in agarose-embedded human chondrocytes subjected to cyclic compression (5-15%, 0.5Hz, 5 – 10 minutes) (Haudenschild et al., 2008b). RHOA can induce actin cytoskeletal protein reorganisation, which is suggested to be a mechanism by which chondrocytes can alter their mechanical properties dependent on the mechanical load applied (Campbell et al., 2007). Increased expression of the WNT inhibitors FBXW11 and AXIN2 was observed, whereas DKK-1 was consistently down-regulated in both loading regimes and post-load time points which may lead to the increase in WNT signalling activation.

Most of the genes had returned to a basal level of expression comparable to the unloaded tissue at 24 hours post-cessation of load, or expression levels were reduced below that of the unloaded controls. In response to 2.5MPa primarily, the canonical WNT signalling components and inhibitors were down-regulated indicating a reduction in load-induced WNT signalling. In contrast, cartilage subjected to the higher load (7MPa) demonstrated a consistent, and sustained up-regulation of WNT target genes (FOSL-1, WISP-1, PPARD, and CCND1); the remainder of the genes exhibited similar expression profiles to the 2.5MPa load and unloaded cartilage. Furthermore, it is interesting to note that the mechano-regulation of the canonical WNT signalling components (at 7MPa),

which had previously been elevated were subsequently down-regulated at 24 hours post-load suggestive that WNT activity is controlled returning it to basal levels. Surprisingly, the only time-point in which DKK-1 was not differentially regulated in either loading regime was at 24 hours post-load. This result reaffirms the possibility that DKK-1 down-regulation was associated with an initial WNT signalling activation (Zhou et al., 2010), as taken together with the confocal data, it is evident that WNT signalling activity is diminished within 24 hours post-cessation of load in comparison to other time points.

Overall, both loading regimes demonstrated similarities in their differential regulation of the WNT signalling genes that were present on the PCR arrays. Furthermore, early-response genes such as MYC and C-JUN were consistently up-regulated in both loading regimes, particularly at 2 and 4 hours post-load, indicating that the transcriptional window for these early mechanical responses is within 4 hours post-stimulation of the tissue which is in line with other studies (Fitzgerald et al., 2006, Huang et al., 2005, Sironen et al., 2002). Importantly, nearly all of the genes, detected using the custom-built PCR arrays, which appeared to be mechanically regulated in the cartilage explants were verified using qPCR (Tables 5-1, 5-2, 5-3). Furthermore, several sub-groups of genes were identified that were either: [1] regulated in response to load, irrespective of the regime, [2] only regulated by either the 2.5MPa or 7MPa loads respectively, or alternatively [3] a load-induced differential effect whereby the effect was more pronounced as the load increased.

5.4 Summary

- Mechanical load activated WNT signalling in explant cartilage chondrocytes.

- Zonal-dependent activation of WNT signalling with enhanced β-catenin nuclear translocation predominantly occurring in the deep zone in response to both loading regimes.

- Differential load induced transcription of WNT signalling components in response to physiological and degradative loads, with predominant WNT activity occurring at 4 hours post-cessation of load.

- Quantitative PCR successfully validated 15 genes selected from the PCR array findings demonstrating mechano-responsive WNT signalling transcripts.

- Transcription of WNT components were either regulated in response to load irrespective of the regime, were regulated by either the 2.5MPa or 7MPa loads respectively, or alternatively a load-induced differential effect whereby the effect was more pronounced as the load increased.

Chapter 6

Functional analysis- Involvement of DKK-1 and NFATc1 in articular cartilage mechanotransduction

6.1 Background

One of the main modulators involved in cartilage development is WNT signalling. During limb development, canonical WNT signalling was demonstrated to be integral for joint formation (Guo et al., 2004). WNT signalling is differentially regulated according to the differentiation state of chondrocytes (Guo et al., 2009). Recent studies have hypothesised that the cellular processes observed during limb development recapitulate in the pathology of OA including chondrocyte hypertrophy and matrix mineralisation (Blom et al., 2009). Canonical WNT signalling predominantly regulates the process of endochondral ossification during the initial stages before involvement of the non-canonical WNT pathway which maintains the cartilage phenotype, and prevents chondrocytes from undergoing terminal differentiation (Logan and Nusse, 2004, Yates et al., 2005). Expression of WNT signalling components are also dys-regulated in OA pathology. In end-stage human OA, significant up-regulation of several canonical and non-canonical WNT ligands Frizzled receptors and WNT targets including NFATC2, WISP-1, and FOSL1 were observed (Thorfve et al., 2012). Furthermore, in mouse models of experimental OA, enhanced expression of WISP-1, WNT2B and WNT16 were observed (Blom et al., 2009). One of the genome-wide association scans demonstrated the existence of single nucleotide polymorphisms in the inhibitors of the WNT signalling pathway in human end-stage OA cartilage (Loughlin et al., 2004). The presence of these mutations reduces their ability to promote inhibition resulting in increased WNT signalling (Loughlin et al., 2004). Furthermore, dys-regulation of the WNT signalling pathway is shown to induce hypertrophic changes in cartilage tissue, which is a factor involved in OA progression (van der Kraan and van den Berg, 2012). Studies have demonstrated that WNT inhibitors were significantly up-regulated in healthy cartilage tissue, which in normal circumstances is resistant to hypertrophic differentiation, however in OA tissue the expression of WNT inhibitors was significantly down-regulated (Leijten et al., 2012, Thorfve et al., 2012). Regulation of WNT signalling is vital for the maintenance of cartilage homeostasis, thus, there are several secreted inhibitors such as DKK-1, secreted

frizzled related proteins (SFRPs) and WIF-1, which ensure that WNT activation is a tightly controlled process.

Of the WNT associated genes verified as being mechano-sensitive in articular cartilage (Chapter 5), several of these have been implicated in cartilage degeneration and are differentially regulated in OA pathology. One of these genes, which has been widely studied and known to be implicated in OA pathology, is DKK-1. DKKs are a family of secreted glycoproteins comprised of four members (DKK-1-4), however it is widely thought that DKK-1 is the most abundant of the DKKs in articular cartilage (Cruciat and Niehrs, 2013). DKK-1 inhibits WNT signalling by binding to lipoprotein receptor-related protein-6, thus preventing the WNT ligand from binding to its receptor to activate this signalling pathway (Li et al., 2010). Knock-out mouse models of DKK-1 are embryonic lethal due to their integral role in facilitating head and limb development (Mukhopadhyay et al., 2001). Expression of DKK-1 is elevated in human OA cartilage (Thorfve et al., 2012), thus studies have investigated the role of DKK-1 in cartilage homeostasis; these studies have produced contradictory results. A study by Weng et al. demonstrated that in a rat model of OA, administration of DKK-1 aggravated symptoms associated with OA (Weng et al., 2010), whereas inhibition of DKK-1 expression alleviated these symptoms (Weng et al., 2010, Oh et al., 2012). In contrast, a recent study by Funk-Brentano et al. indicated that DKK-1 is highly expressed in healthy mouse cartilage, and furthermore that the therapeutic use of DKK-1 in mechanically-induced OA decreased disease severity, however there was still some proteoglycan loss (Funck-Brentano et al., 2014). These latter findings are in line with the proposed role of DKK-1 as an inhibitor of cartilage hypertrophy, which eventually contributes to OA pathology (Leijten et al., 2012).

NFATC1, nuclear factor of activated T cells (NFAT) was another mechano-sensitive gene identified in the PCR arrays of articular cartilage (Chapter 5), and it too has a prominent role in OA pathology (Greenblatt et al., 2013). The NFATs are a family of transcription factors, which were originally identified as mediating transcriptional regulation via T-cell receptor signalling in immune cells (Wang et al., 2009). The NFAT family has five members in which four (NFATC1 - NFATC4) are activated by calcineurin mediated dephosphorylation of serine residues as

part of the WNT/Ca^{2+} pathway (Greenblatt et al., 2013). To date, there is a poor understanding of how these transcription factors promote catabolic activities, through WNT dysregulation and increased expression of degradative enzymes, in OA chondrocytes (Wang et al., 2009). Earlier studies investigating the role of NFAT in cartilage using NFATC1 deficient mice demonstrated predominantly catabolic activities leading to cartilage degeneration (Wang et al., 2009). The NFAT family have an integral role in regulating the metabolism of adult chondrocytes, as studies have shown that mice lacking both NFATC1 and NFATC2 in cartilage develop severe OA affecting multiple joints; furthermore the speed of disease progression is faster than in other OA mouse models (Greenblatt et al., 2013). Interestingly, the symptoms observed in these knockout mice were reminiscent of human OA such as matrix degradation, osteophyte formation and subchondral bone remodelling as well as loss of cartilage tissue and joint instability (Greenblatt et al., 2013, Wang et al., 2009). However, induction of NFATC2 has been associated with modulation of aggrecan degradation in chondrocytes due to increased ADAMTS-4 activity, correlating with the observation of increased NFATC2 expression in human OA cartilage (Thorfve et al., 2012, Thirunavukkarasu et al., 2006).

As previously demonstrated (Chapter 5), DKK-1 and NFATC1 were both highly sensitive to mechanical load. Inhibition of DKK-1 transcription and induction of NFATc1 expression was observed in explant chondrocytes subjected to load, particularly at 4 hours post-cessation of stimulation. Interestingly, increasing the magnitude of load compounded their differential expression. To understand the relevance of the mechano-sensitive nature of these genes, their role in cartilage mechanotransduction was investigated by manipulating the expression of these molecules and subjecting the tissue to a 7MPa load; the higher loading regime was selected as the genes were most significantly regulated under this stimulation.

6.2 Results

To determine the function(s) of DKK-1 and NFATC1 in cartilage chondrocyte mechanotransduction, their expression was manipulated either by exogenous application of human recombinant DKK-1 or by addition of an NFATC inhibitor (VIVIT peptide) to the cartilage explants for 24 hours prior to mechanical load (7MPa, 1Hz, 15 minutes). Explants were then analysed 24 hours post-cessation of load when changes in transcriptional markers of the cartilage ECM had previously been observed (Chapter 4). As mentioned, the NFATs are a family of transcription factors and, to date, there are no isoform specific inhibitors therefore a generic NFAT inhibitor was used for these functional analyses.

6.2.1 Effect of human recombinant DKK-1 and NFAT inhibitor on explant chondrocyte viability

To assess the most efficacious concentration of modifying agents whilst remaining non-toxic, a range of concentrations of recombinant DKK-1 and NFAT inhibitor were tested, and toxicity evaluated using the CyoTox 96 assay. Based on concentrations reported in the literature, explants were either treated with 100ng/ml, 250ng/ml or 500ng/ml of recombinant DKK-1 or 10µM, 25µM or 50µM NFAT inhibitor for 24 hours prior to the application of load (7MPa, 1Hz, 15 minutes) and then retained in the media throughout the experiment. Toxicity was assessed 24 hours post-cessation of load by analyses of media (Figure 6-1). Comparisons of the treatments normalised to media from the untreated explants (subjected to load only), which served as the control, demonstrated no significant differences indicating that within the range of concentrations used the treatments were non-toxic (Figure 6-1).

6.2.2 Effect of recombinant DKK-1 on mechanically-regulated gene expression in cartilage explants

To investigate the role of DKK-1 in cartilage chondrocyte mechanotransduction, mRNA levels of a panel of genes which included aggrecan, collagen type 2, MMPs, ADAMTSs and TIMPs were quantified 24 hours post-cessation of load after stimulation with 100ng/ml, 250ng/ml or 500ng/ml recombinant DKK-1 (Figures 6-2, 6-3, 6-4 and 6-5). The main

components of cartilage ECM, both aggrecan (Figure 6-2A) and collagen type II expression (Figure 6-2B) appeared unaffected by DKK-1 treatment under these experimental conditions. Transcription of several proteolytic enzymes were decreased in response to DKK-1 stimulation; MMP3 transcription was most significantly affected with a reduction in mRNA expression at all concentrations of recombinant DKK-1 tested with respect to control (100ng/ml 2-fold, $p<0.01$; 250ng/ml 2.4-fold, $p<0.01$; 500ng/ml 1.8-fold, $p<0.05$) (Figure 6-3A). Although MMP9 expression appeared to increase in a dose-dependent manner, this was not statistically significant likely due to the large variation between explants (Figure 6-3B). Interestingly, MMP13 expression was significantly decreased (7-fold; $p<0.001$) in response to 100ng/ml recombinant DKK-1 treatment, however there was no effect at the higher concentrations (Figure 6-3C). Although ADAMTS-4 expression appeared to decrease in explants stimulated with 250ng/ml and 500ng/ml DKK-1, this was not statistically significant (Figure 6-4A). As observed with MMP13, ADAMTS-5 expression also decreased significantly in response to 100ng/ml recombinant DKK-1 (3.2-fold, $p<0.05$), and although transcript levels were reduced at the higher concentrations, again this was not statistically significant (Figure 6-4B). Furthermore, there was an overall reduction in TIMP 1 expression which was significant at 100ng/ml (1.7-fold, $p<0.05$) and 500ng/ml recombinant DKK-1 (2.2-fold, $p<0.01$; Figure 6-5A). Surprisingly, TIMP 3 expression was unaffected by treatment under these experimental conditions (Figure 6-5B).

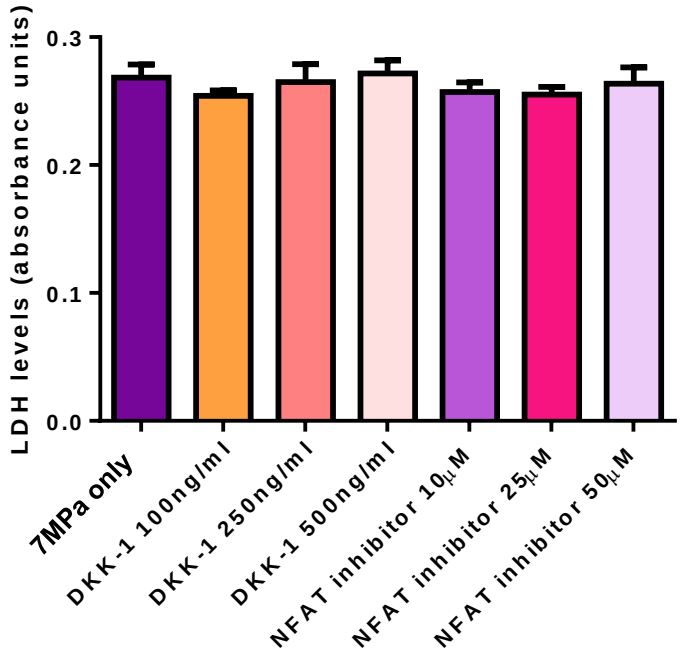

Figure 6-1: Raw absorbances of LDH levels in the media to determine viability of explant tissue treated with different concentrations of recombinant DKK-1 or NFAT inhibitor for 24 hours prior to the application of load (7MPa, 1 Hz, 15 minutes). Media was analysed 24 hours post-cessation of load and absorbance values normalised to the control explants (load only). Data are presented as mean ± SD (n=6) and analysed using a 1-way ANOVA.

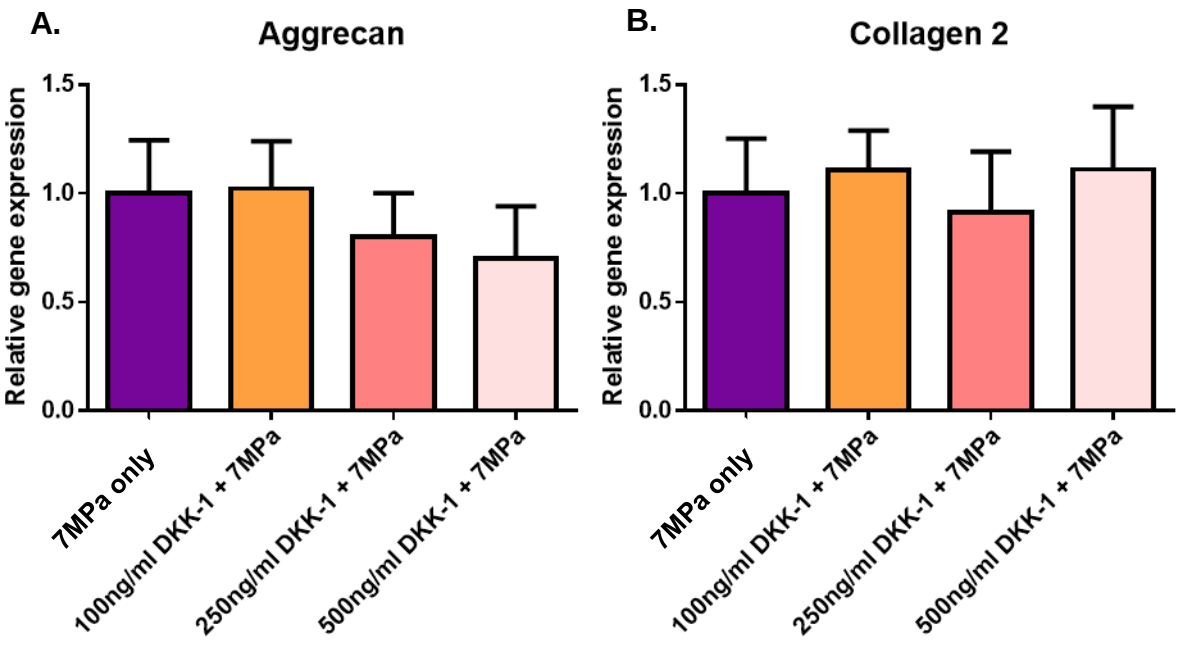

Figure 6-2: mRNA quantification of A) Aggrecan and B) Collagen type II in explants subjected to either 100ng/ml, 250ng/ml or 500ng/ml recombinant DKK-1 for 24 hours prior to application of load (7MPa, 1Hz, 15 minutes). Gene expression was analysed using qPCR in explants processed 24 hours post-cessation of load. Data is presented as mean ± SD (n=6) after normalisation to the housekeeping genes YWHAZ and SDHA and relative to the control (load only). Data was analysed using a 2-way ANOVA.

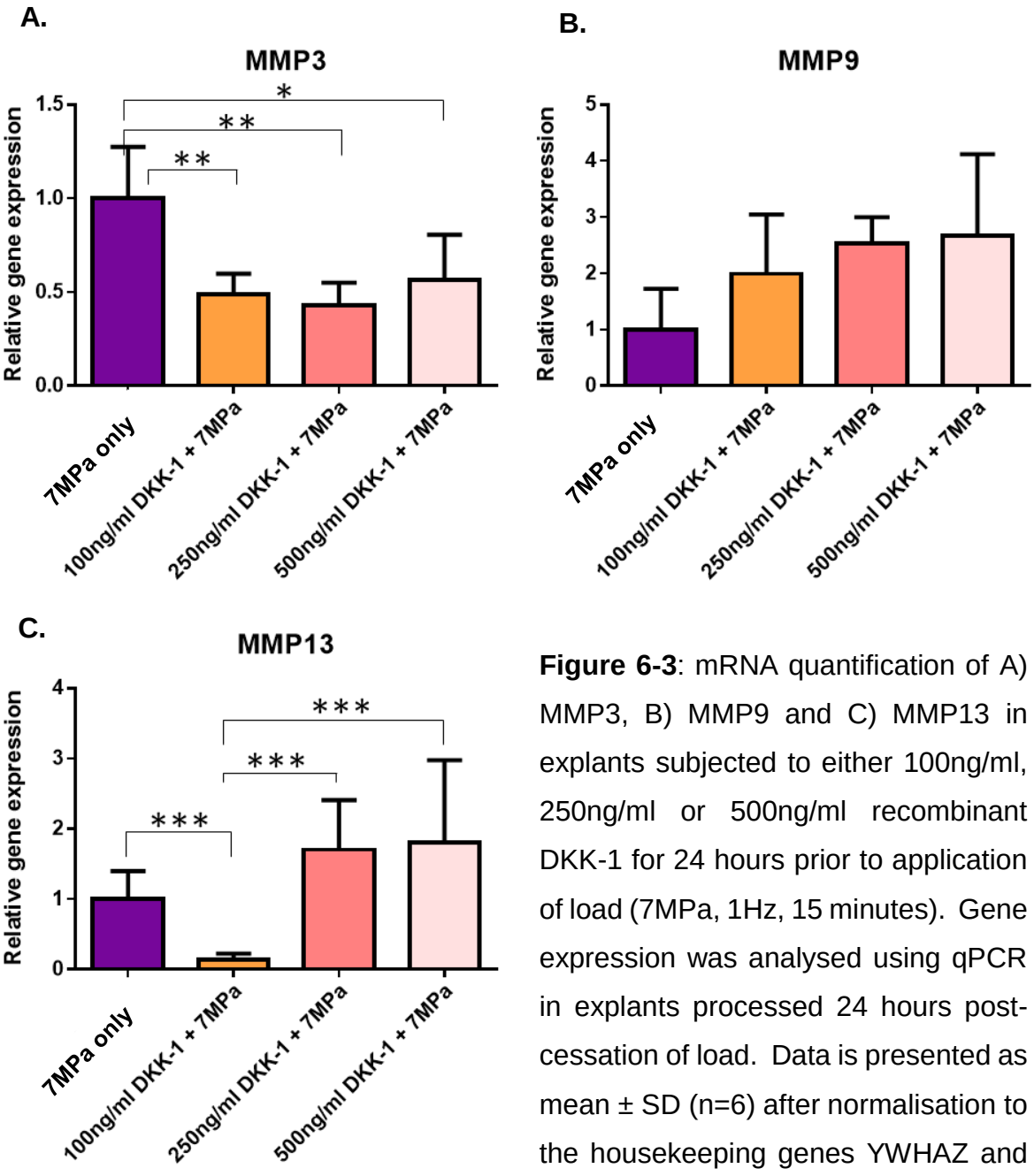

Figure 6-3: mRNA quantification of A) MMP3, B) MMP9 and C) MMP13 in explants subjected to either 100ng/ml, 250ng/ml or 500ng/ml recombinant DKK-1 for 24 hours prior to application of load (7MPa, 1Hz, 15 minutes). Gene expression was analysed using qPCR in explants processed 24 hours post-cessation of load. Data is presented as mean ± SD (n=6) after normalisation to the housekeeping genes YWHAZ and SDHA and relative to the control (load only). Data was analysed using a 2-way ANOVA [* $P < 0.05$, ** $P < 0.01$, *** $P < 0.001$].

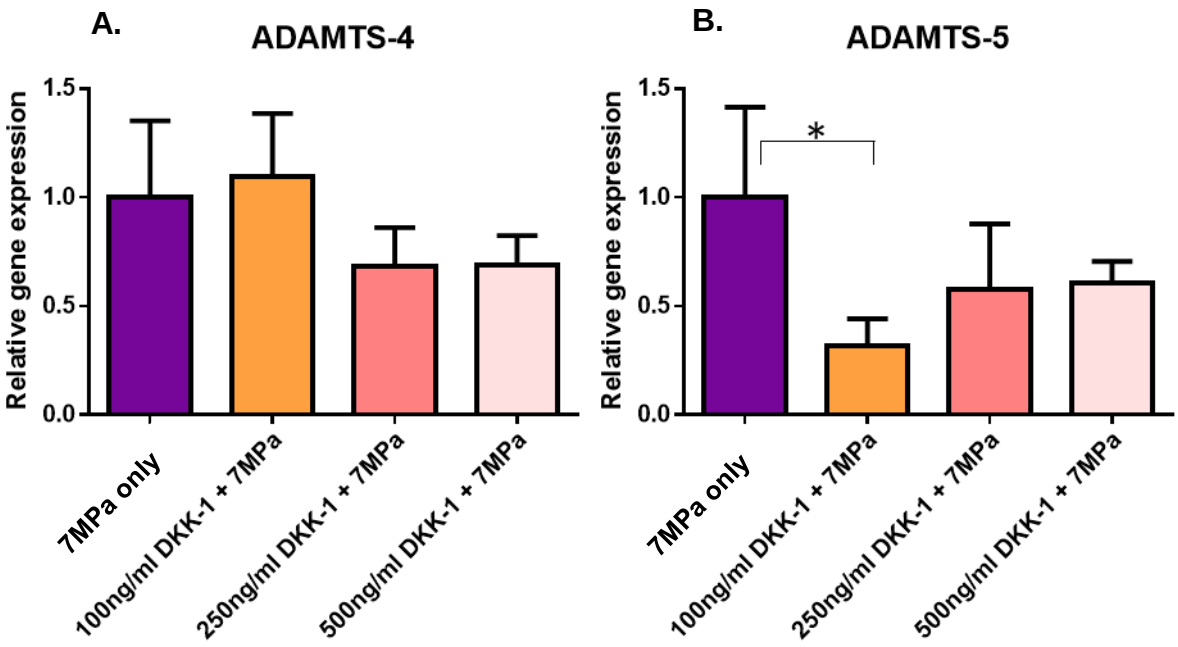

Figure 6-4: mRNA quantification of A) ADAMTS-4 and B) ADAMTS-5 in explants subjected to either 100ng/ml, 250ng/ml or 500ng/ml recombinant DKK-1 for 24 hours prior to application of load (7MPa, 1Hz, 15 minutes). Gene expression was analysed using qPCR in explants processed 24 hours post-cessation of load. Data is presented as mean ± SD (n=6) after normalisation to the housekeeping genes YWHAZ and SDHA and relative to the control (load only). Data was analysed using a 2-way ANOVA [* $P < 0.05$].

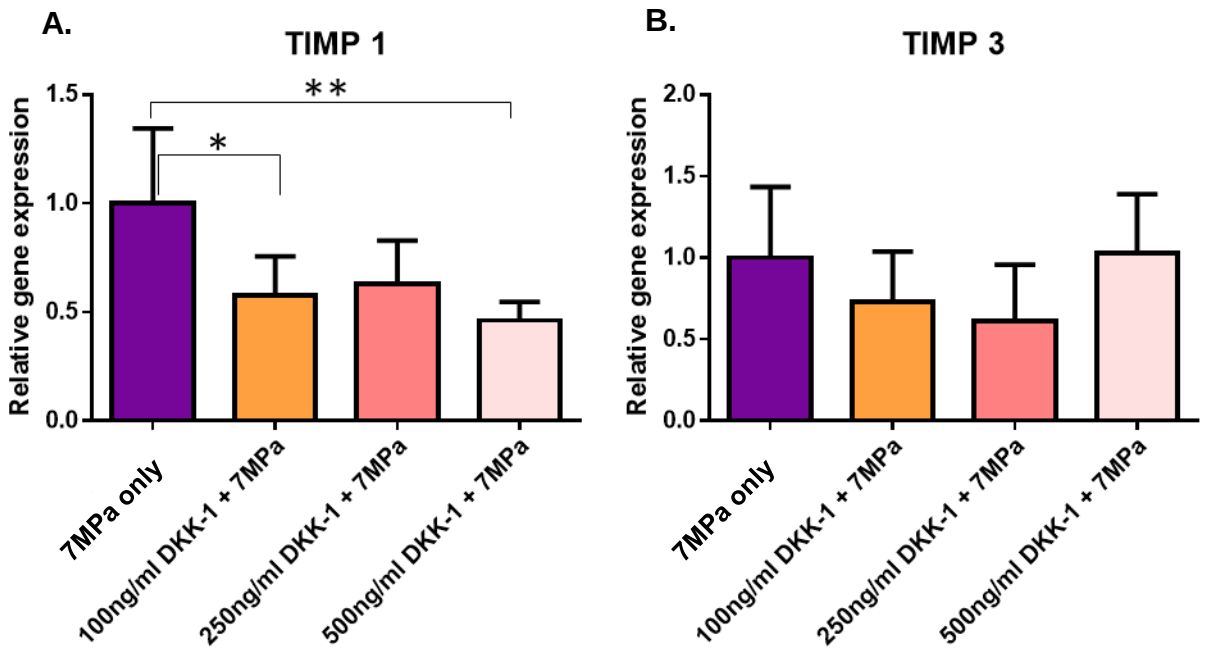

Figure 6-5: mRNA quantification of A) TIMP 1 and B) TIMP 3 in explants subjected to either 100ng/ml, 250ng/ml or 500ng/ml recombinant DKK-1 for 24 hours prior to application of load (7MPa, 1Hz, 15 minutes). Gene expression was analysed using qPCR in explants processed 24 hours post-cessation of load. Data is presented as mean ± SD (n=6) after normalisation to the housekeeping genes YWHAZ and SDHA and relative to the control (load only). Data was analysed using a 2-way ANOVA [* $P < 0.05$, ** $P < 0.01$].

6.2.3 Effect of NFAT inhibitor on mechanically-regulated gene expression in cartilage explants

To investigate the role of NFAT in cartilage chondrocyte mechanotransduction, mRNA levels of a panel of genes as described previously (section 6.2.2) were quantified 24 hours post-cessation of load after stimulation with 10µM, 25µM or 50µM NFAT inhibitor (Figures 6-6, 6-7, 6-8 and 6-9). Of the two major ECM genes analysed, aggrecan expression was significantly reduced at all concentrations tested (10µM 1.6-fold, $p<0.01$; 25µM 1.8-fold, $p<0.01$; 50µM 1.9-fold, $p<0.001$; Figure 6-6A), whereas collagen type 2 mRNA levels were unaffected (Figure 6-6B). Surprisingly, inhibition of NFAT did not significantly affect transcript levels of MMP3 (Figure 6-7A), MMP9 (Figure 6-7B), MMP13 (Figure 6-7C) or ADAMTS-4 (Figure 6-8A) when compared to explants that had been subjected to load (7MPa) only; this may have been attributed to large variations in the experimental samples. In contrast, ADAMTS-5 expression was significantly reduced in response to 25µM NFAT inhibitor (2.6-fold, $p<0.05$; Figure 6-8B). In relation to TIMPs, the NFAT inhibitor elicited a significant overall reduction in TIMP 1 expression (10µM 2.7-fold, $p<0.001$; 25µM 1.9-fold, $p<0.01$; 50µM 2-fold, $p<0.01$; Figure 6-9A), whilst TIMP 3 expression remained unchanged (Figure 6-9B).

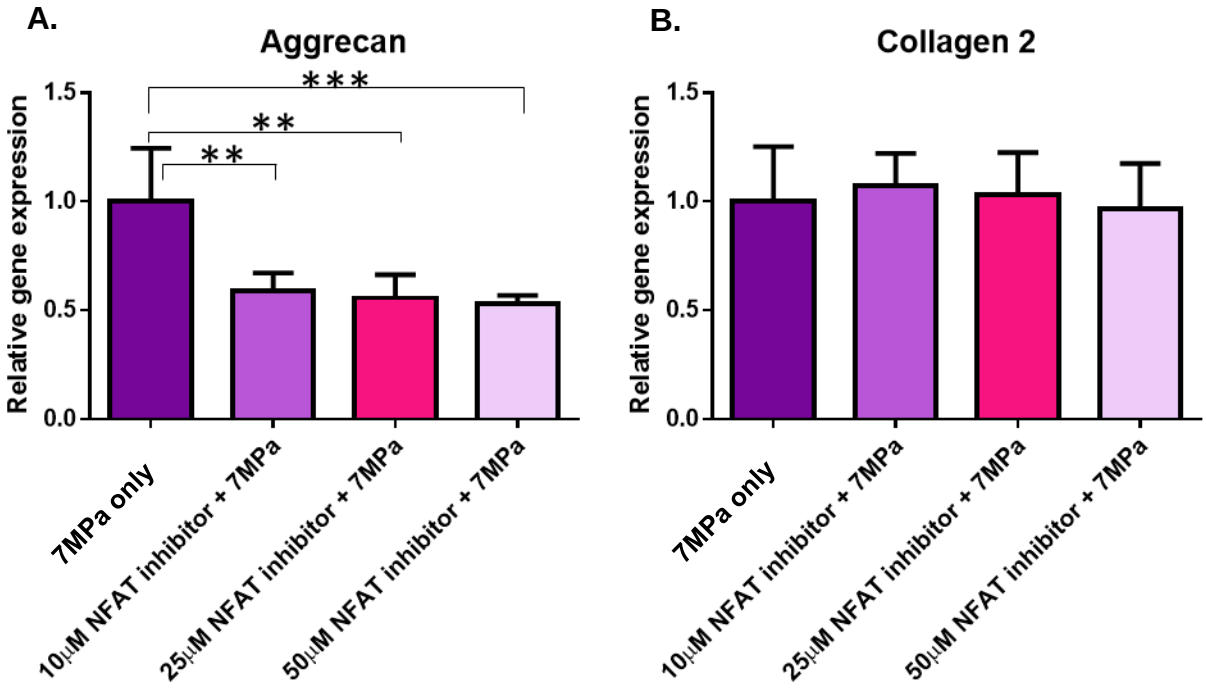

Figure 6-6: mRNA quantification of A) Aggrecan and B) Collagen type II in explants subjected to 10µM, 25µM or 50µM NFAT inhibitor for 24 hours prior to application of load (7MPa, 1Hz, 15 minutes). Gene expression was analysed using qPCR in explants processed 24 hours post-cessation of load. Data is presented as mean ± SD (n=6) after normalisation to the housekeeping genes YWHAZ and SDHA and relative to the control (load only). Data was analysed using a 2-way ANOVA [** $P < 0.01$, *** $P<0.001$].

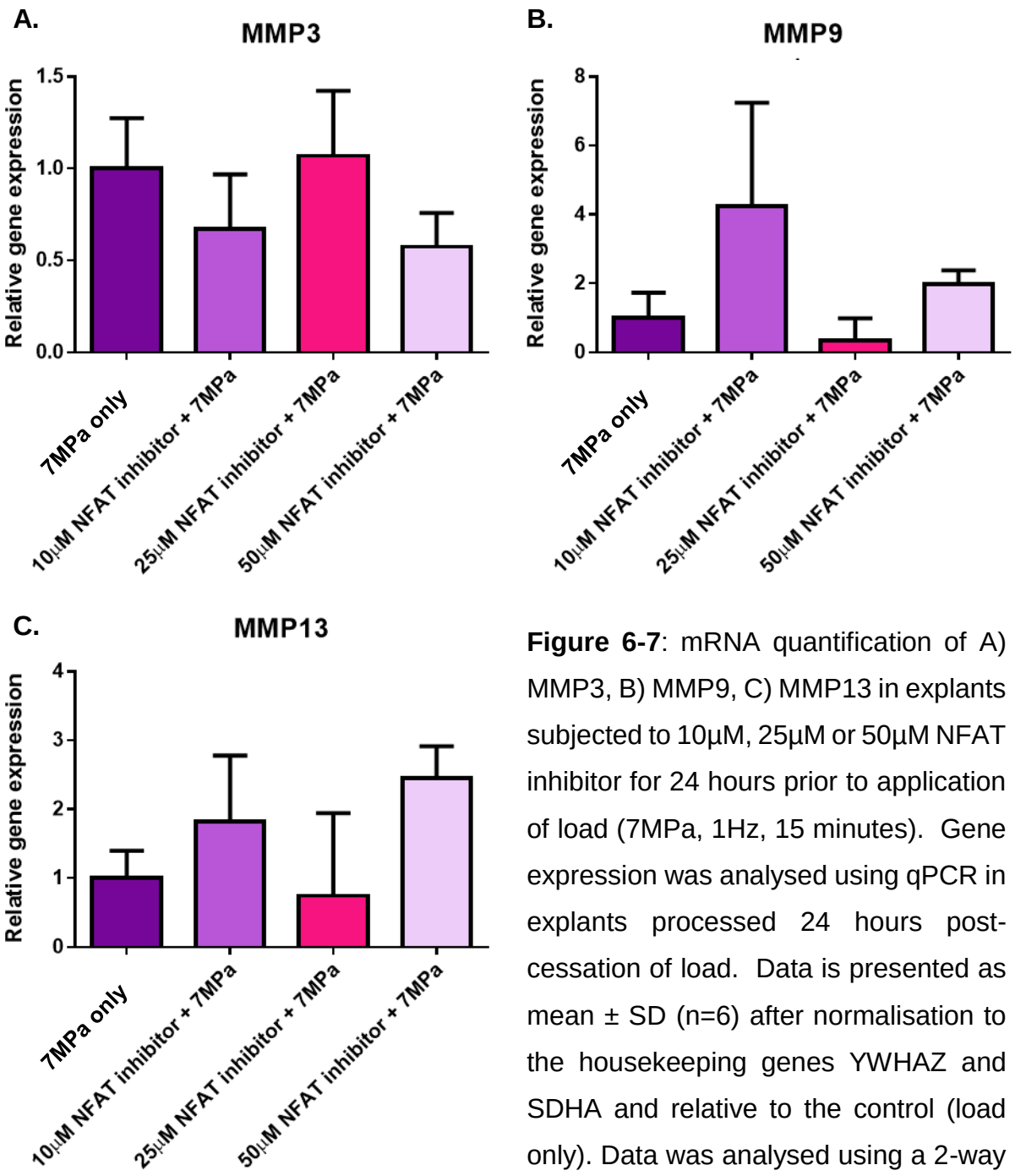

Figure 6-7: mRNA quantification of A) MMP3, B) MMP9, C) MMP13 in explants subjected to 10µM, 25µM or 50µM NFAT inhibitor for 24 hours prior to application of load (7MPa, 1Hz, 15 minutes). Gene expression was analysed using qPCR in explants processed 24 hours post-cessation of load. Data is presented as mean ± SD (n=6) after normalisation to the housekeeping genes YWHAZ and SDHA and relative to the control (load only). Data was analysed using a 2-way ANOVA.

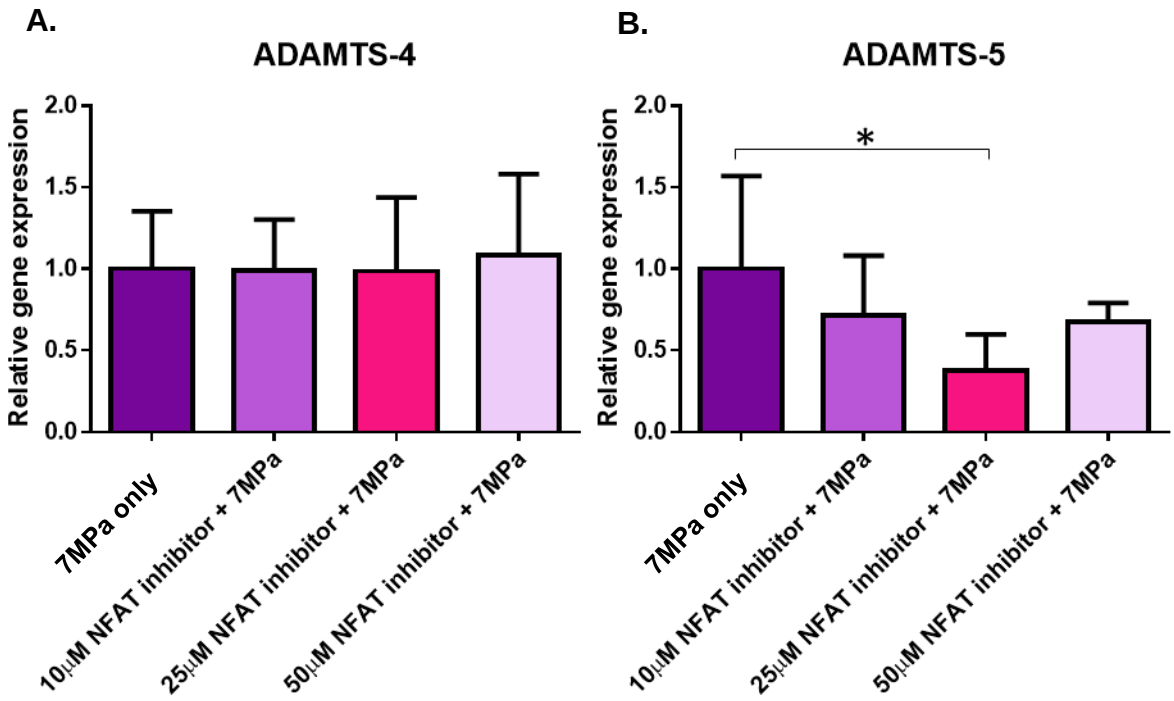

Figure 6-8: : mRNA quantification of A) ADAMTS-4 and B) ADAMTS-5 in explants subjected to 10μM, 25μM or 50μM NFAT inhibitor for 24 hours prior to application of load (7MPa, 1Hz, 15 minutes). Gene expression was analysed using qPCR in explants processed 24 hours post-cessation of load. Data is presented as mean ± SD (n=6) after normalisation to the housekeeping genes YWHAZ and SDHA and relative to the control (load only). Data was analysed using a 2-way ANOVA [* $P < 0.05$].

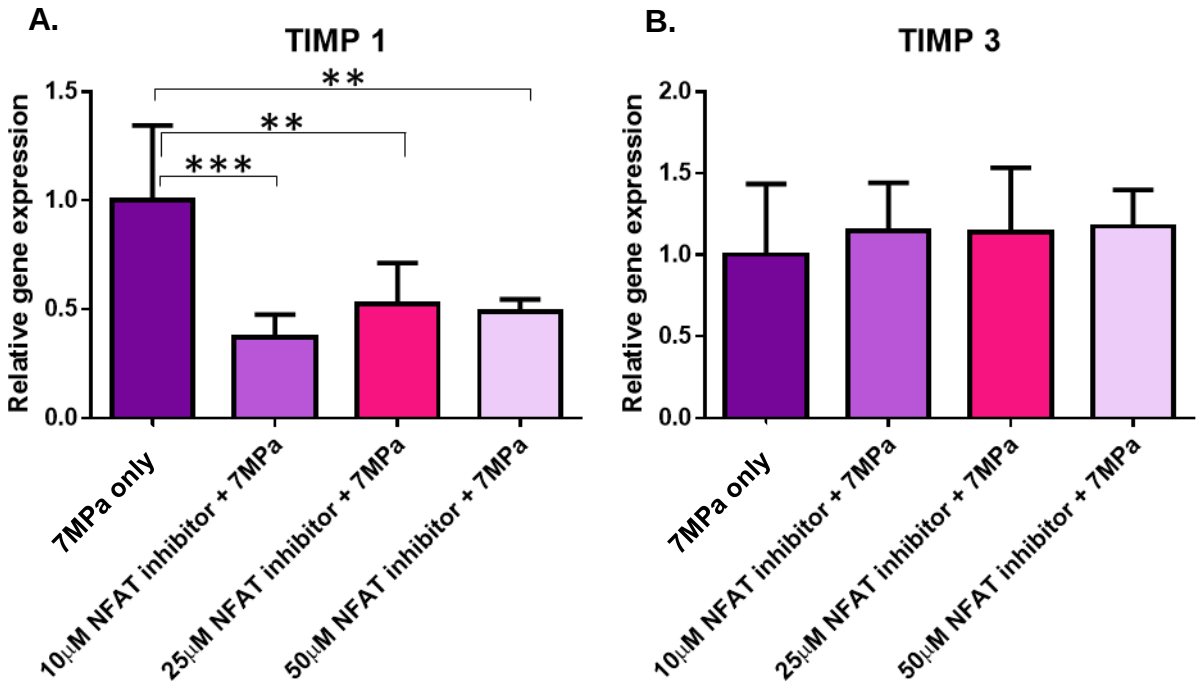

Figure 6-9: : mRNA quantification of A) TIMP 1 and B) TIMP 3 in explants subjected to 10μM, 25μM or 50μM NFAT inhibitor for 24 hours prior to application of load (7MPa, 1Hz, 15 minutes). Gene expression was analysed using qPCR in explants processed 24 hours post-cessation of load. Data is presented as mean ± SD (n=6) after normalisation to the housekeeping genes YWHAZ and SDHA and relative to the control (load only). Data was analysed using a 2-way ANOVA [** $P < 0.01$, *** $P<0.001$].

6.2.4 Effect of recombinant DKK-1 or NFAT inhibitor on the transcriptional expression of mechanically regulated WNT signalling components

After verification that recombinant DKK-1 and NFAT inhibitor treatments were eliciting a transcriptional effect on several ECM markers (sections 6.2.2 and 6.2.3 respectively), their effect on the expression of WNT signalling components was then assessed. Either 250ng/ml recombinant DKK-1 or 25µM NFAT inhibitor was added to explants for 24 hours prior to the application of load (7MPa, 1Hz, 15 minutes). As previously determined for this experimental system (section 5.2.2.2), the optimal transcriptional window to observe alterations in WNT signalling components was 4 hours post-cessation of load, hence WNT signalling PCR arrays were performed at this time point only.

6.2.4.1 Effect of recombinant DKK-1 on the transcriptional expression of mechanically regulated WNT signalling components

Exogenous DKK-1 stimulation of cartilage explants subjected to mechanical load (7MPa, 1 Hz, 15 minutes) modulated approximately a third of the genes present on the PCR array (table 6-1). DKK-1 transcription was elevated in response to exogenous DKK-1 (2.9-fold), and interestingly most of the genes induced in response to load (Figure 5-14B) were inhibited in the presence of DKK-1, particularly noticeable was the inhibition of load-induced FOSL1 amongst the early response/WNT target genes. Of the canonical pathway genes, mRNA levels of several frizzled receptors were decreased including FZD7 (3.5-fold) and FZD9 (4-fold). Furthermore, a reduction in the expression of CBY1 (3.3-fold) and FRAT-1 (3-fold), regulators of the canonical pathway was observed (table 6-1). It is interesting to note that DKK-1 also inhibited the expression of load-induced CTNNB1 transcription i.e. β-catenin (2.1-fold). An unexpected finding was the observation that the expression of several of the non-canonical WNTs were decreased after DKK-1 stimulation including WNT11 (3.1-fold), WNT9A (5.7-fold), WNT2 (2.3-fold) and WNT2B (2.2-fold; table 6-1). Only PRICKLE1 transcription was reduced by DKK-1 treatment (3.8-fold) within the planar cell polarity pathway. A reduction in the transcription of several of the other WNT inhibitors by DKK-1 was observed including SFRP-4 (3.6-fold), DKK-4 (4.5-fold) and WIF-1 (3.3-fold; table 6-1).

Table 6-1: Effect of exogenous DKK-1 on the transcriptional expression of mechanically regulated genes in articular cartilage. WNT signalling PCR arrays were performed on explants pre-treated with 250ng/ml recombinant DKK-1, subjected to load (7MPa, 1Hz, 15 minutes) and analysed 4 hours post-cessation of load. Data are presented as fold change, after normalisation to the housekeeping genes on the plate, and further normalised to explants subjected to load only (n=6).

CANONICAL	
Gene	Recombinant DKK-1 + 7MPa load
CBY1	-3.2716
CTNNB1	-2.114
DVL1	-2.4116
FRAT1	-3.0314
FZD6	-2.0562
FZD7	-3.5554
FZD9	-3.9724
GSK3B	-2.9897
NKD1	-2.5847
TCF7L1	-2.0139
WNT/Ca^{2+}	
NFATC1	-2.4116
WNT11	-3.1167
WNT2	-2.3134
WNT2B	-2.1585
WNT9A	-5.6962
PLANAR CELL POLARITY	
PRICKLE1	-3.8371
WNT INHIBITORS	
AXIN2	-2.0562
BTRC	-2.3457
CTBP1	-2.9282
DKK1	2.9079
DKK4	-4.5002
FBXW4	-2.639
SFRP4	-3.6553
WIF1	-3.3404
WNT TARGETS	
CCND1	-2.2501
CCND2	-2.114
FOSL1	-2.0994

6.2.4.2 Effect of NFAT inhibitor on the transcriptional expression of mechanically regulated WNT signalling components

In contrast to the action of DKK-1, inhibition of NFAT in cartilage explants subjected to mechanical load (7MPa, 1 Hz, 15 minutes) modulated approximately 80% of the genes present on the PCR array (tables 6-2 and 6-3). As expected, NFATc1 transcription was inhibited in the presence of the NFAT inhibitor (3.9-fold), and the majority of the genes that were previously modulated by load (Figure 5-14B) were inhibited too. It is interesting to note that although the NFAT family primarily regulates the WNT/Ca^{2+} pathway, the array data indicates global changes in all WNT signalling components (tables 6-2 and 6-3).

Of the canonical genes present on the array, the expression of the frizzled receptors were substantially decreased by the NFAT inhibitor (table 6-2), specifically FZD5 (5-fold), FZD7 (6.4-fold) and FZD8 (6.4-fold). Furthermore, CBY1 and GSK3β, negative regulators of the canonical WNT signalling pathway, were also down-regulated by 5-fold and 5.5-fold respectively. A reduction in the expression of CTBP1 (5.9-fold) and LEF1 (6.8-fold), transcriptional regulators of canonical WNT signalling targets, was also observed (table 6-2). The greatest fold changes in response to NFAT inhibition involved the WNT/Ca^{2+} pathway genes (table 6-2). It is interesting to note that primarily the WNT ligands were affected including WNT1 (7.8-fold), WNT2B (9.7-fold), WNT5B (6.5-fold), WNT9A (6-fold) and WNT11 (6-fold). Of the genes involved in the planar cell polarity pathway (table 6-3), the greatest transcriptional changes were observed in members of the dishevelled family, namely reductions in DVL1 (6.6-fold) and DVL2 (8-fold). PRICKLE-1 expression, reduced after DKK-1 treatment (table 6-1), was also decreased in response to the NFAT inhibitor (4.7-fold; table 6-3). Treatment of cartilage explants with the NFAT inhibitor affected expression of WNT inhibitor genes (table 6-3), with large reductions in DKK-3 (7.8-fold), DKK-4 (6.7-fold), SFRP-4 (10.8-fold) and FBXW11 transcription (5-fold). Confirmation of an overall reduction in WNT signalling activity was reflected by the decreased expression in WNT signalling target genes (table 6-3). Particularly noticeable was the inhibition of load-induced early response/WNT target genes including FOSL1 (5.5-fold), JUN (2.9-fold) and MYC (3.5-fold), which were previously identified as being highly sensitive to the loading regime (Chapter 5).

Table 6-2: Effect of NFAT inhibitor on the transcriptional expression of mechanically regulated genes in articular cartilage. WNT signalling PCR arrays were performed on explants pre-treated with 25µM NFAT inhibitor, subjected to load (7MPa, 1Hz, 15 minutes) and analysed 4 hours post-cessation of load. Data are presented as fold change, after normalisation to the housekeeping genes on the plate, and further normalised to explants subjected to load only (n=6).

CANONICAL	
Gene	**NFAT inhibitor + 7MPa load**
AES	-2.2038
APC	-2.0279
BCL9	-3.5801
CBY1	-5.0281
CSNK1A1	-4.2281
CSNK2A1	-4.4383
CTBP1	-5.8971
CTNNB1	-4.8568
DIXDC1	-2.2501
FRAT1	-3.2043
FZD1	-2.8089
FZD3	-3.387
FZD4	-3.4105
FZD5	-4.9933
FZD6	-3.7581
FZD7	-6.4531
FZD8	-6.3643
FZD9	-4.6589
GSK3A	-2.6759
GSK3B	-5.5404
LEF1	-6.8211
LRP5	-3.3173
LRP6	-4.1989
NKD1	-4.4383
PORCN	-2.0279
PYGO1	-2.7702
RUVBL1	-3.1167
TCF7	-4.3772
TCF7L1	-4.6589
WNT2	-4.5948
WNT3	-3.7842
WNT/Ca^{2+}	
NFATC1	-3.9449
WNT1	-7.8354
WNT11	-5.9794
WNT2B	-9.7136
WNT5A	-2.3134
WNT5B	-6.498
WNT9A	-5.9794

Table 6-3: Effect of NFAT inhibitor on the transcriptional expression of mechanically regulated genes in articular cartilage. WNT signalling PCR arrays were performed on explants pre-treated with 25µM NFAT inhibitor, subjected to load (7MPa, 1Hz, 15 minutes) and analysed 4 hours post-cessation of load. Data are presented as fold change, after normalisation to the housekeeping genes on the plate, and further normalised to explants subjected to load only (n=6).

PLANAR CELL POLARITY	
Gene	NFAT inhibitor + 7MPa load
DAAM1	-2.5315
DVL1	-6.6346
DVL2	-8
MAPK8	-3.6301
PRICKLE1	-4.6589
RHOA	-3.0951
RHOU	-3.0105
VANGL2	-2.5315
WNT INHIBITORS	
AXIN1	-2.8679
AXIN2	-2.9282
DKK1	-2.4967
DKK2	-2.0994
DKK3	-7.8354
DKK4	-6.774
FBXW11	-5.0281
FBXW4	-4.6589
FRZB	-2.3295
NLK	-3.4822
SFRP1	-3.5554
SFRP4	-10.7779
TLE1	-2.4794
WIF1	-3.605
WNT TARGETS	
BTRC	-5.4642
CCND1	-5.8563
CCND2	-5.3147
DAB2	-2.0705
FOSL1	-5.5404
JUN	-2.8679
MYC	-3.4822
WISP1	-6.0629

6.2.4.3 Effect of recombinant DKK-1 or the NFAT inhibitor on the transcriptional expression of cartilage matrix genes

Having established the optimal concentration of modulating agent and observed a substantial effect on mechanically regulated WNT signalling components, downstream regulation of cartilage matrix genes was investigated further. Explants were stimulated with either 250ng/ml recombinant DKK-1 or 25µM NFAT inhibitor for 24 hours prior to mechanical load (7MPa, 1Hz, 15 minutes). Unlike the previous experiment (section 6.2.2 and 6.2.3), transcript levels of the panel of matrix genes previously described were analysed in explants 4 hours post-cessation of load, as opposed to 24 hours. Although aggrecan mRNA levels were significantly reduced at 24 hours post-load cessation with NFAT inhibitor treatment (Figure 6-6A), this response was not evident after 4 hours (Figure 6-10A). Type II collagen transcription was unaffected by DKK-1 or NFAT inhibitor (Figure 6-10B), reflecting the trends observed at 24 hours (Figure 6-6B). Of the MMPs analysed, MMP3 (Figure 6-11A) and MMP13 (Figure 6-11C) expression was unaffected by either treatment. In contrast, MMP9 expression was significantly reduced by the NFAT inhibitor (4.7-fold, $p<0.01$) and to a lesser extent by recombinant DKK-1 (2-fold, $p<0.05$) relative to the control, comprising explants subjected to load in the absence of modifying agent (Figure 6-11B). Exogenous DKK-1 differentially regulated load-induced expression of the ADAMTSs, with a significant increase in ADAMTS-4 (2.8-fold, $p<0.001$; Figure 6-12A) and significant reduction in ADAMTS-5 (2.5-fold, $p<0.05$; Figure 6-12B). In contrast, ADAMTS-4 transcription was unaffected by the NFAT inhibitor (Figure 6-12A), whereas ADAMTS-5 mRNA levels were also significantly reduced (2.5-fold, $p<0.05$; Figure 6-12B). Although TIMP1 was reduced at 24 hours post-cessation of load after treatment with DKK-1 (Figure 6-5A) and NFAT inhibitor (Figure 6-9A), these effects were not observed at this earlier 4 hour timeframe (Figure 6-13A). However, DKK-1 significantly induced TIMP 3 expression (1.7-fold, $p<0.05$), whereas the NFAT inhibitor had no effect (Figure 6-13B).

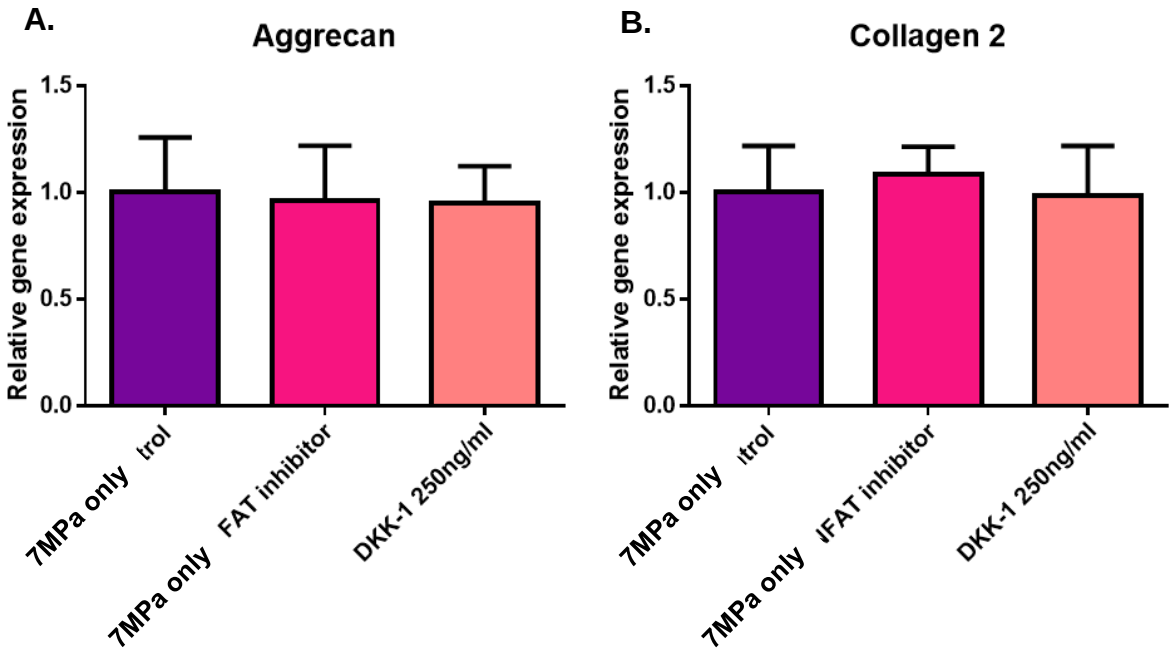

Figure 6-10: mRNA quantification of A) Aggrecan and B) Collagen type II in explants subjected to either 25µM NFAT inhibitor or 250ng/ml recombinant human DKK-1 treatment for 24 hours prior to application of load (7MPa, 1Hz, 15 minutes). Gene expression was analysed using qPCR in explants processed 4 hours post-cessation of load. Data is presented as mean ± SD (n=6) after normalisation to the housekeeping genes YWHAZ and SDHA and relative to the control (load only). Data was analysed using a 2-way ANOVA.

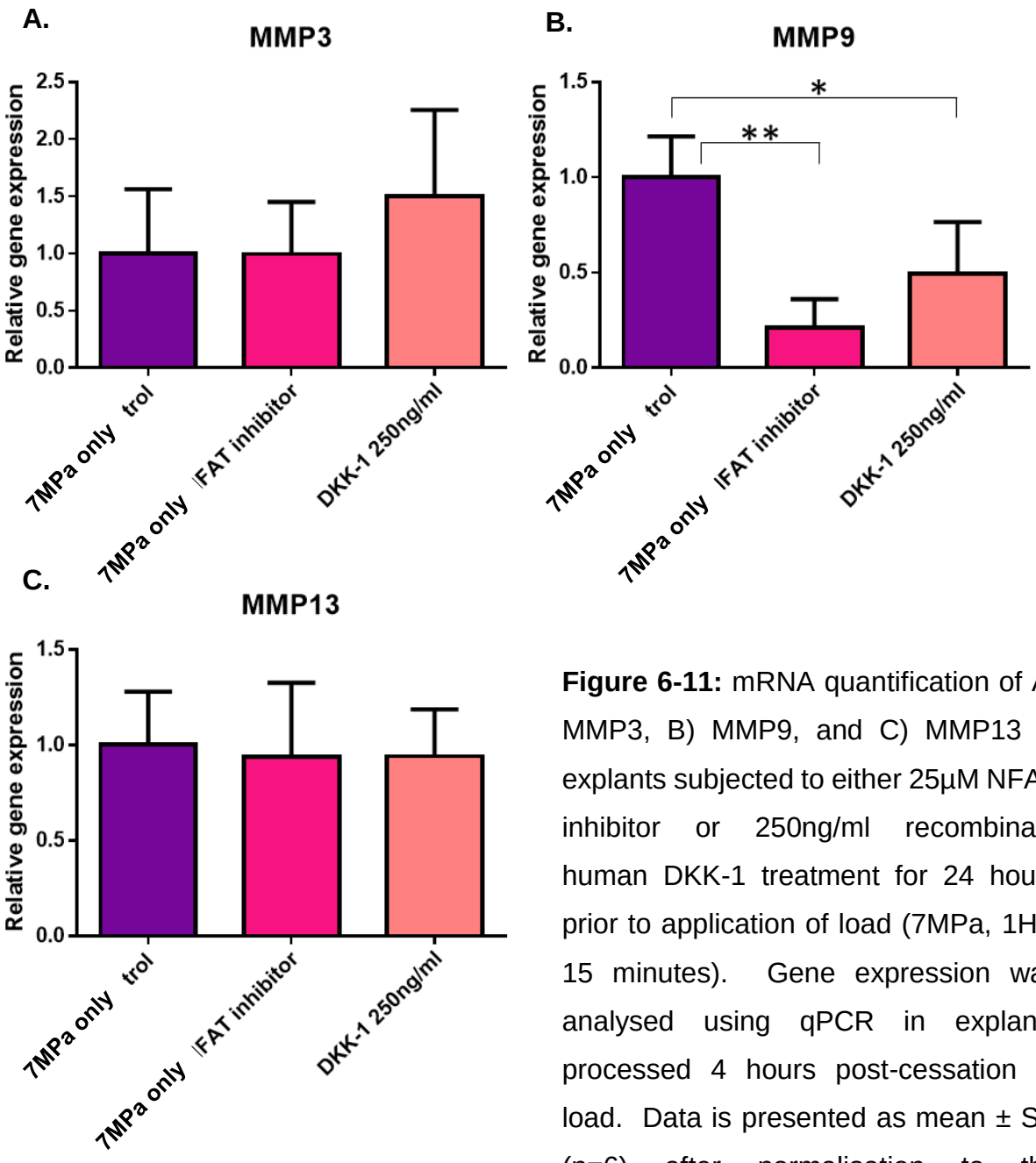

Figure 6-11: mRNA quantification of A) MMP3, B) MMP9, and C) MMP13 in explants subjected to either 25µM NFAT inhibitor or 250ng/ml recombinant human DKK-1 treatment for 24 hours prior to application of load (7MPa, 1Hz, 15 minutes). Gene expression was analysed using qPCR in explants processed 4 hours post-cessation of load. Data is presented as mean ± SD (n=6) after normalisation to the housekeeping genes YWHAZ and SDHA and relative to the control (load only). Data was analysed using a 2-way ANOVA [* $P < 0.05$, ** $P < 0.01$].

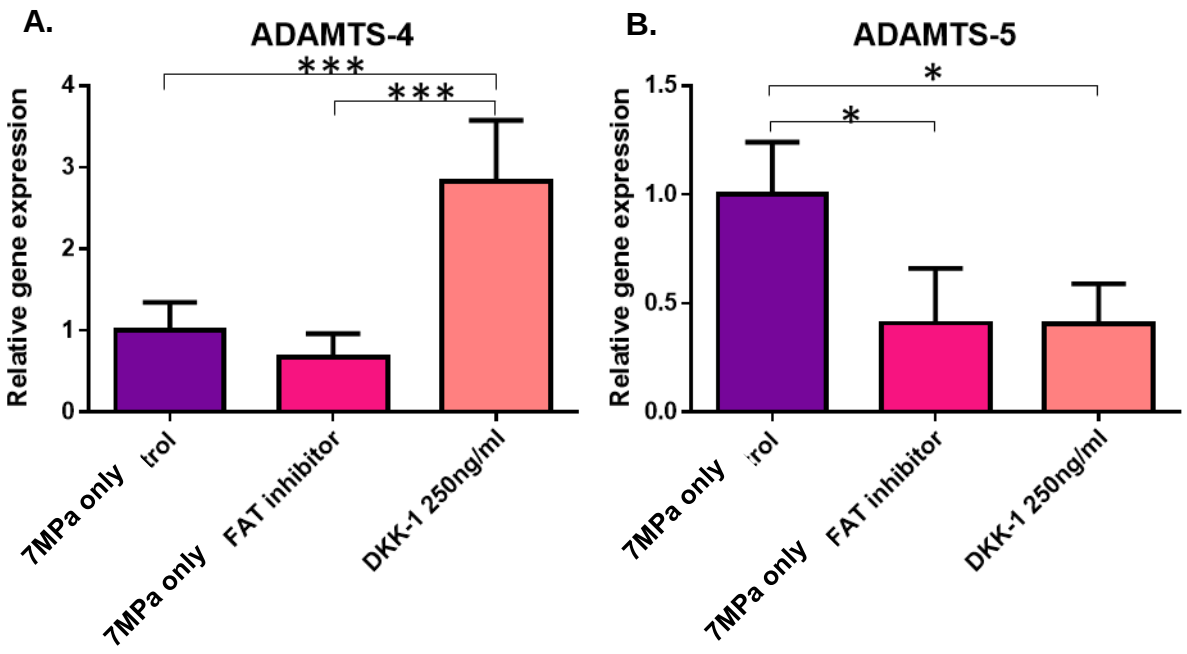

Figure 6-12: mRNA quantification of A) ADAMTS-4 and B) ADAMTS-5 in explants subjected to either 25µM NFAT inhibitor or 250ng/ml recombinant human DKK-1 treatment for 24 hours prior to application of load (7MPa, 1Hz, 15 minutes). Gene expression was analysed using qPCR in explants processed 4 hours post-cessation of load. Data is presented as mean ± SD (n=6) after normalisation to the housekeeping genes YWHAZ and SDHA and relative to the control (load only). Data was analysed using a 2-way ANOVA [* P < 0.05, *** P<0.001].

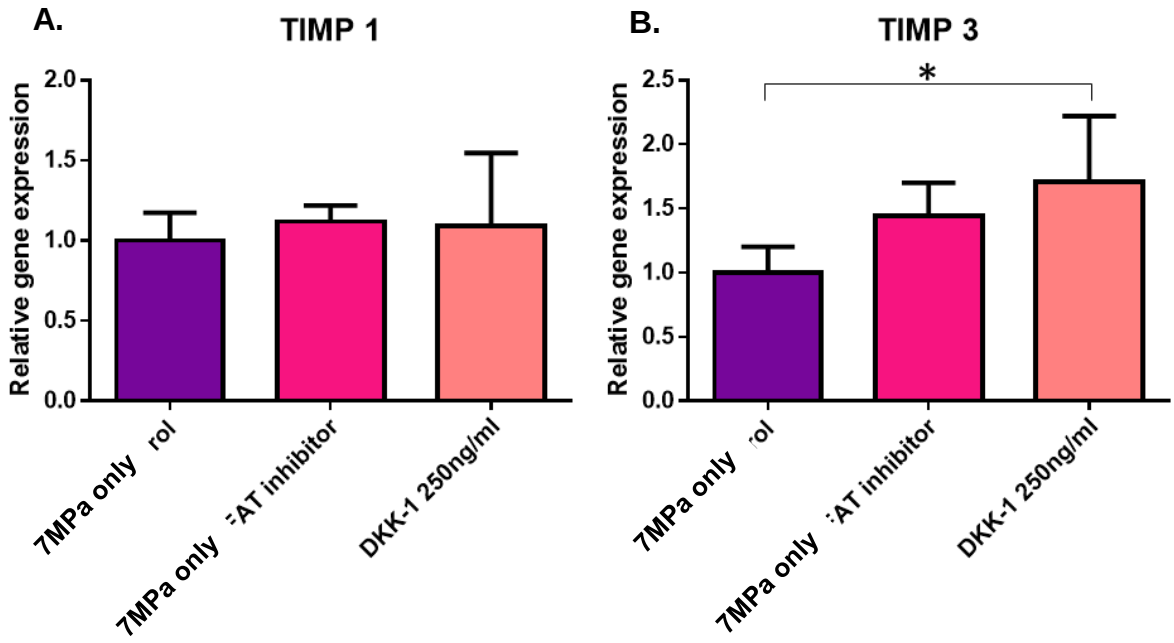

Figure 6-13: mRNA quantification of A) TIMP 1 and B) TIMP 3 in explants subjected to either 25µM NFAT inhibitor or 250ng/ml recombinant Human DKK-1 treatment for 24 hours prior to application of load (7MPa, 1Hz, 15 minutes). Gene expression was analysed using qPCR in explants processed 4 hours post-cessation of load. Data is presented as mean ± SD (n=6) after normalisation to the housekeeping genes YWHAZ and SDHA and relative to the control (load only). Data was analysed using a 2-way ANOVA [* $P < 0.05$].

6.3 Discussion

Regulation of WNT signalling is highly important in maintaining cartilage homeostasis, due to the pivotal role it plays in regulating the balance between anabolic and catabolic processes. WNT signalling is tightly regulated via the action of WNT signalling inhibitors. Our investigation into the mechano-regulation of WNT signalling components in articular cartilage demonstrated that many of the genes (on the PCR array) are differentially regulated by load, but two genes, DKK-1 and NFATC1 were selected for functional analysis. The selection of these genes was based on their role in cartilage homeostasis and OA pathology. DKK-1 is a member of the Dickopff family of secreted glycoproteins. DKK-1 expression is essential during embryonic development as knockout mouse models of DKK-1 are embryonic lethal (Mukhopadhyay et al., 2001). WNT signalling is highly up-regulated in OA tissue, as evident by increased expression of WNT ligands and target genes, and down-regulation of DKK-1 expression (Blom et al., 2009, Funck-Brentano et al., 2014). However, some studies on human OA cartilage have shown an increase in DKK-1 expression (Thorfve et al., 2012). Furthermore, treatment of rat models of OA with DKK-1 antisense oligonucleotide led to a reduction in OA-associated degeneration and symptoms (Weng et al., 2010). The therapeutic use of DKK-1 was also observed in a mouse model of mechanically-induced OA where DKK-1 treatment decreased disease severity (Funck-Brentano et al., 2014).

In contrast, NFATC1 belongs to the NFAT family of transcription factors that are regulated via activation of the WNT/Ca^{2+} pathway. Recent studies have focused on the involvement of NFATC1 and NFATC2 in articular cartilage; knockdown and knockout studies in mice have shown both to have significant roles in maintaining cartilage homeostasis (Rodova et al., 2011, Greenblatt et al., 2013). *In vitro* studies using primary human OA chondrocytes have demonstrated that levels of NFAT were elevated and correlated with cartilage damage (Sun et al., 2014). However, cartilage-specific deletion of NFATC1 and NFACTC2 led to the development of OA with symptoms comparable to the human condition; these events occurred much earlier in this transgenic model than it did in other mouse models of OA suggesting the severity of the NFATC1/NFATC2 deletion (Greenblatt et al., 2013).

Due to their significant mechano-regulation (Chapter 5) and their reported involvement in cartilage homeostasis, the regulatory role of DKK-1 and NFAT in cartilage mechanotransduction was investigated. In order to elucidate the role of DKK-1 and NFAT in load-induced cartilage homeostasis, cartilage explants were stimulated with recombinant DKK-1 or treated with an NFAT inhibitor, which is selective for all NFAT isoforms. Dose-response experiments were performed to determine the optimal concentration for use. A preliminary screen was conducted whereby cartilage explants were pre-treated with either recombinant DKK-1 (100, 250 and 500ng/ml) or NFAT inhibitor (10, 25 and 50μM) for 24 hours, subjected to load (7MPa 1Hz, 15 minutes) and analysed 24 hours post-cessation of load. Cytotoxicity was assessed by measuring lactate dehydrogenase release into the media as a marker of cell death. The results indicated that none of the treatments were toxic within this time frame, therefore the effect of these modifying agents on matrix gene expression was determined.

To determine the effect of increasing DKK-1 and inhibiting NFAT expression, on load-induced cartilage catabolism, transcript levels of a panel of matrix genes including aggrecan, collagen type 2, MMPs, ADAMTSs and TIMPS were quantified.

6.3.1 Effect of recombinant DKK-1 treatment on mechanically-regulated gene expression in cartilage explants (24 hours post-cessation of load)

Surprisingly, DKK-1 had no effect on either aggrecan or collagen type 2 mRNA levels. However, this may be due to the time point chosen post-cessation of load, as opposed to a lack of effect of DKK-1 on the expression of these ECM genes as proteoglycan loss was previously observed in the cartilage of mice over-expressing DKK-1 (Funck-Brentano et al., 2014). Recombinant DKK-1 treatment significantly reduced the expression of MMP3 at all concentrations tested. These results corroborate a previous study in which DKK-1 decreased MMP3 expression through inhibition of the canonical pathway in human cartilage, as MMP3 is a known downstream target (Oh et al., 2012, Lories et al., 2007). Although the data was not statistically significant – likely due to large standard deviations, there was a trend of a DKK-1-dependent increase in MMP9 mRNA

levels. The influence of DKK-1 on MMP9 transcription was previously reported in cancers, where it was suggested that DKK-1 is a marker of poor prognosis in cancer as it promotes metastasis through MMP9 induction (Shi et al., 2013). Interestingly, MMP13 expression was only reduced in response to 100ng/ml DKK-1; MMP13 is also a known downstream target of canonical WNT signalling, as its expression was previously demonstrated to decrease in chondrocytes stimulated with 1µg/ml DKK-1 (Oh et al., 2012, Enochson et al., 2014). Similarly, the activation of canonical WNT signalling is known to induce ADAMTS-4 and ADAMTS-5 expression (Oh et al., 2012). Inhibition of the canonical pathway results in a reduction in the expression of both enzymes, as well as some MMPs, which are downstream targets of WNT signalling, as DKK-1 overexpression results in a reduction in cartilage degeneration (Diarra et al., 2007). Due to large standard deviations, DKK-1 had no effect on mechanically induced ADAMTS-4 transcription, however ADAMTS-5 expression was significantly decreased, again in response to 100ng/ml only, agreeing with the literature above. DKK-1 significantly reduced TIMP 1 expression, corroborating a previous report that one of the initiators of TIMP 1 transcription in human breast tissue is through the canonical WNT pathway (Nakopoulou et al., 2006), therefore this effect on TIMP-1 may be mediated via DKK-1. However, there was no effect on TIMP 3 suggesting a potential different mechanism of regulation.

6.3.2 Effect of NFAT inhibitor on mechanically-regulated gene expression in cartilage explants (24 hours post-cessation of load)

A concentration dependent effect of NFAT inhibition on matrix gene expression was observed in the mechanically loaded cartilage explants. Aggrecan transcription was reduced significantly in response to all concentrations of NFAT inhibitor tested, agreeing with previous studies reporting that NFAT deficiency results in inhibition of aggrecan expression (Sitara and Aliprantis, 2010, Wang et al., 2009). Collagen type 2 expression was not influenced by NFAT inhibition, which was slightly surprising as NFAT1 deficient mice have reduced levels of this matrix gene (Wang et al., 2009). Unlike the effect of DKK-1, NFAT inhibitor did not significantly affect transcript levels of MMP3, MMP9, MMP13 or ADAMTS-4. However, large standard deviations were present in some of the treatment groups, so these experiments would need to be repeated to

validate the observations. ADAMTS-5 expression was significantly reduced in loaded explants stimulated with NFAT inhibitor (25µM only). Previously, NFATC1 was reported to inhibit ADAMTS-5 and induce ADAMTS-4 expression in chondrocytes (Wang et al., 2009), which contradicts my findings. However, this study was conducted in an animal model where only NFAT1 was knocked out, whereas in my study the NFAT inhibitor inhibits all NFAT members which may explain the discrepancy in these results. In this same *in vivo* study (Wang et al., 2009), a reduction in TIMP1 expression was reported, corroborating the reduction in TIMP1 transcription observed in response to NFAT inhibitor. However, TIMP 3 expression was unchanged by treatment, possibly indicative of an alternative regulatory mechanism.

6.3.3 Effect of NFAT inhibitor or recombinant DKK-1 on the transcriptional expression of mechanically regulated WNT signalling components

Although 24 hours post-cessation of load was selected to analyse the effects of DKK-1 and NFAT inhibitor on mechanically regulated matrix transcription (section 6.2.2 and 6.2.3), the optimal window to monitor transcriptional changes in the WNT components was previously determined as 4 hours post-load (Chapter 5). Thus, explants were treated with either 25µM NFAT inhibitor or 250ng/ml recombinant DKK-1 for 24 hours, subjected to load (7MPa, 1Hz, 15 minutes) and analysed 4 hours post-load using WNT signalling PCR arrays, as described (Chapter 5).

Treatment of loaded cartilage with NFAT inhibitor resulted in the differential regulation of approximately 80% of the genes on the array with quite dramatic differences ($\leq$ 11-fold reduction). There was an overall transcriptional reduction in components of the canonical, WNT/Ca^{2+} and PCP pathways, in addition to targets of the WNT signalling pathway. As NFAT is part of the non-canonical WNT/Ca^{2+} pathway, it was initially surprising to observe so many changes in the canonical components. However, recently NFATC1 has been implicated in the negative regulation of canonical WNT signalling through its interaction with dishevelled in a Ca^{2+} dependent manner (Huang et al., 2011). Expression of genes involved in WNT/Ca^{2+} signalling were markedly decreased, primarily involving regulation of the WNT ligands e.g. WNT1, WNT2B, WNT5B,

WNT9A and WNT11. Of the PCP pathway, reductions primarily in dishevelled-1 and -2, as well as PRICKLE-1 were observed. Within the canonical pathway, frizzled receptors, glycogen synthase kinase 3β, and transcriptional regulators of canonical WNT signalling including chibby homolog (CBY1), C-terminal binding protein 1 (CTBP1) and lymphoid enhancer-binding factor 1 were highly down-regulated. It is interesting to note the differential regulation of CBY1 because it has a role in the primary cilium, a mechano-sensing organ. Furthermore, CBY1 is a well-studied cilia-associated protein, its expression is necessary for ciliogenesis and it is known to negatively regulate WNT signalling (Takemaru et al., 2003). NFAT inhibition decreased the expression of many WNT inhibitors but most noticeably DKK-3, DKK-4, SFRP4 and FBXW11 gene expression. Due to NFAT-mediated inhibition of WNT signalling, reductions in the transcription of mechanically regulated WNT target genes, particularly BTRC, cyclin D1 (CCND1), CCND2, FOSL1, MYC, C-JUN and WISP1 were observed. Clearly, mechanically induced transcription of these target genes are likely mediated via activation and translocation of NFATC to the nucleus to orchestrate these events. However, because reports suggest that NFATC can regulate components of the canonical pathway through a Ca^{2+} dependent mechanism, it is difficult to conclude from these observations whether the effect of load is mediated via the non-canonical and/or canonical pathways, although ultimately the WNT pathway is involved.

In contrast, only approximately a third of the array genes were affected by DKK-1 in loaded explants with less dramatic consequences ($\leq$ 5.7-fold reduction). Excepting DKK-1 transcription, which was elevated in response to exogenous DKK-1 treatment, the remainder of the regulated genes were decreased in expression, and mirrored many of the changes resulting from NFAT inhibition.

6.3.4 Effect of NFAT inhibitor or recombinant DKK-1 on the transcriptional expression of cartilage matrix genes (4 hours post-cessation of load)

Having selected the most efficacious concentration of NFAT inhibitor (25µM) and recombinant DKK-1 (250ng/ml) to monitor transcriptional effects on WNT signalling components (section 6.2.2 and 6.2.3), their effects on mechanically regulated matrix gene expression was investigated. In contrast to the dose-response screen, the tissue was analysed 4 hours post-cessation of load to complement the WNT array data. Also, the limited effects of DKK-1 and NFAT inhibition on matrix genes observed at 24 hours post-load indicated that several of the transcriptional events may have occurred earlier. The data from this experiment would partially confirm this, as more effects were observed on matrix gene expression 4 hours post-cessation of load. Aggrecan expression was unaffected by NFAT inhibition at 4 hours post-load, but unlike the other genes, it may require longer to mediate transcriptional effects as it was significantly reduced at 24 hours post-load. However, collagen type 2 expression was unaffected by both modulating agents, a consistent trend observed at 24 hours post-cessation of load. Both NFAT inhibition and DKK-1 significantly reduced MMP9 expression at this earlier analysis time point. As previously mentioned, there is an association of DKK-1 with MMP9 in cancer (Shi et al., 2013). Furthermore, NFATC elements are present in the MMP9 promoter providing a direct mechanism for NFATC1's regulation of MMP9 transcription (Aliprantis et al., 2008, Sundaram et al., 2007). Interestingly, ADAMTS-4 transcription was significantly induced in loaded explants stimulated with DKK-1, which contradicts a study that reported the inhibitory effect of DKK-1 on ADAMTS-4 expression by blocking canonical WNT signalling (Oh et al., 2012), however a study demonstrating that recombinant DKK-1 addition reduced OA severity has shown proteoglycan loss and increased aggrecan neoepitopes demonstrating increased aggrecanase activity (Funck-Brentano et al., 2014). NFAT inhibitor did not influence ADAMTS-4 expression. However, both DKK-1 and NFAT inhibition resulted in significant decreases in ADAMTS-5 expression, an effect also observed 24 hours post-load. Previous studies have demonstrated that using 1, 2 and 10µM cyclosporin A, a generic inhibitor of NFAT, inhibited interleukin-1 induced aggrecanase mediated cartilage degradation in bovine explants,

however our studies have shown changes in only ADAMTS-5 expression (Little et al., 2002). This discrepancy may be due to pre-treatment of explants with interleukin-1 and the use of a non-specific NFATC inhibitor, cyclosporine A. There was no effect on TIMP 1 expression, but again effects were observed at 24 hours post-load, thus this gene may also requires longer to instigate a response to the stimulation. TIMP 3 expression was only elevated by DKK-1 treatment; this appears to have been a transient response as no effects were observed at the 24 hours point.

Collectively, these results demonstrate that NFATs have a major role in the regulation of multiple components of both the canonical and non-canonical WNT signalling pathways, whereas DKK-1 regulation is more restricted to canonical WNT signalling. Furthermore, these studies demonstrate that depending on the specific gene, the length of time necessary to respond to the mechanical stimulus and/or WNT modulating agent is varied. Therefore, careful consideration of the optimal transcriptional timeframe for analysis is necessary i.e. to capture changes in WNT related genes requires earlier analysis post-cessation of load with respect to the ECM genes.

6.4 Summary

- Recombinant DKK-1 and NFAT inhibitor differentially regulate mechanically induced cartilage matrix gene expression.
- Treatment of articular cartilage with either recombinant DKK-1 or NFAT inhibitor ameliorates load-induced expression of WNT signalling genes (Chapter 5).
- DKK-1 primarily regulates canonical WNT signalling in articular cartilage subjected to mechanical load.
- NFATs regulate both the canonical and non-canonical WNT pathways in articular cartilage subjected to mechanical load.

Chapter 7

General discussion

7.1 Importance of WNT signalling in articular cartilage

The WNTs, a family of secreted glycoproteins, are one of the most influential signalling pathways in nearly all tissues in the body, and articular cartilage is no exception. As a result, WNT signalling is normally tightly regulated by a host of inhibitors, as aberrant WNT signalling is known to have severe consequences in disease development e.g. cancer (Clevers and Nusse, 2012). WNT signalling is commonly divided into two pathways referred to as canonical and non-canonical. The canonical WNT signalling pathway is activated as a result of a WNT ligand binding to lipoprotein receptor-related protein (LRP) 5/6 which leads to the accumulation of β-catenin in the cytoplasm, followed by its nuclear translocation resulting in an alteration in transcriptional activity (Habas and Dawid, 2005).

However, the non-canonical WNT signalling pathway is comprised of two pathways: the WNT/Ca^{2+} pathway and the planar cell polarity (PCP) pathway mediated by WNT ligand association with either Frizzled or ROR receptors, respectively. WNT/Ca^{2+} pathway activation leads to WNT-induced intracellular Ca^{2+} release which activates downstream enzymes such as PKC, CAMKII and calcineurin, which subsequently activates NFAT transcription (Kestler and Kuhl, 2008). In contrast, PCP pathway activation involves a cascade of signalling events which comprise activation of Rho GTPases such as RHOA, RAC and CDC42 which facilitate the reorganisation of cytoskeletal elements (Lories et al., 2013, Kestler and Kuhl, 2008). During embryonic development, the process of chondrogenesis is primarily regulated by WNT signalling. Mesenchymal precursors are stimulated to differentiate into chondrocytes by the non-canonical pathway, whereas the canonical pathway promotes chondrocytes to further differentiate into hypertrophic chondrocytes (Yates et al., 2005). Furthermore, WNT signalling in cartilage is necessary to maintain tissue homeostasis. Studies have demonstrated that the ablation or overexpression of β-catenin leads to disastrous effects on cartilage such as apoptosis and cartilage degradation (Zhu et al., 2008, Zhu et al., 2009). Some of the downstream targets of WNT signalling include the MMPS, suggestive of a possible role for the WNTs in cartilage degradation (Yuasa et al., 2008). Due to the prominent role of WNT signalling in

the maintenance of cartilage homeostasis, studies have investigated whether it may have a role in degenerative diseases such as OA.

OA is a multi-factorial degenerative disease which causes cartilage degeneration and subchondral bone remodelling. Some of the factors that are associated with the prevalence of OA are altered mechanical loading, genetics, obesity, age and injury (Rothschild, 2012). Studies assessing human OA tissue have identified a link between enhanced activation of WNT signalling and cartilage degradation. Canonical WNT components including WNT inducible signalling protein-1 (WISP1), WNT16 and WNT2B are elevated in OA cartilage (Blom et al., 2009). Furthermore, single nucleotide polymorphisms identified in FRZB, an inhibitor of WNT signalling, have been shown to reduce its potency to inhibit the WNTs, thus resulting in inappropriate WNT signalling (Loughlin et al., 2004, Min et al., 2005). Related to these human studies was the observation that conditional activation of *β-catenin* in mice resulted in cartilage exhibiting an OA-like phenotype which included surface fibrillation, osteophyte formation and cartilage degeneration (Zhu et al., 2009). These human studies, taken together with evidence from the *in vivo* mouse models of β-catenin manipulation, clearly demonstrate a correlation between aberrant WNT signalling and cartilage degeneration.

Mechanical load is a primary risk factor for OA development, and alterations in weight-bearing can be mediated as a consequence of obesity, sports injuries or previous trauma to the joint. The skeleton is subjected to a range of loads during every day movement e.g. tensile, hydrostatic and shear forces, but it is predominantly exposed to compression in the joints. *In vivo* studies in the hip have suggested that compressive forces ranging from 0.5 – 6.3MPa are exerted during normal weight-bearing activities (Hodge et al., 1986). Therefore, loads which are either below (joint immobilisation) or above (high impact activities) this physiological range, have been shown to have detrimental effects on cartilage homeostasis. In such scenarios, signalling pathways which induce inflammation, apoptosis and increased syntheses of *MMP* and *ADAMTS* become activated resulting in cartilage degeneration (Blain, 2007). As already mentioned, one of the pathways implicated in promoting cartilage degradation in OA is WNT

signalling (Zhu et al., 2009). However, these findings implicate WNT signalling in late-stage OA and have not taken into consideration the role of mechanical load in influencing this pathway. Therefore, ***I hypothesise that the application of mechanical load will (i) induce the activation of the canonical and non-canonical WNT pathways, and (ii) induce a differential response based on the type of load applied, and the magnitude and duration of the loading regime.***

7.2. Is WNT signalling mechanically regulated in articular cartilage?

To verify these hypotheses, two models and loading systems were used. A chondrocyte monolayer cell culture system was used in conjunction with the Flexcell apparatus to initially verify mechano-regulation of WNT signalling in response to tensile strain. Upon determining WNT mechano-regulation in chondrocyte cultures, this observation was confirmed in cartilage explants subjected to compressive loading regimes replicating load-induced physiological and degradative metabolic responses.

The novel findings of this thesis are:

- Canonical WNT signalling is activated in response to tensile strain in primary chondrocytes.
- Canonical WNT signalling is activated in response to compressive load in articular cartilage.
- WNT signalling is differentially regulated in response to physiological and degradative loads, as evidenced by the differential localisation of *β-catenin* in the zones of cartilage tissue.
- Physiological and degradative loads result in differential transcriptional expression of WNT signalling components.
- Addition of exogenous DKK-1 primarily inhibited load-induced transcription of canonical WNT signalling components, impacting on observed changes in the expression of markers of cartilage metabolism.

- Inhibition of NFATC ameliorates load-induced transcription of canonical and non-canonical WNT signalling components, impacting on observed changes in the expression of markers of cartilage metabolism.

These results suggest that WNT signalling has an integral role in mechanically-regulated cartilage homeostasis, as demonstrated by the differential response to physiological and degradative loading regimes. Based on the chondrocyte monolayer model, activation of WNT signalling, as determined by confocal visualisation of nuclear β-catenin translocation, was evident in response to physiological levels of tensile strain (7.5%, 1Hz), in agreement with a study previously performed in our laboratory (Thomas et al., 2011). When subjected to different durations of an identical strain (7.5%, 1Hz), it was observed that 2 hours induced maximal nuclear β-catenin translocation, suggesting that in this model system 2 hours was the approximate time required for the chondrocyte to adapt to the mechanical stimulus. This mechano-response was transient as after 4 hours of tensile strain, the localisation of β-catenin returned to a cytoplasmic distribution comparable to the unloaded chondrocytes. Based on these initial observations, different magnitudes of strain (7.5%, 10% and 14%) were applied, and a differential response was observed where β-catenin was localised to the nucleus in response to 7.5% (as previously observed) as well as 10% strain. In response to higher tensile strain (14%), there was an overall increase in both cytoplasmic and nuclear β-catenin expression, possibly suggesting that once a load exceeds a certain threshold WNT signalling is sustained. This then provides the opportunity whereby catabolic genes may be activated downstream as it is well known that some of the down-stream WNT signalling effector genes include MMPs and ADAMTSs (Yuasa et al., 2008, Wang et al., 2009). In addition, localisation of WIF-1, a secreted inhibitor of WNT signalling, was investigated as it was previously reported to possibly regulate the canonical WNT pathway via a negative feedback mechanism (Stock et al., 2013). Confocal visualisation of WIF-1 demonstrated an enhanced labelling intensity, primarily at the strains which exhibited higher activation of canonical WNT signalling, indicating a possible negative feedback mechanism. To fully

characterise this response to strain, further experiments are needed to examine expression of other WNT signalling genes as well as quantification of phosphorylated versus non-phosphorylated β-catenin protein expression using western blotting. However, having observed activation of WNT signalling in response to tensile strain in high density chondrocyte cultures, the focus of the project was to then examine the role of WNT signalling in a more physiologically relevant model, hence the use of cartilage explants.

Before examination of WNT signalling in cartilage explants, physiological and degradative loading regimes had to be determined in our model system. Previous studies have used well characterised loading regimes (Leong et al., 2011b, Loening et al., 2000, Fitzgerald et al., 2004), however these loading regimes were not compatible with my experimental design. One of my aims was to investigate the early transcriptional changes which occur in response to compressive load, thus shorter loading regimes were needed in addition to optimisation of the period post-cessation of load in which transcriptional events occurred for downstream analysis. The characterised loading regimes in the literature investigated matrix changes that occur after hours of loading, whereas the loading regimes characterised in this thesis were shorter and hence representative of physiological and degradative loads at the gene level i.e. induced transcriptional changes in genes involved in metabolism or predominantly catabolism respectively. Furthermore, characterisation of appropriate loading regimes were accompanied with optimisation of housekeeping genes suitable for qPCR data normalisation, as it is well known that the use of unstable housekeeping genes can lead to inaccurate results. Using a panel of housekeeping genes, SDHA and YWHAZ were identified as the most stable housekeeping genes tested in cartilage subjected to different loading regimes or in the absence of load, and were used for all subsequent experiments. The loading regimes, referred to in this thesis as physiological or degradative in genotype, were characterised by assessing the expression of anabolic and catabolic matrix genes.

As observed in the high density chondrocyte monolayer system, canonical WNT signalling was also activated in cartilage explants in response to

compressive load. Furthermore, canonical WNT signalling was shown to be differentially regulated in response to the magnitude of load applied, confirming my previous observations in cells exposed to increasing levels of strain. Confocal visualisation of β-catenin localisation indicated that canonical WNT signalling was less active in explants subjected to physiological load, but was enhanced in response to degradative load. Of the time points analysed, these effects were observed primarily by 4 hours post cessation of load. This contrasts to the 2 hours observed in the cells, but is likely due to the extended period of time necessary for a mechanical stimulus to elicit a response within the chondrocyte, particularly if it was dependent on feedback mechanisms or release of sequestered molecules e.g. growth factors in the ECM, as would occur *in vivo*. Interestingly, both loading regimes induced WNT activation mainly in the deep zone chondrocytes. A differential response of chondrocytes through the cartilage depth was suggested to be as a result of the differences in matrix composition (Shieh and Athanasiou, 2006, Lee et al., 1998). The chondrocytes' response to a mechanical stimulus may be affected by the stiffness of the matrix, where deformation of a subpopulation of chondrocytes in a specific zone may be more or less than another zone (Lee et al., 1998). Deep zone chondrocytes are embedded in a matrix rich in proteoglycans, therefore the differential activation of WNT signalling could be an adaptive response to compressive load, as the deep zone matrix can deform more than their superficial/mid zone counterparts. This suggestion further supports my hypothesis that the differential WNT signalling observed may be an adaptive response to maintain cartilage tissue integrity (Shieh and Athanasiou, 2006, Vanderploeg et al., 2008, Aydelotte et al., 1988).

7.3 Involvement of canonical and non-canonical WNT pathways in cartilage chondrocyte mechanotransduction

Having confirmed the mechano-regulation of canonical WNT signalling, i.e. as evidenced by nuclear translocation of β-catenin, in cartilage explants, the transcriptional expression of WNT signalling components was assessed to further dissect which of the WNT pathways were activated. Custom-built bovine PCR arrays contained 84 WNT signalling genes encompassing canonical, non-canonical i.e. WNT/Ca^{2+} and PCP, WNT inhibitors and targets of WNT signalling.

Assessment of WNT signalling components at defined periods post-cessation of load, illustrated a fascinating picture of how WNT signalling is differentially regulated by physiological and/or degradative loads. At the early phase post-cessation of load, effects on transcription of the WNT signalling target genes was similar in both loading regimes; however, the fold-change was higher in response to degradative load, as well as the regulation of WNT5B and WNT9A - genes belonging to the WNT/Ca^{2+} pathway. A recent study demonstrated that inhibition of L-type Ca^{2+} channels in cartilage reduced activation of canonical WNT signalling via induction of FRZB expression, thus demonstrating that this pathway is able to regulate the canonical signalling pathway (Takamatsu et al., 2014).

Transcript levels of most WNT signalling components were affected by 4 hours post-cessation of load, and there was a clear demarcation between those genes regulated by physiological load and those by the degradative loading regime. WNT signalling components, already identified as being up-regulated 2 hours post-cessation of load, were also similarly affected at 4 hours in response to physiological load. Overall, mechano-regulation of more genes associated with canonical WNT signalling activation was observed, compared to the earlier time point, as demonstrated by the increased number of WNT signalling target genes transcribed and the reduced expression of WNT signalling inhibitors. In contrast, the majority of the genes which were up-regulated in response to the degradative loading regime were associated with canonical WNT signalling, including transcription of ligands and frizzled receptors. In addition, activation of WNT signalling was further enhanced in response to the higher loading regime as indicated by the transcription of more WNT target genes, frizzled receptors and WNT ligands, when compared to the effect of the physiological regime. Interestingly, several of the WNT-related genes which were altered in response to the degradative loading regime have very similar expression patterns to the levels observed in human OA cartilage. For example, FOSL1 expression was the most highly up-regulated gene at 2 (35-fold), 4 (109-fold) and 24 hours (26.5-fold) post-cessation of the degradative load; interestingly, the expression of this gene is significantly enhanced in OA (Thorfve et al., 2012). FOSL1 is part of the activated protein-1 (AP-1) complex which is implicated in the regulation of MMP expression, among many targets, and involved in increased bone mass, both of

which are features of OA pathology (Newberry et al., 1997, Desvergne and Wahli, 1999, Eferl et al., 2004). Expression of PRICKLE-1 and DVL2 were down-regulated in cartilage subjected to the degradative load; similar responses were observed in OA tissue, although it was the PRICKLE-2 isoform down-regulated in human diseased cartilage (Thorfve et al., 2012). In addition, degradative load was shown to up-regulate the transcription of NFATC1 and NFATC2 (data not shown). Interestingly, NFATC2 mRNA levels were also elevated in OA cartilage, as well as enhanced expression of other WNT/Ca^{2+} related genes indicating activation of this pathway in OA (Thorfve et al., 2012, Sun et al., 2014).

By 24 hours post-cessation of load, both loading regimes showed a reduction in the transcription of WNT signalling genes demonstrating the transient nature of this signalling pathway to regulate the consequences of its activation. All WNT components which were previously transcribed in response to physiological load were subsequently decreased in expression at this later time point. In contrast, the remnants of WNT signalling activation were still evident in explants subjected to the higher loading regime, as a few target genes e.g. FOSL1, were transcribed. The remainder of the previously mechanically regulated WNT components returned to basal levels comparable with the unloaded explants and those subjected to the physiological load. These results indicate that WNT signalling is a complex pathway and although specific components have previously been assigned to a specific WNT pathway i.e. canonical, PCP or WNT/Ca^{2+} pathway, essentially all of these pathways overlap and are found to counter-regulate the expression and/or activation of the other respective pathways. In essence, these pathways do not exist in isolation, as demonstrated by a recent study by Nalesso et al. (2011). They demonstrated that both the canonical and WNT/Ca^{2+} pathways were activated in chondrocytes in response to WNT3A, a classical canonical WNT ligand (Nalesso et al., 2011). Moreover, several studies indicated that the WNT/Ca^{2+} pathway inhibit canonical WNT signalling in human chondrocytes (Nalesso et al., 2011, Kuhl et al., 2000). Previous studies have shown that short episodes of mechanical load i.e. application of 10 cycles (10% strain, 1Hz or 0.3Hz) results in Ca^{2+} mobilisation in chondrocytes (Pingguan-Murphy et al., 2006). One of the earliest mechano-responsive events in chondrocytes is Ca^{2+} mobilisation (Guilak et al., 1999, Wann

et al., 2012). Taking these into consideration, for future studies it would be interesting to investigate how mechanically regulated Ca^{2+} mobilisation affects downstream WNT signalling by loading cartilage explants in the presence or absence of Ca^{2+} channel blockers. This would allow us to further understand the importance of Ca^{2+} in the mechanism of WNT signalling activation and its downstream effects.

7.4 Understanding the functional consequences of differential transcription of DKK-1 and NFATC1 in cartilage chondrocyte mechanotransduction

A preliminary study was conducted to determine the functional effects of the mechanically regulated genes DKK-1 and NFATC1 in articular cartilage homeostasis, as mediated by WNT signalling. Explants were treated with either recombinant DKK-1 or an NFATC inhibitor and subjected to the higher load (7MPa). One of the limitations of this experiment was the inability to source an inhibitor that was specific to NFATC1. Instead, an NFATC inhibitor was used which is reported to selectively inhibit calcineurin-mediated dephosphorylation of NFATCs; it does not disrupt other calcineurin-dependent pathways, but selectively inhibits activation of NFATC1-4 (Roehrl et al., 2004). Previous studies utilised the fungal metabolite cyclosporine A to inhibit NFATCs as it targets the upstream calcineurin, preventing it from dephosphorylating NFATC. However, cyclosporine A has many off-target interactions making it less than ideal for elucidating mechanisms of action in this study (Hu et al., 2014).

Treatment with either recombinant DKK-1 or NFATC inhibitor exhibited significant changes in the transcription of mechano-sensitive downstream effectors including the matrix genes as well as WNT signalling related genes, at 4 and 24 hours post-load. DKK-1 treatment affected the expression of several of the mechanically regulated WNT signalling components, demonstrating that the canonical WNT pathway was being repressed. In contrast, transcript levels were dramatically decreased in the presence of the NFATC inhibitor, as it induced global decreases in many WNT signalling components including WNT ligands, WNT target genes as well as inhibitors and effector genes such as DVL1 and DVL2. NFATC-mediated inhibition of mechanically regulated WNT signalling

molecules emphasises the prominent role the NFATs play in the regulation of WNT homeostasis. These results clearly demonstrate that NFATCs play a crucial role in facilitating both canonical and non-canonical WNT signalling (Huang et al., 2011). Further studies are required to understand the exact role of NFATs in cartilage chondrocyte mechanotransduction. Investigating how mechanical load affects NFATC protein expression and its downstream targets would be interesting to investigate. In addition, further functional studies such as the reciprocal to what was conducted in this series of experiments, i.e. inhibition of DKK-1 and addition of recombinant NFATC1 or 2, are required to further understand how these components are able to regulate WNT signalling in mechanically loaded cartilage to elicit the observed responses.

However, the expression of several of the genes which were altered at 4 hours post-cessation of load were not affected after 24 hours and *vice versa*. This may reflect the fact that some of the genes require even longer periods of application of mechanical load or longer period post-load to show any transcriptional differences. This was demonstrated to be the case in previous temporal studies, where application of 3% strain (0.1Hz, 24 hours) on bovine explants was sufficient to induce significant changes in aggrecan, collagen type II, MMP3 and ADAMTS-5 transcription (Fitzgerald et al., 2006). Shorter durations of load (1, 4, and 8 hours), followed by harvesting of tissue directly post-cessation of load, did not produce a comparable response to those identified at 24 hours (Fitzgerald et al., 2006). The significance of post-load duration is particularly evident with TIMP mechano-regulation. At 4 hours post-load, only TIMP 3 was altered by NFATC inhibition, whereas at 24 hours post-load, only TIMP 1 expression was affected, but its expression was altered by both DKK-1 stimulation and NFATC inhibitor. It is interesting to note that it was mainly the catabolic genes that exhibited significant changes in transcription at both time points. As DKK-1 and NFATC are known to have downstream effects on matrix genes the changes observed here were expected (Yuasa et al., 2008, Sitara and Aliprantis, 2010). MMPs are some of the downstream targets that are directly regulated by canonical WNT signalling, thus the reduction in their expression due to exogenous DKK-1 treatment provides further evidence for a role of WNT signalling in promoting cartilage homeostasis. Furthermore, it suggests that the

reduced expression of DKK-1 in cartilage subjected to the degradative load may be a mechanism by which this regime induces the MMP and ADAMTS transcription observed. Activation of canonical WNT signalling, via exogenous WNT3A or forced expression of constitutive-active β-catenin was shown to induce expression of MMP2, MMP3, MMP9, MMP13, ADAMTS-4 and ADAMTS-5, thus as a regulator of WNT signalling DKK-1 is expected to regulate these downstream targets (Yuasa et al., 2008). This was further shown in mouse models where intra-articular administration of DKK-1 into the joint or in mice overexpressing DKK-1 in cartilage, the presence of exogenous DKK-1 inhibited the progression of OA induced by destabilisation of the medial meniscus (Oh et al., 2012). Furthermore, induction of the canonical WNT signalling targets i.e. MMP13 and ADAMTS-4 by WNT3A stimulation were significantly inhibited by DKK-1 treatment, demonstrating the ability of DKK-1 to regulate expression of catabolic genes induced by canonical WNT activation (Oh et al., 2012). However, contradictory studies by Weng et al. have implicated the involvement of DKK-1 in the progression of OA (Weng et al., 2009, Weng et al., 2010, Weng et al., 2012). Inhibition of DKK-1, using DKK-1 antisense in rat OA models, significantly attenuated OA progression as assessed by cartilage fibrillation and degradation markers (Weng et al., 2010). In addition, DKK-1 expression was enhanced in patients with knee OA, and IL-1β stimulation of cartilage induced the concomitant expression of DKK-1 and caspase-3, an apoptotic marker (Weng et al., 2009). Neutralization using monoclonal DKK-1 antibodies reduced caspase-3 cleavage and cytokine-mediated apoptosis (Weng et al., 2009). In a more recent study, the same group demonstrated that endogenous DKK-1 expression induces MMP3 and ADAMTS-5 expression in human OA synovium, however neutralization of DKK-1 reduced their expression and returned aggrecan expression to basal levels in chondrocyte cultures (Weng et al., 2012).

In contrast, NFATC inhibition modulated aggrecan transcription as well as catabolic gene expression; these observations have been previously reported. Mice deficient in NFATC1 had reduced aggrecan expression (Wang et al., 2009). In addition, these mice had enhanced expression of catabolic genes such as ADAMTS-5 and MMP13, and reduced levels of TIMP 1 (Wang et al., 2009). NFATC *cis*-elements have been identified in the promoters of some of these

matrix genes such as collagen type II, aggrecan, TIMP1, MMP9 and ADAMTS-4 (Thirunavukkarasu et al., 2006, Aliprantis et al., 2008, Sitara and Aliprantis, 2010), suggesting a direct mechanism by which mechanically induced NFATC1 expression can modulate transcription of these catabolic markers. Although my data demonstrates an NFATC-mediated reduction in aggrecan transcription, expression of the MMPs and ADAMTSs were also reduced or remained unaffected by this inhibition. This contradiction illustrates the conflicting data that has previously been reported. NFATC1 knockout mice had no phenotype and were unaffected by destabilisation of the medial meniscus (Wang et al., 2009). However, when NFATC1 and 2 were knocked out, NFATC1 exacerbated the extent of OA in these mice, but the effects were related to abnormal joint development rather than specific defects in articular cartilage (Greenblatt et al., 2013). Evidence provided by the NFATC knockout mouse model supports a role for NFATC as an "OA suppressor" gene as this molecule repressed the OA phenotype (Greenblatt et al., 2013, Wang et al., 2009). However, within the literature, a recent study demonstrated that in human OA cartilage there were increased levels of NFATC1 (Sun et al., 2014). Furthermore, knockdown of NFATC1 reduced the mRNA levels of the catabolic genes, which were found to be induced via interleukin-1β (Sun et al., 2014). In addition, a further study demonstrated similar findings in human OA tissue with significant up-regulation in expression of the NFAT family (Thorfve et al., 2012), thus supporting my findings. However, it has also been previously documented that NFATC1 mRNA levels were significantly reduced in lesional sites from human OA cartilage (Greenblatt et al., 2013). Interestingly, the NFATCs have also been positively implicated in chondrogenesis, but again there is conflicting evidence as NFATC2 had previously been interpreted as a repressor/inhibitor of chondrogenesis in adult NfATC2 knockout mouse joints (Ranger et al., 2000, Tomita et al., 2002). Forced expression of NFATC2 using lentiviral vectors in chondrocytes isolated from these mice rescued the abnormal catabolic and anabolic activities of these cells (Ranger et al., 2000). NFATC activity is tightly regulated by upstream signalling pathways, but it is still unclear which extracellular signals regulate these transcription factors. Many mechanical and biochemical stimuli can regulate both the activators (calcineurin) and inhibitors (e.g. GSK-3) of NFAT activity in

chondrocytes. However, recent studies have demonstrated that manipulating the intracellular regulators of NFAT signalling in chondrocytes i.e. pharmacological inhibition of GSK-3 signalling or inhibition of calcineurin did not yield the anticipated results of rescuing cartilage homeostasis. Instead, increased cartilage degeneration was observed in rats treated with a GSK-3 inhibitor and a decreased severity of OA in mouse models treated with a calcineurin inhibitor: cyclosporine A, correlating with the outcomes of the data from my study (Miclea et al., 2011, Yoo et al., 2007). Collectively, I think that the previous publications and my data clearly demonstrates that like many other fundamental signalling molecules including β-catenin, either enhanced or substantially reduced levels of these proteins confer similar properties i.e. cartilage degeneration. It is a balance of the expression of these molecules which is vital for maintaining cartilage integrity and function, which would explain why the two extremes i.e. too little or too much show similar effects in being detrimental. However, further experiments would need to be performed to determine if this was definitely true. What I can conclude from this particular experimental chapter is that NFATC1 and NFATC2 are mechano-sensitive, their expression increases with magnitude of load, and inhibition of NFATC reduces the expression of specific mechanically-regulated genes mediated via this pathway.

7.5 Future Directions

There were a few limitations in the experimental design, partly due to the use of immature bovine tissue. A limited number of WNT component targets could be investigated as a result of lack of cross-species reactivity between bovine and the other species in which arrays were readily available; as complete elucidation of the bovine genome advances, this will ultimately be rectified. A second limitation was the age of the animals from which the tissue was derived for use in these studies; the animals were approximately 1 – 3 weeks of age i.e. immature. The advantage of using immature cartilage is that it is very cellular, thus providing more material to work with in comparison to mature tissue. Interestingly, although the bovine tissue used in these studies was immature, many of the mechanically induced transcriptional effects observed corroborated gene changes that had been identified either in mature animal tissue or in human

diseased cartilage, giving confidence to the validity of the studies performed. However, comparative studies between immature and mature cartilage should be conducted to elucidate if maturity of tissue influences activation of WNT signalling components in articular cartilage mechanotransduction. It is widely reported that bone remodelling is also regulated by WNT signalling (Baron and Kneissel, 2013, Robinson et al., 2006, Lories et al., 2013), therefore future studies could focus on applying these loading regimes to cartilage explants with subchondral bone attached, as it would be interesting to observe how mechanical load alters WNT signalling in each of the tissues. Furthermore, by comparing the response of cartilage to load in the presence or absence of subchondral bone may provide information on potential crosstalk between these two tissues.

Of the fifteen mechanically-regulated WNT signalling genes validated, only two i.e. DKK-1 and NFATC1 were pursued further to investigate their role in cartilage chondrocyte mechanotransduction. Therefore, it would be interesting to ascertain how important the remainder of these genes are in mechanically induced ECM catabolism, particularly WISP-1 which is also associated with experimental OA, and has been suggested as a potential candidate for OA therapy (Blom et al., 2009, Leask, 2011). Although the expression of the validated genes from my *in vitro* mechanical studies correlate with observations in human studies, it would be useful to characterise their expression in an *in vivo* model. In Cardiff, we have established an *in vivo* model of cartilage degeneration induced by the non-surgical rupture of the cruciate ligament (12N). In this model, early events include swelling and inflammation, and by 3 weeks post-rupture, extensive cartilage degeneration is observed (Blain et al., unpublished observations); this model provides an excellent tool to delineate the early initiating factors of cartilage degradation. Determining the expression levels of these identified genes in this model system would reinforce the importance of these molecules in cartilage mechanobiology and disease progression. Furthermore, this model could also be used to then test whether manipulation of the identified molecules e.g. exogenous DKK-1 or NFATC inhibitor, administered by intra-articular injection, could confer protection against joint degeneration enabling potential therapies to be identified. The alternative strategy would be to mechanically load the relevant transgenic model to elucidate whether the joint

damage was improved or exacerbated in response to the cruciate rupture. Clearly, having identified these mechano-responsive WNT molecules, there is huge scope to further these studies to elucidate their importance in joint degeneration and their potential as therapeutic targets.

7.6 Concluding statement

This thesis presents novel findings demonstrating the mechano-regulation of both canonical and non-canonical WNT signalling in cartilage explants. Elucidating how these mechanically regulated WNT signalling components affects cartilage homeostasis could shed light on the initiating events involved in cartilage degeneration and may offer therapeutic potential in the treatment of OA.

Reference list

AKIMOTO, T., USHIDA, T., MIYAKI, S., AKAOGI, H., TSUCHIYA, K., YAN, Z., WILLIAMS, R. S. & TATEISHI, T. 2005. Mechanical stretch inhibits myoblast-to-adipocyte differentiation through Wnt signaling. *Biochemical and Biophysical Research Communications,* 329**,** 381-385.

AKIYAMA, H., LYONS, J. P., MORI-AKIYAMA, Y., YANG, X., ZHANG, R., ZHANG, Z., DENG, J. M., TAKETO, M. M., NAKAMURA, T., BEHRINGER, R. R., MCCREA, P. D. & DE CROMBRUGGHE, B. 2004. Interactions between Sox9 and beta-catenin control chondrocyte differentiation. *Genes Dev,* 18**,** 1072-87.

ALIPRANTIS, A. O., UEKI, Y., SULYANTO, R., PARK, A., SIGRIST, K. S., SHARMA, S. M., OSTROWSKI, M. C., OLSEN, B. R. & GLIMCHER, L. H. 2008. NFATc1 in mice represses osteoprotegerin during osteoclastogenesis and dissociates systemic osteopenia from inflammation in cherubism. *J Clin Invest,* 118**,** 3775-89.

ALLEN, J. L., COOKE, M. E. & ALLISTON, T. 2012. ECM stiffness primes the TGFbeta pathway to promote chondrocyte differentiation. *Mol Biol Cell,* 23**,** 3731-42.

ANSTAETT, O. L., BROWNLIE, J., COLLINS, M. E. & THOMAS, C. J. 2010. Validation of endogenous reference genes for RT-qPCR normalisation in bovine lymphoid cells (BL-3) infected with Bovine Viral Diarrhoea Virus (BVDV). *Vet Immunol Immunopathol,* 137**,** 201-7.

ARNER, E. C. 2002. Aggrecanase-mediated cartilage degradation. *Curr Opin Pharmacol,* 2**,** 322-9.

AROKOSKI, J. P. A., JURVELIN, J. S., VÄÄTÄINEN, U. & HELMINEN, H. J. 2000. Normal and pathological adaptations of articular cartilage to joint loading. *Scandinavian Journal of Medicine & Science in Sports,* 10**,** 186-198.

ASPBERG, A. 2012. The different roles of aggrecan interaction domains. *J Histochem Cytochem,* 60**,** 987-96.

ATHANASIOU, K. A., DARLING, E. M., HU, J. C., DURAINE, G. D. & REDDI, A. H. 2013. *Articular Cartilage*, Taylor & Francis.

AYDELOTTE, M. B., GREENHILL, R. R. & KUETTNER, K. E. 1988. Differences between sub-populations of cultured bovine articular chondrocytes. II. Proteoglycan metabolism. *Connect Tissue Res,* 18**,** 223-34.

BADER, D. L., SALTER, D. & CHOWDHURY, T. 2011. Biomechanical influence of cartilage homeostasis in health and disease. *Arthritis,* 2011.

BALACESCU, L., BALACESCU, O., CRISAN, N., FETICA, B., PETRUT, B., BUNGARDEAN, C., RUS, M., TUDORAN, O., MEURICE, G., IRIMIE, A., DRAGOS, N. & BERINDAN-NEAGOE, I. 2011. Identifying molecular features for prostate cancer with Gleason 7 based on microarray gene expression profiles. *Rom J Morphol Embryol,* 52**,** 1195-202.

BALACHANDRAN, K., ALFORD, P. W., WYLIE-SEARS, J., GOSS, J. A., GROSBERG, A., BISCHOFF, J., AIKAWA, E., LEVINE, R. A. & PARKER, K. K. 2011. Cyclic strain induces dual-mode endothelial-mesenchymal transformation of the cardiac valve. *Proc Natl Acad Sci U S A,* 108**,** 19943-8.

BARON, R. & KNEISSEL, M. 2013. WNT signaling in bone homeostasis and disease: from human mutations to treatments. *Nat Med,* 19**,** 179-192.

BENNINGHOFF, A. 1925. Form und Bau der Gelenkknorpel in ihren Beziehungen zur Funktion. *Zeitschrift für Zellforschung und Mikroskopische Anatomie,* 2**,** 783-862.

BLAIN, E. J. 2007. Mechanical regulation of matrix metalloproteinases. *Front Biosci,* 12**,** 507-27.
BLAIN, E. J. 2009. Involvement of the cytoskeletal elements in articular cartilage homeostasis and pathology. *Int J Exp Pathol,* 90**,** 1-15.
BLAIN, E. J. 2011. Involvement of the cytoskeletal elements in articular cartilage mechanotransduction. *Mechanosensitivity and Mechanotransduction.* Springer.
BLAIN, E. J., ALI, A. Y. & DUANCE, V. C. 2010. Boswellia frereana (frankincense) suppresses cytokine-induced matrix metalloproteinase expression and production of pro-inflammatory molecules in articular cartilage. *Phytotherapy Research,* 24**,** 905-912.
BLOM, A. B., BROCKBANK, S. M., VAN LENT, P. L., VAN BEUNINGEN, H. M., GEURTS, J., TAKAHASHI, N., VAN DER KRAAN, P. M., VAN DE LOO, F. A., SCHREURS, B. W., CLEMENTS, K., NEWHAM, P. & VAN DEN BERG, W. B. 2009. Involvement of the Wnt signaling pathway in experimental and human osteoarthritis: prominent role of Wnt-induced signaling protein 1. *Arthritis Rheum,* 60**,** 501-12.
BLOM, A. B., VAN LENT, P. L., VAN DER KRAAN, P. M. & VAN DEN BERG, W. B. 2010. To seek shelter from the WNT in osteoarthritis? WNT-signaling as a target for osteoarthritis therapy. *Curr Drug Targets,* 11**,** 620-9.
BONDESON, J., WAINWRIGHT, S., HUGHES, C. & CATERSON, B. 2008. The regulation of the ADAMTS4 and ADAMTS5 aggrecanases in osteoarthritis: a review. *Clin Exp Rheumatol,* 26**,** 139-45.
BOUDREAULT, F. & TSCHUMPERLIN, D. J. 2010. Stretch-induced mitogen-activated protein kinase activation in lung fibroblasts is independent of receptor tyrosine kinases. *Am J Respir Cell Mol Biol,* 43**,** 64-73.
BOURBOULIA, D. & STETLER-STEVENSON, W. G. 2010. Matrix metalloproteinases (MMPs) and tissue inhibitors of metalloproteinases (TIMPs): Positive and negative regulators in tumor cell adhesion. *Seminars in Cancer Biology,* 20**,** 161-168.
BOUTROS, M., PARICIO, N., STRUTT, D. I. & MLODZIK, M. 1998. Dishevelled activates JNK and discriminates between JNK pathways in planar polarity and wingless signaling. *Cell,* 94**,** 109-18.
BREW, K. & NAGASE, H. 2010. The tissue inhibitors of metalloproteinases (TIMPs): an ancient family with structural and functional diversity. *Biochim Biophys Acta,* 1803**,** 55-71.
BUCKWALTER, J. A., MANKIN, H. J. & GRODZINSKY, A. J. 2005. Articular cartilage and osteoarthritis. *Instr Course Lect,* 54**,** 465-80.
BURGERS, T. A. & WILLIAMS, B. O. 2013. Regulation of Wnt/β-catenin signaling within and from osteocytes. *Bone,* 54**,** 244-249.
BUSCHMANN, M. D., GLUZBAND, Y. A., GRODZINSKY, A. J. & HUNZIKER, E. B. 1995. Mechanical compression modulates matrix biosynthesis in chondrocyte/agarose culture. *J Cell Sci,* 108 (Pt 4)**,** 1497-508.
BUSCHMANN, M. D., GLUZBAND, Y. A., GRODZINSKY, A. J., KIMURA, J. H. & HUNZIKER, E. B. 1992. Chondrocytes in agarose culture synthesize a mechanically functional extracellular matrix. *J Orthop Res,* 10**,** 745-58.
BUSCHMANN, M. D., HUNZIKER, E. B., KIM, Y. J. & GRODZINSKY, A. J. 1996. Altered aggrecan synthesis correlates with cell and nucleus structure in statically compressed cartilage. *J Cell Sci,* 109 (Pt 2)**,** 499-508.

CADIGAN, K. M. & NUSSE, R. 1997. Wnt signaling: a common theme in animal development. *Genes Dev,* 11**,** 3286-305.
CAMPBELL, J. J., BLAIN, E. J., CHOWDHURY, T. T. & KNIGHT, M. M. 2007. Loading alters actin dynamics and up-regulates cofilin gene expression in chondrocytes. *Biochem Biophys Res Commun,* 361**,** 329-34.
CASE, N., MA, M., SEN, B., XIE, Z., GROSS, T. S. & RUBIN, J. 2008. Beta-catenin levels influence rapid mechanical responses in osteoblasts. *J Biol Chem,* 283**,** 29196-205.
CHAHINE, N. O., CHEN, F. H., HUNG, C. T. & ATESHIAN, G. A. 2005. Direct measurement of osmotic pressure of glycosaminoglycan solutions by membrane osmometry at room temperature. *Biophys J,* 89**,** 1543-50.
CHAKRABORTI, S., MANDAL, M., DAS, S., MANDAL, A. & CHAKRABORTI, T. 2003. Regulation of matrix metalloproteinases: an overview. *Mol Cell Biochem,* 253**,** 269-85.
CHAO, P. H., WEST, A. C. & HUNG, C. T. 2006. Chondrocyte intracellular calcium, cytoskeletal organization, and gene expression responses to dynamic osmotic loading. *Am J Physiol Cell Physiol,* 291**,** C718-25.
CHAPMAN, K. & VALDES, A. M. 2012. Genetic factors in OA pathogenesis. *Bone,* 51**,** 258-64.
CHEN, C., TAMBE, D. T., DENG, L. & YANG, L. 2013. Biomechanical properties and mechanobiology of the articular chondrocyte. *Am J Physiol Cell Physiol,* 305**,** C1202-8.
CHEN, C. H., CHUANG, S. M., YANG, M. F., LIAO, J. W., YU, S. L. & CHEN, J. J. 2012. A novel function of YWHAZ/beta-catenin axis in promoting epithelial-mesenchymal transition and lung cancer metastasis. *Mol Cancer Res,* 10**,** 1319-31.
CHEN, C. T., BURTON-WURSTER, N., BORDEN, C., HUEFFER, K., BLOOM, S. E. & LUST, G. 2001. Chondrocyte necrosis and apoptosis in impact damaged articular cartilage. *J Orthop Res,* 19**,** 703-11.
CHEN, M., ZHU, M., AWAD, H., LI, T. F., SHEU, T. J., BOYCE, B. F., CHEN, D. & O'KEEFE, R. J. 2008. Inhibition of beta-catenin signaling causes defects in postnatal cartilage development. *J Cell Sci,* 121**,** 1455-65.
CHIGITA, S., SUGIURA, T., ABE, M., KOBAYASHI, Y., SHIMODA, M., ONODA, M. & SHIRASUNA, K. 2012. CD82 inhibits canonical Wnt signalling by controlling the cellular distribution of beta-catenin in carcinoma cells. *Int J Oncol,* 41**,** 2021-8.
CHIQUET, M., MATTHISSON, M., KOCH, M., TANNHEIMER, M. & CHIQUET-EHRISMANN, R. 1996. Regulation of extracellular matrix synthesis by mechanical stress. *Biochem Cell Biol,* 74**,** 737-44.
CHUN, J. S., OH, H., YANG, S. & PARK, M. 2008. Wnt signaling in cartilage development and degeneration. *BMB Rep,* 41**,** 485-94.
CHURCH, V., NOHNO, T., LINKER, C., MARCELLE, C. & FRANCIS-WEST, P. 2002. Wnt regulation of chondrocyte differentiation. *J Cell Sci,* 115**,** 4809-18.
CLEVERS, H. & NUSSE, R. 2012. Wnt/β-Catenin Signaling and Disease. *Cell,* 149**,** 1192-1205.
CONNELLY, J. T., VANDERPLOEG, E. J. & LEVENSTON, M. E. 2004. The influence of cyclic tension amplitude on chondrocyte matrix synthesis: experimental and finite element analyses. *Biorheology,* 41**,** 377-87.
CRUCIAT, C. M. & NIEHRS, C. 2013. Secreted and transmembrane wnt inhibitors and activators. *Cold Spring Harb Perspect Biol,* 5**,** a015081.

DANIELS, D. L. & WEIS, W. I. 2005. Beta-catenin directly displaces Groucho/TLE repressors from Tcf/Lef in Wnt-mediated transcription activation. *Nat Struct Mol Biol,* 12**,** 364-71.
DAS, P., SCHURMAN, D. J. & SMITH, R. L. 1997. Nitric oxide and G proteins mediate the response of bovine articular chondrocytes to fluid-induced shear. *J Orthop Res,* 15**,** 87-93.
DAY, T. F., GUO, X., GARRETT-BEAL, L. & YANG, Y. 2005. Wnt/beta-catenin signaling in mesenchymal progenitors controls osteoblast and chondrocyte differentiation during vertebrate skeletogenesis. *Dev Cell,* 8**,** 739-50.
DE, A. 2011. Wnt/Ca2+ signaling pathway: a brief overview. *Acta Biochim Biophys Sin (Shanghai),* 43**,** 745-56.
DELLETT, M., HU, W., PAPADAKI, V. & OHNUMA, S. 2012. Small leucine rich proteoglycan family regulates multiple signalling pathways in neural development and maintenance. *Dev Growth Differ,* 54**,** 327-40.
DENG, Y., HU, J. C. & ATHANASIOU, K. A. 2007. Isolation and chondroinduction of a dermis-isolated, aggrecan-sensitive subpopulation with high chondrogenic potential. *Arthritis & Rheumatism,* 56**,** 168-176.
DERFUS, B., KRANENDONK, S., CAMACHO, N., MANDEL, N., KUSHNARYOV, V., LYNCH, K. & RYAN, L. 1998. Human osteoarthritic cartilage matrix vesicles generate both calcium pyrophosphate dihydrate and apatite in vitro. *Calcif Tissue Int,* 63**,** 258-62.
DESVERGNE, B. & WAHLI, W. 1999. Peroxisome proliferator-activated receptors: nuclear control of metabolism. *Endocr Rev,* 20**,** 649-88.
DHEDA, K., HUGGETT, J. F., BUSTIN, S. A., JOHNSON, M. A., ROOK, G. & ZUMLA, A. 2004. Validation of housekeeping genes for normalizing RNA expression in real-time PCR. *Biotechniques,* 37**,** 112-4, 116, 118-9.
DHEDA, K., HUGGETT, J. F., CHANG, J. S., KIM, L. U., BUSTIN, S. A., JOHNSON, M. A., ROOK, G. A. & ZUMLA, A. 2005. The implications of using an inappropriate reference gene for real-time reverse transcription PCR data normalization. *Anal Biochem,* 344**,** 141-3.
DIARRA, D., STOLINA, M., POLZER, K., ZWERINA, J., OMINSKY, M. S., DWYER, D., KORB, A., SMOLEN, J., HOFFMANN, M., SCHEINECKER, C., VAN DER HEIDE, D., LANDEWE, R., LACEY, D., RICHARDS, W. G. & SCHETT, G. 2007. Dickkopf-1 is a master regulator of joint remodeling. *Nat Med,* 13**,** 156-163.
DONNAN, F. G. 1924. The theory of membrane equilibria. *Chemical Reviews,* 1**,** 73-90.
DOUDNA, J. A. & RATH, V. L. 2002. Structure and Function of the Eukaryotic Ribosome: The Next Frontier. *Cell,* 109**,** 153-156.
DRISSI, H., ZUSCIK, M., ROSIER, R. & O'KEEFE, R. 2005. Transcriptional regulation of chondrocyte maturation: potential involvement of transcription factors in OA pathogenesis. *Mol Aspects Med,* 26**,** 169-79.
DUANCE, V. C., CREAN, J. K., SIMS, T. J., AVERY, N., SMITH, S., MENAGE, J., EISENSTEIN, S. M. & ROBERTS, S. 1998. Changes in collagen cross-linking in degenerative disc disease and scoliosis. *Spine (Phila Pa 1976),* 23**,** 2545-51.
DURRANT, L. A., ARCHER, C. W., BENJAMIN, M. & RALPHS, J. R. 1999. Organisation of the chondrocyte cytoskeleton and its response to changing mechanical conditions in organ culture. *J Anat,* 194 (Pt 3)**,** 343-53.

EA, H. K., MONCEAU, V., CAMORS, E., COHEN-SOLAL, M., CHARLEMAGNE, D. & LIOTE, F. 2008. Annexin 5 overexpression increased articular chondrocyte apoptosis induced by basic calcium phosphate crystals. *Ann Rheum Dis,* 67**,** 1617-25.

EFERL, R., HOEBERTZ, A., SCHILLING, A. F., RATH, M., KARRETH, F., KENNER, L., AMLING, M. & WAGNER, E. F. 2004. The Fos-related antigen Fra-1 is an activator of bone matrix formation. *EMBO J,* 23**,** 2789-99.

ENOCHSON, L., STENBERG, J., BRITTBERG, M. & LINDAHL, A. 2014. GDF5 reduces MMP13 expression in human chondrocytes via DKK1 mediated canonical Wnt signaling inhibition. *Osteoarthritis and Cartilage,* 22**,** 566-577.

ERICKSON, G. R., NORTHRUP, D. L. & GUILAK, F. 2003. Hypo-osmotic stress induces calcium-dependent actin reorganization in articular chondrocytes. *Osteoarthritis Cartilage,* 11**,** 187-97.

ESKO, J. D., KIMATA, K. & LINDAHL, U. 2009. Proteoglycans and Sulfated Glycosaminoglycans. *In:* VARKI, A., CUMMINGS, R. D., ESKO, J. D., FREEZE, H. H., STANLEY, P., BERTOZZI, C. R., HART, G. W. & ETZLER, M. E. (eds.) *Essentials of Glycobiology.* 2nd ed. Cold Spring Harbor (NY).

EVANGELOU, E., CHAPMAN, K., MEULENBELT, I., KARASSA, F. B., LOUGHLIN, J., CARR, A., DOHERTY, M., DOHERTY, S., GÓMEZ-REINO, J. J., GONZALEZ, A., HALLDORSSON, B. V., HAUKSSON, V. B., HOFMAN, A., HART, D. J., IKEGAWA, S., INGVARSSON, T., JIANG, Q., JONSDOTTIR, I., JONSSON, H., KERKHOF, H. J. M., KLOPPENBURG, M., LANE, N. E., LI, J., LORIES, R. J., VAN MEURS, J. B. J., NÄKKI, A., NEVITT, M. C., RODRIGUEZ-LOPEZ, J., SHI, D., SLAGBOOM, P. E., STEFANSSON, K., TSEZOU, A., WALLIS, G. A., WATSON, C. M., SPECTOR, T. D., UITTERLINDEN, A. G., VALDES, A. M. & IOANNIDIS, J. P. A. 2009. Large-scale analysis of association between GDF5 and FRZB variants and osteoarthritis of the hip, knee, and hand. *Arthritis & Rheumatism,* 60**,** 1710-1721.

EYRE, D. 2002. Collagen of articular cartilage. *Arthritis Res,* 4**,** 30-5.

EYRE, D. & WU, J.-J. 2005. Collagen Cross-Links. *In:* BRINCKMANN, J., NOTBOHM, H. & MÜLLER, P. K. (eds.) *Collagen.* Springer Berlin Heidelberg.

FEHRENBACHER, A., STECK, E., RICKERT, M., ROTH, W. & RICHTER, W. 2003. Rapid regulation of collagen but not metalloproteinase 1, 3, 13, 14 and tissue inhibitor of metalloproteinase 1, 2, 3 expression in response to mechanical loading of cartilage explants in vitro. *Archives of Biochemistry and Biophysics,* 410**,** 39-47.

FITZGERALD, J. B., JIN, M., DEAN, D., WOOD, D. J., ZHENG, M. H. & GRODZINSKY, A. J. 2004. Mechanical compression of cartilage explants induces multiple time-dependent gene expression patterns and involves intracellular calcium and cyclic AMP. *J Biol Chem,* 279**,** 19502-11.

FITZGERALD, J. B., JIN, M. & GRODZINSKY, A. J. 2006. Shear and compression differentially regulate clusters of functionally related temporal transcription patterns in cartilage tissue. *J Biol Chem,* 281**,** 24095-103.

FUJISAWA, T., HATTORI, T., TAKAHASHI, K., KUBOKI, T., YAMASHITA, A. & TAKIGAWA, M. 1999. Cyclic mechanical stress induces extracellular matrix degradation in cultured chondrocytes via gene expression of matrix metalloproteinases and interleukin-1. *J Biochem,* 125**,** 966-75.

FUKUDA, K., ASADA, S., KUMANO, F., SAITOH, M., OTANI, K. & TANAKA, S. 1997. Cyclic tensile stretch on bovine articular chondrocytes inhibits protein

kinase C activity. *The Journal of laboratory and clinical medicine,* 130**,** 209-215.
FUNCK-BRENTANO, T., BOUAZIZ, W., MARTY, C., GEOFFROY, V., HAY, E. & COHEN-SOLAL, M. 2014. Dkk1-mediated inhibition of Wnt signaling in bone ameliorates osteoarthritis. *Arthritis Rheumatol*.
GANEA, E., TRIFAN, M., LASLO, A. C., PUTINA, G. & CRISTESCU, C. 2007. Matrix metalloproteinases: useful and deleterious. *Biochem Soc Trans,* 35**,** 689-91.
GARVICAN, E. R., VAUGHAN-THOMAS, A., CLEGG, P. D. & INNES, J. F. 2010. Biomarkers of cartilage turnover. Part 2: Non-collagenous markers. *Vet J,* 185**,** 43-9.
GELSE, K., POSCHL, E. & AIGNER, T. 2003. Collagens--structure, function, and biosynthesis. *Adv Drug Deliv Rev,* 55**,** 1531-46.
GLARE, E. M., DIVJAK, M., BAILEY, M. J. & WALTERS, E. H. 2002. beta-Actin and GAPDH housekeeping gene expression in asthmatic airways is variable and not suitable for normalising mRNA levels. *Thorax,* 57**,** 765-70.
GOLDRING, M. B. & MARCU, K. B. 2009. Cartilage homeostasis in health and rheumatic diseases. *Arthritis Res Ther,* 11**,** 224.
GORDON, M. D. & NUSSE, R. 2006. Wnt signaling: multiple pathways, multiple receptors, and multiple transcription factors. *J Biol Chem,* 281**,** 22429-33.
GREENBLATT, M. B., RITTER, S. Y., WRIGHT, J., TSANG, K., HU, D., GLIMCHER, L. H. & ALIPRANTIS, A. O. 2013. NFATc1 and NFATc2 repress spontaneous osteoarthritis. *Proc Natl Acad Sci U S A,* 110**,** 19914-9.
GRUMOLATO, L., LIU, G., MONG, P., MUDBHARY, R., BISWAS, R., ARROYAVE, R., VIJAYAKUMAR, S., ECONOMIDES, A. N. & AARONSON, S. A. 2010. Canonical and noncanonical Wnts use a common mechanism to activate completely unrelated coreceptors. *Genes Dev,* 24**,** 2517-30.
GUILAK, F. 1995. Compression-induced changes in the shape and volume of the chondrocyte nucleus. *J Biomech,* 28**,** 1529-41.
GUILAK, F., ERICKSON, G. R. & TING-BEALL, H. P. 2002. The effects of osmotic stress on the viscoelastic and physical properties of articular chondrocytes. *Biophys J,* 82**,** 720-7.
GUILAK, F., RATCLIFFE, A. & MOW, V. C. 1995. Chondrocyte deformation and local tissue strain in articular cartilage: a confocal microscopy study. *J Orthop Res,* 13**,** 410-21.
GUILAK, F., ZELL, R. A., ERICKSON, G. R., GRANDE, D. A., RUBIN, C. T., MCLEOD, K. J. & DONAHUE, H. J. 1999. Mechanically induced calcium waves in articular chondrocytes are inhibited by gadolinium and amiloride. *J Orthop Res,* 17**,** 421-9.
GUO, X., DAY, T. F., JIANG, X., GARRETT-BEAL, L., TOPOL, L. & YANG, Y. 2004. Wnt/beta-catenin signaling is sufficient and necessary for synovial joint formation. *Genes Dev,* 18**,** 2404-17.
GUO, X., MAK, K. K., TAKETO, M. M. & YANG, Y. 2009. The Wnt/beta-catenin pathway interacts differentially with PTHrP signaling to control chondrocyte hypertrophy and final maturation. *PLoS One,* 4**,** e6067.
GUTERL, C. C., GARDNER, T. R., RAJAN, V., AHMAD, C. S., HUNG, C. T. & ATESHIAN, G. A. 2009. Two-dimensional strain fields on the cross-section of the human patellofemoral joint under physiological loading. *J Biomech,* 42**,** 1275-81.
HAAPALA, J., AROKOSKI, J. P., HYTTINEN, M. M., LAMMI, M., TAMMI, M., KOVANEN, V., HELMINEN, H. J. & KIVIRANTA, I. 1999. Remobilization does

not fully restore immobilization induced articular cartilage atrophy. *Clin Orthop Relat Res*, 218-29.
HABAS, R. & DAWID, I. B. 2005. Dishevelled and Wnt signaling: is the nucleus the final frontier? *J Biol,* 4, 2.
HABAS, R., KATO, Y. & HE, X. 2001. Wnt/Frizzled activation of Rho regulates vertebrate gastrulation and requires a novel Formin homology protein Daam1. *Cell,* 107, 843-54.
HAGIWARA, H., SCHROTER-KERMANI, C. & MERKER, H. J. 1993. Localization of collagen type VI in articular cartilage of young and adult mice. *Cell Tissue Res,* 272, 155-60.
HAN, Z., CHANG, L., YAMANISHI, Y., KARIN, M. & FIRESTEIN, G. S. 2002. Joint damage and inflammation in c-Jun N-terminal kinase 2 knockout mice with passive murine collagen-induced arthritis. *Arthritis & Rheumatism,* 46, 818-823.
HARTMANN, C. 2002. Wnt-signaling and skeletogenesis. *J Musculoskelet Neuronal Interact,* 2, 274-6.
HARTMANN, C. & TABIN, C. J. 2000. Dual roles of Wnt signaling during chondrogenesis in the chicken limb. *Development,* 127, 3141-59.
HARTMANN, C. & TABIN, C. J. 2001. Wnt-14 plays a pivotal role in inducing synovial joint formation in the developing appendicular skeleton. *Cell,* 104, 341-51.
HAUDENSCHILD, D. R., D'LIMA, D. D. & LOTZ, M. K. 2008a. Dynamic compression of chondrocytes induces a Rho kinase-dependent reorganization of the actin cytoskeleton. *Biorheology,* 45, 219-28.
HAUDENSCHILD, D. R., NGUYEN, B., CHEN, J., D'LIMA, D. D. & LOTZ, M. K. 2008b. Rho kinase-dependent CCL20 induced by dynamic compression of human chondrocytes. *Arthritis Rheum,* 58, 2735-42.
HAUSELMANN, H. J., FERNANDES, R. J., MOK, S. S., SCHMID, T. M., BLOCK, J. A., AYDELOTTE, M. B., KUETTNER, K. E. & THONAR, E. J. 1994. Phenotypic stability of bovine articular chondrocytes after long-term culture in alginate beads. *J Cell Sci,* 107 (Pt 1), 17-27.
HEINEGARD, D. 2009. Proteoglycans and more--from molecules to biology. *Int J Exp Pathol,* 90, 575-86.
HEINEGARD, D. & SAXNE, T. 2011. The role of the cartilage matrix in osteoarthritis. *Nat Rev Rheumatol,* 7, 50-6.
HELMINEN, H. J. 1987. *Joint loading: biology and health of articular structures*, Wright.
HIROSE, J., MASUDA, I. & RYAN, L. M. 2000. Expression of cartilage intermediate layer protein/nucleotide pyrophosphohydrolase parallels the production of extracellular inorganic pyrophosphate in response to growth factors and with aging. *Arthritis Rheum,* 43, 2703-11.
HOANG, B., MOOS, M., JR., VUKICEVIC, S. & LUYTEN, F. P. 1996. Primary structure and tissue distribution of FRZB, a novel protein related to Drosophila frizzled, suggest a role in skeletal morphogenesis. *J Biol Chem,* 271, 26131-7.
HODGE, W. A., FIJAN, R. S., CARLSON, K. L., BURGESS, R. G., HARRIS, W. H. & MANN, R. W. 1986. Contact pressures in the human hip joint measured in vivo. *Proc Natl Acad Sci U S A,* 83, 2879-83.
HONDA, K., OHNO, S., TANIMOTO, K., IJUIN, C., TANAKA, N., DOI, T., KATO, Y. & TANNE, K. 2000. The effects of high magnitude cyclic tensile load on

cartilage matrix metabolism in cultured chondrocytes. *Eur J Cell Biol,* 79**,** 601-9.
HU, G., WANG, K., GROENENDYK, J., BARAKAT, K., MIZIANTY, M. J., RUAN, J., MICHALAK, M. & KURGAN, L. 2014. Human structural proteome-wide characterization of Cyclosporine A targets. *Bioinformatics*.
HUANG, C. Y. C., REUBEN, P. M. & CHEUNG, H. S. 2005. Temporal Expression Patterns and Corresponding Protein Inductions of Early Responsive Genes in Rabbit Bone Marrow–Derived Mesenchymal Stem Cells Under Cyclic Compressive Loading. *STEM CELLS,* 23**,** 1113-1121.
HUANG, J., BALLOU, L. R. & HASTY, K. A. 2007. Cyclic equibiaxial tensile strain induces both anabolic and catabolic responses in articular chondrocytes. *Gene,* 404**,** 101-109.
HUANG, T., XIE, Z., WANG, J., LI, M., JING, N. & LI, L. 2011. Nuclear factor of activated T cells (NFAT) proteins repress canonical Wnt signaling via its interaction with Dishevelled (Dvl) protein and participate in regulating neural progenitor cell proliferation and differentiation. *J Biol Chem,* 286**,** 37399-405.
HWANG, S. G., YU, S. S., LEE, S. W. & CHUN, J. S. 2005. Wnt-3a regulates chondrocyte differentiation via c-Jun/AP-1 pathway. *FEBS Lett,* 579**,** 4837-42.
IM, G. I. & QUAN, Z. 2010. The effects of Wnt inhibitors on the chondrogenesis of human mesenchymal stem cells. *Tissue Eng Part A,* 16**,** 2405-13.
IRIANTO, J., RAMASWAMY, G., SERRA, R. & KNIGHT, M. M. 2014. Depletion of chondrocyte primary cilia reduces the compressive modulus of articular cartilage. *Journal of Biomechanics,* 47**,** 579-582.
ITALIANO, A., CHEN, C. L., SUNG, Y. S., SINGER, S., DEMATTEO, R. P., LAQUAGLIA, M. P., BESMER, P., SOCCI, N. & ANTONESCU, C. R. 2012. SDHA loss of function mutations in a subset of young adult wild-type gastrointestinal stromal tumors. *BMC Cancer,* 12**,** 408.
IWAKURA, T., INUI, A. & REDDI, A. H. 2013. Stimulation of superficial zone protein accumulation by hedgehog and Wnt signaling in surface zone bovine articular chondrocytes. *Arthritis Rheum,* 65**,** 408-17.
JAHN, K., STRUPP, M., SCHNEIDER, E., DIETERICH, M. & BRANDT, T. 2000. Differential effects of vestibular stimulation on walking and running. *Neuroreport,* 11**,** 1745-8.
JIN, M., FRANK, E. H., QUINN, T. M., HUNZIKER, E. B. & GRODZINSKY, A. J. 2001. Tissue shear deformation stimulates proteoglycan and protein biosynthesis in bovine cartilage explants. *Arch Biochem Biophys,* 395**,** 41-8.
JONES, A. R. C., GLEGHORN, J. P., HUGHES, C. E., FITZ, L. J., ZOLLNER, R., WAINWRIGHT, S. D., CATERSON, B., MORRIS, E. A., BONASSAR, L. J. & FLANNERY, C. R. 2007. Binding and localization of recombinant lubricin to articular cartilage surfaces. *Journal of Orthopaedic Research,* 25**,** 283-292.
JORTIKKA, M. O., INKINEN, R. I., TAMMI, M. I., PARKKINEN, J. J., HAAPALA, J., KIVIRANTA, I., HELMINEN, H. J. & LAMMI, M. J. 1997. Immobilisation causes longlasting matrix changes both in the immobilised and contralateral joint cartilage. *Ann Rheum Dis,* 56**,** 255-61.
JULKUNEN, P., IIVARINEN, J., BRAMA, P. A., AROKOSKI, J., JURVELIN, J. S. & HELMINEN, H. J. 2010. Maturation of collagen fibril network structure in tibial and femoral cartilage of rabbits. *Osteoarthritis Cartilage,* 18**,** 406-15.
JURVELIN, J., KIVIRANTA, I., TAMMI, M. & HELMINEN, H. J. 1986. Effect of physical exercise on indentation stiffness of articular cartilage in the canine knee. *Int J Sports Med,* 7**,** 106-10.

KAMINENI, S., WANI, Z., LUO, Z.-P., RURIKO, Y. & AN, K.-N. 2012. Chondrocyte response to tensile and compressive cyclic loading modalities. *Journal of Musculoskeletal Research,* 15.
KANBE, K., YANG, X., WEI, L., SUN, C. & CHEN, Q. 2007. Pericellular matrilins regulate activation of chondrocytes by cyclic load-induced matrix deformation. *J Bone Miner Res,* 22**,** 318-28.
KANG, T. H., PARK, Y., BADER, J. S. & FRIEDMANN, T. 2013. The housekeeping gene hypoxanthine guanine phosphoribosyltransferase (HPRT) regulates multiple developmental and metabolic pathways of murine embryonic stem cell neuronal differentiation. *PLoS One,* 8**,** e74967.
KASHIWAGI, M., ENGHILD, J. J., GENDRON, C., HUGHES, C., CATERSON, B., ITOH, Y. & NAGASE, H. 2004. Altered proteolytic activities of ADAMTS-4 expressed by C-terminal processing. *J Biol Chem,* 279**,** 10109-19.
KAWAKAMI, Y., WADA, N., NISHIMATSU, S. I., ISHIKAWA, T., NOJI, S. & NOHNO, T. 1999. Involvement of Wnt-5a in chondrogenic pattern formation in the chick limb bud. *Dev Growth Differ,* 41**,** 29-40.
KERR, A. P. D. 2010. *Introductory biomechanics,* Edinburgh, Churchill Livingstone.
KESTLER, H. A. & KUHL, M. 2008. From individual Wnt pathways towards a Wnt signalling network. *Philos Trans R Soc Lond B Biol Sci,* 363**,** 1333-47.
KIANI, C., CHEN, L., WU, Y. J., YEE, A. J. & YANG, B. B. 2002. Structure and function of aggrecan. *Cell Res,* 12**,** 19-32.
KIM, W., KIM, M. & JHO, E. H. 2013. Wnt/beta-catenin signalling: from plasma membrane to nucleus. *Biochem J,* 450**,** 9-21.
KIRALY, K., HYTTINEN, M. M., PARKKINEN, J. J., AROKOSKI, J. A., LAPVETELAINEN, T., TORRONEN, K., KIVIRANTA, I. & HELMINEN, H. J. 1998. Articular cartilage collagen birefringence is altered concurrent with changes in proteoglycan synthesis during dynamic in vitro loading. *Anat Rec,* 251**,** 28-36.
KISIDAY, J. D., KURZ, B., DIMICCO, M. A. & GRODZINSKY, A. J. 2005. Evaluation of medium supplemented with insulin-transferrin-selenium for culture of primary bovine calf chondrocytes in three-dimensional hydrogel scaffolds. *Tissue Eng,* 11**,** 141-51.
KITAGAKI, J., IWAMOTO, M., LIU, J. G., TAMAMURA, Y., PACIFCI, M. & ENOMOTO-IWAMOTO, M. 2003. Activation of β–catenin-LEF/TCF signal pathway in chondrocytes stimulates ectopic endochondral ossification. *Osteoarthritis and Cartilage,* 11**,** 36-43.
KIVIRANTA, I., JURVELIN, J., TAMMI, M., SAAMANEN, A. M. & HELMINEN, H. J. 1987. Weight bearing controls glycosaminoglycan concentration and articular cartilage thickness in the knee joints of young beagle dogs. *Arthritis Rheum,* 30**,** 801-9.
KIVIRANTA, I., TAMMI, M., JURVELIN, J., SAAMANEN, A. M. & HELMINEN, H. J. 1988. Moderate running exercise augments glycosaminoglycans and thickness of articular cartilage in the knee joint of young beagle dogs. *J Orthop Res,* 6**,** 188-95.
KLATT, A. R., BECKER, A. K., NEACSU, C. D., PAULSSON, M. & WAGENER, R. 2011. The matrilins: modulators of extracellular matrix assembly. *Int J Biochem Cell Biol,* 43**,** 320-30.
KNIGHT, M. M., TOYODA, T., LEE, D. A. & BADER, D. L. 2006. Mechanical compression and hydrostatic pressure induce reversible changes in actin cytoskeletal organisation in chondrocytes in agarose. *J Biomech,* 39**,** 1547-51.

KOH, J. Y. & CHOI, D. W. 1987. Quantitative determination of glutamate mediated cortical neuronal injury in cell culture by lactate dehydrogenase efflux assay. *J Neurosci Methods,* 20**,** 83-90.
KOMIYA, Y. & HABAS, R. 2008. Wnt signal transduction pathways. *Organogenesis,* 4**,** 68-75.
KORVER, T. H., VAN DE STADT, R. J., KILJAN, E., VAN KAMPEN, G. P. & VAN DER KORST, J. K. 1992. Effects of loading on the synthesis of proteoglycans in different layers of anatomically intact articular cartilage in vitro. *J Rheumatol,* 19**,** 905-12.
KOZERA, B. & RAPACZ, M. 2013. Reference genes in real-time PCR. *J Appl Genet,* 54**,** 391-406.
KUHL, M., SHELDAHL, L. C., MALBON, C. C. & MOON, R. T. 2000. Ca(2+)/calmodulin-dependent protein kinase II is stimulated by Wnt and Frizzled homologs and promotes ventral cell fates in Xenopus. *J Biol Chem,* 275**,** 12701-11.
KUMAR, P., OKA, M., TOGUCHIDA, J., KOBAYASHI, M., UCHIDA, E., NAKAMURA, T. & TANAKA, K. 2001. Role of uppermost superficial surface layer of articular cartilage in the lubrication mechanism of joints. *J Anat,* 199**,** 241-50.
KURZ, B., JIN, M., PATWARI, P., CHENG, D. M., LARK, M. W. & GRODZINSKY, A. J. 2001. Biosynthetic response and mechanical properties of articular cartilage after injurious compression. *J Orthop Res,* 19**,** 1140-6.
KURZ, B., LEMKE, A. K., FAY, J., PUFE, T., GRODZINSKY, A. J. & SCHUNKE, M. 2005. Pathomechanisms of cartilage destruction by mechanical injury. *Ann Anat,* 187**,** 473-85.
LAU, K. H., BAYLINK, D. J., ZHOU, X. D., RODRIGUEZ, D., BONEWALD, L. F., LI, Z., RUFFONI, D., MULLER, R., KESAVAN, C. & SHENG, M. H. 2013. Osteocyte-derived insulin-like growth factor I is essential for determining bone mechanosensitivity. *Am J Physiol Endocrinol Metab,* 305**,** E271-81.
LEASK, A. 2011. Will o' the wisp: CCN4 as a novel molecular target in osteoarthritis. *Journal of Cell Communication and Signaling,* 5**,** 51-52.
LEE, C., GRAD, S., WIMMER, M. & ALINI, M. 2005a. The influence of mechanical stimuli on articular cartilage tissue engineering. *Topics in tissue engineering,* 2**,** 1-32.
LEE, D. A. & BADER, D. L. 1997. Compressive strains at physiological frequencies influence the metabolism of chondrocytes seeded in agarose. *Journal of Orthopaedic Research,* 15**,** 181-188.
LEE, D. A., KNIGHT, M. M., BOLTON, J. F., IDOWU, B. D., KAYSER, M. V. & BADER, D. L. 2000. Chondrocyte deformation within compressed agarose constructs at the cellular and sub-cellular levels. *J Biomech,* 33**,** 81-95.
LEE, D. A., NOGUCHI, T., KNIGHT, M. M., O'DONNELL, L., BENTLEY, G. & BADER, D. L. 1998. Response of chondrocyte subpopulations cultured within unloaded and loaded agarose. *J Orthop Res,* 16**,** 726-33.
LEE, H. S., MILLWARD-SADLER, S. J., WRIGHT, M. O., NUKI, G., AL-JAMAL, R. & SALTER, D. M. 2002. Activation of Integrin-RACK1/PKCalpha signalling in human articular chondrocyte mechanotransduction. *Osteoarthritis Cartilage,* 10**,** 890-7.
LEE, J. H., FITZGERALD, J. B., DIMICCO, M. A. & GRODZINSKY, A. J. 2005b. Mechanical injury of cartilage explants causes specific time-dependent changes in chondrocyte gene expression. *Arthritis Rheum,* 52**,** 2386-95.

LEIJTEN, J. C., EMONS, J., STICHT, C., VAN GOOL, S., DECKER, E., UITTERLINDEN, A., RAPPOLD, G., HOFMAN, A., RIVADENEIRA, F., SCHERJON, S., WIT, J. M., VAN MEURS, J., VAN BLITTERSWIJK, C. A. & KARPERIEN, M. 2012. Gremlin 1, frizzled-related protein, and Dkk-1 are key regulators of human articular cartilage homeostasis. *Arthritis Rheum,* 64**,** 3302-12.

LEONG, D. J., HARDIN, J. A., COBELLI, N. J. & SUN, H. B. 2011a. Mechanotransduction and cartilage integrity. *Annals of the New York Academy of Sciences,* 1240**,** 32-37.

LEONG, D. J., LI, Y. H., GU, X. I., SUN, L., ZHOU, Z., NASSER, P., LAUDIER, D. M., IQBAL, J., MAJESKA, R. J., SCHAFFLER, M. B., GOLDRING, M. B., CARDOSO, L., ZAIDI, M. & SUN, H. B. 2011b. Physiological loading of joints prevents cartilage degradation through CITED2. *FASEB J,* 25**,** 182-91.

LI, R., BEEBE, T., JEN, N., YU, F., TAKABE, W., HARRISON, M., CAO, H., LEE, J., YANG, H., HAN, P., WANG, K., SHIMIZU, H., CHEN, J., LIEN, C. L., CHI, N. C. & HSIAI, T. K. 2014. Shear stress-activated wnt-angiopoietin-2 signaling recapitulates vascular repair in zebrafish embryos. *Arterioscler Thromb Vasc Biol,* 34**,** 2268-75.

LI, S., ESTERBERG, R., LACHANCE, V., REN, D., RADDE-GALLWITZ, K., CHI, F., PARENT, J.-L., FRITZ, A. & CHEN, P. 2011a. Rack1 is required for Vangl2 membrane localization and planar cell polarity signaling while attenuating canonical Wnt activity. *Proceedings of the National Academy of Sciences,* 108**,** 2264-2269.

LI, S., JIA, X., DUANCE, V. C. & BLAIN, E. J. 2011b. The effects of cyclic tensile strain on the organisation and expression of cytoskeletal elements in bovine intervertebral disc cells: an in vitro study. *Eur Cell Mater,* 21**,** 508-22.

LI, Y., LU, W., KING, T. D., LIU, C. C., BIJUR, G. N. & BU, G. 2010. Dkk1 stabilizes Wnt co-receptor LRP6: implication for Wnt ligand-induced LRP6 down-regulation. *PLoS One,* 5**,** e11014.

LI, Y., RANKIN, S. A., SINNER, D., KENNY, A. P., KRIEG, P. A. & ZORN, A. M. 2008. Sfrp5 coordinates foregut specification and morphogenesis by antagonizing both canonical and noncanonical Wnt11 signaling. *Genes Dev,* 22**,** 3050-63.

LIANG, P., GUO, Y., ZHOU, X. & GAO, X. 2014. Expression profiling in Bemisia tabaci under insecticide treatment: indicating the necessity for custom reference gene selection. *PLoS One,* 9**,** e87514.

LITTLE, C. B., HUGHES, C. E., CURTIS, C. L., JONES, S. A., CATERSON, B. & FLANNERY, C. R. 2002. Cyclosporin A inhibition of aggrecanase-mediated proteoglycan catabolism in articular cartilage. *Arthritis & Rheumatism,* 46**,** 124-129.

LIVAK, K. J. & SCHMITTGEN, T. D. 2001. Analysis of relative gene expression data using real-time quantitative PCR and the 2(-Delta Delta C(T)) Method. *Methods,* 25**,** 402-8.

LOENING, A. M., JAMES, I. E., LEVENSTON, M. E., BADGER, A. M., FRANK, E. H., KURZ, B., NUTTALL, M. E., HUNG, H.-H., BLAKE, S. M., GRODZINSKY, A. J. & LARK, M. W. 2000. Injurious Mechanical Compression of Bovine Articular Cartilage Induces Chondrocyte Apoptosis. *Archives of Biochemistry and Biophysics,* 381**,** 205-212.

LOESER, R. F. 2014. Integrins and chondrocyte-matrix interactions in articular cartilage. *Matrix Biol*.

LOGAN, C. Y. & NUSSE, R. 2004. THE WNT SIGNALING PATHWAY IN DEVELOPMENT AND DISEASE. *Annual Review of Cell and Developmental Biology,* 20**,** 781-810.

LORIES, R. J., CORR, M. & LANE, N. E. 2013. To Wnt or not to Wnt: the bone and joint health dilemma. *Nat Rev Rheumatol,* 9**,** 328-39.

LORIES, R. J., PEETERS, J., BAKKER, A., TYLZANOWSKI, P., DERESE, I., SCHROOTEN, J., THOMAS, J. T. & LUYTEN, F. P. 2007. Articular cartilage and biomechanical properties of the long bones in Frzb-knockout mice. *Arthritis Rheum,* 56**,** 4095-103.

LOUGHLIN, J., DOWLING, B., CHAPMAN, K., MARCELLINE, L., MUSTAFA, Z., SOUTHAM, L., FERREIRA, A., CIESIELSKI, C., CARSON, D. A. & CORR, M. 2004. Functional variants within the secreted frizzled-related protein 3 gene are associated with hip osteoarthritis in females. *Proc Natl Acad Sci U S A,* 101**,** 9757-62.

LUO, J., CHEN, J., DENG, Z. L., LUO, X., SONG, W. X., SHARFF, K. A., TANG, N., HAYDON, R. C., LUU, H. H. & HE, T. C. 2007. Wnt signaling and human diseases: what are the therapeutic implications? *Lab Invest,* 87**,** 97-103.

MACDONALD, B. T., TAMAI, K. & HE, X. 2009. Wnt/beta-catenin signaling: components, mechanisms, and diseases. *Dev Cell,* 17**,** 9-26.

MACKIE, E. J., AHMED, Y. A., TATARCZUCH, L., CHEN, K. S. & MIRAMS, M. 2008. Endochondral ossification: How cartilage is converted into bone in the developing skeleton. *The International Journal of Biochemistry & Cell Biology,* 40**,** 46-62.

MADEJ, W., VAN CAAM, A., BLANEY DAVIDSON, E. N., VAN DER KRAAN, P. M. & BUMA, P. 2014. Physiological and excessive mechanical compression of articular cartilage activates Smad2/3P signaling. *Osteoarthritis and Cartilage,* 22**,** 1018-1025.

MAO, B., WU, W., DAVIDSON, G., MARHOLD, J., LI, M., MECHLER, B. M., DELIUS, H., HOPPE, D., STANNEK, P., WALTER, C., GLINKA, A. & NIEHRS, C. 2002. Kremen proteins are Dickkopf receptors that regulate Wnt/beta-catenin signalling. *Nature,* 417**,** 664-7.

MAROUDAS, A. 1976. Balance between swelling pressure and collagen tension in normal and degenerate cartilage. *Nature,* 260**,** 808-809.

MARTIN, J. A. & BUCKWALTER, J. A. 1998. Effects of fibronectin on articular cartilage chondrocyte proteoglycan synthesis and response to insulin-like growth factor-I. *Journal of Orthopaedic Research,* 16**,** 752-757.

MATUSEK, T., DJIANE, A., JANKOVICS, F., BRUNNER, D., MLODZIK, M. & MIHALY, J. 2006. The Drosophila formin DAAM regulates the tracheal cuticle pattern through organizing the actin cytoskeleton. *Development,* 133**,** 957-66.

MAUCK, R. L., SOLTZ, M. A., WANG, C. C., WONG, D. D., CHAO, P. H., VALHMU, W. B., HUNG, C. T. & ATESHIAN, G. A. 2000. Functional tissue engineering of articular cartilage through dynamic loading of chondrocyte-seeded agarose gels. *J Biomech Eng,* 122**,** 252-60.

MAWATARI, T., LINDSEY, D. P., HARRIS, A. H., GOODMAN, S. B., MALONEY, W. J. & SMITH, R. L. 2010. Effects of tensile strain and fluid flow on osteoarthritic human chondrocyte metabolism in vitro. *J Orthop Res,* 28**,** 907-13.

MELROSE, J. & WHITELOCK, J. M. 2006. Extracellular Matrix. *Wiley Encyclopedia of Biomedical Engineering.* John Wiley & Sons, Inc.

METCALFE, C., MENDOZA-TOPAZ, C., MIESZCZANEK, J. & BIENZ, M. 2010. Stability elements in the LRP6 cytoplasmic tail confer efficient signalling upon DIX-dependent polymerization. *J Cell Sci,* 123**,** 1588-99.

MICLEA, R. L., SIEBELT, M., FINOS, L., GOEMAN, J. J., LOWIK, C. W., OOSTDIJK, W., WEINANS, H., WIT, J. M., ROBANUS-MAANDAG, E. C. & KARPERIEN, M. 2011. Inhibition of Gsk3beta in cartilage induces osteoarthritic features through activation of the canonical Wnt signaling pathway. *Osteoarthritis Cartilage,* 19**,** 1363-72.

MII, Y. & TAIRA, M. 2011. Secreted Wnt "inhibitors" are not just inhibitors: regulation of extracellular Wnt by secreted Frizzled-related proteins. *Dev Growth Differ,* 53**,** 911-23.

MILLWARD-SADLER, S. & SALTER, D. 2004. Integrin-dependent signal cascades in chondrocyte mechanotransduction. *Annals of biomedical engineering,* 32**,** 435-446.

MILLWARD-SADLER, S. J., WRIGHT, M. O., DAVIES, L. W., NUKI, G. & SALTER, D. M. 2000. Mechanotransduction via integrins and interleukin-4 results in altered aggrecan and matrix metalloproteinase 3 gene expression in normal, but not osteoarthritic, human articular chondrocytes. *Arthritis Rheum,* 43**,** 2091-9.

MIN, J. L., MEULENBELT, I., RIYAZI, N., KLOPPENBURG, M., HOUWING-DUISTERMAAT, J. J., SEYMOUR, A. B., POLS, H. A., VAN DUIJN, C. M. & SLAGBOOM, P. E. 2005. Association of the Frizzled-related protein gene with symptomatic osteoarthritis at multiple sites. *Arthritis Rheum,* 52**,** 1077-80.

MOLLENHAUER, J., MOK, M. T., KING, K. B., GUPTA, M., CHUBINSKAYA, S., KOEPP, H. & COLE, A. A. 1999. Expression of anchorin CII (cartilage annexin V) in human young, normal adult, and osteoarthritic cartilage. *J Histochem Cytochem,* 47**,** 209-20.

MOW, V. & HUNG, C. 2001. Chapter 3: Biomechanics of articular cartilage. *In:* NORDIN, M. & FRANKLIN, V. (eds.) *Basic biomechanics of the musculoskeletal system.* 3rd ed.: Lippincott Williams & Wilkins.

MOW, V. & RATCLIFFE, A. 1997. Structure and function of articular cartilage and meniscus. *In:* MOW, V. & HAYES, W. (eds.) *Basic Orthopaedic Biomechanics.* 2 ed.: Lippincott-Raven.

MUKHOPADHYAY, M., SHTROM, S., RODRIGUEZ-ESTEBAN, C., CHEN, L., TSUKUI, T., GOMER, L., DORWARD, D. W., GLINKA, A., GRINBERG, A., HUANG, S. P., NIEHRS, C., IZPISUA BELMONTE, J. C. & WESTPHAL, H. 2001. Dickkopf1 is required for embryonic head induction and limb morphogenesis in the mouse. *Dev Cell,* 1**,** 423-34.

MURAD, S., GROVE, D., LINDBERG, K. A., REYNOLDS, G., SIVARAJAH, A. & PINNELL, S. R. 1981. Regulation of collagen synthesis by ascorbic acid. *Proc Natl Acad Sci U S A,* 78**,** 2879-82.

MURPHY, G. 2011. Tissue inhibitors of metalloproteinases. *Genome Biol,* 12**,** 233.

MURPHY, G., KNAUPER, V., ATKINSON, S., BUTLER, G., ENGLISH, W., HUTTON, M., STRACKE, J. & CLARK, I. 2002. Matrix metalloproteinases in arthritic disease. *Arthritis Res,* 4 Suppl 3**,** S39-49.

MURPHY, G. & NAGASE, H. 2008. Progress in matrix metalloproteinase research. *Mol Aspects Med,* 29**,** 290-308.

NAGASE, H. & KASHIWAGI, M. 2003. Aggrecanases and cartilage matrix degradation. *Arthritis Res Ther,* 5**,** 94-103.

NAGASE, H., VISSE, R. & MURPHY, G. 2006. Structure and function of matrix metalloproteinases and TIMPs. *Cardiovasc Res,* 69**,** 562-73.
NAKAMURA, Y., WAKITANI, S., SAITO, N. & TAKAOKA, K. 2005. Expression profiles of BMP-related molecules induced by BMP-2 or -4 in muscle-derived primary culture cells. *J Bone Miner Metab,* 23**,** 426-34.
NAKOPOULOU, L., MYLONA, E., PAPADAKI, I., KAVANTZAS, N., GIANNOPOULOU, I., MARKAKI, S. & KERAMOPOULOS, A. 2006. Study of phospho-[beta]-catenin subcellular distribution in invasive breast carcinomas in relation to their phenotype and the clinical outcome. *Mod Pathol,* 19**,** 556-563.
NALESSO, G., SHERWOOD, J., BERTRAND, J., PAP, T., RAMACHANDRAN, M., DE BARI, C., PITZALIS, C. & DELL'ACCIO, F. 2011. WNT-3A modulates articular chondrocyte phenotype by activating both canonical and noncanonical pathways. *J Cell Biol,* 193**,** 551-64.
NEU, C. P., KHALAFI, A., KOMVOPOULOS, K., SCHMID, T. M. & REDDI, A. H. 2007. Mechanotransduction of bovine articular cartilage superficial zone protein by transforming growth factor beta signaling. *Arthritis Rheum,* 56**,** 3706-14.
NEWBERRY, E. P., WILLIS, D., LATIFI, T., BOUDREAUX, J. M. & TOWLER, D. A. 1997. Fibroblast growth factor receptor signaling activates the human interstitial collagenase promoter via the bipartite Ets-AP1 element. *Mol Endocrinol,* 11**,** 1129-44.
NICODEMUS, G. D. & BRYANT, S. J. 2010. Mechanical loading regimes affect the anabolic and catabolic activities by chondrocytes encapsulated in PEG hydrogels. *Osteoarthritis Cartilage,* 18**,** 126-37.
NUKI, G. & SALTER, D. 2007. The impact of mechanical stress on the pathophysiology of osteoarthritis. *Osteoarthritis: a companion to rheumatology. Philadelphia: Mosby***,** 33-52.
NUSSE, R. 2005. Wnt signaling in disease and in development. *Cell Res,* 15**,** 28-32.
O'KEEFFE, S. A., HOGAN, B. A., EUSTACE, S. J. & KAVANAGH, E. C. 2009. Overuse Injuries of the Knee. *Magnetic Resonance Imaging Clinics of North America,* 17**,** 725-739.
OEGEMA, T. R., CARPENTER, R. J., HOFMEISTER, F. & THOMPSON, R. C. 1997. The interaction of the zone of calcified cartilage and subchondral bone in osteoarthritis. *Microscopy Research and Technique,* 37**,** 324-332.
OH, H., CHUN, C. H. & CHUN, J. S. 2012. Dkk-1 expression in chondrocytes inhibits experimental osteoarthritic cartilage destruction in mice. *Arthritis Rheum,* 64**,** 2568-78.
OTTERNESS, I. G., ESKRA, J. D., BLIVEN, M. L., SHAY, A. K., PELLETIER, J. P. & MILICI, A. J. 1998. Exercise protects against articular cartilage degeneration in the hamster. *Arthritis Rheum,* 41**,** 2068-76.
PALMOSKI, M. J. & BRANDT, K. D. 1981. Running inhibits the reversal of atrophic changes in canine knee cartilage after removal of a leg cast. *Arthritis & Rheumatism,* 24**,** 1329-1337.
PALMOSKI, M. J., COLYER, R. A. & BRANDT, K. D. 1980. Joint motion in the absence of normal loading does not maintain normal articular cartilage. *Arthritis Rheum,* 23**,** 325-34.
PARKKINEN, J. J., LAMMI, M. J., INKINEN, R., JORTIKKA, M., TAMMI, M., VIRTANEN, I. & HELMINEN, H. J. 1995. Influence of short-term hydrostatic

pressure on organization of stress fibers in cultured chondrocytes. *J Orthop Res,* 13**,** 495-502.
PATWARI, P., COOK, M. N., DIMICCO, M. A., BLAKE, S. M., JAMES, I. E., KUMAR, S., COLE, A. A., LARK, M. W. & GRODZINSKY, A. J. 2003. Proteoglycan degradation after injurious compression of bovine and human articular cartilage in vitro: interaction with exogenous cytokines. *Arthritis Rheum,* 48**,** 1292-301.
PEARLE, A. D., WARREN, R. F. & RODEO, S. A. 2005. Basic science of articular cartilage and osteoarthritis. *Clin Sports Med,* 24**,** 1-12.
PERERA, P., WYPASEK, E., MADHAVAN, S., RATH-DESCHNER, B., LIU, J., NAM, J., RATH, B., HUANG, Y., DESCHNER, J., PIESCO, N., WU, C. & AGARWAL, S. 2010. Mechanical signals control SOX-9, VEGF, and c-Myc expression and cell proliferation during inflammation via integrin-linked kinase, B-Raf, and ERK1/2-dependent signaling in articular chondrocytes. *Arthritis Research & Therapy,* 12**,** R106.
PINGGUAN-MURPHY, B., EL-AZZEH, M., BADER, D. L. & KNIGHT, M. M. 2006. Cyclic compression of chondrocytes modulates a purinergic calcium signalling pathway in a strain rate- and frequency-dependent manner. *J Cell Physiol,* 209**,** 389-97.
PREMARAJ, S., SOUZA, I. & PREMARAJ, T. 2011. Mechanical loading activates beta-catenin signaling in periodontal ligament cells. *Angle Orthod,* 81**,** 592-9.
RAMAGE, L. 2011. Integrins and extracellular matrix in mechanotransduction. *Cell Health and Cytoskeleton,* 4**,** 1-9.
RAMAGE, L., NUKI, G. & SALTER, D. M. 2009. Signalling cascades in mechanotransduction: cell–matrix interactions and mechanical loading. *Scandinavian Journal of Medicine & Science in Sports,* 19**,** 457-469.
RANGER, A. M., GERSTENFELD, L. C., WANG, J., KON, T., BAE, H., GRAVALLESE, E. M., GLIMCHER, M. J. & GLIMCHER, L. H. 2000. The nuclear factor of activated T cells (NFAT) transcription factor NFATp (NFATc2) is a repressor of chondrogenesis. *J Exp Med,* 191**,** 9-22.
RATCLIFFE, A. & MOW, V. 1996. Articular cartilage. *In:* COMPER, W. D. (ed.) *Extracellular matrix.* Amsterdam Harwood Academic Pubs.
ROBINSON, J. A., CHATTERJEE-KISHORE, M., YAWORSKY, P. J., CULLEN, D. M., ZHAO, W., LI, C., KHARODE, Y., SAUTER, L., BABIJ, P., BROWN, E. L., HILL, A. A., AKHTER, M. P., JOHNSON, M. L., RECKER, R. R., KOMM, B. S. & BEX, F. J. 2006. Wnt/beta-catenin signaling is a normal physiological response to mechanical loading in bone. *J Biol Chem,* 281**,** 31720-8.
RODOVA, M., LU, Q., LI, Y., WOODBURY, B. G., CRIST, J. D., GARDNER, B. M., YOST, J. G., ZHONG, X. B., ANDERSON, H. C. & WANG, J. 2011. Nfat1 regulates adult articular chondrocyte function through its age-dependent expression mediated by epigenetic histone methylation. *J Bone Miner Res,* 26**,** 1974-86.
ROEHRL, M. H., KANG, S., ARAMBURU, J., WAGNER, G., RAO, A. & HOGAN, P. G. 2004. Selective inhibition of calcineurin-NFAT signaling by blocking protein-protein interaction with small organic molecules. *Proc Natl Acad Sci U S A,* 101**,** 7554-9.
ROTHSCHILD, B. M., AND J., W.R. 2012. Epidemiology and Biomechanics of Osteoarthritis. *In:* ROTHSCHILD, B. M. (ed.) *Principles of Osteoarthritis- Its Definition, Character, Derivation and Modality-Related Recognition.* InTech.

ROUGHLEY, P. J. 2001. Articular cartilage and changes in arthritis: noncollagenous proteins and proteoglycans in the extracellular matrix of cartilage. *Arthritis Res,* 3**,** 342-7.
ROUGHLEY, P. J. 2006. The structure and function of cartilage proteoglycans. *Eur Cell Mater,* 12**,** 92-101.
RYU, J. H. & CHUN, J. S. 2006. Opposing roles of WNT-5A and WNT-11 in interleukin-1beta regulation of type II collagen expression in articular chondrocytes. *J Biol Chem,* 281**,** 22039-47.
SAHEBJAM, S., KHOKHA, R. & MORT, J. S. 2007. Increased collagen and aggrecan degradation with age in the joints of Timp3−/− mice. *Arthritis & Rheumatism,* 56**,** 905-909.
SALTER, D. M., HUGHES, D. E., SIMPSON, R. & GARDNER, D. L. 1992. Integrin expression by human articular chondrocytes. *Br J Rheumatol,* 31**,** 231-4.
SCHLESSINGER, K., HALL, A. & TOLWINSKI, N. 2009. Wnt signaling pathways meet Rho GTPases. *Genes Dev,* 23**,** 265-77.
SEAL, B. L., OTERO, T. C. & PANITCH, A. 2001. Polymeric biomaterials for tissue and organ regeneration. *Materials Science and Engineering: R: Reports,* 34**,** 147-230.
SHI, R.-Y., YANG, X.-R., SHEN, Q.-J., YANG, L.-X., XU, Y., QIU, S.-J., SUN, Y.-F., ZHANG, X., WANG, Z., ZHU, K., QIN, W.-X., TANG, Z.-Y., FAN, J. & ZHOU, J. 2013. High expression of Dickkopf-related protein 1 is related to lymphatic metastasis and indicates poor prognosis in intrahepatic cholangiocarcinoma patients after surgery. *Cancer,* 119**,** 993-1003.
SHI, Y., FU, Y., TONG, W., GENG, Y., LUI, P. P. Y., TANG, T., ZHANG, X. & DAI, K. 2012. Uniaxial mechanical tension promoted osteogenic differentiation of rat tendon-derived stem cells (rTDSCs) via the Wnt5a-RhoA pathway. *Journal of Cellular Biochemistry,* 113**,** 3133-3142.
SHIEH, A. C. & ATHANASIOU, K. A. 2006. Biomechanics of single zonal chondrocytes. *J Biomech,* 39**,** 1595-602.
SIRONEN, R. K., KARJALAINEN, H. M., ELO, M. A., KAARNIRANTA, K., TORRONEN, K., TAKIGAWA, M., HELMINEN, H. J. & LAMMI, M. J. 2002. cDNA array reveals mechanosensitive genes in chondrocytic cells under hydrostatic pressure. *Biochim Biophys Acta,* 1591**,** 45-54.
SITARA, D. & ALIPRANTIS, A. O. 2010. Transcriptional regulation of bone and joint remodeling by NFAT. *Immunological Reviews,* 233**,** 286-300.
SOFAT, N., ROBERTSON, S. D., HERMANSSON, M., JONES, J., MITCHELL, P. & WAIT, R. 2012. Tenascin-C fragments are endogenous inducers of cartilage matrix degradation. *Rheumatol Int,* 32**,** 2809-17.
SOKOLOFF, L. 2014. *The Joints and Synovial Fluid*, Elsevier Science.
STEINMEYER, J., KNUE, S., RAISS, R. X. & PELZER, I. 1999. Effects of intermittently applied cyclic loading on proteoglycan metabolism and swelling behaviour of articular cartilage explants. *Osteoarthritis Cartilage,* 7**,** 155-64.
STOCK, M., BOHM, C., SCHOLTYSEK, C., ENGLBRECHT, M., FURNROHR, B. G., KLINGER, P., GELSE, K., GAYETSKYY, S., ENGELKE, K., BILLMEIER, U., WIRTZ, S., VAN DEN BERG, W. & SCHETT, G. 2013. Wnt inhibitory factor 1 deficiency uncouples cartilage and bone destruction in tumor necrosis factor alpha-mediated experimental arthritis. *Arthritis Rheum,* 65**,** 2310-22.
SUN, R., ZHANG, B., CHEN, L. & SUN, J. 2014. Role of nuclear factor of activated T cells 1 in the pathogenesis of osteoarthritis. *Exp Ther Med,* 7**,** 195-198.

SUNDARAM, K., NISHIMURA, R., SENN, J., YOUSSEF, R. F., LONDON, S. D. & REDDY, S. V. 2007. RANK ligand signaling modulates the matrix metalloproteinase-9 gene expression during osteoclast differentiation. *Exp Cell Res,* 313**,** 168-78.

SURMANN-SCHMITT, C., WIDMANN, N., DIETZ, U., SAEGER, B., EITZINGER, N., NAKAMURA, Y., RATTEL, M., LATHAM, R., HARTMANN, C. & VON DER MARK, H. 2009. Wif-1 is expressed at cartilage-mesenchyme interfaces and impedes Wnt3a-mediated inhibition of chondrogenesis. *Journal of cell science,* 122**,** 3627-3637.

TAKAMATSU, A., OHKAWARA, B., ITO, M., MASUDA, A., SAKAI, T., ISHIGURO, N. & OHNO, K. 2014. Verapamil protects against cartilage degradation in osteoarthritis by inhibiting Wnt/beta-catenin signaling. *PLoS One,* 9**,** e92699.

TAKEMARU, K., YAMAGUCHI, S., LEE, Y. S., ZHANG, Y., CARTHEW, R. W. & MOON, R. T. 2003. Chibby, a nuclear beta-catenin-associated antagonist of the Wnt/Wingless pathway. *Nature,* 422**,** 905-9.

THALI, M., BUKOVSKY, A., KONDO, E., ROSENWLRTH, B., WALSH, C. T., SODROSKI, J. & GOTTLINGER, H. G. 1994. Functional association of cyclophilin A with HIV-1 virions. *Nature,* 372**,** 363-365.

THELLIN, O., ZORZI, W., LAKAYE, B., DE BORMAN, B., COUMANS, B., HENNEN, G., GRISAR, T., IGOUT, A. & HEINEN, E. 1999. Housekeeping genes as internal standards: use and limits. *J Biotechnol,* 75**,** 291-5.

THIRUNAVUKKARASU, K., PEI, Y., MOORE, T. L., WANG, H., YU, X. P., GEISER, A. G. & CHANDRASEKHAR, S. 2006. Regulation of the human ADAMTS-4 promoter by transcription factors and cytokines. *Biochem Biophys Res Commun,* 345**,** 197-204.

THOMAS, R. S., CLARKE, A. R., DUANCE, V. C. & BLAIN, E. J. 2011. Effects of Wnt3A and mechanical load on cartilage chondrocyte homeostasis. *Arthritis Res Ther,* 13**,** R203.

THORFVE, A., DEHNE, T., LINDAHL, A., BRITTBERG, M., PRUSS, A., RINGE, J., SITTINGER, M. & KARLSSON, C. 2012. Characteristic Markers of the WNT Signaling Pathways Are Differentially Expressed in Osteoarthritic Cartilage. *Cartilage,* 3**,** 43-57.

TOMITA, M., REINHOLD, M. I., MOLKENTIN, J. D. & NASKI, M. C. 2002. Calcineurin and NFAT4 induce chondrogenesis. *J Biol Chem,* 277**,** 42214-8.

TOPOL, L., JIANG, X., CHOI, H., GARRETT-BEAL, L., CAROLAN, P. J. & YANG, Y. 2003. Wnt-5a inhibits the canonical Wnt pathway by promoting GSK-3-independent beta-catenin degradation. *J Cell Biol,* 162**,** 899-908.

TRICKEY, W. R., VAIL, T. P. & GUILAK, F. 2004. The role of the cytoskeleton in the viscoelastic properties of human articular chondrocytes. *J Orthop Res,* 22**,** 131-9.

TROEBERG, L. & NAGASE, H. 2012. Proteases involved in cartilage matrix degradation in osteoarthritis. *Biochim Biophys Acta,* 1824**,** 133-45.

VAN AMERONGEN, R. & NUSSE, R. 2009. Towards an integrated view of Wnt signaling in development. *Development,* 136**,** 3205-14.

VAN DER KRAAN, P. M., BUMA, P., VAN KUPPEVELT, T. & VAN DEN BERG, W. B. 2002. Interaction of chondrocytes, extracellular matrix and growth factors: relevance for articular cartilage tissue engineering. *Osteoarthritis and Cartilage,* 10**,** 631-637.

VAN DER KRAAN, P. M. & VAN DEN BERG, W. B. 2012. Chondrocyte hypertrophy and osteoarthritis: role in initiation and progression of cartilage degeneration? *Osteoarthritis and Cartilage,* 20**,** 223-232.
VAN WEEREN, P. R., FIRTH, E. C., BROMMER, H., HYTTINEN, M. M., HELMINEN, A. E., ROGERS, C. W., DEGROOT, J. & BRAMA, P. A. 2008. Early exercise advances the maturation of glycosaminoglycans and collagen in the extracellular matrix of articular cartilage in the horse. *Equine Vet J,* 40**,** 128-35.
VANDERPLOEG, E. J., IMLER, S. M., BRODKIN, K. R., GARCIA, A. J. & LEVENSTON, M. E. 2004. Oscillatory tension differentially modulates matrix metabolism and cytoskeletal organization in chondrocytes and fibrochondrocytes. *J Biomech,* 37**,** 1941-52.
VANDERPLOEG, E. J., WILSON, C. G. & LEVENSTON, M. E. 2008. Articular chondrocytes derived from distinct tissue zones differentially respond to in vitro oscillatory tensile loading. *Osteoarthritis Cartilage,* 16**,** 1228-36.
VIDYA PRIYADARSINI, R., SENTHIL MURUGAN, R. & NAGINI, S. 2012. Aberrant activation of Wnt/β-catenin signaling pathway contributes to the sequential progression of DMBA-induced HBP carcinomas. *Oral Oncology,* 48**,** 33-39.
VISSE, R. & NAGASE, H. 2003. Matrix metalloproteinases and tissue inhibitors of metalloproteinases: structure, function, and biochemistry. *Circ Res,* 92**,** 827-39.
WALLINGFORD, J. B., FRASER, S. E. & HARLAND, R. M. 2002. Convergent extension: the molecular control of polarized cell movement during embryonic development. *Dev Cell,* 2**,** 695-706.
WANG, J., GARDNER, B. M., LU, Q., RODOVA, M., WOODBURY, B. G., YOST, J. G., ROBY, K. F., PINSON, D. M., TAWFIK, O. & ANDERSON, H. C. 2009. Transcription factor Nfat1 deficiency causes osteoarthritis through dysfunction of adult articular chondrocytes. *J Pathol,* 219**,** 163-72.
WANN, A. K., ZUO, N., HAYCRAFT, C. J., JENSEN, C. G., POOLE, C. A., MCGLASHAN, S. R. & KNIGHT, M. M. 2012. Primary cilia mediate mechanotransduction through control of ATP-induced Ca2+ signaling in compressed chondrocytes. *FASEB J,* 26**,** 1663-71.
WARDALE, R. J. & DUANCE, V. C. 1993. Quantification and immunolocalisation of porcine articular and growth plate cartilage collagens. *J Cell Sci,* 105 (Pt 4)**,** 975-84.
WATKINS, J. 2014. *Fundamental Biomechanics of Sport and Exercise*, Taylor & Francis.
WENG, L. H., KO, J. Y., WANG, C. J., SUN, Y. C. & WANG, F. S. 2012. Dkk-1 promotes angiogenic responses and cartilage matrix proteinase secretion in synovial fibroblasts from osteoarthritic joints. *Arthritis Rheum,* 64**,** 3267-77.
WENG, L. H., WANG, C. J., KO, J. Y., SUN, Y. C., SU, Y. S. & WANG, F. S. 2009. Inflammation induction of Dickkopf-1 mediates chondrocyte apoptosis in osteoarthritic joint. *Osteoarthritis Cartilage,* 17**,** 933-43.
WENG, L. H., WANG, C. J., KO, J. Y., SUN, Y. C. & WANG, F. S. 2010. Control of Dkk-1 ameliorates chondrocyte apoptosis, cartilage destruction, and subchondral bone deterioration in osteoarthritic knees. *Arthritis Rheum,* 62**,** 1393-402.
WISSMANN, C., WILD, P. J., KAISER, S., ROEPCKE, S., STOEHR, R., WOENCKHAUS, M., KRISTIANSEN, G., HSIEH, J. C., HOFSTAEDTER, F., HARTMANN, A., KNUECHEL, R., ROSENTHAL, A. & PILARSKY, C. 2003.

WIF1, a component of the Wnt pathway, is down-regulated in prostate, breast, lung, and bladder cancer. *J Pathol,* 201**,** 204-12.
WONG, M., SIEGRIST, M. & CAO, X. 1999. Cyclic compression of articular cartilage explants is associated with progressive consolidation and altered expression pattern of extracellular matrix proteins. *Matrix Biol,* 18**,** 391-9.
WONG, M., WUETHRICH, P., BUSCHMANN, M. D., EGGLI, P. & HUNZIKER, E. 1997. Chondrocyte biosynthesis correlates with local tissue strain in statically compressed adult articular cartilage. *J Orthop Res,* 15**,** 189-96.
WRIGHT, M. O., NISHIDA, K., BAVINGTON, C., GODOLPHIN, J. L., DUNNE, E., WALMSLEY, S., JOBANPUTRA, P., NUKI, G. & SALTER, D. M. 1997. Hyperpolarisation of cultured human chondrocytes following cyclical pressure-induced strain: evidence of a role for alpha 5 beta 1 integrin as a chondrocyte mechanoreceptor. *J Orthop Res,* 15**,** 742-7.
WU, J. Q., SEAY, M., SCHULZ, V. P., HARIHARAN, M., TUCK, D., LIAN, J., DU, J., SHI, M., YE, Z., GERSTEIN, M., SNYDER, M. P. & WEISSMAN, S. 2012. Tcf7 is an important regulator of the switch of self-renewal and differentiation in a multipotential hematopoietic cell line. *PLoS Genet,* 8**,** e1002565.
YAMAGUCHI, T. P., BRADLEY, A., MCMAHON, A. P. & JONES, S. 1999. A Wnt5a pathway underlies outgrowth of multiple structures in the vertebrate embryo. *Development,* 126**,** 1211-23.
YANAGAWA, S., VAN LEEUWEN, F., WODARZ, A., KLINGENSMITH, J. & NUSSE, R. 1995. The dishevelled protein is modified by wingless signaling in Drosophila. *Genes Dev,* 9**,** 1087-97.
YANG, H., HENNING, D. & VALDEZ, B. C. 2005. Functional interaction between RNA helicase II/Guα and ribosomal protein L4. *FEBS Journal,* 272**,** 3788-3802.
YANG, Y., TOPOL, L., LEE, H. & WU, J. 2003. Wnt5a and Wnt5b exhibit distinct activities in coordinating chondrocyte proliferation and differentiation. *Development,* 130**,** 1003-15.
YAO, Z., NAKAMURA, H., MASUKO-HONGO, K., SUZUKI-KUROKAWA, M., NISHIOKA, K. & KATO, T. 2004. Characterisation of cartilage intermediate layer protein (CILP)-induced arthropathy in mice. *Ann Rheum Dis,* 63**,** 252-8.
YATES, K. E., SHORTKROFF, S. & REISH, R. G. 2005. Wnt influence on chondrocyte differentiation and cartilage function. *DNA Cell Biol,* 24**,** 446-57.
YOKOTA, H., LEONG, D. & SUN, H. 2011. Mechanical Loading: Bone Remodeling and Cartilage Maintenance. *Current Osteoporosis Reports,* 9**,** 237-242.
YOO, S. A., PARK, B. H., YOON, H. J., LEE, J. Y., SONG, J. H., KIM, H. A., CHO, C. S. & KIM, W. U. 2007. Calcineurin modulates the catabolic and anabolic activity of chondrocytes and participates in the progression of experimental osteoarthritis. *Arthritis Rheum,* 56**,** 2299-311.
YUASA, T., KONDO, N., YASUHARA, R., SHIMONO, K., MACKEM, S., PACIFICI, M., IWAMOTO, M. & ENOMOTO-IWAMOTO, M. 2009. Transient activation of Wnt/{beta}-catenin signaling induces abnormal growth plate closure and articular cartilage thickening in postnatal mice. *Am J Pathol,* 175**,** 1993-2003.
YUASA, T., OTANI, T., KOIKE, T., IWAMOTO, M. & ENOMOTO-IWAMOTO, M. 2008. Wnt/beta-catenin signaling stimulates matrix catabolic genes and activity in articular chondrocytes: its possible role in joint degeneration. *Lab Invest,* 88**,** 264-74.

ZHOU, X. L., QIN, X. R., ZHANG, X. D. & YE, L. H. 2010. Downregulation of Dickkopf-1 is responsible for high proliferation of breast cancer cells via losing control of Wnt/beta-catenin signaling. *Acta Pharmacol Sin,* 31**,** 202-10.

ZHU, M., CHEN, M., ZUSCIK, M., WU, Q., WANG, Y.-J., ROSIER, R. N., O'KEEFE, R. J. & CHEN, D. 2008. Inhibition of β-catenin signaling in articular chondrocytes results in articular cartilage destruction. *Arthritis & Rheumatism,* 58**,** 2053-2064.

ZHU, M., TANG, D., WU, Q., HAO, S., CHEN, M., XIE, C., ROSIER, R. N., O'KEEFE, R. J., ZUSCIK, M. & CHEN, D. 2009. Activation of β-Catenin Signaling in Articular Chondrocytes Leads to Osteoarthritis-Like Phenotype in Adult β-Catenin Conditional Activation Mice. *Journal of Bone and Mineral Research,* 24**,** 12-21.

Appendices

Appendix 1

β-catenin localisation in unloaded primary articular chondrocytes. Cells were labelled with monoclonal anti-β-catenin antibody in conjunction with goat anti-mouse FITC-conjugated secondary antibody (green): nuclei were counterstained with DAPI (blue) and visualised using confocal microscopy. Representative serial sections depicting the location of the staining i.e. in the cytoplasm and/or nucleus are shown.

Appendix 2

Effect of tensile strain (7.5%, 1Hz) on β-catenin localisation in primary articular chondrocytes loaded for 2 hours. Cells were labelled with monoclonal anti-β-catenin antibody in conjunction with goat anti-mouse FITC-conjugated secondary antibody (green): nuclei were counterstained with DAPI (blue) and visualised using confocal microscopy. Representative serial sections depicting the location of the staining i.e. in the cytoplasm and/or nucleus are shown.

Appendix 3

A. **B.**

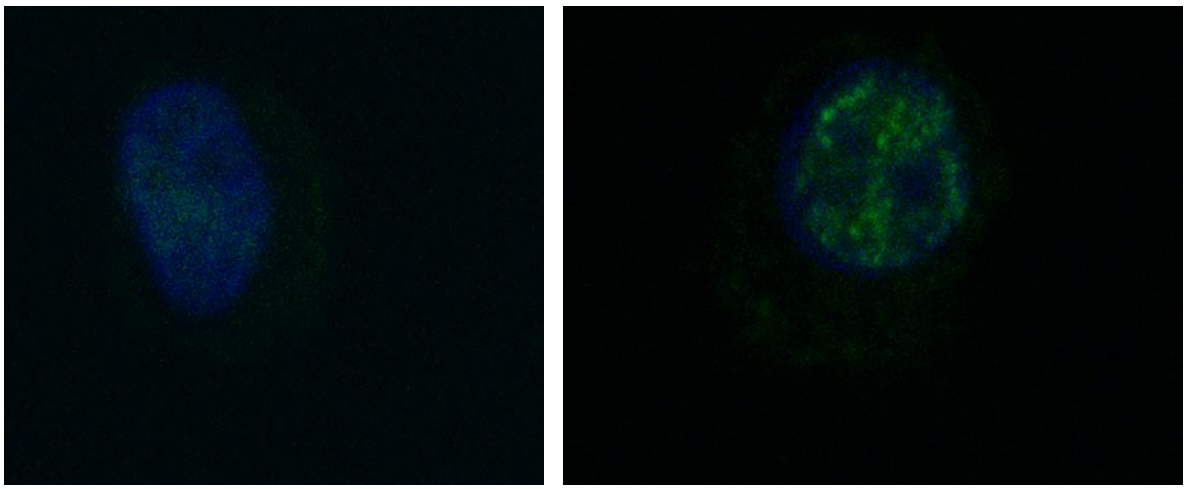

Effect of tensile strain (7.5%, 1Hz) on β-catenin localisation in primary articular chondrocytes loaded for 2 hours. Cells were labelled with monoclonal anti-β-catenin antibody in conjunction with goat anti-mouse FITC-conjugated secondary antibody (green): nuclei were counterstained with DAPI (blue) and visualised using confocal microscopy. Representative serial section depicting β-catenin labelling in A) unloaded and B) loaded chondrocytes.

Appendix 4

Table of the genes present on RT^2 Profiler WNT PCR array (Qiagen).

Position	UniGene	GenBank	Symbol	Description
A01	Bt.9945	NM_001128497	AES	Amino-terminal enhancer of split
A02	Bt.11086	NM_001075986	APC	Adenomatous polyposis coli
A03	Bt.21602	NM_001191398	AXIN1	Axin 1
A04	Bt.4412	NM_001192299	AXIN2	Axin 2
A05	N/A	XM_002686086	BCL9	B-cell CLL/lymphoma 9
A06	Bt.25271	NM_001083475	BTRC	Beta-transducin repeat containing
A07	Bt.88783	NM_001046273	CCND1	Cyclin D1
A08	Bt.4895	NM_001076372	CCND2	Cyclin D2
A09	Bt.65222	NM_174711	CSNK1A1	Casein kinase 1, alpha 1
A10	Bt.64603	NM_174635	CSNK2A1	Casein kinase 2, alpha 1 polypeptide
A11	Bt.1780	XM_002688450	CTBP1	C-terminal binding protein 1
A12	Bt.33687	NM_001076141	CTNNB1	Catenin (cadherin-associated protein), beta 1, 88kDa
B01	Bt.8208	NM_001081588	DAAM1	Dishevelled associated activator of morphogenesis 1
B02	Bt.15382	NM_001193246	DAB2	Disabled homolog 2, mitogen-responsive phosphoprotein (Drosophila)
B03	N/A	XM_002693011	DIXDC1	DIX domain containing 1
B04	Bt.13880	NM_001205544	DKK1	Dickkopf homolog 1 (Xenopus laevis)
B05	Bt.18710	NM_001100306	DKK3	Dickkopf homolog 3 (Xenopus laevis)
B06	Bt.27892	NM_001206601	DVL1	Dishevelled, dsh homolog 1 (Drosophila)
B07	Bt.17972	NM_001191382	DVL2	Dishevelled, dsh homolog 2 (Drosophila)
B08	Bt.30467	XM_002696250	FBXW11	F-box and WD repeat domain containing 11
B09	Bt.26327	NM_001101985	FBXW4	F-box and WD repeat domain containing 4
B10	Bt.62944	NM_001040605	FGF4	Fibroblast growth factor 4
B11	Bt.17885	NM_001205985	FOSL1	FOS-like antigen 1
B12	Bt.88317	NM_001192452	FOXN1	Forkhead box N1
C01	N/A	XM_002698415	FRAT1	Frequently rearranged in advanced T-cell lymphomas
C02	Bt.121	NM_174059	FRZB	Frizzled-related protein
C03	Bt.26635	NM_001101048	FZD1	Frizzled family receptor 1
C04	Bt.79602	NM_001192964	FZD3	Frizzled family receptor 3
C05	Bt.67879	NM_001206269	FZD4	Frizzled family receptor 4
C06	N/A	XM_005197510	FZD5	Frizzled family receptor 5
C07	Bt.104004	XM_863880	FZD6	Frizzled homolog 6 (Drosophila)
C08	Bt.105583	NM_001144091	FZD7	Frizzled family receptor 7
C09	N/A	XM_005194311	FZD8	Frizzled family receptor 8
C10	N/A	XM_002698189	FZD9	Frizzled family receptor 9

Appendix 5

Table of the genes present on RT^2 Profiler WNT PCR array (Qiagen).

Position	UniGene	GenBank	Symbol	Description
C11	Bt.33944	NM_001102192	GSK3A	Glycogen synthase kinase 3 alpha
C12	Bt.48740	NM_001101310	GSK3B	Glycogen synthase kinase 3 beta
D01	Bt.11159	NM_001077827	JUN	Jun proto-oncogene
D02	N/A	XM_002694622	KREMEN1	Kringle containing transmembrane protein 1
D03	Bt.18467	NM_001192856	LEF1	Lymphoid enhancer-binding factor 1
D04	Bt.45360	XM_002699405	LRP5	Low density lipoprotein receptor-related protein 5
D05	Bt.60913	XM_002687783	LRP6	Low density lipoprotein receptor-related protein 6
D06	Bt.14050	NM_001192974	MAPK8	Mitogen-activated protein kinase 8
D07	Bt.13092	NM_001075130	MMP7	Matrix metallopeptidase 7 (matrilysin, uterine)
D08	Bt.21164	NM_001046074	MYC	V-myc myelocytomatosis viral oncogene homolog (avian)
D09	Bt.45162	NM_001166615	NFATC1	Nuclear factor of activated T-cells, cytoplasmic, calcineurin-dependent 1
D10	Bt.60075	NM_001105453	NKD1	Naked cuticle homolog 1 (Drosophila)
D11	Bt.43996	NM_001193253	NLK	Nemo-like kinase
D12	Bt.18496	NM_001097991	PITX2	Paired-like homeodomain 2
E01	Bt.38004	NM_001101208	PORCN	Porcupine homolog (Drosophila)
E02	Bt.13264	NM_001083636	PPARD	Peroxisome proliferator-activated receptor delta
E03	Bt.57449	NM_001102534	PRICKLE1	Prickle homolog 1 (Drosophila)
E04	N/A	XM_002690892	PYGO1	Pygopus homolog 1 (Drosophila)
E05	Bt.49678	NM_176645	RHOA	Ras homolog gene family, member A
E06	Bt.2846	NM_001098147	RHOU	Ras homolog gene family, member U
E07	Bt.41723	NM_001101076	RUVBL1	RuvB-like 1 (E. coli)
E08	Bt.5226	NM_174460	SFRP1	Secreted frizzled-related protein 1
E09	Bt.3540	NM_001075764	SFRP4	Secreted frizzled-related protein 4
E10	Bt.112292	NM_001206251	SOX17	SRY (sex determining region Y)-box 17
E11	Bt.44634	NM_001099186	TCF7	Transcription factor 7 (T-cell specific, HMG-box)
E12	N/A	XM_002691408	TCF7L1	Transcription factor 7-like 1 (T-cell specific, HMG-box)
F01	Bt.3589	NM_001098020	TLE1	Transducin-like enhancer of split 1 (E(sp1) homolog, Drosophila)
F02	Bt.87234	NM_001205875	VANGL2	Vang-like 2 (van gogh, Drosophila)
F03	Bt.63013	NM_001075996	WIF1	WNT inhibitory factor 1
F04	N/A	XM_002692603	WISP1	WNT1 inducible signaling pathway protein 1
F05	Bt.101628	NM_001114191	WNT1	Wingless-type MMTV integration site family, member 1
F06	Bt.61102	NM_001099078	WNT10A	Wingless-type MMTV integration site family, member 10A
F07	Bt.21876	NM_001082456	WNT11	Wingless-type MMTV integration site family, member 11
F08	Bt.37171	NM_001014949	WNT16	Wingless-type MMTV integration site family, member 16
F09	Bt.37360	NM_001013001	WNT2	Wingless-type MMTV integration site family member 2
F10	Bt.27254	NM_001099363	WNT2B	Wingless-type MMTV integration site family, member 2B
F11	Bt.112395	NM_001206024	WNT3	Wingless-type MMTV integration site family, member 3
F12	N/A	XM_002688509	WNT3A	Wingless-type MMTV integration site family, member 3A
G01	Bt.88484	NM_001205971	WNT5A	Wingless-type MMTV integration site family, member 5A
G02	Bt.6367	NM_001205628	WNT5B	Wingless-type MMTV integration site family, member 5B
G03	Bt.27385	NM_001205563	WNT6	Wingless-type MMTV integration site family, member 6

Appendix 6

Table of the genes present on RT2 Profiler WNT PCR array (Qiagen).

G04	Bt.69615	NM_001192788	WNT7A	Wingless-type MMTV integration site family, member 7A
G05	N/A	XM_603482	WNT7B	Wingless-type MMTV integration site family, member 7B
G06	Bt.106446	NM_001192370	WNT8A	Wingless-type MMTV integration site family, member 8A
G07	N/A	XM_002688510	WNT9A	Wingless-type MMTV integration site family, member 9A
G08	Bt.17918	NM_174739	CBY1	Chibby homolog 1 (Drosophila)
G09	Bt.24868	NM_001082615	DKK2	Dickkopf homolog 2 (Xenopus laevis)
G10	N/A	XM_002698709	DKK4	Dickkopf homolog 4 (Xenopus laevis)
G11	Bt.9084	XM_002697867	KREMEN2	Kringle containing transmembrane protein 2
G12	N/A	XM_001254723	MAP2K7	Mitogen-activated protein kinase kinase 7
H01	Bt.14186	NM_173979	ACTB	Actin, beta
H02	Bt.87389	NM_001034034	GAPDH	Glyceraldehyde-3-phosphate dehydrogenase
H03	Bt.49238	NM_001034035	HPRT1	Hypoxanthine phosphoribosyltransferase 1
H04	Bt.22662	NM_001075742	TBP	TATA box binding protein
H05	Bt.111451	NM_174814	YWHAZ	Tyrosine 3-monooxygenase/tryptophan 5-monooxygenase activation protein, zeta polypeptide
H06	N/A	SA_00137	BGDC	Cow Genomic DNA Contamination
H07	N/A	SA_00104	RTC	Reverse Transcription Control
H08	N/A	SA_00104	RTC	Reverse Transcription Control
H09	N/A	SA_00104	RTC	Reverse Transcription Control
H10	N/A	SA_00103	PPC	Positive PCR Control
H11	N/A	SA_00103	PPC	Positive PCR Control
H12	N/A	SA_00103	PPC	Positive PCR Control

Glossary of biomechanical terms:

Compression: The application of a pushing stress resulting in the object becoming shorter and thinner.

Hydrostatic pressure: Pressure which arises from the restriction of fluid flow within the tissue.

Shear: The movement of fluid flow through the tissue ECM or experienced at the tissue surface due to friction and/or contact stresses.

Strain: The deformation of the tissue resulting from the application of load.

Stress: Defined as the ratio of the force applied to the cross-sectional area of the tissue.

Tension: The application of a pulling force resulting in the tissue stretching and becoming longer and thinner.